UNIVERSITA' DEGLI STUDI DI PARMA

Dottorato di ricerca in
Biologia e Patologia Molecolare

Ciclo XXV

NOVEL THERAPIES IN NON-SMALL CELL LUNG CANCER

Coordinatore:
Chiar.mo Prof. Valeria Dall'Asta

Tutor:
Chiar.mo Prof. Roberta Alfieri

Dottorando: Elena Galvani

CONTENTS

Chapter 1

General Introduction

LUNG CANCER

Lung cancer is the leading cause of cancer-related death worldwide [1]. Approximately 1.2 million new cases of lung cancer are diagnosed every year, and 1.1 million patients die of the disease. Prolonged tobacco smoke has been identified as the cause of 90% of this unimaginable death toll [2]. In Europe and US lung cancer in never-smokers is rare (<10% of cases), and most cases in the US are now represented by ex-smokers. Radon gas, asbestos or genetic factors have been described as possible causes for lung cancer development in never-smokers [3-5]. The histological or cytological diagnosis of lung cancer is usually obtained by bronchoscopic examination or fine needle aspiration, and malaise, weight loss and dyspnea are the most common symptoms at onset.

Two main distinctions are made among the several histological types of lung cancer: small cell lung carcinoma (SCLC) and non-small cell lung carcinoma (NSCLC). For more than 50 years, SCLC has been mainly staged as either limited or extensive stage disease. Recent publications suggested the use of the Tumor-Node-Metastasis (TNM) classification in NSCLC as well as in SCLC [6-7]. This system which was initially introduced in 1972 has been modified over the years, and recently some additional adjustments have been proposed [8]. The TNM staging system includes a pretreatment clinical classification (cTNM), which is used to identify the guidance of treatment, and a postsurgical histopathologic classification (pTNM), which permits to estimate prognosis and select the most appropriate treatment approach. The TNM staging system takes into account the size and the degree of spread of the primary tumor (T), whether and to what extent lymph nodes are involved (N) and the presence of distant metastasis (M). NSCLCs, which account for about 85% of all lung cancers, consist of several different histological subtypes, including squamous cell lung carcinoma, adenocarcinoma and large cell carcinoma. Whereas squamous cell carcinoma was the most frequent histological type a decade ago, adenocarcinoma represents at present over 50% of NSCLCs in the US, North European countries and Japan. This change in histological prevalence is most likely related to a change in type of cigarette smoke and potentially to pollution in urban areas [9]. In spite of advances in early detection, the prognosis for both SCLC and NSCLC remains poor. The overall 5-year survival for patients with limited stage SCLC is about 20% while for patients with extensive stage is less than 1% [6]. For NSCLC, the overall 5-year survival of patients with stage IA is 76.9% and for patients with stage IIA this is 48.5%. For patients with stage IIIA disease, 30.6% is still alive 5 years after surgery, whereas for patients with stage IV this is only 1% [10].

LUNG CANCER TREATMENT

The histological type, together with the stage of disease, and the performance status, are used as parameters to define the treatment for lung cancer patients. Since SCLC is usually diagnosed in advanced stage, chemotherapy represents the mainstay treatment for this disease, while surgery is rarely applied. Commonly, the combination with cisplatin and etoposide is used in the treatment of SCLC, which response is about 90% in patients with limited disease, and 50-60% in patients with extensive disease [11]. Of these, about 10-50% achieves a complete radiological response. Concomitant chest radiotherapy with chemotherapy is used in patients with limited disease, and prophylactic cranial irradiation is also recommended in patients who respond to systemic treatment, to prevent brain relapse.

For early stage NSCLC, surgery is the most important curative modality. However, only approximately 20-30% of patients are diagnosed at resectable stage (stage I-II). For advanced NSCLC patients with good performance status (0-1), platinum-based chemotherapy represents the standard treatment and partial responses can be achieved in 30-40% of the cases while complete responses are very rare [12]. Combinations with cisplatin or carboplatin, and third generation cytotoxic drugs, such as gemcitabine, paclitaxel, docetaxel, etoposide or vinorelbine, are used. Moreover, both chemo- and radiotherapy can be used in neo-adjuvant setting to shrink the tumor before surgery or as adjuvant therapy to improve outcome after resection. The use of both neo-adjuvant and adjuvant chemotherapy has been shown to improve patient survival [13-15]. Despite advances in these combined treatment modalities for lung cancer, prognosis remains poor and severe side effects are often observed. Therefore, more effective and less toxic treatments are needed and, as a result, a variety of molecular targeted therapies have been recently introduced for the treatment of advanced NSCLC.

TARGETED THERAPY

The novel targeted therapies are based on advances in our understanding of key cellular networks and genetic nodal points around which tumors could arise and progress [16, 17]. Genome characterization efforts have highlighted the importance of “driver” somatic alterations that activate crucial oncoproteins originating tumor with a pivotal dependency. Single-agent therapeutic regimens especially designed to intercept deregulated dominant oncogenes have proven to be effective treatment in these “oncogene addicted” tumors [18,19].

A number of molecular aberrations have been identified in NSCLC including EGFR mutations/amplifications, EML4-ALK translocation fusions, KRAS mutations, PIK3CA mutations, IGF-1R overexpression, and MET amplification/overexpression [20]. Conflicting results have demonstrated marginal benefit with targeted agents in unselected populations of patients with advanced NSCLC. However, many targeted agents have been approved in different line setting for the treatment of specific subgroups of patients. In particular, the epidermal growth factor receptor (EGFR) has been successfully targeted in this disease either by monoclonal antibodies (mAbs) or small molecules inhibiting the tyrosine kinase domain (gefitinib and erlotinib). Cetuximab is a mAb which blocks the extracellular domain of EGFR, thereby competing with the ligands, resulting in the inhibition of the receptor. This mAb, which is approved for the treatment of advanced colorectal cancer, has also been approved as first-line treatment combined with platinum-based chemotherapy in EGFR-positive NSCLC patients with good performance status [21, 22].

Gefitinib (Iressa) has been approved by U.S. Food and Drug Administration (FDA) and EMEA as upfront therapy replacing chemotherapy in late-stage NSCLC patients harboring activating-EGFR mutations [23]. Furthermore, the manageable toxicity, along with its efficacy, make erlotinib (Tarceva) an important option as maintenance therapy, and both erlotinib and gefitinib are also the only drugs of proven efficacy in the third-line setting for patients with NSCLC previously treated with chemotherapy [24]. Another example of targeted therapy for the treatment of advanced NSCLC is the antiangiogenic agent bevacizumab (Avastin), in combination with carboplatin-paclitaxel or any platinum-based chemotherapy, which has been recently approved as first-line treatment for patients bearing tumors with non-squamous histology [25]. More recently,

the anaplastic lymphoma kinase (ALK) inhibitor crizotinib (Xalkori) has also been approved by FDA for the treatment of locally advanced or metastatic NSCLCs that express the abnormal ALK gene [26]. Aberrations in other key molecules and signaling pathways, such as RAS/RAF/MEK, PI3K/Akt/mTOR, or c-MET, have been identified as crucial targets, especially in resistant patients. Novel drugs aimed to interact with these abnormal molecules are actively being investigated in the clinic, including the histone deacetylase (HDAC) inhibitor vorinostat [27], the BRAF inhibitor sorafenib [28], the Src/Abl inhibitor dasatinib [29] and many others [30].

EGFR SIGNALING PATHWAY

EGFR is a member of the ErbB family of receptor tyrosine kinases including EGFR (HER1; ErbB-1), HER2/c-neu (ErbB-2), HER3 (ErbB-3) and HER4 (ErbB-4). These receptors are present as monomers on the cell surface and are activated by binding of specific ligands, such as EGF and transforming growth factor alpha (TNF-α) [31]. Upon ligand binding, EGFR undergoes homo- or heterodimerization which results in autophosphorylation of several tyrosine residues. Downstream signaling pathways are activated which associate with the phosphorylated tyrosines through their phosphotyrosine-binding SH2 domains. These proteins initiate several transduction cascades, mainly involving the PI3K/Akt/mTOR, STATs and RAS/MEK/ERK pathways, which regulate cell survival, differentiation, proliferation, motility and angiogenesis (Figure 1). The EGFR inhibition is intensively being explored as cancer therapeutic approach because of its overexpression/mutation in many solid tumors including NSCLC and the evidence that aberrant signaling can lead to cancer transformation [32].

EGFR TYROSINE KINASE INHIBITORS

Small molecules have been used to inhibit EGFR kinase domain, thereby competing with ATP for the activation of signaling cascade on the cytoplasmic side of the receptor. Gefitinib and erlotinib are two examples of tyrosine kinase inhibitors (TKIs) which have been approved in several countries for the treatment of advanced NSCLC [33].

Initial studies with EGFR-TKIs showed about 10-20% response rates (RR) in unselected NSCLC patients when used as second- or third-line treatment [34-36]. Asians, women, non-smokers, and patients with adenocarcinoma were subsequently identified as subgroups more likely to benefit from gefitinib or erlotinib treatment [37]. Despite four large phase III trials failed to demonstrate any survival advantage from the combination of EGFR-TKIs with chemotherapy in first-line treatment, additional overall survival (OS) benefits were observed with erlotinib as second-/third-line or maintaining setting [38, 39]. However, the identification of somatic EGFR mutations, followed by retrospective analyses and prospective trials with EGFR-TKIs in selected patients, explained the previous conflicting results and defined the stage for more specific use of these agents [40, 41].

EGFR AS PREDICTOR FOR RESPONSE TO EGFR-TKIs

To date, several somatic EGFR mutations have been described in NSCLC, part of which are located in the region of the *EGFR* gene encoding the TK-domain (exons 18-24) [42, 43]. Nearly 90% of the detected EGFR mutations are either in-frame deletions in exon 19 affecting the amino acids ELREA (Del746-750), or

missense mutation in exon 21 replacing leucine-858 by arginine (L858R). EGFR mutations have been investigated in much detail in analyses *in vitro* which showed the specific activation of anti-apoptotic pathways via Akt and STAT signaling being sustained by the mutated receptors [44, 45]. Furthermore, *in vivo* assays showed that persistent EGFR signaling is required for the maintenance of tumors harboring mutations of the receptor [46, 47]. These studies reported the correlation between the development of adenocarcinoma in mice and the expression of mutant EGFR. Moreover, tumor regression was observed after gene silencing or treatment with erlotinib.

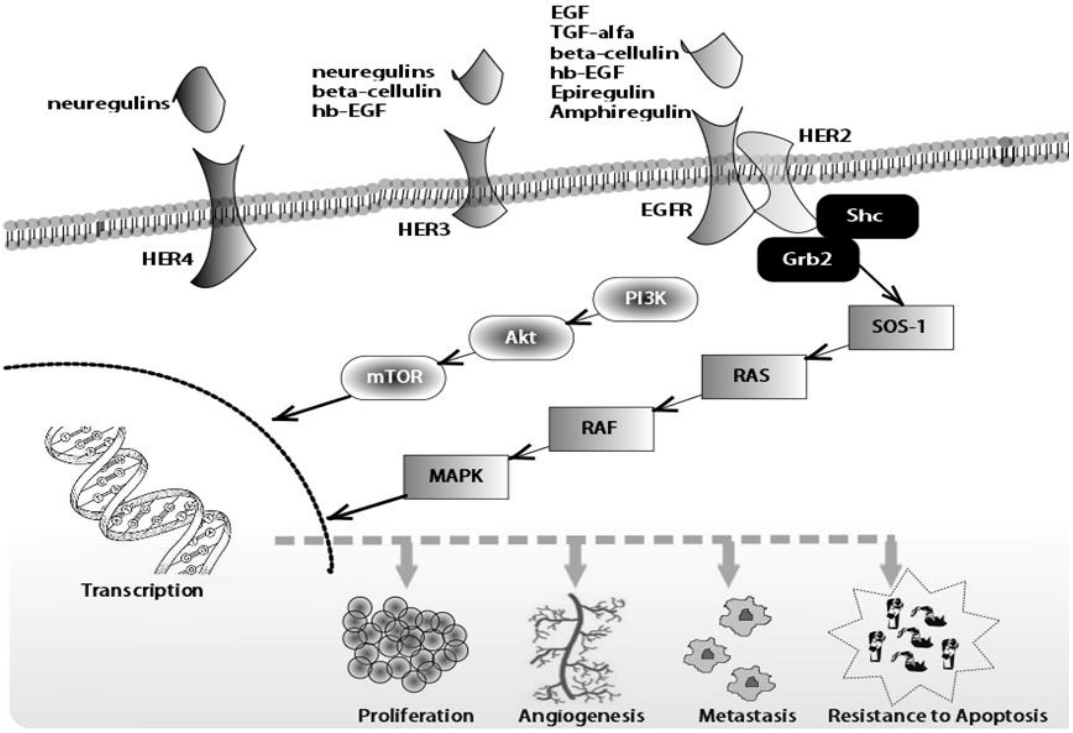

Figure 1. EGFR signaling pathway. ErbB family of receptors and signaling pathways involved in the tumorigenesis of NSCLC. Autophosphorylation of EGFR after heterodimerization (i.e. HER2) induces downstream activation of PI3K/Akt and RAS/MAPK pathways regulating various cellular responses.

Evidences suggest that different EGFR mutations correlate with differential levels of sensitivity to EGFR-TKIs treatment. The exon 19 deletions have been shown to be superior in predicting the response to TKIs than the other EGFR mutations [48, 49] (Figure 2). It has also been shown that among the patients treated with erlotinib or gefitinib, those which harbor this type of EGFR aberrations have a significantly longer survival time than patients harboring the L858R mutation [50]. Other recurrent but less frequent EGFR mutations correlated with response to EGFR-TKIs include the point mutation G719S in exon 18 and the L861Q substitution in exon 21 [51]. In addition to activating mutations which increase the sensitivity to EGFR-TKIs, a secondary mutation correlating with resistance to these agents has been identified which replaces methionine for threonine at residue 790 (T790M) [52].

Despite a large number of trials validated the predictive role of EGFR mutations as biomarkers of sensitivity to EGFR-TKIs, a limited group of NSCLC patients bearing wild-type EGFR also significantly benefits from the treatment with these drugs [53]. These findings suggest the existence of additional mechanisms involved in the response to gefitinib or erlotinib in EGFR mutation-negative patients. EGFR expression as assessed by

immunohistochemistry (IHC) or changes in EGFR copy-number detected by fluorescent in situ hybridization (FISH) or quantitative PCR were reported by several studies to be predictive markers for response to EGFR-TKIs treatment in NSCLC patients [54, 55]. However, controversial results were observed regarding the role of EGFR expression or gene amplification in the response to TKIs; thus, their validity as predictive biomarkers in NSCLC patients remains controversial [56-60]. During the past decades, several studies based on DNA/RNA microarrays have also tried to develop predictive signatures to decide the most suitable therapy approach for specific types or subtypes of tumors. Conflicting results and difficulties in replicating the data led to a limited impact on clinical practice. However, recent technical advancements in the development of rapid whole-genome studies could potentially change the pharmacogenomic approach to personalized treatment. These techniques are represented mainly by massively parallel or next-generation sequencing and GWASs [61, 62]. Prospective randomized trials are presently ongoing with EGFR-TKIs on patients selected on the basis of clinical characteristics and/or molecular markers and will help to clarify several of the open questions [63].

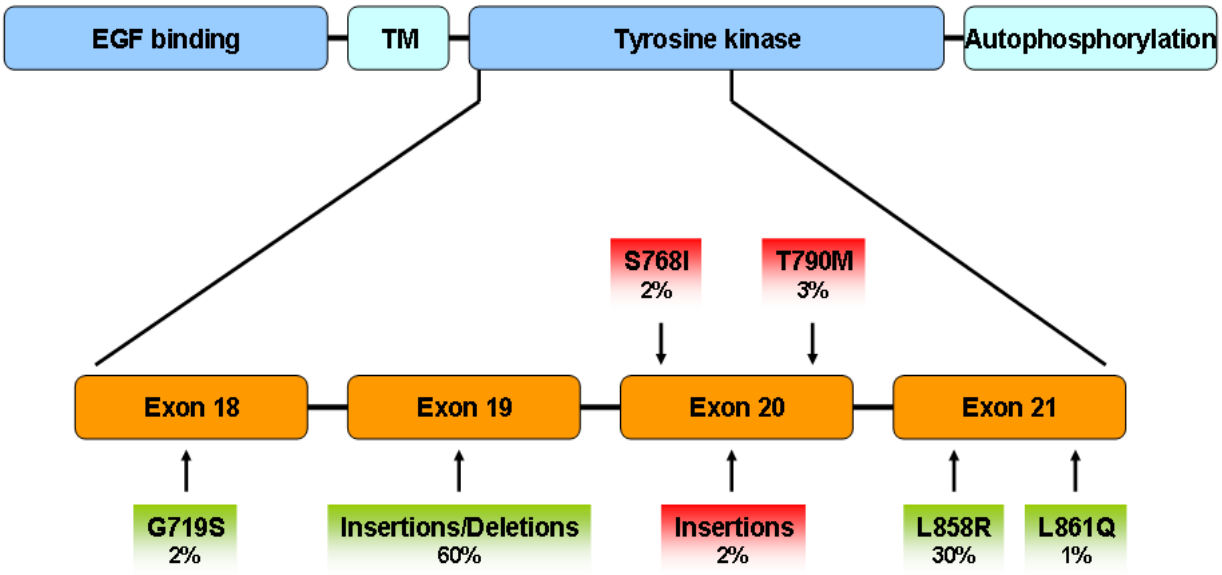

Figure 2. EGFR hotspot mutations. Localization of EGFR mutations in hotspot regions of the tyrosine kinase domain. Mutations which correlate with EGFR-TKI sensitivity are highlighted in green, while in red are reported those associated with resistance. Approximated percentages of each mutation as observed of total mutations detected in NSCLC patients are indicated (source: COSMIC). TM, transmembrane.

ANTIANGIOGENIC AGENTS

Angiogenesis is the multi-step process whereby new blood vessels are formed from the existing vasculature. Being involved in tumor progression and metastasis, angiogenesis represents an attractive therapeutic target for cancer treatment. The vascular endothelial growth factor (VEGF) pathway is key player in tumor angiogenesis. In hypoxic conditions, tumor cells secrete VEGF which binds the transmembrane TK receptors VEGFR-1, VEGFR-2 and VEGFR-3. The activation of the downstream signaling cascade stimulates endothelial cells proliferation, differentiation, migration and survival, and thereby the formation of new blood vessels [64]. Two main strategies are currently available to inhibit the VEGF pathway: i) direct VEGF inhibition by mAbs like bevacizumab, or ii) VEGFR inhibition by TKIs such as sorafenib, sunitinib,

montasenib and cediranib.

When added to standard chemotherapy, the mAb against VEGF bevacizumab increased survival in NSCLC patients [65]. In the pivotal phase III study ECOG 4599, non-squamous NSCLC patients were randomized to receive either chemotherapy or the combination of chemotherapy with the mAb. The addition of bevacizumab prolonged the OS from 10.3 months to 12.3 months, and increased the RR from 15% to 35%. Based on this study, bevacizumab gained FDA and EMEA approval as first-line therapy for advanced non-squamous NSCLC [66].

Several agents have been investigated which are active against multiple tyrosine kinases, including VEGFR, such as sorafenib and sunitinib. Sorafenib (Bay 43–9006, Nexavar®, Bayer; Leverkusen, Germany) is a TKI targeting VEGFR-2 and VEGFR-3, PDGFR-β, stem cell factor receptor (c-kit), v-raf 1 murine leukemia viral oncogene homolog 1 (Raf), and fms-like tyrosine kinase-3 (flt-3) [67]. Data from a phase II trial demonstrated the activity of sorafenib as single-agent in NSCLC patients pretreated with either chemotherapy or EGFR-TKIs [68]. Recently, the placebo-controlled, randomized phase III trial ESCAPE also evaluated sorafenib in the first-line setting in combination with platinum-based chemotherapy [69]. No improvement in OS or PFS was reported for patients randomized to chemotherapy plus sorafenib, and subgroups analyses revealed a reduction in OS for squamous histology type. A similarly designed phase III trial of sorafenib in combination with gemcitabine/cisplatin in non-squamous NSCLC (NExUS, NCT00449033) was stopped early as it failed to meet its primary endpoint of improving OS. Sorafenib has also been studied as second-line therapy in combination with pemetrexed compared to pemetrexed alone. No difference in median PFS (3.4 vs. 4.1 months; P = 0.22) and OS (9.4 vs. 9.7 months; P = 0.49) was reported in this phase II trial enrolling non-squamous NSCLC patients [70]. The combination of sorafenib with erlotinib has also been evaluated in multiple phase II trials either in pretreated or chemotherapy-naïve patients [71-74].

Similarly to sorafenib, the multi-kinase inhibitor sunitinib (SU11248, Sutent®, Pfizer; New London, CT, USA) has been tested in a number of settings and combinations in advanced and metastatic NSCLC [75-77]. To date, the inhibition of both the EGFR and angiogenesis pathways using the combination of sorafenib/sunitinib plus erlotinib did not appear to improve the outcome in unselected NSCLC patients, despite single agent studies suggest that either sorafenib or sunitinib are active in NSCLC patients. The identification of predictive biomarkers of response is needed to improve driven treatment selection for advanced NSCLCs. Up to now the available data on both sorafenib and sunitinib do not support their use outside the setting of clinical trials.

EML4-ALK FUSION GENE

The EML4-ALK fusion translocation oncogene is a rare abnormality which has been detected in 6% of patients with NSCLC, and might constitutively switch the growth signal on the RAS/RAF pathway [78, 79]. EML4-ALK fusion, is generally associated with wild-type EGFR and KRAS, and correlates with EGFR-TKIs resistance, while the response to standard chemotherapy does not seem to be affected by the presence of this aberration [79]. The extraordinary response seen in ALK-positive NSCLC patients accelerated the FDA approval of the potent ALK/c-MET inhibitor crizotinib. In a phase I dose escalation study overall response

rate among ALK-positive patients was 61%, with 10 months median survival [80]. The promising results obtained with crizotinib prompted the start of both a phase II trial in patients who relapsed after first-line chemotherapy and a phase III randomized trial of the drug compared to second-line therapy. To date, a 54% RR with a 91% disease control rate [partial response + stable disease] has been reported in the phase II study [81]. Recently, another phase III trial comparing crizotinib with first-line standard chemotherapy has also been launched.

THE EMERGING MOLECULAR TARGET c-MET

The hepatocyte growth factor receptor c-MET triggers key intracellular signal cascades involved in cell proliferation and angiogenesis, epithelial-mesenchymal transition, cell invasion and metastasis. Similarly to EGFR, c-MET overexpression, gene amplification, or mutation has been shown to have an important role in lung cancer [82]. Importantly, c-MET amplification has been especially observed in lung cancer patients who developed resistance to the first-line treatment with gefitinib or erlotinib [83, 84]. As a result, new targeted drugs against c-MET or its ligand are now in the clinic, also in combination with EGFR inhibitors, and have shown promising results.

OUTLINE OF THIS THESIS

The prognosis of NSCLC remains poor, mainly due to advanced stage of the disease at the time of diagnosis. The standard platinum-based doublet therapy leads to modest increased survival. The introduction of targeted agents in this disease has started improving the outcome of selected patients. Particularly, never-smokers, Asians, females and patients bearing adenocarcinoma were initially recognized as subgroups most likely to benefit from EGFR-TKIs. The correlation with clinical response after EGFR-TKI treatment was improved with the discovery of EGFR specific mutations. The correlations between different treatments and clinical outcomes in NSCLC patients were discussed in this thesis, with a particular focus on the role of EGFR in the response to TKIs. Furthermore, the effects of combinations with known targeted drugs and the activity of novel EGFR-TKIs in NSCLC preclinical models were investigated with the aim to improve the current therapeutic setting for selected NSCLCs.

In CHAPTER 1, a general introduction about lung cancer treatment approaches is given. This chapter focuses on the role of EGFR expression and mutations in the response to tyrosin kinase inhibitors, together with insights into current targeted therapies approved or in development for the treatment of advanced NSCLC.

In CHAPTER 2 the folate-dependent enzyme thymidylate synthase is presented as target for the treatment of several tumor types. Preclinical and clinical testing of several TS inhibitors are discussed with particular attention on pemetrexed which emerged for its approval and widespread use as first-/second-line and maintenance in the treatment of NSCLC.

In CHAPTER 3 the development and approval of the EGFR-TKIs gefitinib and erlotinib for the treatment of advanced NSCLC are illustrated. The results from the clinical studies and the mechanisms of primary and secondary resistance to these drugs are described. Furthermore, this chapter analyzes the current status and evolving role of inhibiting EGFR through the development of novel TKIs able to overcome the principal acquired resistance mechanism to gefitinib and erlotinib.

A focus on the correlation between different clinical and biological parameters and the clinical activity of gefitinib and erlotinib is shown in CHAPTER 4. In particular, germline polymorphisms of EGFR, ABCG2 and other molecules which have been related to EGFR-TKIs response are described and novel approaches that could potentially change the pharmacogenomic approach to future perzonalized treatment are discussed.

In addition to genetic aberrations, it has been demonstrated that drug resistance can emerge also from epigenetic changes, including regulation of different signaling pathways by microRNAs which act as key post-transcriptional regulators of gene expression. CHAPTER 5 highlights several recent and clinically relevant aspects of regulation of drug resistance by microRNAs from the perspective of current anti-EGFR-targeted therapies in NSCLC.

The development of innovative EGFR-TKIs able to overcome the resistance to gefitinib and erlotinib conferred by a secondary mutation of the receptor is described in CHAPTER 6. The synthesis, stability and in vitro activity on EGFR are illustrated. Furthermore, other molecular mechanisms of action of these new compounds are highlighted in CHAPTER 7, with particular focus on the effects related with the epithelial to mesenchymal transition and cancer stem like cells transformation.

Many efforts are ongoing trying to identify new biomarkers for response to EGFR-TKIs and much information has been gathered on the EGFR pathway. Combination of drugs with different targets is a logical approach to overcome multilevel cross-stimulation among key pathways in NSCLC progression. CHAPTER 8 highlights the mechanisms underlying the synergism of sorafenib-erlotinib combination, which already showed clinical activity and acceptable safety, in NSCLC cell lines selected for their heterogeneous pattern of EGFR and Raf-kinase-inhibitor protein expression, and EGFR/K-Ras mutations.

Even though a large number of trials firmly established the predictive role of EGFR mutations as biomarkers of response to gefitinib or erlotinib, a small group of wild-type EGFR NSCLC patients also significantly benefits from the treatment with the EGFR-TKIs. These findings suggest the existence of additional mechanisms involved in sensitivity or resistance to these agents in EGFR mutation-negative patients. In CHAPTER 9 gefitinib metabolism by CYP1A1 is described as early assessment of responsiveness to the drug in NSCLC cells lacking activating mutations. In metabolizing cells, the role of this enzyme as potential target to increase gefitinib potency is discussed. Furthermore, the increased surface expression of EGFR and/or HER2 in wild-type EGFR-TKI sensitive NSCLC cell lines by erlotinib which leads to increased susceptibility to ADCC is illustrated in CHAPTER 10. In this chapter the combination of erlotinib with monoclonal antibodies is presented as a potential strategy to improve the treatment of EGFR mutation-negative NSCLC patients sensitive to erlotinib.

Finally, in CHAPTER 11 the findings of all the investigations, as well as future perspectives in these areas are summarized and discussed.

REFERENCES

1. Siegel R, et al. Cancer Statistics 2012. CA Cancer J Clin 2012; (62): 10- 29.
2. Hecht SS. Lung carcinogenesis by tobacco smoke. Int J Cancer 2012; 131(12):2724-32.
3. Gorlova OY, et al. Aggregation of cancer among relatives of never-smoking lung cancer patients. Int J Cancer 2007; 121(1): 111-8.
4. Tirmarche M, et al. Risk of lung cancer from radon exposure: contribution of recently published studies of uranium miners. Ann ICRP 2012; 41(3-4):368-77.
5. Wei S, et al. Genome-wide gene-environment interaction analysis for asbestos exposure in lung cancer susceptibility. Carcinogenesis. 2012; 33(8):1531-7.
6. Vallières E, et al. The IASLC Lung Cancer Staging Project: proposals regarding the relevance of TNM in the pathologic staging of small cell lung cancer in the forthcoming (seventh) edition of the TNM classification for lung cancer. J Thorac Oncol 2009; 4(9):1049-59.
7. Mountain CF, Dresler CM. Regional lymph node classification for lung cancer staging. Chest 1997; 111: 1718-23.
8. Goldstraw P. The 7th Edition of TNM in Lung Cancer: what now? J Thorac Oncol 2009; 4: 671-3.
9. Chen F, et al. Time trend and geographic patterns of lung adenocarcinoma in the United States, 1973-2002. Cancer Epidemiol Biomarkers Prev 2007; 16(12): 2724-9.
10. Fibla JJ, et al. Validation of the lung cancer staging system revisions using a large prospective clinical trial database (ACOSOG Z0030). Eur J Cardiothorac Surg. 2012 [Epub ahead of print].
11. Murray N, Turrisi AT. A review of first-line treatment for small-cell lung cancer. J Thorac Oncol 2006; 1(3): 270-8.
12. Azzoli CG, et al. 2011 Focused Update of 2009 American Society of Clinical Oncology Clinical Practice Guideline Update on Chemotherapy for Stage IV Non-Small-Cell Lung Cancer. J Clin Oncol 2011; 29(28):3825-31.
13. Kim AW, et al. Neoadjuvant chemoradiation for clinically advanced non-small cell lung cancer: an analysis of 233 patients. Ann Thorac Surg 2011; 92(1):233-41.
14. Douillard JY, et al. Adjuvant vinorelbine plus cisplatin versus observation in patients with completely resected stage IB-IIIA non-small-cell lung cancer (Adjuvant Navelbine International Trialist Association [ANITA]): a randomised controlled trial. Lancet Oncol 2006; 7(9): 719-27.
15. Le Chevalier T, et al. Cisplatin-based adjuvant chemotherapy in patients with completely resected non-small-cell lung cancer. N Engl J Med 2004; 350(4): 351-60.
16. Tsuruo T. Molecular cancer therapeutics: recent progress and targets in drug resistance. Int Med 2003; 42(3): 237-43.
17. Herbst RS, et al. Lung cancer. N Engl J Med 2008; 359(13): 1367-80.
18. Hoang T, Schiller JH. Advanced NSCLC: from cytotoxic systemic chemotherapy to molecularly targeted therapy. Exp Rev Anticanc 2002; 2(4): 393-401.
19. Gutierrez ME, et al. Next generation oncology drug development: opportunities and challenges. Nat Rev Clin Oncol 2009;6:259-65.
20. Sharma SV, et al. Cell line-based platforms to evaluate the therapeutic efi cacy of candidate anticancer agents. Nat Rev Cancer 2010; 10:241–253.
21. Pirker R, et al. Cetuximab plus chemotherapy in patients with advanced non-small-cell lung cancer (FLEX): an open-label randomised phase III trial. Lancet 2009; 373:1525-31
22. Cunningham D, et al. Cetuximab monotherapy and cetuximab plus irinotecan in irinotecan-refractory metastatic colorectal cancer. N Engl J Med 2004; 351(4): 337-45.
23. Ku GY, et al. Gefitinib vs. chemotherapy as first-line therapy in advanced non-small cell lung cancer: meta-analysis of phase III trials. Lung Cancer 2011; 74(3):469-73.
24. Reck M, et al. Reviewing the safety of erlotinib in non-small cell lung cancer. Exp Opin Drug Saf 2011; 10:147-57.
25. Reck M, et al. Phase III trial of cisplatin plus gemcitabine with either placebo or bevacizumab as first-line therapy for nonsquamous non-small-cell lung cancer: AVAil. J Clin Oncol 2009; 27:1227-34.
26. Gandhi L, Jänne PA. Crizotinib for ALK-rearranged non-small cell lung cancer: a new targeted therapy for a new target. Clin Cancer Res. 2012; 18(14):3737-42.
27. Ramalingam SS, et al. Carboplatin and Paclitaxel in combination with either vorinostat or placebo for first-line therapy of advanced non-small-cell lung cancer. J Clin Oncol. 2010; 28(1):56-62.
28. Paz-Ares LG, et al. Phase III, randomized, double-blind, placebo-controlled trial of gemcitabine/cisplatin alone or with sorafenib for the first-line treatment of advanced, nonsquamous non-small-cell lung cancer. J Clin Oncol. 2012; 30(25):3084-92.
29. Johnson FM, et al. Phase II study of dasatinib in patients with advanced non-small-cell lung cancer. J Clin Oncol 2010; 28(30):4609-15.

30. Langer CJ, et al. Targeted agents in the third-/fourth-line treatment of patients with advanced (stage III/IV) non-small cell lung cancer (NSCLC). Cancer Treat Rev. 2012 [Epub ahead of print].

31. Zhang H, et al. ErbB receptors: from oncogenes to targeted cancer therapies. J Clin Invest 2007; 117(8): 2051–2058.

32. Franklin WA, et al. Epidermal growth factor receptor family in lung cancer and premalignancy. Semin Oncol 2002; 29(1): 3-14.

33. Giaccone G. Epidermal growth factor receptor inhibitors in the treatment of non-small-cell lung cancer. J Clin Oncol 2005; 23(14): 3235-42.

34. Fukuoka M, et al. Multi-institutional randomized phase II trial of gefitinib for previously treated patients with advanced non-small-cell lung cancer (The IDEAL 1 Trial) [corrected]. J Clin Oncol 2003; 21(12): 2237-46.

35. Kris MG, et al. Efficacy of gefitinib, an inhibitor of the epidermal growth factor receptor tyrosine kinase, in symptomatic patients with non-small cell lung cancer - A randomized trial. JAMA 2003; 290(16): 2149-58.

36. Shepherd FA, et al. Erlotinib in previously treated non- small-cell lung cancer. N Engl J Med 2005; 353(2): 123-32.

37. Thatcher N, et al. Gefitinib plus best supportive care in previously treated patients with refractory advanced non small- cell lung cancer: results from a randomised, placebocontrolled, multicentre study (Iressa Survival Evaluation in Lung Cancer). Lancet 2005; 366(9496): 1527-37.

38. Shepherd FA, et al. Erlotinib in previously treated non-small-cell lung cancer. N Engl J Med 2005; 353(2): 123-32.

39. Cappuzzo F, et al. Erlotinib as maintenance treatment in advanced non-small-cell lung cancer: a multicentre, randomised, placebo-controlled phase 3 study. Lancet Oncol 2010; 11(6): 521-9.

40. Lynch TJ, et al. Activating mutations in the epidermal growth factor receptor underlying responsiveness of non-small-cell lung cancer to gefitinib. N Engl J Med 2004; 350(21): 2129-39.

41. Paez JG, et al. EGFR mutations in lung cancer: correlation with clinical response to gefitinib therapy. Science 2004; 304(5676): 1497-500.

42. Wellcome trust sanger institute: Catalogue of somatic mutations in cancer. Available on: http: //www.sanger.ac.uk/perl/genetics/CGP/cosmic?action=gene&ln=EGFR

43. De Pas T, et al. Activity of epidermal growth factor receptor- tyrosine kinase inhibitors in patients with non-small cell lung cancer harboring rare epidermal growth factor receptor mutations. J Thorac Oncol 2011; 6(11): 1895-901.

44. Sordella R, et al. Gefitinib-sensitizing EGFR mutations in lung cancer activate anti-apoptotic pathways. Science 2004; 305(5687): 1163-7.

45. Tracy S, et al. Gefitinib induces apoptosis in the EGFR (L858R) non small-cell lung cancer cell line H3255. Cancer Res 2004; 64(20): 7241-4.

46. Ji HB, et al. The impact of human EGFR kinase domain mutations on lung tumorigenesis and in vivo sensitivity to EGFR-targeted therapies. Cancer Cell 2006; 9(6): 485-95.

47. Politi K, et al. Lung adenocarcinomas induced in mice by mutant EGF receptors found in human lung cancers respond to a tyrosine kinase inhibitor or to down-regulation of the receptors. Genes & Development 2006; 20(11): 1496-510.

48. Mitsudomi T, et al. Mutations of the epidermal growth factor receptor gene predict prolonged survival after gefitinib treatment in patients with non-small-cell lung cancer with postoperative recurrence. J Clin Oncol 2005; 23(11): 2513-20.

49. Pao W, et al. EGF receptor gene mutations are common in lung cancers from “never smokers” and are associated with sensitivity of tumors to gefitinib and erlotinib. P Natl Acad Sci USA 2004; 101(36): 13306-11.

50. Riely GJ, et al. Clinical course of patients with non-small cell lung cancer and epidermal growth factor receptor exon 19 and exon 21 mutations treated with gefitinib or erlotinib. Clin Cancer Res 2006; 12(3): 839-44.

51. Pao W, Miller VA. Epidermal growth factor receptor mutations, small-molecule kinase inhibitors, and non-small-cell lung cancer: current knowledge and future directions. J Clin Oncol 2005; 23(11): 2556-68.

52. Pao W, et al. Acquired resistance of lung adenocarcinomas to gefitinib or erlotinib is associated with a second mutation in the EGFR kinase domain. Plos Med 2005; 2(3): 225-35.

53. Kobayashi S, et al. A phase II trial of erlotinib in patients with EGFR wild-type advanced non-small-cell lung cancer. Cancer Chemother Pharmacol 2012; 69(5): 1241-6.

54. Hirsch FR, et al. Predictive value of EGFR and HER2 overexpression in advanced non-small-cell lung cancer. Oncogene 2009; 28 Suppl 1: S32-7.

55. Hirsch FR, et al. Fluorescence in situ hybridization subgroup analysis of TRIBUTE, a phase III trial of erlotinib plus carboplatin and paclitaxel in non-small cell lung cancer. Clin Cancer Res 2008; 14(19): 6317-23.

56. Tsao MS, et al. Molecular analysis of the epidermal growth factor receptor (EGFR) gene and protein expression in patients treated with erlotinib in National Cancer Institute of Canada Clinical Trials Group (NCIC CTG) trial BR.21. J Clin Oncol 2005; 23(16): 622S.

57. Bell DW, et al. Epidermal growth factor receptor mutations and gene amplification in non-small-cell lung cancer: Molecular analysis

of the IDEAL/INTACT gefitinib trials. J Clin Oncol 2005; 23(31): 8081-92.

58. Dziadziuszko R, et al. EGFR mRNA expression detected by RT-PCR predicts sensitivity to gefitinib in advanced non-small cell lung cancer (NSCLC) patients. Clin Cancer Res 2005; 11(24): 9028S-9S.
59. Crinò L, et al. Gefitinib versus vinorelbine in chemotherapy-naive elderly patients with advanced non small-cell lung cancer (INVITE): a randomized, phase II study. J Clin Oncol 2008; 26(26): 4253-60.
60. Hirsch FR, et al. Molecular predictors of outcome with gefitinib in a phase III placebo-controlled study in advanced non-small-cell lung cancer. J Clin Oncol 2006; 24(31): 5034-42.
61. Metzker ML. Sequencing technologies - the next generation. Nat Rev Genet 2010; 11(1):31-46.
62. Wu X, et al. Genome-wide association study of survival in non-small cell lung cancer patients receiving platinum-based chemotherapy. J Natl Cancer I 2011; 103(10):817-25.
63. Murray S, et al. Molecular predictors of response to tyrosine kinase inhibitors in patients with Non-Small-Cell Lung Cancer. J Exp Clin Cancer Res. 2012; 31(1):77.
64. Ferrara N. Vascular endothelial growth factor: basic science and clinical progress. Endocr Rev. 2004; 25(4):581-611.
65. Sandler, A. et al. Paclitaxel-carboplatin alone or with bevacizumab for non-small-cell lung cancer. N. Engl. J. Med 2006; 355, 2542–2550.
66. Soria JC, et al. Systematic review and meta-analysis of randomised, phase II/III trials adding bevacizumab to platinum-based chemotherapy as first-line treatment in patients with advanced non-small-cell lung cancer. Ann Oncol 2012 [Epub ahead of print].
67. S.M. Wilhelm, et al. BAY 43-9006 exhibits broad spectrum oral antitumor activity and targets the RAF/MEK/ERK pathway and receptor tyrosine kinases involved in tumor progression and angiogenesis Cancer Res 2004; 64:7099–7109.
68. G.R. Blumenschein, et al. Phase II, Multicenter, uncontrolled trial of single-agent sorafenib in patients with relapsed or refractory, advanced non small-cell lung cancer J Clin Oncol 2009; 27:4274–4280.
69. G. Scagliotti, et al. Phase III study of carboplatin and paclitaxel alone or with sorafenib in advanced non-small-cell lung cancer J Clin Oncol 2010; 28:1835–1842.
70. J.R. Molina, et al. A randomized phase II study of pemetrexed (PEM) with or without sorafenib (S) as second-line therapy in advanced non-small cell lung cancer (NSCLC) of nonsquamous histology: NCCTG N0626 study. J Clin Oncol 2011; 29 [Abstract 7513].
71. B. Cho, et al. A multicenter phase II study of sorafenib in combination with erlotinib in patients with advanced non-small cell lung cancer (NSCLC). J Clin Oncol 2010; 28:7547.
72. D.R. Spigel, et al. Randomized, double-blind, placebo-controlled, phase II trial of sorafenib and erlotinib or erlotinib alone in previously treated advanced non-small-cell lung cancer. J Clin Oncol 2011; 29:2582–2589.
73. J.S.W Lind, et al. A multicenter phase II study of erlotinib and sorafenib in chemotherapy-naive patients with advanced non-small cell lung cancer. Clin Cancer Res 2010, 16:3078–3087.
74. C. Gridelli, et al. Sorafenib in combination with erlotinib or with gemcitabine in elderly patients with advanced non-small-cell lung cancer: a randomized phase II study. Ann Oncol 2010; 21:417P
75. S. Novello, et al. Phase II study of continuous daily sunitinib dosing in patients with previously treated advanced non-small cell lung cancer. Brit J Cancer 2009; 101:1543–1548.
76. M.A Socinski, et al. Safety and efficacy of combining sunitinib with bevacizumab + paclitaxel/carboplatin in non-small cell lung cancer. J Thorac Oncol 2010; 5:354–360.
77. G.V. Scagliotti, et al. Sunitinib (SU) in combination with erlotinib (E) for the treatment of advanced/metastatic nonsmall cell lung cancer (NSCLC): a phase III study. Ann Oncol 2010; 21:LBA6.
78. Soda, M. et al. Identification of the transforming EML4-ALK fusion gene in non-small-cell lung cancer. Nature 2007; 448: 561–566.
79. Wong, D. W. et al. The EML4-ALK fusion gene is involved in various histologic types of lung cancers from nonsmokers with wild-type EGFR and KRAS. Cancer 2009; 115:1723–1733.
80. Camidge DR, et al. Progression-free survival (PFS) from a phase I study of crizotinib (PF-02341066) in patients with ALK-positive non-small cell lung cancer. J Clin Oncol 2011; 29 (suppl; abstr 2501).
81. Crinó L, et al. Initial phase II results with crizotinib in advanced ALK-positive nonsmall cell lung cancer (NSCLC): PROFILE 1005. J Clin Oncol 2011; 29 (suppl; abstr 7514).
82. Herbst, R. S., et al. Lung cancer. N. Engl. J. Med 2008; 359:1367–1380
83. Cappuzzo, F. et al. Increased MET gene copy number negatively affects survival of surgically resected non-small-cell lung cancer patients. J. Clin. Oncol 2009; 27:1667–1674.
84. Bean, J. et al. MET amplification occurs with or without T790M mutations in EGFR mutant lung tumors with acquired resistance to gefitinib or erlotinib. Proc Natl Acad Sci USA 2007; 104, 20932–20937.

Chapter 2

Thymidylate synthase inhibitors for non-small cell lung cancer

Galvani E, Peters GJ & Giovannetti E.

EXPERT OPINION ON INVESTIGATIONAL DRUGS 2011

20:1343-56.

ABSTRACT

Introduction: The folate-dependent enzyme thymidylate synthase (TS) plays a pivotal role in DNA replication/repair and cancer cell proliferation, and represents a valid target for the treatment of several tumor types, including NSCLC. NSCLC is the leading cause of cancer-related mortality, and several TS inhibitors have gone into preclinical and clinical testing, with pemetrexed emerging for its approval and widespread use as first-/second-line and maintenance therapy for this disease.

Areas covered: This review summarizes the therapeutic options in NSCLC, as well as the background and rationale for targeting TS. The authors also review recent pharmacogenetic studies and data from clinical trials evaluating novel TS inhibitors, hoping that the reader will gain a comprehensive overview of the field of TS inhibition, specifically relating to drugs used or being developed for lung cancer patients.

Expert opinion: TS is a validated target in NSCLC. However, benefits from conventional chemotherapy in NSCLC have plateaued, and more costeffective results should be obtained with individualized treatment. Accordingly, the clinical success for TS inhibitors may depend on our ability to correctly administer these agents following biomarker-driven patient selection, including TS genotype and expression, and using the right combination therapy.

1.INTRODUCTION

There are few drug targets in oncology that are as old but still so widely used as chemotherapeutic targets such as thymidylate synthase (TS). For the last 5 decades, the TS inhibitor 5-fluorouracil (5-FU) has remained the treatment of choice in both the adjuvant and the palliative setting of colorectal cancer therapy, and in recent years, combinations of both 5-FU and its oral prodrug capecitabine with irinotecan, oxaliplatin and the novel biological agents bevacizumab and cetuximab have increased responses in first-line therapy of metastatic colorectal cancer patients up to 40% [1].

However, TS inhibitors have shown an effective antitumor activity also in other tumor types, and the approval of pemetrexed in combination with cisplatin for the upfront treatment of advanced non-squamous NSCLC, as well as the recent positive results of a Phase III trial comparing oral S-1 plus carboplatin with paclitaxel plus carboplatin in chemotherapy-naive patients with advanced NSCLC, highlighted their pivotal role for the treatment of lung cancer [2,3].

These drugs belong to the same class of agents and seemto have similar mechanisms of action, but differ in the potency of target inhibition, aswell as in their clinical activity, toxicity, dosing schedules and pharmacology [4]. Several studies focussed on the clinical trials and molecular determinants of TS inhibitors, and in this review we highlight the aspects that are more important for their activity inNSCLC.Other issues are the identification of new pharmacodynamics and pharmacogenetic biomarkers which would help in the selection of the optimal dose, and the development of molecular biology technologies to decipher markers of chemosensitivity and/or resistance, which might be applied to the patient before and during treatment, in order to tailor TS inhibitors-based chemotherapy to individual patients.

2.THERAPEUTIC OPTIONS IN NON-SMALL CELL LUNG CANCER (NSCLC)

Lung cancer represents the leading cause of cancer mortality worldwide. The Surveillance, Epidemiology and End Results assessed the 5-year survival rate at 15% in the US and 10% in Europe across all stages of disease, with < 7% of patients alive 10 years after diagnosis. For modern oncology, modifying the outcome of lung cancer in terms of disease-free survival and overall survival (OS) is still a major challenge [5].

The diagnosis of early stage (I-II) NSCLCs leads to surgery, which is the only curative treatment. Radiotherapy is an option for those patients who are not candidates for lobectomy because of severe medical co-morbidities [6]. Moreover, in the last 10 years, different clinical trials demonstrated that cisplatin-based doublet treatment after complete resection improves disease-free survival and 5-year OS, supporting the role of adjuvant chemotherapy in early stage NSCLC after surgery [7].

Locally advanced or stage IIIA disease accounts for almost 30% of patients with NSCLC. Unfortunately, only few of these cases undergo curative resection and, given the poor survival, adjuvant chemo- and/or radiotherapy is strongly recommended [8].

However, because of the lack of symptoms in early stage, the majority of patients affected by NSCLC have locally advanced or metastatic tumor (i.e., stage IIIB or IV NSCLC) at diagnosis, and the chemotherapy armamentarium against these tumors includes various classes of therapeutic agents, as described in Figure 1. Platinum-based doublet therapy is the standard of care in patients with good performance status. In order to prove that chemotherapy leads to a modest but statistically significant improvement in survival when

compared with best supportive care only, several prospective trials and meta-analyses were required. In these trials, patients were treated with the so called old- or second-generation of chemotherapeutic drugs including cisplatin, ifosfamide, mitomycinC, vindesine and vinblastine. Each of these drugs significantly improved the response rate of the disease, and polychemotherapy demonstrated better results than single agent treatment both in terms of response and survival [9], while three-drug combinations were better than two-drugs only in terms of response [10]. Given these results, single-agent chemotherapy is now recommended only in patients with poor performance status. Moreover, because of the lower incidence of serious side effects, carboplatin has largely replaced cisplatin, but severalmeta-analyses have demonstrated higher response rates for cisplatin combinations when compared with carboplatin combinations [11].

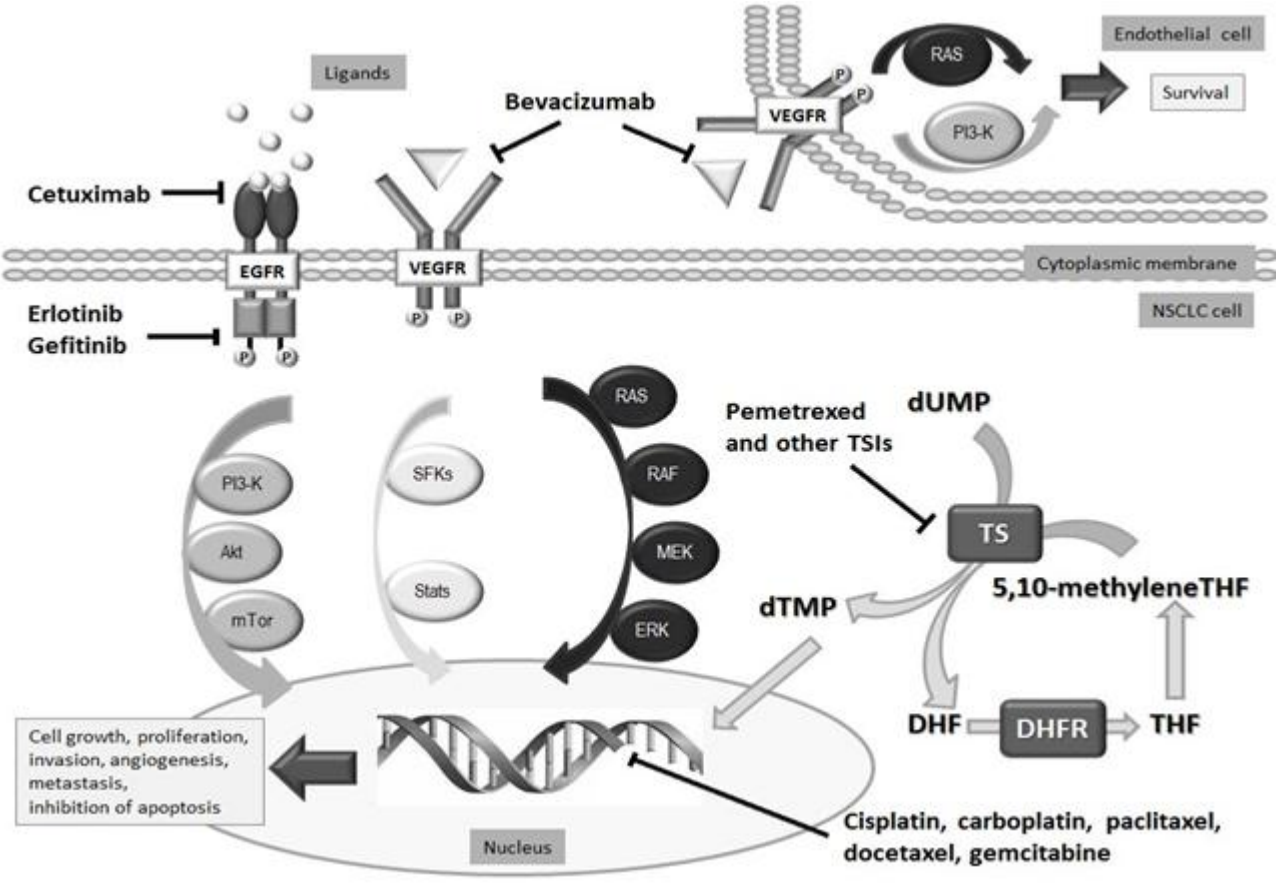

Figure 1. Therapeutic agents approved for the treatment of advanced NSCLC. DHF: Dihytrofolate; DHFR: Dihydrofolate reductase; dUMP: Deoxyuridine monophosphate; SFKs: Src family kinases; THF: Tetrahydrofolate; TS: Thymidylate syntase; dTMP: Deoxythymidine monophosphate; VEGFR: Vascular endothelial growth factor receptor.

The introduction of third-generation drugs, such as gemcitabine, taxanes, irinotecan and vinorelbine, in combination with platinum compounds, further improved chemotherapy results in advanced NSCLC. A number of recent randomized studies demonstrated that the addition of platinum to any one of the reported single agents resulted in an improved outcome compared with best supportive care [12]. However, according to results of several meta-analyses, non-platinum-based combination chemotherapy of third-generation agents can be considered as an alternative first-line treatment in those cases in which platinum therapy is contraindicated [13]. In patients bearing tumors with non-squamous histology, recently both the FDA and the

European Medicines Agency (EMEA) approved the combination of pemetrexed with cisplatin [2]. Similar approval for first-line therapy in nonsquamous NSCLC was obtained by the antiangiogenic agent bevacizumab, in combination with carboplatin-paclitaxel or any platinum-based chemotherapy despite disagreement among lung cancer specialists regarding the actual benefit [2,14].

Advances in our understanding of the molecular basis of NSCLC have enabled the development of new, rationally designed, biological agents targeting critical pathways in lung cancer cells. These biological agents interact with receptors, ligands, signaling molecules or genes that are pivotal in tumor growth and development, and have produced fruitful results [15]. Because of its overexpression in NSCLC and involvement in cell growth and proliferation, EGFR is the most commonly studied target in this disease. EGFR has been targeted either by mAbs blocking the receptor (such as cetuximab) or small molecules inhibiting the kinase domain (such as erlotinib and gefitinib). Cetuximab has been approved for first-line treatment with platinum-based chemotherapy in EGFR-protein expressing NSCLC patients with good performance status [16]. However, the OS advantage from adding cetuximab was only 1.2 months (hazard ratio (HR) = 0.871, p = 0.04), and this extra time was accompanied by a substantially higher rate of adverse reactions, raising once again questions on what counts as a benefit in cancer treatment [17].

Conversely, the results of the Phase III IPASS study, leading to the approval of gefitinib as first-line treatment of patients with activating mutations of the EGFR tyrosine kinase domain, represent a milestone toward personalized medicine in NSCLC oncology. This trial demonstrated superior progression-free survival (PFS), greater objective response rate, improved tolerability and significant quality of life benefits for gefitinib compared to carboplatin--paclitaxel doublet chemotherapy in selected first-line patients. Therefore, the FDA and EMEA approved gefitinib as first-line of treatment replacing chemotherapy in locally advanced or metastatic NSCLC patients harboring EGFR activating mutations [18].

Most current guidelines recommend a limited number of cycles (four to six) for first-line chemotherapy for advanced NSCLC [19]. However, due to the positive results of several studies that tested the prolonged duration of first-line treatment in patients without progression at the end of the planned cycles of chemotherapy, this way of treatment has recently received great attention. The second-line of treatment can be realized with chemotherapy, using one or all the drugs administered in first-line treatment or switching to a different agent, or with a targeted agent continuing the one previously administered in addition to chemotherapy (as is common practice with bevacizumab and cetuximab) or starting a new targeted agent [20].

The first drug approved for the prolonged treatment of NSCLC was docetaxel. This agent had demonstrated clinical activity in the second-line setting with response rates around 15-22%, median survival times from 5.8 to 11 months, while the estimated 1-year survival rate ranged from 25 to 40% [21].

Because of its comparable efficacy outcomes and better safety profile than docetaxel, sequential therapy with pemetrexed has also been approved to treat patients with NSCLC after receiving first-line chemotherapy treatment [22]. Similarly, the oral administration and manageable toxicity, along with its comparable efficacy, make erlotinib an important option as maintenance therapy for patients with NSCLC previously treated with first-line chemotherapy [23]. Erlotinib and gefitinib are also the only drugs of proven efficacy in the third-line setting. Several chemotherapy drugs, including pemetrexed, as well as many new biological agents, such as

cetuximab, bevacizumab, sunitinib, sorafenib, everolimus, lapatinib and bortezomib, are being investigated as maintenance therapy [24]. However, larger studies are needed to examine the effectiveness and safety of potential third-line regimens in an effort to prolong survival while maintaining quality of life of patients with advanced NSCLC.

3. ROLE OF THYMIDYLATE SYNTASE AS THERAPEUTIC TARGET

TS is a folate-dependent enzyme that catalyzes the methylation of deoxyuridine-5'-monophosphate (dUMP) using 5,10-methylene-tetrahydrofolate (5,10-CH2-THF) as the methyl donor to form deoxythymidine-5'-monophosphate (dTMP) [25]. This function maintains the dTMP pool, which is critical for DNA replication and repair, which in turn is essential for cell proliferation (Figure 2). Furthermore, TS protein and mRNA levels are elevated in several tumors, and ectopic expression of catalytically active TS is able to induce a transformed phenotype in mammalian cells as manifested by foci formation, anchorage independent growth, hyperplasia and tumor formation in nude mice [26,27]. These studies highlighted the role of TS as a transforming factor and a potential oncogene. Therefore, inhibition of TS represents an anti-metabolite approach to control tumor cell growth, and using a definition that is often overused in the last years to describe drug development, TS inhibitors can be considered one of the first 'targeted' drugs because they were specifically designed in order to interfere with a precise molecular target. However, normal proliferating tissues, such as bone marrow and gastrointestinal mucosa, are also dependent on DNA synthesis and thus sensitive to TS inhibition, leading to myelosuppression, mucositis and diarrhea.

The first fluorinated pyrimidines were synthesized by Heidelberger > 50 years ago, and fluorinated uracil was introduced into clinical use almost immediately [28]. The active metabolite of 5-FU, fluoro-dUMP, inhibits TS by the formation of a covalent ternary complex with TS and CH2-THF. This results in depletion of dTMP and thereby inhibition of DNA synthesis which can lead to thymine-less death. This phenomenon was first reported in Escherichia coli when thymine requiring mutants of the bacterium lost viability when grown nutrients, and was commonly attributed to 'unbalanced growth' wherein cells continued fundamental processes of RNA transcription, protein synthesis and metabolism in the absence of DNA replication [29]. TS inhibition also results in an increase in 2'-deoxyuridine-5'-triphosphate (dUTP), which leads to misincorporation of dUTP into DNA: its excision, catalyzed by uracil-DNA glycosylase, results in DNA damage. Moreover, a specific interaction exists between oncogenes and TS, by binding of TS protein to p53 and c-myc RNA [30,31], while wild-type p53 can also inhibit TS promoter activity [32].

At transcriptional level, TS expression is activated by the transcription factor E2F-1, which plays a key role in cell cycle progression [33]. In addition, TS protein functions as an RNA-binding protein repressing the translation of its own mRNA [34]. Specifically, the translation of human TS mRNA is negatively regulated by direct binding of TS to two different cis-acting elements in its cognate mRNA. The first element is a 30-nt sequence found within the 59-untranslated region (59-UTR) that includes the translational start site in a stable stem-loop structure [34], while the second binding site is a 70-nt sequence corresponding to the nucleotides 480 - 550 [35]. When TS inhibitors bind to TS, the complex cannot interact with its cognate mRNA, which results in increased TS protein expression, while variant RNAs with either a deletion or mutation in the core motif of TS were unable to bind to the TS protein [36]. This study, as well as other studies in cancer cells, demonstrated also that the elevated expression of TS after exposure to TS inhibitors

was in part attributable to increased protein stability [36,37]. Finally, TS expression might be affected by specific polymorphisms, gene-copy number and also microRNA (miRNA), and new molecular biology analyses to decipher these factors as possible regulators of TS as well as determinants of TS inhibitors are described in Section 5, 'Expert opinion, novel drug combinations and future perspectives'.

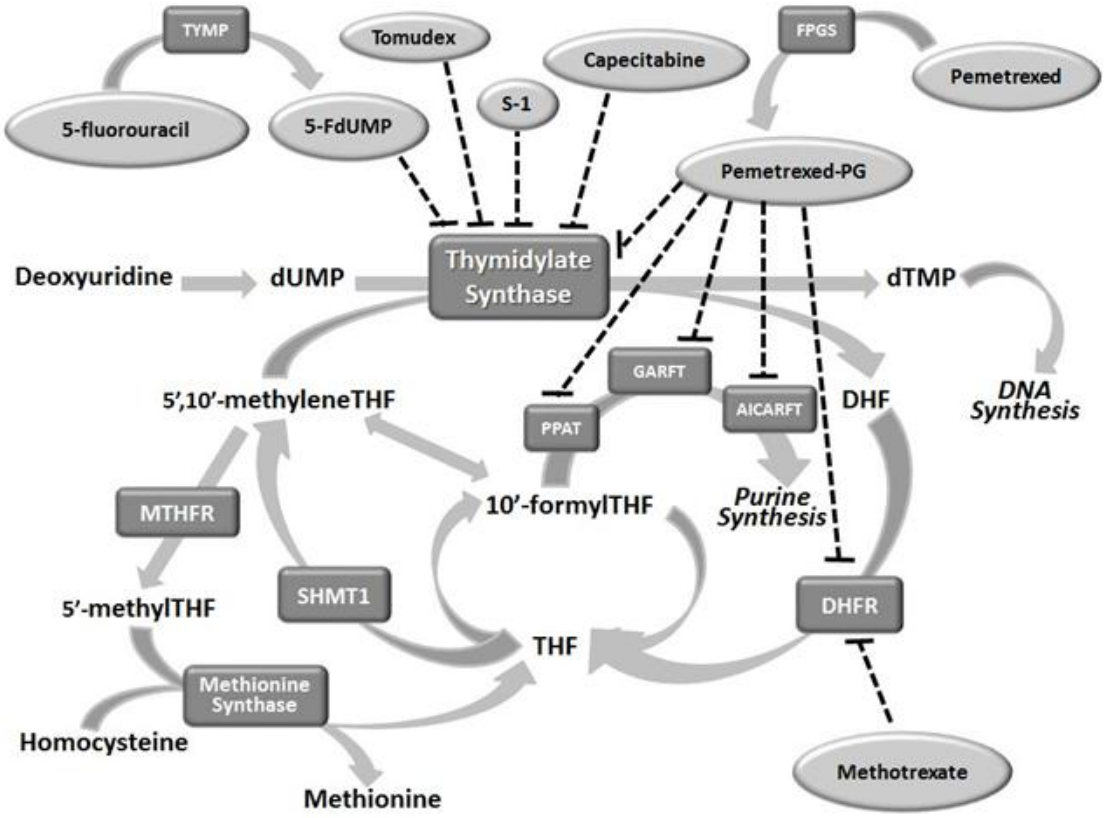

Figure 2. Pivotal role of TS in DNA synthesis, and drugs affecting TS activity and its related pathways. AICARFT: Aminoimidazole carboxamide ribonucleotide tranformylase; DHF: Dihytrofolate; DHFR: Dihydrofolate reductase; 5-FdUMP: 5-fluoro-deoxyuridine monophosphate; FPGS: Folypolyglutamate syntethase; GARFT: Glycinamide ribonucleotide formyl transferase; MTHFR: Methylene tetrahydrofolate reductase; PG: Polyglutamate; PPAT: Phosphoribosyl pyrophosphate amidotransferase; SHMT: Serine hydroxymethyltransferase; dUMP: Deoxyuridine monophosphate; THF: Tetrahydrofolate; dTMP: Deoxythymidine monophosphate; TYMP: Thymidine phosphorylase.

4. THYMIDYLATE SYNTHASE INHIBITORS IN NSCLC

4.1 Pemetrexed

We have included pemetrexed in this review because TS is its most important target [38], although it has often been referred to as a multitargeted antifolate. Moreover, pemetrexed represents the first TS inhibitor to be approved in the treatment of NSCLC and is currently in widespread use for both first-/second-line and maintenance therapy of this disease (Box 1).

The multitargeted antifolate pemetrexed was first registered by the FDA for the treatment of malignant pleural mesothelioma, based on a randomized, Phase III, single-blind, multicenter trial which compared cisplatin alone versus cisplatin plus pemetrexed. In that trial, the addition of pemetrexed to cisplatin significantly improved both the survival, by 3 months, and the overall response rate [39].

Pemetrexed demonstrated to be also active as a single agent in Phase II and III trials involving patients

with locally advanced or metastatic NSCLC previously treated with chemotherapy. On the basis of data from a randomized, Phase III trial, in August 2004, the FDA approved pemetrexed for second-line treatment of NSCLC [22]. In that trial which compared pemetrexed (500 mg/m2 every 3 weeks, with vitamin B12 and folic acid supplementation) to docetaxel (75 mg/m2 every 3 weeks; not significantly different), median survival was 8.3 versus 7.9 months, respectively. However, while response rates and time-to-progression for both agents resulted comparable, the incidence of side effects (grade 3 or 4 neutropenia, febrile neutropenia and neutropenia with infections) as well as hospitalizations for neutropenic fever and other drug-related adverse events with pemetrexed was significantly lower than with docetaxel.

Box 1. Drug summary.

Drug name	Pemetrexed
Phase	Launched
Launched indications	Malignant pleural mesothelioma First/second-line treatment and maintenanace after chemotherapy of advanced non-squamous NSCLC
Pharmacology description	Thymidylate shyntase (TS) inhibitor AICARFT inhibitor DHFR inhibitor GARFT inhibitor PPAT inhibitor
Route of administration	Infusion
Chemical structure	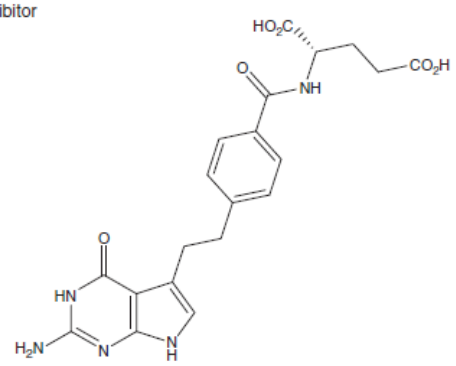
Pivotal trials	[2,22,39]

Subsequently, the combination with pemetrexed plus cisplatin was tested as first-line therapy in advanced NSCLC patients in a Phase III randomized trial in comparison to gemcitabine plus cisplatin [2]. Another trial comparing carboplatin plus pemetrexed or gemcitabine was developed with quality of life measured by European Organization for the Research and Treatment of Cancer QLQ-C30 and LC 13 questionnaires as primary end point. A total of 436 patients were randomized and no difference was observed for the primary outcome in terms of survival with the median OS of 7.3 for the pemetrexed-carboplatin arm and 7 months for the gemcitabine-carboplatin arm. Patients receiving pemetrexed-carboplatin experienced significantly less toxicity with respect to leucopenia, neutropenia and thrombocytopenia [40]. However, a previous randomized, non-inferiority, Phase III trial enrolling 1725 chemotherapy-naive patients with advanced NSCLC to receive either cisplatin 75 mg/m^2 on day 1 plus gemcitabine 1250 mg/m^2 on days 1 and 8 or cisplatin at the same dose plus pemetrexed 500 mg/m^2 on day 1, every 3 weeks for a maximum of six cycles, showed that cisplatin-pemetrexed provided similar efficacy with better tolerability and more convenient administration than cisplatin-gemcitabine [2]. The comparison of the OS between the two regimens was the primary objective of that trial which resulted in 10.3 months OS in

both arms (HR = 0.94; 95%CI, 0.84 - 1.05). Survival rates at 12 months were 43.5 and 41.9% for cisplatin-pemetrexed and cisplatin-gemcitabine, respectively, and also PFS was non inferior (4.8 vs. 5.1 months, respectively; HR = 1.04; 95% CI, 0.94 - 1.15). Response rate reached 30.6% in the pemetrexed-cisplatin arm and 28.2% in the gemcitabine-cisplatin arm. For cisplatin-pemetrexed, the rates of grade 3 or 4 neutropenia, anemia and thrombocytopenia ($p \leq 0.001$), febrile neutropenia ($p = 0.002$) and alopecia ($p < 0.001$) were significantly lower [2].

An intriguing aspect of this study occurred in the prespecified analyses for survival with respect to histology. In patients with adenocarcinoma (n = 847; 12.6 vs 10.9 months) or large-cell carcinoma histology (n = 153; 10.4 vs 6.7 months), OS resulted statistically superior in the cisplatin-pemetrexed treatment arm. Conversely, in squamous cell histology, there was a significant longer survival with cisplatin-gemcitabine (n = 473; 9.4 vs 10.8 months). This was the first Phase III study in NSCLC prospectively showing survival differences based on histological subtype [2]. Phase II studies and the combined retrospective review of two large, randomized, Phase III trials also supported the predictive role of histology for pemetrexed [41]. Furthermore, the differential activity of pemetrexed in nonsquamous histology has been confirmed in a multi-center, double-blind Phase III trial evaluating the efficacy and safety of pemetrexed versus placebo in stage IIIB/IV NSCLC patients who did not progress after four cycles of first-line platinum-based chemotherapy [42]. A total of 663 patients were enrolled (441 in the pemetrexed and 222 in the placebo arm) and histological subtyping was as follows: adenocarcinoma, 50%; squamous-cell carcinoma, 27%; large-cell carcinoma, 3%; and not otherwise specified/indeterminate histology, 20% of cases. Pemetrexed treatment resulted in a significantly improved PFS (4.3 vs 2.6 months; HR = 0.502; 95% CI, 0.42 - 0.61; $p < 0.00001$) and tumor response ($p < 0.001$). Furthermore, pemetrexed showed a statistically significant superior activity in non-squamous (n = 482; 4.5 vs 2.6 months) than in squamous histology (n = 182; 2.8 vs 2.6 months). On the basis of the results of these studies, the EMEA and FDA approved pemetrexed for use in the first-line treatment of advanced non-squamous NSCLC.

Moreover, in July 2009, both the EMEA and FDA approved pemetrexed as maintenance therapy in patients with other than predominantly squamous cell histology in locally advanced or metastatic NSCLC whose disease has not progressed after four cycles of platinum-based chemotherapy with different agents. In particular, the PARAMOUNT trial investigated whether pemetrexed maintenance therapy after first-line platinum-based chemotherapy in patients with advanced NSCLC improved PFS [43]. This double-blind, placebo-controlled trial enrolled 939 patients treated with four cycles of pemetrexed (500 mg/m^2) and cisplatin (75 mg/m^2) on day 1 of a 21-day cycle. Of those patients, 539 (57.4%) who had not progressed during pemetrexed--cisplatin induction were randomized to maintenance pemetrexed (same dose on day 1 of a 21-day cycle) with best supportive care (359 patients) or placebo plus best supportive care (180 patients) until disease progression. The risk of disease progression resulted in a 36% reduction in the pemetrexed arm (HR = 0.64, 95% CI, 0.51 - 0.81; $p = 0.00025$) with a median of 3.9 versus 2.6 months on the placebo arm. The disease control rate with pemetrexed treatment was statistically significantly superior ($p = 0.009$) versus placebo. The drug-related serious adverse event rate obtained with pemetrexed was higher than with placebo but the study demonstrated that pemetrexed maintenance therapy following pemetrexed-cisplatin chemotherapy is an effective and well-tolerated treatment for patients with advanced

non-squamous NSCLC.

4.1.1 Studies on TS expression and other molecular determinants of pemetrexed activity

One potential explanation of the different results obtained with pemetrexed treatment in various histological subtypes of NSCLC might relate to the differential TS expression in those tumors. Indeed, the baseline expression of the TS gene and protein were significantly higher in NSCLC tissues from chemotherapy-naive patients affected by squamous cell carcinoma compared with patients affected by adenocarcinoma ($p < 0.0001$) [44].

Pemetrexed is a multitargeted agent that enters the cell via the reduced folate carrier (RFC) and is converted by folypolyglutamate syntethase (FPGS) to a series of active polyglutamate derivatives able to inhibit several folate-dependent enzymes such as TS, dihydrofolate reductase (DHFR), glycinamide ribonucleotide formyl transferase (GARFT) and, to a lesser extent, aminoimidazole carboxamide ribonucleotide tranformylase and CI-tetrahydrofolate synthase [45]. This mechanism of action leads to depletion of fully reduced folates and results in disruption of nucleotide synthesis for both purines and pyrimidines. These metabolites retained intracellularly longer than the parent compound, resulting in more prolonged cytotoxic effects.

While GARFT is inhibited just weakly by pemetrexed, TS represents the main target of this drug and its inhibition leads to the interruption of tetrahydrofolate oxidation with consequential lack of DHFR activity [38]. However, GARFT inhibition may become important in case of TS overexpression or mutation, and the multitargeted effects of pemetrexed explains its broader spectrumof cytotoxic activity when compared in preclinical studies with other antimetabolites such as 5-FU, and antifolates such as methotrexate (MTX) or raltitrexed [46,47].

Preclinical data showed a significant correlation between overexpression of TS mRNA or protein with reduced sensitivity to pemetrexed in NSCLC cell lines [48,49], and a recent study investigating the effect of TS overexpression on pemetrexed sensitivity reported that the chemosensitivity of NSCLC cells overexpressing TS was markedly reduced compared with that of control cells. The inhibition of DNA synthesis and induction of apoptotic cell death by pemetrexed were also significantly reduced by overexpression of TS [50]. mRNA expression of genes involved in the mechanism of action of pemetrexed was correlated with in vitro sensitivity of 61 freshly explanted human tumor specimens, and low gene expression levels of TS, as well as of GARFT and DHFR, significantly correlated with chemosensitivity to pemetrexed [51]. Moreover, xenografts obtained with TS-overexpressing cells were more resistant to the growth-inhibitory effect of pemetrexed [50].

Simple logistic regression suggested a potential relationship between mRNA expression of TS and pemetrexed response in a study performed in specimens from patients enrolled within a Phase II trial of pemetrexed in advanced breast cancer. On the basis of threshold analysis, patients with ‘low’ baseline TS were more likely to respond to pemetrexed than patients with ‘high’ baseline TS [52]. Two recent studies on mesothelioma samples reported that both TS protein and mRNA expression significantly correlated with survival and response rates in patients treated with pemetrexed-based regimens [53,54]. Similarly, the immunohistochemical analysis of TS expression in 24 NSCLC specimens from pemetrexed non-responding patients was significantly higher than that in those of responders [50]. In another study, the analysis of 49

tumor specimens available from advanced NSCLC patients treated with pemetrexed showed that low TS expression was correlated with longer median PFS (4.8 vs 3.4 months; p = 0.01). In patients with adenocarcinoma, the low TS patient group had a longer median survival as compared with patients with high TS expression [55]. More recently, an immunohistochemical study on 285 patients with non-squamous NSCLC treated with pemetrexed-based chemotherapy also showed that low TS protein expression was significantly associated with better clinical outcomes [56].

However, the potential prognostic role of TS has not been clarified. Several studies suggested that TS levels may be associated with stage of disease, lymph node metastasis, tumor differentiation, prognosis and tumor cell proliferation, but many results were controversial [57-59]. A recent analysis of cytoplasmic tumoral TS by automated in situ protein quantification, demonstrating improved survival for NSCLC patients with high TS protein expression [59], appears to contrast a report of improved survival for patients with low tumoral TS expression in colorectal cancer, as detected by immunohistochemistry [60]. However, standard immunohistochemistry with visual scoring in an attempt to quantify protein expression has significant technical limitations, including the non-quantitative chemistry of routine immunoperoxidase stains and the subjective light intensity perception of the human eye [60]. Moreover, it is noteworthy that confocal analyses in lung and colon cancer cell lines indicate that TS is expressed mostly cytoplasmic in lung and nuclear in colon cancers, respectively [59].

Additional studies with consistent methodology and broader validation cohorts are needed to define the precise value of TS. In order to obtain a prospective validation of the role of TS for pemetrexed-based chemotherapy in the adjuvant setting, a Phase III multi-center, randomized study named ITACA (International TAilored Chemotherapy Adjuvant) is ongoing in Europe. In all registered patients, before randomization, expression of ERCC1 and TS is assessed by PCR on paraffin-embedded tumor specimens in a central laboratory. Within 45 days post-surgery, patients in each genetic profile are randomized to receive either a standard chemotherapy selected by the investigator (cisplatin-vinorelbine, cisplatin-docetaxel or cisplatin-gemcitabine) or an experimental treatment (tailored arms) selected as follows: i) high ERCC1 and high TS, four cycles of single agent paclitaxel; ii) high ERCC1 and low TS, four cycles of single agent pemetrexed; iii) low ERCC1 and high TS, four cycles of cisplatin-gemcitabine and iv) low ERCC1 and low TS, four cycles of cisplatin-pemetrexed. All chemotherapy regimens are administered for a total of four cycles on a 3-weekly basis. Primary end point is OS and currently 180 patients have been enrolled from24 institutions, while the expected total number of patients is 700 [61].

Although overexpression of TS is the most studied mechanism involved in resistance to pemetrexed, multiple mechanisms of antifolate resistance might also affect pemetrexed activity in vitro and in vivo. In particular, curative antifolate-based chemotherapy of various human cancers is still hampered by several acquired drug resistance phenomena including: i) impaired uptake due to loss of transporters function; ii) overexpression of ATP-driven multi-drug resistance (MDR) transporters which increases drug efflux; iii) defective antifolate polyglutamylation due to decreased FPGS expression and/or inactivating mutations; iv) increased expression of g-glutamyl hydrolase (GGH), overexpression of DHFR and mutations that decrease its affinity and v) expansion of intracellular 5,6,7,8-tetrahydrofolate (THF) cofactor pools [62].

Among the studies focusing on pemetrexed, a PCR analysis in tumor explants demonstrated that

sensitive tumors expressed statistically significantly less MDR transporter MDR associated protein (MRP)4 mRNA than resistant tumors, while there was a trend in mRNA expression of MRP5 protein to be increased in resistant tumors [51]. These data are in agreement with previous findings, showing that MRP1 through MRP5 and breast cancer resistance protein (BCRP) have the facility to transport folates and antifolates including MTX, raltitrexed and pemetrexed. Another recent study showed that gene and protein expression of ABCC11/MRP8 was higher in pemetrexed-resistant cells than in the parental cells [63]. However, there was no correlation between ABCC11 gene expression and pemetrexed sensitivity of 13 lung adenocarcinoma cells [63], and no overexpression of any of the MRPs or BCRP has been reported in most antifolate-resistant selected cell lines [64].

In contrast, in a systematic study using various polyglutamatable inhibitors of DHFR, TS and GARFT, isolating 14 antifolate-resistant human leukemia cell lines after a repeated high-dose intermittent schedule mimicking the chemotherapeutic treatment, the vast majority of these antifolate-resistant cell lines displayed a 90 - 99% loss of FPGS activity, frequently associated with the absence of any substantial decrease in FPGS mRNA levels. These cell lines displayed up to five orders of magnitude of cross-resistance to polyglutamylation-dependent antifolates including pemetrexed, while retaining sensitivity to polyglutamylation-independent antifolates [65]. However, although inactivating FPGS mutations do exist, they do not appear to be a frequent mechanism underlying loss of FPGS function [66], while multiple tumor cell lines with resistance to various polyglutamatable antifolates showed a marked suppression of FPGS activity in the absence of decreased FPGS mRNA levels [67]. These findings warrant further studies to characterize the post-transcriptional mechanisms involved in the loss of FPGS activity in antifolate-resistant tumor cells in the absence of decreased FPGS mRNA levels, such as FPGS alternative splicing, as demonstrated in leukemia cells [68].

The impact of the intracellular folate pool size on the cytotoxic activity of multiple antifolates was evaluated by other studies showing that, as the THF cofactor pool size increased, the 50% inhibitory concentrations for the polyglutamatable antifolates lometrexol, pemetrexed and raltitrexed markedly increased. This appeared to result from a significant suppression of the formation of antifolate polyglutamates and is in agreement with studies showing that loss of RFC function and folate depletion result in enhanced pemetrexed inhibition of purine synthesis [69,70]. Indeed, pemetrexed is an excellent substrate for RFC, but in a HCT-15 clone (PT1) with a glycine to arginine substitution at amino acid 401, resulting in the loss of RFC function, albeit the initial uptake of pemetrexed in PT1 cells was markedly reduced, there was increased pemetrexed inhibition of TS. This was likely due to cellular folate pool contraction resulting in partial preservation of pemetrexed polyglutamylation and increased target enzyme inhibition [71].

Of note, impaired RFC function is an important mechanism of resistance to MTX and other antifolates in vitro [72], and may be associated with clinical resistance to this agent in the treatment of acute lymphoblastic leukemia [73]. The transport for pemetrexed appears to be quite different and has been attributed, in part, also to an RFC-independent, pH-dependent pathway, which serves as an alternative transport route for this drug and it is likely mediated by the proton coupled folate transporter (PCFT) [74]. In particular, a recent study showed that PCFT increased the growth inhibitory activity of pemetrexed, illustrating its unique role in the transport and pharmacological activity of pemetrexed. Because of the ubiquitous expression of PCFT in

human tumors, and the ability of PCFT to sustain pemetrexed activity even in the absence of RFC, tumor cells are unlikely to become resistant to pemetrexed as a result of impaired transport because of the redundancy of these genetically distinct routes [75].

However, the promoter of PCFT is highly methylated [76], eventually reducing its activity in cancer cell systems. Indeed, a recent study showed that promoter silencing through methylation and gene copy loss accounted for the loss of PCFT activity in antifolate-resistant HeLa R1 - 11 cells [77], suggesting that one plausible modality to overcome antifolate-resistance in cells that are devoid of PCFT activity due to promoter methylation may be to pulse-treat cells with relatively well-tolerated demethylating agents, such as 5-Aza-dC. Therefore, data about the possible association of PCFT promoter methylation and clinical outcome in NSCLC patients treated with pemetrexed can be very useful to offer alternative therapies to resistant patients.

In conclusion, several factors might cause resistance to pemetrexed and further studies are needed to clarify other mechanisms involved in its activity. However, the established clinical safety profiles of pemetrexed make this drug an attractive agent for polychemotherapy regimens, which should overcome the tumor resistance and improve clinical outcome.

4.2 UFT and S-1

Because primary lung cancers are characterized by high expression and activity of dihydropyrimidine dehydrogenase (DPD), which is the key enzyme of 5-FU degradation, studies on the activity of oral 5-FU derivatives preventing 5-FU degradation appeared of interest for NSCLC treatment. The first oral 5-FU derivatives were tegafur [78], and 5¢-deoxy-5-fluorouridine. These drugs yielded a response rate lower than 15% [107], but other rationally engineered and metabolically-activated DPD inhibiting fluoropyrimidines (DIF), such as UFT [79], and S-1 [80] have proved to be effective in several randomized controlled studies in NSCLC patients.

The DIF UFT combines uracil, a competitive inhibitor of DPD, with the 5-FU prodrug tegafur in a 4:1 molar ratio. In Japan, UFT is approved for several tumors, including NSCLC [81], while in the UK UFT with folinic acid is approved as firstline treatment by the National Institute forHealth and Clinical Excellence for metastatic colorectal cancer.

The combination of UFT, etoposide and leucovorin resulted as active in second- or third-line therapy of Caucasian NSCLC patients [82] and because of its favorable toxicity profile warranted further investigation.

However, most recent trials focused on S-1, in which a more potent DPD inhibitor is combined. Indeed, S-1 combines the 5-FU prodrug tegafur (ftorafur, FT) with two enzyme inhibitors, CDHP (5-chloro-2,4-dihydroxypyridine) and OXO (potassium oxonate), in a molar ratio of 1 (FT):0.4 (CDHP):1(OXO). CDHP is a reversible competitive inhibitor of DPD, preventing the degradation of FT derived 5-FU. Therefore, 5-FU remains in plasma and tumor tissue longer and at higher levels than when low-dose 5-FU is continuously infused intravenously. OXO is a reversible competitive inhibitor of orotate phosphoribosyltransferase, a phosphoenzyme for 5-FU, which is distributed at high levels in the gastrointestinal tract after oral administration, resulting in a reduction in diarrhea and mucositis caused by 5-FU.

A recent Phase III trial evaluated whether treatment with carboplatin plus S-1 was non-inferior than

carboplatin plus paclitaxel with regard to OS in 564 chemotherapy-naive Japanese patients [3]. These patients were randomly assigned to receive either carboplatin (AUC, 5) on day-1 plus oral S-1 (40 mg/m^2 twice a day) on days 1 - 14 or carboplatin (AUC, 6) plus paclitaxel (200mg/m^2) on day-1 every 21 days. Although the patients treated within the carboplatin and S-1 arm had significantly more dose delays, median OS was 15.2 months in the patients given carboplatin and S-1 armand 13.3 months in the carboplatin and paclitaxel arm, with 1-year survival rates of 57.3 and 55.5%, respectively. These results demonstrated the non inferiority of carboplatin plus S-1 in comparison with carboplatin-paclitaxel combination, suggesting that it might be a valid treatment option in patients with advanced NSCLC.

Conversely, the combination of S-1 with cisplatin as first line treatment did not achieve an objective response rate over 30% during a Phase II study in caucasian patients. Therefore, while oral bioavailability and preliminary evidence of activity make this compound an appealing choice for additional investigations, further studies are needed to determine the optimal patient population or S-1 combination [83].

Preclinical studies showed a synergistic antitumor effect of S-1 with the EGFR tyrosin kinase inhibitor (TKI) gefitinib in NSCLC cell lines. In these cells, gefitinib inhibited the expression of the transcription factor E2F-1, resulting in the downregulation of TS at the mRNA and protein levels, favoring the activity of S-1 [84]. Furthermore, the combination of S-1 and gefitinib synergistically inhibited also the growth of NSCLC gefitinib-resistant NSCLC cells and xenografts with MET amplification, suggesting that the addition of S-1 to EGFR-TKIs is a promising strategy to overcome EGFR-TKI resistance in NSCLC with MET amplification [85].

However, although a recent study showed that tumor expression levels of TS and DPD were predictive of response to S-1-carboplatin chemotherapy [86], a pooled analysis of S-1 trials I NSCLC demonstrated that the activity of S-1 was independent of tumor histology [87].

4.3 Others TS inhibitors

Only a few clinical studies evaluated the activity of other TS inhibitors in NSCLC, such as the quinazoline folate analog raltitrexed, which acts as a direct and specific TS inhibitor, and the oral prodrug of 5-FU capecitabine. In particular, a Phase I, dose-escalation study evaluated the combination of raltitrexed and cisplatin in patients with previously untreated metastatic NSCLC. Of 19 patients evaluated for response, 3 achieved a partial response, 13 had stable disease and 3 progressed [88]. However, withdrawal of the sponsor's support has left raltitrexed (i.e., Tomudex®) without the level of continuing investigation afforded to pemetrexed.

Regarding capecitabine, the increase in thymidine phosphorylase (TP) expression which mediates the final step of the capecitabine activation pathway could provide a rationale for the use of this drug in NSCLC, as described in a recent case of a patient with metastatic lung adenocarcinoma with high levels of lactate dehydrogenase and carcinoembryonic antigen with a clear partial response to capecitabine after several lines of chemotherapy [89]. A previous study showed that TP expression in lung cancer cells and stroma was associated with response to capecitabine-docetaxel chemotherapy [90], and might be a useful predictor of NSCLC response to capecitabine-based chemotherapy. Interestingly, preclinical data on the bioactive anthraquinone derivatives emodin demonstrated its synergistic effects with capecitabine in NSCLC cells through upregulation of TP mRNA and protein expression in capecitabine treated NSCLC cell lines [91]. These data, as well as the high response rate observed in a Phase II trial of docetaxel plus capecitabine in

pretreated NSCLC patients [92], encourage further evaluation of capecitabine in NSCLC. However, further larger prospective trials are needed to confirm the prognostic significance of TP expression in NSCLC, as well as the possible role of capecitabine in the chemotherapy armamentarium against lung cancer.

5. EXPERT OPINION, NOVEL DRUG COMBINATIONS & FUTURE PERSPECTIVES

TS is a validated target in NSCLC, and the TS inhibitor pemetrexed emerged for its approval and widespread use for first-/second-line and maintenance therapy for this disease.

However, benefits from conventional chemotherapy in NSCLC have plateaued, while much more cost-effective results should be obtained with individualized patient treatment. Accordingly, the clinical success for TS inhibitors may ultimately be dependent on our ability to correctly administer these agents following appropriate biomarker-driven patient selection, including TS genotype and expression, and using the right combination therapy.

As reported in Section 4.1.1, 'Studies on TS expression and other molecular determinants of pemetrexed activity', the levels of TS expression have been correlated with resistance to therapy with pemetrexed, and a prospective validation of the role of TS for pemetrexed-based chemotherapy is ongoing in a Phase III randomized study [61]. However, this trial is enrolling patients in the adjuvant setting, while further prospective randomized trials, with a control and a genotypic arm, should be performed in patients affected by advanced/metastatic NSCLC.

Further studies should also evaluate the genetic and epigenetic factors involved in the regulation of TS.

Assessing germ-line genetic polymorphisms as either predictive or prognostic markers is very appealing, especially in the advanced cancer setting. In this setting, diagnosis is usually done from small needle biopsy samples and tumors are either not resected or resected after neoadjuvant therapy, so that the handling of tumormaterial can be problematic. Polymorphisms are inherited genetic variants harbored by all the cells of the body and, although a genotype represents a static value unable to change in response to a different situation, such as exposure to chemotherapy, and it may not reflect changes in tumor DNA, such as loss of heterozygosity, previous studies showed no differences in polymorphisms analyzed in tumor and normal tissues [93]. Moreover, polymorphism analysis can be easily performed in blood tissue and is easier to adopt in the routine clinical setting than tumor gene expression arrays, which need core needle biopsies of patient's tumors with immediate freezing, laser microdissection and subsequent sophisticated infrastructure.

The promoter of the human TS gene contains a 28-bp tandem repeat near the initiation codon in its 5'-UTR. This tandem repeat region functions as an enhancer element for the TS gene promoter, the TS enhancer region (TSER). TSER has been shown to be polymorphic, and several studies evaluated two known polymorphisms in this region: i) a variable number of tandem repeats of a 28 bp sequence (2R/3R) and ii) a G > C single nucleotide substitution within the repeats, altering the E-box sequence binding an upstream stimulatory factor-1 [94]. In vitro expression studies have suggested an association between the number of repeats and TS expression: the presence of a triple-repeat (3R/3R) results in a 2.6-fold greater TS expression than a double-repeat [95]. However, the relationship among these polymorphisms, regulation of TS expression and patient response to fluoropyrimidine treatment has been inconsistent, and no correlation between TS polymorphisms and survival was observed in patients enrolled in a randomized Phase II study

of pemetrexed compared with pemetrexed plus carboplatin in pretreated patients with advanced NSCLC [96]. Of note, the other pharmacogenomic analysis performed during this trial showed that patients with MTHFR C677T homozygous mutation had increased PFS compared with patients with wild-type or heterozygous mutations [96]. However, a study in 48 NSCLC subjects enrolled in a Phase II trial of pemetrexed in combination with bevacizumab for second-line therapy showed that two polymorphisms in GGH, IVS1(1307)CT and IVS5(1042)TC, one in RFC, IVS2(4935)GA, and the wild-type genotype in FPGS, 5'-UTR(-63)GA, correlated significantly with toxicity. Furthermore, a significant association was observed for the GGH polymorphism IVS1(1307)CT and median OS [97].

Conversely, negative results were reported in a study on TS gene copy number, which was increased more frequently in squamous cell carcinomas, but was not associated with prognosis [98]. Future studies should test whether TS gene copy number predicts clinical benefit from treatment with pemetrexed.

A recent study evaluated two miRNA targeting TS, miR-192 and miR-215. However, downregulation of TS by miR-192/215 did not lead to an increase in 5-FU sensitivity, suggesting that the activity of miR-192/215 was not mediated by TS. In contrast, overexpression of both miRNAs resulted in a reduction of cell proliferation and, therefore, diminished the effectiveness of S-phase-specific drugs like 5-FU, suggesting that miR-192 and miR-215 can still play a role in resistance to TS inhibitors [99]. Therefore, further studies should evaluate whether miRNA expressed in NSCLC cells might regulate resistance mechanisms towards pemetrexed, as reported for other chemotherapeutic agents [100]. Additional information will be gained with the integration of data from 'next-generation' or 'massively parallel' sequencing platforms.

Hopefully, in the near future the availability of validated, commercial FDA-approved array/sequencing platforms will lead to the discovery of key genes, miRNAs and pathways responsible of the chemosensitivity/resistance of NSCLC to TS inhibitor-based treatments and guide in the selection of more effective rationally-based tailor-made treatments, and drug combinations for each patient.

Regarding drug combinations, another intriguing observation is the downregulation of TS by several biological targeted drugs. In particular, the EGFR-TKI erlotinib decreased TS expression and activity, possibly through E2F-1 reduction, showing synergistic interaction with pemetrexed in NSCLC cells [51,101].

More recently, similar results were observed with the novel EGFR-TKI BIBW2992, providing a scientific rationale for testing the combination of BIBW 2992 with pemetrexed in patients who develop acquired resistance after harboring the EGFR T790M mutation [102].

Other targeted agents modulating TS included the PKC-β inhibitor enzastaurin and the Src-inhibiting agent dasatinib, which synergistically enhanced pemetrexed cytotoxicity in NSCLC cells [103,104]. Of note, the results observed in the preclinical study on pemetrexed-enzastaurin combination are in agreement with the data on deoxyuridine levels, measured as a surrogate marker of TS inhibition using a specific LCMS/MS validated method, in blood samples from 15 patients treated with the enzastaurin-pemetrexed combination [105,106]. The enzastaurin-pemetrexed regimen after 22 days induced 2- to 3.5-fold increased deoxyuridine levels with respect to baseline in all patients, indicating an increased TS inhibition by this combination with respect to data obtained in patients treated with pemetrexed alone.

These data suggest innovative combinations improving the efficacy of TS-inhibiting agents for the treatment of NSCLC that should be tested and validated in the clinical setting.

REFERENCES

1. Meyerhardt JA, Mayer RJ. Systemic therapy for colorectal cancer. N Engl J Med 2005;20:476-87
2. Scagliotti GV, Parikh P, von PJ, et al. Phase III study comparing cisplatin plus gemcitabine with cisplatin plus pemetrexed in chemotherapy-naive patients with advanced-stage non-small-cell lung cancer. J Clin Oncol 2008;26:3543-51
3. Okamoto I, Yoshioka H,Morita S, et al. Phase III trial comparing oral S-1 plus carboplatin with paclitaxel plus carboplatin in chemotherapy-naive patients with advanced non-small-cell lung cancer: results of a west Japan oncology group study. J Clin Oncol 2010;28:5240-6
4. Lehman NL. Future potential of thymidylate synthase inhibitors in cancer therapy. Expert Opin Investig Drugs 2002;11:1775-87
5. Sant M, Aareleid T, Berrino F, et al. EUROCARE-3: survival of cancer patients diagnosed 1990-94--results and commentary. Ann Oncol 2003;14(Suppl 5):v61-118
6. Qiao X, Tullgren O, Lax I, et al. The role of radiotherapy in treatment of stage I non-small cell lung cancer. Lung Cancer 2003;41:1-11
7. Keller SM, Adak S, Wagner H, et al. A randomized trial of postoperative adjuvant therapy in patients with completely resected stage II or IIIA non-small-cell lung cancer. Eastern Cooperative Oncology Group. N Engl J Med 2000;343:1217-22
8. Crino L, Weder W, van MJ, et al. Early stage and locally advanced (non-metastatic) non-small-cell lung cancer: ESMO Clinical Practice Guidelines for diagnosis, treatment and follow-up. Ann Oncol 2010;21(Suppl 5):v103-15
9. Marino P, Preatoni A, Cantoni A, et al. Single-agent chemotherapy versus combination chemotherapy in advanced non-small cell lung cancer: a quality and meta-analysis study. Lung Cancer 1995;13:1-12
10. Delbaldo C, Michiels S, Syz N, et al. Benefits of adding a drug to a single-agent or a 2-agent chemotherapy regimen in advanced non-small-cell lung cancer: a meta-analysis. JAMA 2004;292:470-84
11. Ardizzoni A, Boni L, Tiseo M, et al. Cisplatin- versus carboplatin-based chemotherapy in first-line treatment of advanced non-small-cell lung cancer: an individual patient data meta-analysis. J Natl Cancer Inst 2007;99:847-57
12. Schiller JH, Harrington D, Belani CP, et al. Comparison of four chemotherapy regimens for advanced non-small-cell lung cancer. N Engl J Med 2002;346:92-8
13. D'Addario G, Pintilie M, Leighl NB, et al. Platinum-based versus non-platinum-based chemotherapy in advanced non-small-cell lung cancer: a meta-analysis of the published literature. J Clin Oncol 2005;23:2926-36
14. Reck M, von PJ, Zatloukal P, et al. Phase III trial of cisplatin plus gemcitabine with either placebo or bevacizumab as first-line therapy for nonsquamous non-small-cell lung cancer: AVAil. J Clin Oncol 2009;27:1227-34
15. Gutierrez ME, Kummar S, Giaccone G. Next generation oncology drug development: opportunities and challenges. Nat Rev Clin Oncol 2009;6:259-65
16. Pirker R, Pereira JR, Szczesna A, et al. Cetuximab plus chemotherapy in patients with advanced non-small-cell lung cancer (FLEX): an open-label randomised phase III trial. Lancet 2009;373:1525-31
17. Fojo T, Grady C. How much is life worth: cetuximab, non-small cell lung cancer, and the $440 billion question. J Natl Cancer Inst 2009;101:1044-8
18. Ku GY, Haaland BA, de Lima LG. Gefitinib vs. chemotherapy as first-line therapy in advanced non-small cell lung cancer: meta-analysis of phase III trials. Lung Cancer 2011 May 10. [Epub ahead of print]
19. Azzoli CG, Baker S Jr, Temin S, et al. American Society of Clinical Oncology Clinical Practice Guideline update on chemotherapy for stage IV non-small-cell lung cancer. J Clin Oncol 2009;27:6251-66
20. Arango BA, Castrellon AB, Santos ES, et al. Second-line therapy for non-small-cell lung cancer. Clin Lung Cancer 2009;10:91-8
21. Fossella FV, Lee JS, Shin DM, et al. Phase II study of docetaxel for advanced or metastatic platinum-refractory non-small-cell lung cancer. J Clin Oncol 1995;13:645-51
22. Hanna N, Shepherd FA, Fossella FV, et al. Randomized phase III trial of pemetrexed versus docetaxel in patients with non-small-cell lung cancer previously treated with chemotherapy. J Clin Oncol 2004;22:1589-97
23. Reck M, Mok T, Wolf J, et al. Reviewing the safety of erlotinib in non-small cell lung cancer. Expert Opin Drug Saf 2011;10:147-57
24. Gridelli C, Maione P, Rossi A, et al. New avenues for second-line treatment of metastatic non-small-cell lung cancer. Expert Rev Anticancer Ther 2009;9:115-24
25. Carreras CW, Santi DV. The catalytic mechanism and structure of thymidylate synthase. Annu Rev Biochem 1995;64:721-62
26. Rahman L, Voeller D, Rahman M, et al. Thymidylate synthase as an oncogene: a novel role for an essential DNA synthesis enzyme. Cancer Cell 2004;5:341-51
27. Chen M, Rahman L, Voeller D, et al. Transgenic expression of human thymidylate synthase accelerates the development of hyperplasia and tumors in the endocrine pancreas. Oncogene 2007;26:4817-24

28. Muggia FM, Peters GJ, Landolph JR. XIII International Charles Heidelberger Symposium and 50 Years of Fluoropyrimidines in Cancer Therapy Held on september 6 to 8, 2007 at New York University Cancer Institute, Smilow Conference Center. Mol Cancer Ther 2009;8:992-9
29. Longley DB, Harkin DP, Johnston PG. 5-fluorouracil: mechanisms of action and clinical strategies. Nat Rev Cancer 2003;3:330-8
30. Ju J, Pedersen-Lane J, Maley F, et al. Regulation of p53 expression by thymidylate synthase. Proc Natl Acad Sci USA 1999;96:3769-74
31. Chu E, Takechi T, Jones KL, et al. Thymidylate synthase binds to c-myc RNA in human colon cancer cells and in vitro. Mol Cell Biol 1995;15:179-85
32. Giovannetti E, Backus HH, Wouters D, et al. Functional inactivity and mutations of p53 differentially affect sensitivity to 5-fluorouracil and antifolate inhibitors of thymidylate synthase (TS) by altering TS levels in colorectal cancer cells. Nucleosides Nucleotides Nucleic Acids 2008;27:740-5
33. DeGregori J, Kowalik T, Nevins JR. Cellular targets for activation by the E2F1 transcription factor include DNA synthesis- and G1/S-regulatory genes. Mol Cell Biol 1995;15:4215-24
34. Chu E, Voeller D, Koeller DM, et al. Identification of an RNA binding site for human thymidylate synthase. Proc Natl Acad Sci USA 1993;90:517-21
35. Lin X, Parsels LA, Voeller DM, et al. Characterization of a cis-acting regulatory element in the protein coding region of thymidylate synthase mRNA. Nucleic Acids Res 2000;28:1381-9
36. Zhang Y, Yang S, Liu M, et al. Interaction between thymidylate synthase and its cognate mRNA in zebrafish embryos. PLoS One 2010;5:e10618
37. Kitchens ME, Forsthoefel AM, Rafique Z, et al. Ligand-mediated induction of thymidylate synthase occurs by enzyme stabilization. Implications for autoregulation of translation. J Biol Chem 1999;274:12544-7
38. Chattopadhyay S, Moran RG, Goldman ID. Pemetrexed: biochemical and cellular pharmacology, mechanisms, and clinical applications. Mol Cancer Ther 2007;6:404-17
39. Vogelzang NJ, Rusthoven JJ, Symanowski J, et al. Phase III study of pemetrexed in combination with cisplatin versus cisplatin alone in patients with malignant pleural mesothelioma. J Clin Oncol 2003;21:2636-44
40. Gronberg BH, Bremnes RM, Flotten O, et al. Phase III study by the Norwegian lung cancer study group: pemetrexed plus carboplatin compared with gemcitabine plus carboplatin as first-line chemotherapy in advanced non-small-cell lung cancer. J Clin Oncol 2009;27:3217-24
41. Scagliotti G, Hanna N, Fossella F, et al. The differential efficacy of pemetrexed according to NSCLC histology: a review of two Phase III studies. Oncologist 2009;14:253-63
42. Ciuleanu T, Brodowicz T, Zielinski C, et al. Maintenance pemetrexed plus best supportive care versus placebo plus best supportive care for non-small-cell lung cancer: a randomised, double-blind, phase 3 study. Lancet 2009;374:1432-40
43. Paz-Ares LG, De Marinis F, Dediu M, et al. PARAMOUNT: Phase III study of maintenance pemetrexed (pem) plus best supportive care (BSC) versus placebo plus BSC immediately following induction treatment with pem plus cisplatin for advanced nonsquamous non-small cell lung cancer (NSCLC). J Clin Oncol 2011;29(Suppl):abstract CRA7510
44. Ceppi P, Volante M, Saviozzi S, et al. Squamous cell carcinoma of the lung compared with other histotypes shows higher messenger RNA and protein levels for thymidylate synthase. Cancer 2006;107:1589-96
45. Shih C, Chen VJ, Gossett LS, et al. LY231514, a pyrrolo[2,3-d]pyrimidinebased antifolate that inhibits multiple folate-requiring enzymes. Cancer Res 1997;57:1116-23
46. Chen VJ, Bewley JR, Andis SL, et al. Preclinical cellular pharmacology of LY231514 (MTA): a comparison with methotrexate, LY309887 and raltitrexed for their effects on intracellular folate and nucleoside triphosphate pools in CCRF-CEM cells. Br J Cancer 1998;78(Suppl 3):27-34
47. Takimoto CH. New antifolates: pharmacology and clinical applications. Oncologist 1996;1:68-81
48. Giovannetti E, Mey V, Nannizzi S, et al. Cellular and pharmacogenetics foundation of synergistic interaction of pemetrexed and gemcitabine in human non-small-cell lung cancer cells. Mol Pharmacol 2005;68:110-18
49. Giovannetti E, Lemos C, Tekle C, et al. Molecular mechanisms underlying the synergistic interaction of erlotinib, an epidermal growth factor receptor tyrosine kinase inhibitor, with the multitargeted antifolate pemetrexed in non-small-cell lung cancer cells. Mol Pharmacol 2008;73:1290-300
50. Takezawa K, Okamoto I, Okamoto W, et al. Thymidylate synthase as a determinant of pemetrexed sensitivity in non-small cell lung cancer. Br J Cancer 2011;104:1594-601
51. Hanauske AR, Eismann U, Oberschmidt O, et al. In vitro chemosensitivity of freshly explanted tumor cells to pemetrexed is correlated with target gene expression. Invest New Drugs 2007;25:417-23
52. Gomez HL, Santillana SL, Vallejos CS, et al. A phase II trial of pemetrexed in advanced breast cancer: clinical response and association with molecular target expression. Clin Cancer Res 2006;12:832-8

53. Righi L, Papotti MG, Ceppi P, et al. Thymidylate synthase but not excision repair cross-complementation group 1 tumor expression predicts outcome in patients with malignant pleural mesothelioma treated with pemetrexed-based chemotherapy. J Clin Oncol 2010;28:1534-9

54. Zucali PA, Giovannetti E, Destro A, et al. Thymidylate synthase and excision repair cross-complementing group-1 as predictors of responsiveness in mesothelioma patients treated with pemetrexed/carboplatin. Clin Cancer Res 2011;17:2581-90

55. Chen CY, Chang YL, Shih JY, et al. Thymidylate synthase and dihydrofolate reductase expression in non-small cell lung carcinoma: the association with treatment efficacy of pemetrexed. Lung Cancer 2011; [Epub ahead of print]

56. Sun JM, Han J, Ahn JS, et al. Significance of thymidylate synthase and thyroid transcription factor 1 expression in patients with nonsquamous non-small cell lung cancer treated with pemetrexed-based chemotherapy. J Thorac Oncol 2011; [Epub ahead of print]

57. Higashiyama M, Kodama K, Yokouchi H, et al. Thymidylate synthase and dihydropyrimidine dehydrogenase activities in non-small cell lung cancer tissues: relationship with in vitro sensitivity to 5-fluorouracil. Lung Cancer 2001;34:407-16

58. Nakagawa T, Tanaka F, Otake Y, et al. Prognostic value of thymidylate synthase expression in patients with p-stage I adenocarcinoma of the lung. Lung Cancer 2002;35:165-70

59. Zheng Z, Li X, Schell MJ, et al. Thymidylate synthase in situ protein expression and survival in stage I nonsmall-cell lung cancer. Cancer 2008;112:2765-73

60. Edler D, Kressner U, Ragnhammar P, et al. Immunohistochemically detected thymidylate synthase in colorectal cancer: an independent prognostic factor of survival. Clin Cancer Res 2000;6:488-92

61. Novello S, Scagliotti G, Torri V, et al. International tailored chemotherapy adjuvant trial: ITACA trial. J Clin Oncol 2011;29(Suppl):abstract e17514

62. Assaraf YG. Molecular basis of antifolate resistance. Cancer Metastasis Rev 2007;26:153-81

63. Uemura T, Oguri T, Ozasa H, et al. ABCC11/MRP8 confers pemetrexed resistance in lung cancer. Cancer Sci 2010;101:2404-10

64. Assaraf YG. The role of multidrug resistance efflux transporters in antifolate resistance and folate homeostasis. Drug Resist Updat 2006;9:227-46

65. Liani E, Rothem L, Bunni MA, et al. Loss of folylpoly-gamma-glutamate synthetase activity is a dominant mechanism of resistance to polyglutamylation-dependent novel antifolates in multiple human leukemia sublines. Int J Cancer 2003;103:587-99

66. Zhao R, Titus S, Gao F, et al. Molecular analysis of murine leukemia cell lines resistant to 5, 10-dideazatetrahydrofolate identifies several amino acids critical to the function of folylpolyglutamate synthetase. J Biol Chem 2000;275:26599-606

67. Pizzorno G, Moroson BA, Cashmore AR, et al. Multifactorial resistance to 5,10-dideazatetrahydrofolic acid in cell lines derived from human lymphoblastic leukemia CCRF-CEM. Cancer Res 1995;55:566-73

68. Stark M, Wichman C, Avivi I, et al. Aberrant splicing of folylpolyglutamate synthetase as a novel mechanism of antifolate resistance in leukemia. Blood 2009;113:4362-9

69. Zhao R, Gao F, Goldman ID. Marked suppression of the activity of some, but not all, antifolate compounds by augmentation of folate cofactor pools within tumor cells. Biochem Pharmacol 2001;61:857-65

70. Zhao R, Zhang S, Hanscom M, et al. Loss of reduced folate carrier function and folate depletion result in enhanced pemetrexed inhibition of purine synthesis. Clin Cancer Res 2005;11:1294-301

71. Chattopadhyay S, Zhao R, Krupenko SA, et al. The inverse relationship between reduced folate carrier function and pemetrexed activity in a human colon cancer cell line. Mol Cancer Ther 2006;5:438-49

72. Matherly LH, Goldman DI. Membrane transport of folates. Vitam Horm 2003;66:403-56

73. Gorlick R, Goker E, Trippett T, et al. Defective transport is a common mechanism of acquired methotrexate resistance in acute lymphocytic leukemia and is associated with decreased reduced folate carrier expression. Blood 1997;89:1013-18

74. Zhao R, Gao F, Hanscom M, et al. A prominent low-pH methotrexate transport activity in human solid tumors: contribution to the preservation of methotrexate pharmacologic activity in HeLa cells lacking the reduced folate carrier. Clin Cancer Res 2004;10:718-27

75. Zhao R, Qiu A, Tsai E, et al. The proton-coupled folate transporter: impact on pemetrexed transport and on antifolates activities compared with the reduced folate carrier. Mol Pharmacol 2008;74:854-62

76. Gonen N, Bram EE, Assaraf YG. PCFT/SLC46A1 promoter methylation and restoration of gene expression in human leukemia cells. Biochem Biophys Res Commun 2008;376:787-92

77. Diop-Bove NK, Wu J, Zhao R, et al. Hypermethylation of the human proton-coupled folate transporter (SLC46A1) minimal transcriptional regulatory region in an antifolate-resistant HeLa cell line. Mol Cancer Ther 2009;8:2424-31

78. Ansfield FJ, Kallas GJ, Singson JP. Phase I-II studies of oral tegafur (ftorafur). J Clin Oncol 1983;1:107-10

79. Keicho N, Saijo N, Shinkai T, et al. Phase II study of UFT in patients with advanced non-small cell lung cancer. Jpn J Clin Oncol

1986;16:143-6

80. Shirasaka T, Shimamato Y, Ohshimo H, et al. Development of a novel form of an oral 5-fluorouracil derivative (S-1) directed to the potentiation of the tumor selective cytotoxicity of 5-fluorouracil by two biochemical modulators. Anticancer Drugs 1996;7:548-57
81. Tanaka F, Wada H, Fukushima M. UFT and S-1 for treatment of primary lung cancer. Gen Thorac Cardiovasc Surg 2010;58:3-13
82. Surmont V, Aerts JG, Pouw E, et al. Oral UFT, etoposide and leucovorin in recurrent non-small cell lung cancer: a non-randomized phase II study. Lung Cancer 2009;66:333-7
83. Sandler A, Graham C, Baggstrom M, et al. An open-label, multicenter, three-stage, phase ii study of S-1 in combination with cisplatin as first-line therapy for patients with advanced non-small cell lung cancer. J Thorac Oncol 2011; Epub ahead of print
84. Okabe T, Okamoto I, Tsukioka S, et al. Synergistic antitumor effect of S-1 and the epidermal growth factor receptor inhibitor gefitinib in non-small cell lung cancer cell lines: role of gefitinib-induced down-regulation of thymidylate synthase. Mol Cancer Ther 2008;7:599-606
85. Okabe T, Okamoto I, Tsukioka S, et al. Addition of S-1 to the epidermal growth factor receptor inhibitor gefitinib overcomes gefitinib resistance in non-small cell lung cancer cell lines withMET amplification. Clin Cancer Res 2009;15:907-13
86. Takeda M, Okamoto I, Hirabayashi N, et al. Thymidylate synthase and dihydropyrimidine dehydrogenase expression levels are associated with response to S-1 plus carboplatin in advanced non-small cell lung cancer. Lung Cancer 2011;73:103-9
87. Yamamoto N, Yamanaka T, Ichinose Y, et al. Pooled analysis of S-1 trials in non-small cell lung cancer according to histological type. Anticancer Res 2010;30:2985-90
88. Manegold C, Buchholz E, Kloeppel R, et al. Phase I dose-escalating study of raltitrexed ('Tomudex') and cisplatin in metastatic non-small cell lung cancer. Lung Cancer 2002;36:183-9
89. Mendiola C, Vaz MA. Is capecitabine a new choice of treatment for lung adenocarcinoma? A case report involving partial response in second line of treatment and hypothesis of the biological basis. Clin Transl Oncol 2009;11:554-7
90. Han JY, Hong EK, Lee SY, et al. Thymidine phosphorylase expression in tumour cells and tumour response to capecitabine plus docetaxel chemotherapy in non-small cell lung cancer. J Clin Pathol 2005;58:650-4
91. Ko JC, Tsai MS, Kuo YH, et al. Modulation of Rad51, ERCC1, and thymidine phosphorylase by emodin result in synergistic cytotoxic effect in combination with capecitabine. Biochem Pharmacol 2011;81:680-90
92. Kindwall-Keller T, Otterson GA, Young D, et al. Phase II evaluation of docetaxel-modulated capecitabine in previously treated patients with non-small cell lung cancer. Clin. Cancer Res 2005;11:1870-6
93. Giovannetti E, Zucali PA, Peters GJ, et al. Association of polymorphisms in AKT1 and EGFR with clinical outcome and toxicity in non-small cell lung cancer patients treated with gefitinib. Mol Cancer Ther 2010;9:581-93
94. Mandola MV, Stoehlmacher J, Muller-Weeks S, et al. A novel single nucleotide polymorphism within the 5' tandem repeat polymorphism of the thymidylate synthase gene abolishes USF-1 binding and alters transcriptional activity. Cancer Res 2003;63:2898-904
95. Horie N, Aiba H, Oguro K, et al. Functional analysis and DNA polymorphism of the tandemly repeated sequences in the 5'-terminal regulatory region of the human gene for thymidylate synthase. Cell Struct Funct 1995;20:191-7
96. Smit EF, Burgers SA, Biesma B, et al. Randomized phase II and pharmacogenetic study of pemetrexed compared with pemetrexed plus carboplatin in pretreated patients with advanced non-small-cell lung cancer. J Clin Oncol 2009;27:2038-45
97. Adjei AA, Mandrekar SJ, Dy GK, et al. Phase II trial of pemetrexed plus bevacizumab for second-line therapy of patients with advanced non-small-cell lung cancer: NCCTG and SWOG study N0426. J Clin Oncol 2010;28:614-19
98. Wynes MW, Dziadziuszko R, Singh S, et al. Thymidylate synthase (TS) gene copy number in NSCLC. J Clin Oncol 2010;28(Suppl):abstract e21063
99. Boni V, Bitarte N, Cristobal I, et al. miR-192/miR-215 influence 5-fluorouracil resistance through cell cycle-mediated mechanisms complementary to its post-transcriptional thymidilate synthase regulation. Mol Cancer Ther 2010;9:2265-75
100. Giovannetti E, Erozenci A, Smit J, et al. Molecular mechanisms underlying the role of microRNAs (miRNAs) in anticancer drug resistance and implications for clinical practice. Crit Rev Oncol Hematol 2011; [Epub ahead of print]
101. Li T, Ling YH, Goldman ID, et al. Schedule-dependent cytotoxic synergism of pemetrexed and erlotinib in human non-small cell lung cancer cells. Clin Cancer Res 2007;13:3413-22
102. Takezawa K, Okamoto I, Tanizaki J, et al. Enhanced anticancer effect of the combination of BIBW2992 and thymidylate synthase-targeted agents in non-small cell lung cancer with the T790M mutation of epidermal growth factor receptor. Mol Cancer Ther 2010;9:1647-56
103. Tekle C, Giovannetti E, Sigmond J, et al. Molecular pathways involved in the synergistic interaction of the PKC beta inhibitor enzastaurin with the antifolate pemetrexed in non-small cell lung cancer cells. Br J Cancer 2008;99:750-9
104. Ceppi P, Rapa I, Lo IM, et al. Expression and pharmacological inhibition of thymidilate synthase and Src kinase in non-small cell lung cancer. Int J Cancer 2011; [Epub ahead of print]

105.Hanauske AR, Lahn M, Musib LC, et al. Phase Ib safety and pharmacokinetic evaluation of daily and twice daily oral enzastaurin in combination with pemetrexed in advanced/metastatic cancer. Ann Oncol 2009;20:1565-75

106.Giovannetti E, Honeywell R, Hanauske AR, et al. Pharmacological aspects of the enzastaurin-pemetrexed combination in non-small cell lung cancer (NSCLC). Curr Drug Targets 2010;11:12-28

107.Ota K, Taguchi T, Kimura K. Report on nationwide pooled data and cohort investigation in UFT phase II study. Cancer Chemother Pharmacol 1988;22(4):333-8

Chapter 3

EGFR-TKIs: current status and future perspectives in the development of novel irreversible inhibitors for the treatment of mutant NSCLC

Galvani E, Alfieri RR, Giovannetti E, Cavazzoni A, La Monica S, Galetti M, Fumarola C, Bonelli MA, Mor M, Tiseo M, Peters GJ, Petronini PG & Ardizzoni A.

CURRENT PHARMACEUTICAL DESIGN 2013

19(5):818-832.

ABSTRACT

Conventional chemotherapeutic regimens have reached an efficacy plateau against most solid tumors and deal with significant toxicity. Recently, the goal of the oncologic research to improve outcome and reduce treatment-related side-effects has led to the development of novel anticancer treatments targeting specific proteins or genes involved in cancer growth and progression. In particular, the tyrosine-kinase inhibitors (TKIs) gefitinib and erlotinib targeting the epidermal growth factor receptor (EGFR) have been approved for the treatment of non-small-cell lung cancer (NSCLC). Their clinical activity has been related to different clinical and biological parameters, such as the presence of activating mutations in the kinase domain of the target. Disappointingly, their clinical efficacy is limited by the development of resistance which is caused in more than 50% of the cases by the emergence of a secondary point-mutation (T790M) in the ATP-binding cleft of EGFR. Several novel EGFR inhibitors, able to covalently bind the target and prolong its inactivation, have been developed with the aim to overcome such resistance and are evaluated in ongoing clinical studies. However, not all clinical outcomes, including tolerability, are explained, and the identification/validation of novel biomarkers of sensitivity or resistance to such agents is a viable area of research to improve their clinical use. This review summarizes the current knowledge on the functional role of activating mutations of EGFR, pivotal primary/acquired resistance mechanisms as well as clinical data of small molecule EGFR-TKIs, and discusses the future of such therapeutic approach in NSCLC.

1.INTRODUCTION

1.1 Background

Non-small cell lung cancer (NSCLC), which currently accounts for nearly 85% of primary malignant lung tumors, remains the leading global cause of cancer-related death worldwide [1]. Unfortunately, in spite of advances in early detection, the majority of patients with NSCLC are diagnosed with advanced-stage disease. For such patients the prognosis remains poor, with a median survival of only 10-12 months [2,3], and a 5-year survival rate of around 16% in the U.S. [4]. Based on the associated moderate improvement in survival and quality of life, platinum-based chemotherapy constitutes the standard first-line treatment for advanced NSCLC patients with good performance status [5,6]. Despite the improvement of the conventional treatment and the development of the second-line chemotherapy agents, NSCLC patients show rapid emergence of resistance against platinum-based regimens resulting in limited overall survival (OS) [7,8]. Therefore, new treatment approaches have been thoroughly investigated in the last decade. These novel therapies are based on advances in our understanding of key cellular networks and genetic nodal points around which tumors could arise and progress [9,10]. Genome characterization efforts have highlighted the importance of “driver” somatic alterations that activate crucial oncoproteins originating tumor with a pivotal dependency. Single-agent therapeutic regimens especially designed to intercept deregulated dominant oncogenes have proven to be effective treatment in “oncogene addicted” tumors [11]. The clinical development and usage of the inhibitor of the ABL tyrosine kinase imatinib in the treatment of chronic myeloid leukemia (CML) is a successful example of the efficacy of targeting such oncogenic pathways [12]. Based on their role in maintenance of cellular homeostasis, protein kinases, including tyrosine kinases (PTKs), have been identified as important targets in cancer treatment. Furthermore, it has been largely demonstrated that mutations or abnormal activation of PTKs lead to the development and progression of many cancers [13].

1.2. Role of EGFR in the Pathogenesis of NSCLC

The epidermal growth factor receptor (EGFR) is a member of the ErbB family of receptor tyrosine kinases together with HER2 (ErbB2), HER3 (ErbB3), and HER4 (ErbB4) (Fig. 1). The ErbB receptors are normally expressed in various tissues of epithelial, mesenchymal and neural origin. The pivotal role of ErbBs in normal individual development has been largely investigated by multiple research groups through the use of knockout mouse models [14-17] and their involvement in the regulation of important tumorigenic processes, such as proliferation, apoptosis, angiogenesis, and invasion has also been demonstrated. However, it is easy to imagine that dysregulation of such genes or proteins can lead to cancer development.

The ErbB receptors are plasma membrane glycoproteins composed of an extracellular ligand-binding domain, a single transmembrane region and an intracellular TK-domain [18]. These molecules exist as inactive monomers and, on binding to ligands, they undergo conformational changes that allow homo- or heterodimerization with the other members of the family of receptors [19,20]. Dimerization, an essential requirement for the transactivation of the intrinsic kinase domain, leads to the phosphorylation on specific tyrosine residues within the cytoplasmic region of the receptor [21]. Activated ErbB dimers stimulate many intracellular signalling pathways and, despite the extensive overlap in the recruited proteins, different ErbBs

preferentially modulate specific signalling pathways (Fig. 1). Among the ErbBs downstream pathways, the phosphatidylinositol 3-kinase (PI3K)-Akt-mammalian target of rapamycin (mTOR) and the mitogen-activated protein kinase (MAPK) pathways have been demonstrated to play a key role in the control of numerous fundamental cellular processes [22-24]. In particular, cell survival has been mainly associated with Akt signalling [25] which is initiated by binding of the Src homology 2 (SH2) domain of PI3K with activated EGFR-HER3 dimers [26]. Although ordinary PI3K binding sites are not included in the autophosphorylation sites on EGFR, this receptor can activate PI3K via the docking protein Gab1 [27]. Conversely, cell proliferation process is primarily linked to the activation of Ras, which triggers the Raf/MEK/ERK cascade, by binding of Grb2 SH2-domain to EGFR [28]. The signal transducer and activator of transcription proteins (STATs) [29], the steroid receptor coactivator (SRC) tyrosine kinase, are other important signaling effectors of the ErbB receptors. Furthermore, in response to the binding of the ligand, the complex with the receptor is rapidly internalized, allowing EGFR to interact with many cytosolic proteins, and is either proteolytically degraded or recycled back to the cell membrane [30].

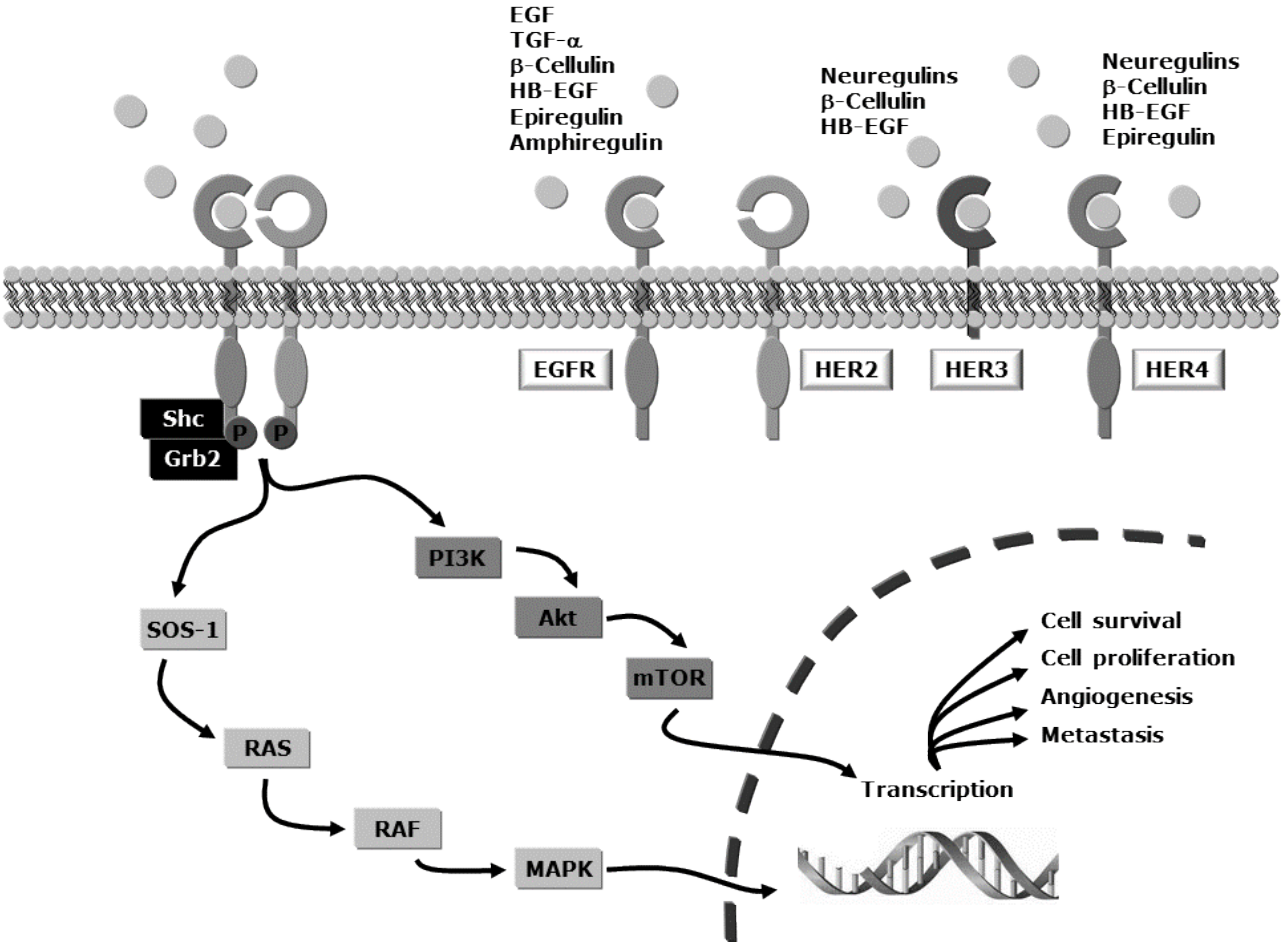

Figure 1. EGFR signaling pathway. Signaling pathways and epidermal growth factor tyrosine kinase receptors involved in the tumorigenesis of NSCLC. Akt, protein kinase B; EGF, epidermal growth factor; EGFR, epidermal growth factor receptor; hb-EGF, heparin binding EGF; MAPK, mitogen-activated protein kinase; PI3K, phosphatidylinositol-3-kinase; Raf, v-raf 1 murine leukemia viral oncogene homolog 1; Ras, retrovirus-associated DNA sequences; SOS, Son of sevenless; TGF, transforming growth factor; mTOR, mammalian target of rapamycin; FGF, fibroblast growth factor; VEGF, vascular endothelial growth factor; Grb2, growth factor receptor-bound protein 2.

Along with its ligands (e.g. EGF, TGF-α, and amphiregulin) EGFR is frequently overexpressed and

negatively correlated with prognosis in many types of human malignancies, including NSCLC [31-33]. In particular, overexpression of EGFR has been found in 40-80% of NSCLC cases and EGFR mutations were also described and correlated with malignancy “oncogene-addiction” [34]. The increased expression of the receptor has been ascribed to various events, such as epigenetic mechanisms, gene amplification, and oncogenic viruses [35]. Besides, overexpression of the ligand for ErbB3 and ErbB4, neuregulin-1, has also been reported in NSCLC [36]. Taken together, these findings make EGFR an attractive target for cancer therapy [37].

To date, two classes of EGFR inhibitors are available for clinical use in many countries, including either, small-molecule TK inhibitors (TKIs) that compete with ATP for the interaction with the intracellular domain, and monoclonal antibodies (mAbs) which contend with ligands at the extracellular domain [38]. Both classes exert antitumor activity with various potential implications for clinical efficacy correlated to the different administration way and mechanism of action. In addition to the receptor, kinase inhibitors against other proteins within the EGFR pathway, such as Raf, MEK, PI3K, Akt and mTOR, are also in clinical development.

1.3. Clinical Development of First-generation EGFR-TKIs

Gefitinib (Iressa®, AstraZeneca, Wilmington, DE, USA) and erlotinib (Tarceva®, Hoffman-La Roche, Basel, Switzerland) are the two EGFR-TKIs currently approved for the treatment of advanced NSCLC in many countries. Both first-generation quinazoline-derived drugs were designed as ATP-mimetics to reversibly block wild-type receptor phosphorylation. Their clinical development in NSCLC treatment preceded the discovery of EGFR activating mutations as key markers of sensitivity.

After being widely investigated in pre-clinical and phase I studies, encouraging results were obtained in multiple phase II trials evaluating the efficacy of these drugs as single agent in the third-line setting treatment of advanced NSCLC patients [39-41]. While 150 mg per day of erlotinib was initially established as the recommended phase 2 dose, gefitinib was used at two different doses (250 mg or 500 mg) in different phase II and phase III clinical studies (Table 1). Diarrhea and acne-like rash, which are extensively reported as the two most common adverse events linked to the use of EGFR-TKIs, are the main causes of treatment discontinuation. Other adverse events are less frequent.

Based on response rates (RRs) of around 10-20% in two randomized phase II trials (IDEAL1 and IDEAL2), gefitinib was approved in 2003 by the US Food and Drug Administration (FDA) as third-line treatment of advanced NSCLC patients after failure of both, platinum-based chemotherapy and docetaxel [39,40,42]. Of note, the randomized phase III trial ISEL, comparing gefitinib to placebo in NSCLC patients who failed the treatment with standard chemotherapy, did not report any significant improvement in OS either in the overall population (5.6 vs. 5.1 months, respectively; HR = 0.89; CI: 0.77-1.02; P = 0.087) and in the subset of adenocarcinoma patients (6.3 vs. 5.4 months; HR = 0.84; CI 0.68-1.03 P = 0.089). In the same study, survival rates at 12 months in the whole population were 27 and 21% for gefitinib and placebo, respectively, while 30 and 18% rates were reported in the adenocarcinoma subgroup [43]. The absence of significant improvement in OS restricted the use of gefitinib in the U.S. to those NSCLC patients who had already derived benefit from the treatment.

Subsequently, two large randomized clinical studies (INTACT-1 and INTACT-2) investigated the

combination of gefitinib with platinum-based chemotherapy regimens as first-line treatment in NSCLC [44,45]. Both trials failed to demonstrate any OS, time to progression (TTP) or progression free survival (PFS) benefit with the addition of gefitinib to chemotherapy versus upfront standard chemotherapy. Furthermore, no significant difference in terms of RR, PFS, or OS was reported in the randomized phase II trial INVITE, comparing gefitinib to vinorelbine in chemotherapy-naïve unselected elderly NSCLC patients [46]. Thus, despite gefitinib better tolerance, no evidence was found to sustain its use as first-line setting in this group of patients. Importantly, gefitinib was non-inferior when compared with docetaxel as second-/third-line treatment in unselected NSCLC patients in terms of OS (7.6 vs. 8.0 months, respectively; HR = 1.020; CI: 0.9065-1.150) [47]. Of note, the INTEREST's subsets of patients of Asian ethnicity, female, never-smokers, and with adenocarcinoma histology were more likely to benefit from either gefitinib or docetaxel (Table 1).

Similar to gefitinib, erlotinib was compared to placebo in stage IIIB or IV NSCLC patients previously treated with one or two cycles of chemotherapy. Benefit in terms of OS was reported for the TKI treated group (6.7 months [erlotinib] vs. 4.7 months [placebo]; HR = 0.70; P < 0.001). Based on the results of the BR.21 trial, erlotinib achieved full regulatory approval in the U.S as second or third-line treatment of advanced NSCLCs [48]. Recently, the phase III trial TITAN comparing erlotinib to single-agent chemotherapy (docetaxel or pemetrexed) in second- or third-line setting in unselected NSCLC patients, failed to report significant survival advantage in the TKI treated arm (HR = 0.96; CI: 0.78-1.19; P = 0.7299) [49]. The phase III, placebo-control study SATURN evaluated the use of erlotinib as maintenance therapy in patients who did not progress after first-line chemotherapy. Longer PFS was reported for the erlotinib treated group (11.1 weeks [erlotinib] vs. 12.3 weeks [placebo]; HR = 0.71; CI: 0.62-0.82; P < 0.0001). More importantly, OS advantage of one month was registered in the TKI arm (12.0 months [erlotinib] vs. 11.0 months [placebo]; HR = 0.81; P = 0.0088) across all considered subgroups (i.e. K-RAS or EGFR mutation status, gender, histology) [50]. However, likewise gefitinib, two phase III trials (TRIBUTE and TALENT) were launched to evaluate whether the addition of erlotinib to first-line chemotherapy would improve treatment efficacy. No significant survival advantage was observed in patients receiving the combination when compared with those treated with conventional chemotherapy regimen [51,52] (Table 1).

Despite four large phase III trials failed to demonstrate additional survival benefit of the combination of EGFR-TKIs with firstline chemotherapy, in the second-/third-line or maintaining setting, OS advantages were observed with erlotinib in the BR.21 and SATURN trials [48,50]. However, the discovery of somatic EGFR mutations, followed by retrospective analyses and prospective phase II trials with EGFR-TKIs in selected patients, explained the previous conflicting observations and defined the stage for more specific use of these agents [53,54].

2. PREDICTIVE BIOMARKERS OF DRUG SENSITIVITY

Several biomarkers, including EGFR expression as assessed by immunohistochemistry (IHC), changes in EGFR copy-number detected by fluorescent in situ hybridization (FISH) or quantitative PCR, and EGFR mutational status evaluated by sequencing or PCR, were identified and evaluated during the key trials which led to EGFR-TKIs approval in second-/third-line treatment for NSCLC [55]. However, controversial results were observed regarding the role of EGFR expression or gene amplification in the response to TKIs; thus,

their validity as predictive biomarkers in NSCLC patients remains controversial [35,46,56,57]. Conversely, clear evidences on the correlation between EGFR mutational status and EGFR-TKIs sensitivity made it the best predictor of clinical response to these targeting agents.

Table 1. Summary of randomized phase II and phase III trials of first-generation EGFR-TKIs in unselected NSCLC patients

Trial	Phase	Patients features	Treatment	ORR (%)	Median PFS/TTP (months)	Median OS (months)
Gefitinib						
IDEAL-1 *(ref #39)*	2	210 patients with 1 or 2 prior CT regimens (at least 1 containing platinum)	Gefitinib 250 or 500 mg/day	18.4 (gef 250) 19.0 (gef 500)	2.7 (gef 250) 2.8 (gef 500)	7.6 (gef 250) 8.0 (gef 500)
IDEAL-2 *(ref #40)*	2	221 patients who received at least 2 prior CT regimens	Gefitinib 250 or 500 mg/day	12.0 (gef 250) 9.0 (gef 500)	NA NA	7.0 (gef 250) 6.0 (gef 500)
ISEL *(ref #43)*	3	1692 patients who were refractory to or intolerant of their latest CT regimen	Gefitinib (250 mg/day) or placebo	8.0 (gef) 1.3 (pl)	3.0 (gef) 2.6 (pl)	5.6 (gef) 5.1 (pl)
INTACT-1 *(ref #44)*	3	1093 CT-naïve patients	Cis/gem + gefitinib (250 or 500 mg/day) or placebo	50.3 (gef 250) 49.7 (gef 500) 44.8 (pl)	5.8 (gef 250) 5.5 (gef 500) 6.0 (pl)	9.9 (gef 250) 9.9 (gef 500) 10.9 (pl)
INTACT-2 *(ref #45)*	3	1037 CT-naïve patients	Carbo/pac+ gefitinib (250 or 500 mg/day) or placebo	30.4 (gef 250) 30.0 (gef 500) 28.7 (pl)	5.3 (gef 250) 4.6 (gef 500) 5.0 (pl)	9.8 (gef 250) 8.7 (gef 500) 9.9 (pl)
INVITE *(ref #46)*	2	196 CT-naïve patients (age >or= 70 years)	Gefitinib (250 mg/day) or vinorelbine	3.1(gef) 5.1(vin)	2.7 (gef) 2.9 (vin)	5.9 (gef) 8.0 (vin)
INTEREST *(ref #47)*	3	1466 patients who had 1 or more prior platinum-based regimens	Gefitinib (250 mg/day) or docetaxel	9.1 (gef) 7.6 (doc)	2.2 (gef) 2.7 (doc)	7.6 (gef) 8.0 (doc)
Erlotinib						
BR.21 *(ref #48)*	3	731 patients who had 1 or 2 prior CT regimens	Erlotinib or placebo	8.9 (erl) <1 (pl)	2.2 (erl) 1.8 (pl)	6.7 (erl) 1.8 (pl)
TITAN *(ref #49)*	3	424 patients who progressed after up to four cycles platinum-based CT	Erlotinib or CT (docetaxel or pemetrexed)	7.9 (erl) 6.3 (CT)	6.3 weeks (erl) 8.6 weeks (CT)	5.3 (erl) 5.5 (CT)
SATURN *(ref #50)*	3	889 patients with non-progressive disease following platinum-based CT	Erlotinib or placebo	11.9 (erl) 5.4 (pl)	12.3 weeks (erl) 11.1 weeks (pl)	12.0 (erl) 11.0 (pl)
TRIBUTE *(ref #51)*	3	1059 CT-naive patients	Carbo+pac+ erlotinib or placebo	21.5 (erl) 19.3 (pl)	5.1 (erl) 4.9 (pl)	10.6 (erl) 10.5 (pl)
TALENT *(ref #52)*	3	1172 CT-naïve patients	Cis+gem+ erlotinib or placebo	31.5 (erl) 29.9 (pl)	23.7 weeks (erl) 24.6 weeks (pl)	43 weeks (erl) 44.1 weeks (pl)

Carbo, carboplatin; cis, cisplatin; CT, chemotherapy; doc, docetaxel; erl, erlotinib; gef, gefinib; gem, gemcitabine; NA, not available; pac, paclitaxel; pl, placebo; vin, vinorelbine.

To date, several somatic EGFR mutations have been observed in NSCLC [58,59]. Importantly, multiple aberrations in the region of the EGFR gene encoding the TK-domain (exons 18-24) have been associated with the therapeutic response to EGFR-TKIs [59-61]. The exon 21 missense point mutation L858R and the in-frame deletions in exon 19 are the most frequently observed EGFR alterations in NSCLC. These mutations, also known as activating mutations, confer tumor cell dependency on EGFR signaling and are the most commonly studied predictive biomarkers of response to gefitinib and erlotinib [53,54,62] being observed in 15 to 40% of cases in several published studies [34,63-66]. Of note, sensitizing EGFR mutations are frequently found in certain subsets of patients such as females, Asian individuals, and non-smokers [34]. Other recurrent but less frequent EGFR mutations correlated with response to EGFR-TKIs include the point mutation G719S in exon 18 and the L861Q mutation in exon 21 [67].

Even though the ISEL study failed to demonstrate survival benefit with the use of gefitinib compared to best supportive care (BSC) in unselected patients, preplanned subgroup analyses revealed a significant increase in OS in both Asians (9.5 vs. 5.5 months; HR = 0.66; CI: 0.48-0.91; P = 0.010) and never-smokers (8.9 vs. 6.1 months; HR = 0.67; CI: 0.49-0.92; P = 0.012) when treated with gefitinib [43]. These results identified Asians and never-smokers as individuals who are more likely to benefit from EGFR-TKIs. The following Iressa Pan-Asia Study (IPASS) was designed in order to optimize gefitinib clinical response, comparing the TKI with carboplatin/paclitaxel as upfront treatment in lung adenocarcinoma patients who were light or never-smokers [61] (Table 2). This study enrolled more than 1200 patients and PFS was its primary endpoint. No significant difference in PFS was observed between the treatments. Interestingly, the retrospective EGFR mutation analysis revealed that mutations-positive patients took advantage from gefitinib treatment either in terms of RR (71.2% vs. 47.3%; P < 0.0001), and PFS (9.5 vs. 6.3 months; HR = 0.48; CI: 0.36-0.64; P < 0.0001). Of note, patients presenting wild-type EGFR who were treated with the TKI showed significantly lower RR (1.1% vs. 23.5%; P = 0.001) and worse PFS (1.5 vs. 5.5 months; HR = 2.85; CI: 2.05-3.98; P < 0.001). Therefore, IPASS results provided the missing link between EGFR mutational status and clinical response to EGFR-TKIs and represent a milestone toward personalized medicine. Based on the results of this trial, gefitinib has been recently approved in Europe as first-line treatment of patients harboring EGFR activating mutations. Furthermore, although no difference was observed between the treatments (OS, 18.8 months [gefitinib] vs. 17.4 months [carboplatin/paclitaxel]; HR = 0.90; P = 0.109), EGFR mutation-positive patients had longer OS independently from the received treatment (EGFR mutation-positive: 21.6 months [gefitinib] and 21.9 months [carboplatin/paclitaxel]; EGFR mutation-negative: 11.2 months [gefitinib] and 12.7 months [carboplatin/paclitaxel]) [68]. Thus, the IPASS trial demonstrated that EGFR mutation-positive cases are a clinically distinct entity with a better prognosis compared to non-mutated NSCLCs. Ultimately, despite the large and unpredictable inter-individual variability in toxicity, the IPASS trial demonstrated a more favourable tolerability profile for gefitinib when compared to chemotherapy [69].

Multiple trials enrolling patients selected on the basis of molecular and clinical characteristics were launched after the identification of patient features and EGFR mutational status as predictive biomarkers. A randomized phase II clinical study comparing erlotinib as single agent or in combination with carboplatin/paclitaxel in adenocarcinoma patients who were light or never-smoker, demonstrated the non-inferiority of the TKI alone, when compared to the combination, in terms of PFS (5.0 vs. 6.6 months, respectively; P = 0.1988). Of note, toxic effects (grade 3 to 4 hematologic and non-hematologic toxicity) were greater in the arm treated with the combination of erlotinib with chemotherapy. Similar to IPASS, this study identified EGFR mutation-positive patients as the most likely to benefit from both the treatments [70].

Recently, results from several phase III trials comparing gefitinib or erlotinib to standard chemotherapy as first-line setting for NSCLC patients with activating EGFR mutations have been reported (Table 2). In agreement with the IPASS findings, the randomized trials WJTOG3405 [71] and NEJ002 [72], comparing gefitinib to platinum-based chemotherapy as upfront treatment in prospectively identified EGFR-mutated NSCLC patients, reported advantage derived from the TKI treatment in terms of RR and PFS for this selected population. Similarly, erlotinib prolonged PFS and increased RR when compared to platinum-based chemotherapy in selected EGFR-mutated patients in the OPTIMAL [73] and EURTAC [74] prospective trials. These results definitely validate the IPASS findings sustaining the efficacy of EGFR-TKIs in this setting.

Table 2. First-generation EGFR-TKIs versus chemotherapy as first-line treatment for NSCLC patients with activating EGFR mutations

Trial	Patients features	Treatment	ORR (%)	Median PFS/TTP (months)	Median OS (months)
Gefitinib					
IPASS ***(ref #61,#68)***	261 patients EGFR-mutation positive	Gefitinib or carbo+pac	71.2 (gef) 47.3 (CT)	9.5 (gef) 6.3 (CT)	21.6 (gef) 21.9 (CT)
WJTOG3405 ***(ref #71)***	172 patients EGFR-mutation positive	Gefitinib or cis+doc	62.1 (gef) 32.2 (CT)	9.2 (gef) 6.3 (CT)	30.9 (gef) NA
NEJSG002 ***(ref #72)***	230 patients EGFR-mutation positive	Gefitinib or carbo+pac	73.7 (gef) 30.7 (CT)	10.8 (gef) 5.4 (CT)	30.5 (gef) 23.6 (CT)
First-SIGNAL ***(ref #75)***	313 Korean never-smokers with stage IIIB or IV lung adenocarcinoma	Gefitinib or cis+gem	55.4 (gef) 46.0 (CT)	5.8 (gef) 6.4 (CT)	22.3 (gef) 22.9 (CT)
Erlotinib					
OPTIMAL ***(ref #73)***	165 patients EGFR-mutation positive	Erlotinib or carbo+gem	83.0 (erl) 36.0 (CT)	13.1 (erl) 4.6 (CT)	NA NA
EURTAC ***(ref #74)***	174 patients EGFR-mutation positive	Erlotinib or carbo/cis + doc/gem	58.0 (erl) 15.0 (CT)	9.7 (erl) 5.2 (CT)	19.3 (erl) 19.5 (CT)

Carbo, carboplatin; cis, cisplatin; CT, chemotherapy; doc, docetaxel; erl, erlotinib; gef, gefinib; gem, gemcitabine; NA, not available; pac, paclitaxel; pl, placebo.

Moreover, given the reduced toxicity, the improved quality of life and the rapid symptoms relieve with single agent TKI when compared to chemotherapy, the use of first-generation EGFR-TKIs has become the new standard of care for the upfront treatment of EGFR mutation-positive NSCLC patients. However, the recent South Korean randomized phase III trial First-SIGNAL comparing gefitinib to first-line chemotherapy in 309 Korean never-smokers with lung adenocarcinoma, failed to demonstrate any OS advantage (22.3 vs. 22.9 months, respectively; HR = 0.932; CI: 0.716-1.213; P = 0.604) derived from TKI treatment in this selected population [75] (Table 2).

In contrast, the Chinese study INFORM, comparing gefitinib to BSC as maintenance therapy in unselected NSCLC patients, reported a significantly longer PFS in the TKI treated arm with respect to placebo (4.8 vs. 2.6 months, respectively; HR = 0.42; P < 0.0001). Of note, consistent with other trials, EGFR-mutation positive patients took advantage the most from gefitinib maintenance treatment (median PFS: 16.6 vs. 2.7 months; HR = 0.16), but no difference in term of OS was reported [76]. On the other hand, maintenance therapy with erlotinib in the SATURN study achieved significantly improved PFS and OS among the overall patients. Interestingly, erlotinib was able to improve PFS in both EGFR mutated (HR = 0.10; CI: 0.04-0.25; P < 0.0001) and wild-type (HR = 0.78; CI: 0.63-0.96; P = 0.0185) patients [50]. Taken together, the results from INFORM and SATURN trials suggest that EGFR wild-type patients may benefit from EGFR-TKI maintenance therapy on the basis of the specific EGFR-TKI used.

Even though a large number of trials firmly established the predictive role of EGFR mutations as biomarkers of response to gefitinib or erlotinib, a small group of wild-type EGFR NSCLC patients also significantly benefits from the treatment with the EGFR-TKIs [77]. These findings suggest the existence of additional mechanisms involved in sensitivity or resistance to these agents in EGFR mutation-negative patients.

3. PRIMARY & SECONDARY RESISTANCE TO FIRST-GENERATION EGFR-TKIs

Primary (or de novo) and secondary (or acquired) drug resistance are key issues in targeted therapeutics. Although the majority of lung malignancies have overexpression of EGFR, only a small fraction

of patients significantly benefits from EGFR inhibition while most of the tumors show primary resistance. However, despite the initial promising response to gefitinib or erlotinib as first-line therapy EGFR-TKIs in the overwhelming majority of NSCLC patients harboring sensitising EGFR mutations [78,79], most of these patients inevitably relapse due to the emergence of acquired resistance. The challenge of tumor drug resistance therefore represents a pervasive barrier that confounds the ultimate goal of cure or long-term control of advanced/metastatic cancer.

3.1. Primary Resistance and EGFR Status

De novo resistance includes patients who are initially refractory to EGFR-TKI treatment. The IPASS trial reported for wild-type EGFR patients of Asian origin an objective RR of 2% and reduced TTP with TKI treatment as compared with chemotherapy [61]. These results suggest that wild-type EGFR is a negative biomarker for the response to TKI treatment. Moreover, other genetic alterations than activating EGFR mutations, such as insertions (D770_N771insNPG, D770_N771insSVQ, and D770_N771insG) or the single point mutation T790M in exon 20 of EGFR, have been correlated with primary resistance to TKIs (Table 3).

Table 3. Summary of the mechanisms of resistance to EGFR-TKIs in NSCLC

Primary Resistance		Secondary Resistance	
EGFR aberrations	- D770_N771 (ins NPG) - D770_N771 (ins SVQ) - D770_N771 (ins G) - D770_N771 (ins VDSVDNP) - S768_V769 (ins VAS) - T790M - L861R - L862V	**EGFR: aberrations**	- **T790M** - L474S - D761Y - T854A - altered trafficking
Other mechanisms	- ins in exon 20 HER2 - K-RAS mut - PI3KCA mut - loss of PTEN - BRAF mut - overexpression of MAPKs - overexpression of ABCG2 - overexpression of IGF-1R - overexpression of Bcl-2 - overexpression of angiogenesis regulators - overexpression of SRC-3 - ALK translocations - CSCs - MET amplification	**Other mechanisms**	- **MET amplification** - overexpression or hyperactivation of IGF-1R - constitutive association of IRS-1 with PI3K - overexpression of ABCG2 - PI3KCA mut - SCLC transformation - EMT

ins, insertion; mut, mutation.

These alterations, which preclude the interaction of gefitinib or erlotinib with their target, occur in almost 5% of NSCLCs [59,80]. Of note, somatic insertions in HER2 exon 20 have also been detected in NSCLC and were similarly associated with absence of sensitivity to EGFR-TKIs [81]. However, some studies reported the existence of T790M at a low frequency within the tumor cells before TKI treatment [82-85]. Since this mutation is also correlated with secondary resistance, drug selection pressure of pre-existing kinase domain mutations has been proposed as explanation for the presence of T790M as dominant clone after TKI

treatment. A few cases of germline transmission of T790M have been described and this mutation has been recognised as initiating genetic event, but studies to date failed to demonstrate growth advantage as well as altered signalling conferred by T790M-EGFR compared with the wild-type receptor. However, given the limited sensitivity of detection methods, the question whether T790M is primary rather than acquired is still unanswered.

Despite the low incidence of these mutations, various studies aimed to overcome resistance conferred by exon 20 aberrations of EGFR and HER2 were conducted. In these studies, different strategies, including the use of EGFR-HER2 irreversible inhibitors as well as heat shock protein-90 (HSP-90) inhibitors, were tested [86, 87]. Few other aberrations, such as S784F, S768_V769insVAS, D770_N771insVDSVDNP, L861R and L862V, have been associated with EGFR-TKIs resistance in NSCLC patients [59]. However, for many of the rare EGFR mutations, the effect on responsiveness to TKIs treatment remains unknown.

3.2. Other Mechanisms of Primary Resistance

Mutations in genes other than EGFR and its family members have also been shown to play an important role in conferring primary resistance to EGFR-TKIs (Table 3). The best described examples of such resistance are mutations of the K-RAS oncoprotein which have been correlated with de novo resistance to TKIs in different tumor types including NSCLC [63,88,89]. K-RAS is a member of the RAS family of oncogenes and gene mutations have been reported to be related to the development of many cancers [90]. K-RAS aberrations have been detected in 20-30% of NSCLC patients with >90% localised in codons 12 and 13. Such alterations are responsible for the constitutive activation of RAS signaling, which promotes cell proliferation and reduction of apoptosis through the activation of EGFR downstream pathways such as PI3K and MAPKs [91]. Of note, K-RAS aberrations have been more frequently observed in adenocarcinomas from elderly and heavy smokers patients who have been identified as groups unlikely to benefit from EGFR-TKIs therapy [92,93]. Although mutations in K-RAS and EGFR are almost mutually exclusive, there are rare instances where they coexist. Interestingly, mutations of the catalytic region of PI3K (PIK3CA), exons 9 and 20, in cis- with EGFR mutations have been reported in NSCLC patients who have never been treated with EGFR-TKIs [94,95]. Other uncommon markers for de novo resistance, such as loss of PTEN, BRAF mutations, overexpression of MAPKs, ATP-binding cassette sub-family G member 2 (ABCG2), insulin-like growth factor-1 receptor (IGF-1R), Bcl-2, and angiogenesis regulators, as well as SRC-3 have recently been observed [96,97]. Furthermore, ALK translocations, which have been found to be mutually exclusive with EGFR or KRAS mutations, have also been associated with primary resistance to gefitinib or erlotinib treatment in advanced NSCLC patients [98].

Cancer stem cells (CSCs), together with their self-renewal, maintenance, and plasticity signaling pathways, such as TGF-α, Wnt, Notch, Hedgehog, PI3K/PTEN/mTOR, IGF-1R, histone demethylase and histone deacetylase (HDAC), have been also proposed as potential mechanisms of primary drug-resistance, including EGFR-TKIs [99,100]. Since CSCs seem to be less dependent on growth factor pathways than the abundant non-CSCs in a tumor, they may survive to drug inhibition leading to the failure of the therapy. Indeed, acquisition of secondary mutations in this quiescent stem cell population might cause the emergence of secondary resistance.

3.3. Secondary Resistance and EGFR Status

The acquisition of resistance to kinase inhibitors treatment in clinical oncology is by now a well-documented phenomenon in multiple cancer types. As the major EGFR activating mutations improve the sensitivity of the tumor to anilinoquinazoline inhibitors stabilizing their interactions with crucial amino acids in the ATP-binding pocket [53], to date it seems that after an initial response to such agents all the patients eventually experience progressive disease [101]. Given the rapid increasing number of patients who acquire resistance to gefitinib or erlotinib after their approval as first-line treatment in selected NSCLCs, a clinical definition of secondary resistance to these agents was established to unify treatments and investigate this subgroup of lung tumor [102].

One commonly described mechanism of drug resistance involves additional genetic alterations within the target oncogene itself. This mechanism was first described in patients with CML treated with imatinib. However, while several secondary mutations have been associated with secondary resistance to imatinib treatment, only a few point mutations, such as T790M, L747S [103], D761Y [104] and T854A [105], have been correlated to resistance to gefitinib and erlotinib in NSCLC (Table 3). In particular, the EGFR-T790M secondary mutation of kinase domain is the best characterized and most frequent mechanism of acquired resistance to EGFR-TKIs accounting for approximately 50% of cases relapsed from prior targeting treatment [104,106-108]. The T790M mutation, often referred to as the “gatekeeper”, was initially thought to confer resistance to EGFR-TKIs due to the steric hindrance of the bulkier methionine residue [106,107]. However, this explanation is difficult to reconcile with the evidence that irreversible EGFR-TKIs structurally similar to gefitinib and erlotinib are able to overcome the resistance associated with this mutation, as discussed later. Recently, Yun and colleagues have reported that T790M-mutant retains affinity to gefitinib (Kd 4.6 nM) similar to that observed for the L858R mutant (Kd 2.4 nM) [109]. Interestingly, the acquisition of such mutation increases about 10-fold the ATP affinity with respect to the L858R-mutant receptor. The authors concluded that the increased ATP affinity, and not the sterical blocking binding, is the mechanism by which the T790M mutation confers drug resistance [109].

The T790M mutation has been associated with shorter PFS when compared to the wild-type receptor (7.7 vs. 16.5 months, respectively; $P < 0.001$) [110]. However, this gatekeeper mutation has also been correlated with more indolent disease and better survival outcomes than other mechanisms of acquired resistance to TKIs [111]. Moreover, discontinuing EGFR-TKI treatments and removing the selection pressure for T790M has been associated with mutation-independent tumor growth and loss of the secondary mutation [112].

3.4. Other Mechanisms of Acquired Resistance

In 2007, Engelman and colleagues first reported the amplification of the receptor for the hepatocyte growth factor (MET) as the second major mechanism of acquired resistance to EGFR-TKIs [113] (Table 3). MET amplification has been detected in about 20% of patients who relapsed after gefitinib or erlotinib prior therapy, but only in 3% of untreated patients and cases of coexistence of the gatekeeper mutation with MET amplification have been described [113,114]. Furthermore, MET amplification was reported to sustain the HER3/PI3K/Akt antiapoptotic signaling pathway despite the presence of gefitinib in NSCLC cells [113-115]. Based on these findings, preclinical studies indicate the combination of EGFR and MET-TKIs as treatment

strategy for tumors harboring both EGFR mutation or MET amplification [115,116].

Several other mechanisms have been associated with EGFRTKIs acquired resistance, including expression and hyper-activation of the IGF-1R and constitutive association of IRS-1 with PI3K through loss of expression of IGF-binding proteins [117,118], altered EGFR trafficking [119], and expression of the ABCG2 drug efflux transporter [120]. The alteration of PIK3CA has also been indicated as secondary resistance mechanism to first-generation EGFR-TKIs in vitro [112,121]. Phenotypic transformation of EGFR mutation-positive adenocarcinoma patients who “switched” to small-cell lung cancer (SCLC) and epithelial-to-mesenchymal transition (EMT) processes, identified as acquired vimentin and loss of E-cadherin expression, were also reported as mechanisms of secondary resistance to EGFR-TKIs by Sequist and colleagues [112]. Recently, the activation of TGF-α/IL-6 signaling has been associated with erlotinib resistance because of its involvement in EMT [122]. Of note, in approximately 30% of cases, the mechanisms underlying secondary resistance to EGFR-TKIs treatment are still unknown.

4. SECOND-GENERATION EGFR-TKIs

It is expected that the elucidation of primary and acquired resistance mechanisms affecting “targetable” tumor dependencies will drive the development of rational therapeutic combinations. Here, the purpose is not only to increase the efficacy and the duration of clinical response, but also prevent and exceed the emergence of acquired resistance to first-generation EGFR-TKIs.

Structural insights into the resistance mutation affecting the gatekeeper residue accelerated the design of irreversible EGFRTKIs. These second-generation targeting agents, which covalently bind the residue Cys797 located at the entrance of the ATP binding cleft of the receptor, were active in preclinical models harboring the T790M mutation [123]. Multiple theoretical advantages of these drugs over the first-generation reversible EGFR-TKIs have been described in preclinical models: i) increased affinity and irreversible blockade of the receptor resulting in persistent suppression of ErbBs signaling; ii) inhibition of other ErbB family members, such as HER2 and HER4; iii) partial in vitro efficacy retained against the T790M mutation and other less frequent alterations correlated with resistance to the first-generation inhibitors. Taken together, these properties suggested that irreversible EGFR-TKIs could either delay or suppress the development of T790M in TKI-naïve patients and be used as treatment in patients who relapsed after an initial response to first-generation agents. Alternatively they may substitute the reversible targeting agents as they reach better total inhibition of EGFR signaling. Thus, several second-generation targeting agents are currently undergoing clinical trials.

4.1. Canertinib (CI-1033)

The 4-anilinoquinazoline-derived compound CI-1033 (Pfizer Inc) inhibits ErbB family members by covalently binding to Cys773 of EGFR (or the analogous HER2-Cys784 and HER4-Cys778). The covalent interaction with the target resulted in preclinical models in prolonged inhibition of the receptor activity with respect to first-generation TKIs [124]. Furthermore, a phase I clinical study reported the association of canertinib with paclitaxel and carboplatin as safe and well-tolerated [125]. A randomized phase II trial, evaluating CI-1033 efficacy as second-line treatment in advanced NSCLC patients, has also been performed. In this study, the inhibitor was used at three different dosages in 21-day cycles: 50 or 150 mg

daily for 21 consecutive days, or 450 mg daily for 14 days followed by 7 days of no treatment. One-year survival rate was the primary endpoint. No differences in terms of 1-year survival rate, PFS or OS among the three dose levels were reported. Diarrhea and rash were the major dose-dependent treatment-related adverse events. Furthermore, the RRs were 2%, 2%, and 4% for the three dosages, respectively. Canertinib demonstrated modest activity in unselected NSCLC patients but did not meet its primary endpoint [126]. Thus, canertinib is not being evaluated anymore as potential treatment in NSCLC.

4.2. Neratinib (HKI-272)

Neratinib (Pfizer; New London, CT, USA) is an irreversible EGFR/HER2 inhibitor [127] which demonstrated growth inhibition effect in NCI-H1975 (L858R and T790M) and NCI-H1650 (delE746-A750) cells in preclinical studies [119]. Neratinib was also effective in Ba/F3 cells transformed with EGFRvIII [128] as well as in HER2 mutant/amplified cell lines [129,130]. Neratinib has been evaluated in a single-agent phase II trial in advanced NSCLC patients who had previously undergone chemotherapy [131]. Although, the maximum tolerated dose (MTD) established in a phase I trial was 320 mg [132], during the phase II trial this dose had to be reduced to 240 mg daily due to severe toxicity (grade 3 diarrhea >50%). However, neratinib had a low efficacy both in patients with prior benefit from TKIs and in TKI-naïve patients, potentially because of inadequate bioavailability due to diarrhea imposed dose limitation [131]. Furthermore, as determined from in vitro assays, the reduced dosage does not permit to achieve the level of drug that in patients is required to prevent the emergence of the T790M mutation [133]. As a result, neratinib is not developed anymore for the treatment of NSCLC.

4.3. Dacomitinib (PF-00299804)

Dacomitinib (Pfizer Inc., New York, NY, USA) is an orally administered, highly selective irreversible pan-ErbB (EGFR, HER2, and HER4) TK-inhibitor. This inhibitor was active in preclinical studies against first-generation TKI-resistant tumor cells and human tumor xenograft models [124,134]. Furthermore, dacomitinib showed antitumor activity against tumors with activating EGFR mutations and tumors harbouring the T790M mutation, but very limited response was reported for K-RAS mutated tumors [124,134]. Two phase I dose-escalation studies investigating dacomitinib pharmacokinetics in Western (NCT00225121) and Japanese (NCT007833328) patients with advanced solid tumors assessed the MTD in 45 mg once daily [135,136]. In particular, the U.S. trial enrolled 121 patients, of whom 47% were NSCLC patients and the majority of them had received a previous treatment with first-generation EGFR-TKIs. This study reported positive safety and tolerability profiles, and stomatitis, rash, palmar-plantar erythrodysesthesia syndrome, dehydration and diarrhea as the most common dose limiting toxicity (DLT) events [133]. In agreement with the Western study, the Japanese trial showed that dacomitinib was generally safe and well tolerated. None of the 13 treated patients had DLT, and adverse events were generally of grade 1/2 severity and manageable.

Antitumor activity was also reported, particularly in NSCLC [136]. A phase II trial evaluated dacomitinib efficacy in patients with NSCLC (wild-type K-RAS) who progressed after at least one prior chemotherapy regimen and erlotinib (NCT00548093). In this study, patients were separated in adenocarcinoma and non-adenocarcinoma and received dacomitinib 45 mg once daily. Among the 62 evaluable patients, 3 had partial response (PR) and 35 achieved stable disease (SD) for more than 6 weeks. Patient reported outcomes

suggested diarrhea and mucositis as the most common adverse drug-related effects [137]. The safety and efficacy of the inhibitor were also investigated in a phase I/II study conducted in Asians refractory to chemotherapy, and erlotinib or gefitinib treatment. Preliminary data of the 30 evaluable patients showed PFS (4 months) 35%, OS (6 months) 87%, overall RR 8%, and clinical benefit rate (PR or SD ≥ 24 weeks) 20%. This study demonstrated that dacomitinib is well-tolerated and has antitumor activity without adversely impacting patients' health-related quality of life [138]. Based on the encouraging results provided during previous studies, a randomized, phase III trial (JBR.26) comparing dacomitinib to placebo as third-line setting is ongoing in advanced NSCLC patients with varying histology and molecular subtypes, who have failed chemotherapy and EGFR-TKIs (NCT01000025) (Table 4). A randomized phase II study comparing dacomitinib with erlotinib as second-line therapy in 188 patients with advanced NSCLC who progressed after upfront chemotherapy has been designed (NCT00769067) [139]. Baseline features were equally distributed between the two treatments with the exception of performance status 2 (19.1% [dacomitinib] and 3.2% [erlotinib]) and positive EGFR-mutation status (20.2% [dacomitinib] and 11.7% [erlotinib]).

Among the overall population, longer median PFS was achieved with dacomitinib treatment compared to erlotinib (12.4 vs. 8.3 weeks, respectively; HR = 0.681; CI, 0.490-0.945; P = 0.019), as well as increased RR (17% vs. 4%) and clinical benefit (PR or SD for ≥ 24 weeks: 27.7% vs. 13.8%, respectively). Moreover, consistent benefits from dacomitinib treatment were observed across several subsets including wild-type EGFR patients (PFS: 11.1 weeks [dacomitinib] vs. 8.0 weeks [erlotinib]; HR = 0.624; CI, 0.389-1.002; P = 0.047). Diarrhea and dermatitis acneiform were more severe but tolerable with dacomitinib treatment compared to erlotinib group. Thus, based on phase II data, a randomized phase III trial was launched to compare the efficacy of dacomitinib with erlotinib as second-line treatment setting in unselected advanced NSCLC patients (ARCHER 1009; NCT01360554) (Table 4) [140].

Furthermore, an open-label phase II study evaluating dacomitinib as first-line treatment in adenocarcinoma patients who were never-smokers/former light-smokers, or patients who harbour EGFR mutations is ongoing (NCT00818441) [141]. A total of 92 patients have been already enrolled. Thirty-four of 46 EGFR-activating mutation-positive patients had PR (74%; CI: 59-86; exon 19 = 72%; exon 21 = 76%) and the reported median PFS was 17 months. PR rates and preliminary PFS were not significantly different for exons 19 and 21. Patients with wild-type EGFR had PR 7% (n=14; CI: 0-34) and PFS at 4 months 33% (n=14; CI: 11-58). The most common treatment-related side effects reported were dermatitis acneiform and diarrhea. Importantly, in these EGFR-TKI treatment-naïve patients, the daily dose of dacomitinib was reduced from 45 mg to 30 mg among some patients due to drug-related toxicity. Another multi-cohort, phase II safety study is now ongoing to assess the impact of daily dacomitinib as prophylactic treatment on the incidence of adverse events in advanced refractory NSCLC patients (ARCHER 1042 - NCT01465802). Moreover, the impact of an interrupted drug dosing schedule in first-line treatment of EGFR mutation-positive NSCLC patients (EGFR mutation or HER2 mutation/amplification) will be investigated.

More recently, a dose-related tumor shrinkage rate was observed in the combined analysis of multiple tumor size measurements collected from 200 patients from 4 clinical trials (3 phase I and 1 phase II) treated with 15 mg to 45 mg once daily dacomitinib [142]. Of note, 83% less shrinkage was observed in patients with wild-type EGFR when compared with mutants. Thus, further research is ongoing to evaluate the potential of this inhibitor in the treatment of EGFR-mutated NSCLCs.

Table 4. Summary of randomized phase III trials of second-generation irreversible EGFR-TKIs

Trial	Phase	Patients features	Treatment	Primary endpoint	Status (as of July 2012)
Dacomitinib					
JBR.26 *(NCT01000025)*	3	720 patients failing CT and EGFR-TKI	Dacomitinib or placebo	OS	Ongoing, recruiting
ARCHER 1009 *(NCT01360554)*	3	800 patients with 1–2 prior therapies (at least 1 must be standard CT for advanced NSCLC)	Dacomitinib or erlotinib	PFS	Ongoing, recruiting
Afatinib					
LUX-Lung 1 *(NCT00656136)*	3	585 patients failing CT and EGFR-TKI for at least 12 weeks	Afatinib or placebo	OS	Completed
LUX-Lung 3 *(NCT00949650)*	3	330 patients with treatment-naive adenocarcinoma harboring *EGFR*-activating mutations	Afatinib or cis+pem	PFS	Ongoing but no longer recruiting
LUX-Lung 5 *(NCT01085136)*	3	1100 patients failing CT and EGFR-TKI who subsequently achieved benefit with afatinib monotherapy	Afatinib followed by afatinib + pac or CT	PFS	Ongoing but no longer recruiting
LUX-Lung 6 *(NCT01121393)*	3	364 patients with treatment-naive adenocarcinoma harboring *EGFR*-activating mutations	Afatinib or cis+gem	PFS	Ongoing but no longer recruiting
LUX-Lung 8 *(NCT01523587)*	3	Estimated enrollment 800 patients with advanced squamous cell carcinoma of the lung who failed CT	Afatinib or erlotinib	PFS	Ongoing, recruiting

Cis, cisplatin; CT, chemotherapy; gem, gemcitabine; pac, paclitaxel; pem, pemetrexed.

4.4. Afatinib (BIBW 2992)

The anilinoquinazoline derivative afatinib (Boehringer Ingelheim; Ingelheim, Germany), is a compound designed to covalently bind EGFR and HER2, and inhibit the kinase activity of both wild-type and mutant receptors [143]. In a phase I study 50 mg once daily was determined as the MTD and recommended phase 2 dose of afatinib in solid tumors [144]. Gastrointestinal events, such as diarrhea, nausea and vomiting, together with fatigue and rash were the most common treatment-related side effects reported [144]. Afatinib is systemically evaluated in multiple major clinical studies in NSCLC (LUX-Lung trials) testing different treatment strategies [145].

The Japanese phase I/II trial LUX-Lung 4, confirmed the MTD of 50 mg once daily of afatinib in Asian patients who had received previous standard therapy (chemotherapy and/or EGFR-TKIs) or ineligible for existing therapies [146]. The phase II part of the trial included patients who failed chemotherapy treatment and subsequently received advantage, for at least 3 months, from gefitinib or erlotinib (NCT00711594) [147]. Grade 3 mucositis was reported as reversible DLT with 50 mg afatinib once daily treatment. Similar to non-Asian patients, other treatment-related adverse events of grade 2 severity, such as stomatitis, diarrhea, anorexia, rash, dry skin, and paronychia were observed in this population [146].

The randomized phase IIb/III trial LUX-Lung 1 compared afatinib to placebo (both plus BSC) in patients with NSCLC whose disease progressed either after receiving one or two previous lines of chemotherapy and gefitinib or erlotinib for at least 12 weeks (NCT00656136) (Table 4). The primary endpoint was OS. Five hundred eighty five patients were randomly assigned to treatment (n=390 [afatinib], n=195 [placebo]). The reported median PFS was prolonged with afatinib when compared with placebo (3.3 vs. 1.1 months, respectively: HR = 0.38; P < 0.0001). However, where the median OS was 10.8 months in the afatinib arm and 12.0 months in the placebo group (HR = 1.08; CI: 0.86-1.35; P = 0.74) the endpoint was not achieved. Diarrhea and rash/acne were reported as the most common side effects with afatinib treatment (87% and

78%, respectively) [148]. Despite the LUX-Lung 1 trial failed to meet the primary endpoint of prolonging OS, a trend towards an extended OS (11% improvement in survival probability, HR = 0.9; CI: 0.69-1.18) for the subgroup of EGFR mutation-positive patients (n=391) was reported [149].

The LUX-Lung 2 is a phase II trial evaluating afatinib in stage IIIB/IV lung adenocarcinoma patients with activating EGFR mutations, either chemotherapy-naïve or after one line of neoadjuvant/adjuvant chemotherapy (NCT00525148). Among the 129 mutation-positive patients who were treated with the inhibitor, the objective RR was 61%. Of note, 66% of the 106 patients with the two common activating EGFR mutations (deletion exon 19 or L858R mutation) had an objective response, and no difference in the RR between these mutations was observed. Diarrhea and rash/acne were reported as the most common adverse events with dose-related severity [150].

The observations collected in the LUX-Lung 2 study, set the stage for the registration trials LUX-Lung 3 (NCT00949650) and LUX-Lung 6 (NCT01121393). These two ongoing phase III trials, are evaluating the efficacy and safety profile of afatinib versus chemotherapy as first-line treatment for EGFR mutation-positive NSCLC patients in different geographical regions, with PFS as the primary endpoint. Preliminary data from the LUX-Lung 3 trial on 345 patients showed prolonged PFS with afatinib treatment (11.1 months [afatinib] vs. 6.9 months [pemetrexed/cisplatin]; HR = 0.58; P=0.0004) suggesting the use of the TKI as potential first-line setting option. Interestingly, a longer PFS with afatinib treatment was also observed in the subset of patients with common activating EGFR mutations when compared to those treated with chemotherapy (13.6 vs. 6.9 months, respectively; HR = 0.47; P<0.0001). Objective RR was higher with afatinib (56% vs. 23%; P<0.001) and adverse events related to such treatment were manageable and with a lower discontinuation rate than pemetrexed/cisplatin treatment (8% versus 12%) [151].

Furthermore, a randomized, open-label, phase IIb trial (LUX-Lung 7) is now ongoing comparing afatinib to gefitinib as first-line treatment setting in EGFR mutation-positive adenocarcinoma patients (NCT01466660). A randomized phase III trial evaluating the efficacy of afatinib given as an add-on to paclitaxel compared to chemotherapy alone in NSCLC patients progressing after afatinib monotherapy is ongoing (LUX-Lung 5 - NCT01085136). The estimated enrollment for this study is 1100 patients and PFS the primary endpoint. Another ongoing randomized, phase III trial (LUX-Lung 8), will evaluate the efficacy of afatinib compared to erlotinib as second-line treatment in patients with advanced squamous cell carcinoma of the lung (NCT01523587) (Table 4).

Given the promising results of the previous studies, several phase I/II clinical trials are now ongoing to explore efficacy and safety profile of afatinib in different settings and combinations for the treatment of advanced NSCLC patients (NCT01156545, NCT00730925, NCT00796549, NCT00993499, NCT01003899, NCT01090011, NCT01415011, NCT01553942).

5. THIRD-GENERATION EGFR-TKIs

The currently available second-generation EGFR-TK inhibitors showed reduced efficacy in cell-line models harbouring the gatekeeper mutation with respect to those having activating-EGFR mutations. Thus, at clinically achievable concentrations, these agents do not inhibit EGFR-T790M in vitro [124,133,141,152].

Furthermore, because the ATP affinity of the T790M-mutant receptor is similar to the one of the wild-type, the concentrations of inhibitors which are required to inhibit the mutant EGFR also effectively inhibit the

wild-type receptor. Clinically, the inhibition of wild-type EGFR results in side effects, such as diarrhea and skin rash, and limits drug dosage, reducing the chances to achieve plasma concentrations able to inhibit the T790M mutant receptor. Consequently, the clinical efficacy of second-generation irreversible EGFR inhibitors, including canertinib and neratinib, has been limited in NSCLC patients who relapsed after first-generation EGFR-TKIs treatment [126,133]. Moreover, focal amplification of EGFR, that preferentially involves the T790M-containing allele, has been reported as mechanism of acquired resistance to dacomitinib in preclinical models. Importantly, the growth of these cell lines resistant to second-generation inhibitor was observed to remain dependent on EGFR signaling [153]. Based on these findings, multiple mutant selective irreversible inhibitors have recently been identified as potential drug candidates for the treatment of NSCLC patients with the aim to overcome T790M mutation-related resistance to EGFR-TKIs.

The irreversible WZ4002 pyrimidine EGFR-TKI was effective in preclinical NSCLC models harboring T790M-EGFR. In particular, this agent was 30- to 100-fold more potent against T790MEGFR, and up to 100-fold less potent against wild-type EGFR, than quinazoline-based EGFR inhibitors in vitro [154]. A recent study also reported the efficacy of this third-generation TKI, in combination with the Bcl-2 inhibitor ABT-263 and trichostatin A as HDAC inhibitor, in suspended EGFR-mutant lung adenocarcinoma cells which seem to depend more on EGFR signaling for survival than adherent cells do [155]. Furthermore, preclinical models of resistance to WZ4002 have been established from cell lines harbouring common EGFR mutations, and novel secondary mutations of the receptor have been identified and correlated with the acquired resistance to the treatment. Interestingly, such mutations not always lead to cross-resistance to other EGFR-TKIs suggesting the combination of EGFR-TKIs as potential scenario for NSCLC patients [156].

CO-1686 is also a novel irreversible EGFR-TKI which preferentially targets the mutant forms of the receptor. In particular, this compound showed inhibitory activity against both common activating mutations and the T790M mutation, in vitro and in vivo, but not in cell lines harboring wild-type EGFR [157]. Furthermore, CO-1686 caused tumor shrinkage as a single agent in EGFR exon 19 deletion and T790M-mutation positive NSCLC tumor models. Importantly, this agent inhibited mutant EGFR signaling in tumor tissue, but no inhibitory effect was reported towards wild-type EGFR signaling in normal lung tissue. A phase I/II trial evaluating CO-1686 safety and efficacy profile in NSCLC patients who relapsed after upfront treatment with erlotinib or gefitinib, is now ongoing (NCT01526928).

6. ALTERNATIVE APPROACHES

6.1. Combination of Targeted Agents with Chemotherapy

As previously discussed, a randomized, phase II trial (CALGB 30406) is now ongoing to test erlotinib as single agent or in combination with carboplatin/paclitaxel as first-line treatment for never-smokers/light-smokers with PFS as the primary endpoint [70]. No difference in the PFS of the whole population was found between the treatments, either in the retrospective analysis of EGFR mutational status. Of note, even if not statistically significant, a prolonged OS for EGFR mutation-positive patients treated with the combination of erlotinib with carboplatin/paclitaxel was reported [70]. Thus, the evaluation of the potential effects of combining EGFR-TKI and chemotherapy as upfront therapy for EGFR mutation-positive NSCLC patients becomes a tempting future prospective.

Furthermore, since tumors harboring activating EGFR mutations depend on the receptor signals to grow

and proliferate, the continuous suppression of the EGFR-dependent clones by the inhibitor may be necessary after disease progression, while the addition of chemotherapy abolishes the growth of EGFR-independent clones. Considering the “oncogene addiction” concept, the combination of paclitaxel with gefitinib after failure of first-line TKI treatment has been investigated in advanced NSCLC patients [158]. A retrospective cohort study reported RR of 13%, control disease rate of 75%, median PFS of 4.3 months and median OS 8.1 months. These results suggested the combination of paclitaxel and gefitinib as eventually advantageous in patients who relapsed after first-line EGFR-TKI therapy. The same idea represents the base of the previously reported LUX-Lung 5 study evaluating afatinib in combination with paclitaxel with respect to chemotherapy alone. Alternative schedules of EGFR-TKI and chemotherapy are being evaluated.

6.2. Signaling Pathways Inhibition at Different Levels

Concomitant inhibition of EGFR and other key molecules involved in its signaling pathways may be an alternative approach to bypass resistance to first-generation EGFR-TKIs for the treatment of lung cancers. Since MET amplification accounts for around 20% of the cases of acquired resistance to gefitinib or erlotinib treatment, the combination of EGFR and MET inhibitors may delay the emergence of resistance to single-agent gefitinib or erlotinib through such mechanism. The combination of erlotinib with the MET-TKI tivantinib (ARQ197) has been investigated in a phase I study demonstrating to be well tolerated [159]. So far, a phase II clinical study comparing the combination of such agents with erlotinib alone in the second-line treatment of NSCLC patients, failed to meet the primary endpoint of prolonging PFS [160]. However, multiple phase II/III trials are now ongoing to determine whether this combination approach may be effective in the treatment of advanced NSCLC patients who relapsed after first-line chemotherapy or single-agent EGFR-TKI (NCT01580735, NCT01377376, NCT01244191). Further clarification of the pathways leading to acquired resistance is essential to maximize the efficacy of targeting treatment in advanced NSCLC patients.

6.3. Target Inhibition at Different Levels

The approach of combining TKIs and monoclonal antibodies directed against different regions of the same target may result in improved inhibition of such target. Recently published preclinical and clinical studies evaluating the combination of erlotinib with the anti-EGFR mAb cetuximab, reported the synergism of such combination in colon cancer cell lines and in chemotherapy-refractory colorectal cancer patients [161]. However, the same combination did not result in any response in a phase I/II clinical study conducted in advanced NSCLC patients who acquired resistance to first-line erlotinib treatment [162]. Interestingly, in a NSCLC xenograft model of tumor harbouring the T790M mutation, the combination of the second-generation EGFR-TKI afatinib with cetuximab, but not the combination of gefitinib with the antibody, resulted in a significant tumor size reduction [163]. Furthermore, a phase I study reported PR of about 30% obtained with the combination of afatinib with cetuximab in NSCLC patients harbouring T790M tumors [164]. All the 22 patients treated with the recommended phase 2 dose for the combination (40 mg once daily of afatinib and 500 mg/m2 IV every 2 weeks of cetuximab) showed disease control with tumor shrinkage of up to 76% at the time of reporting. The encouraging preliminary results led to the expansion of the testing cohort for further evaluation of such treatment strategy [164].

7. CONCLUSIONS

In the last few years, multiple TKIs have been approved for cancer treatment, while several others are currently under evaluation. Based on the findings on the critical involvement of EGFR in tumor development and progression, small molecules, such as gefitinib and erlotinib, were rationally designed to inhibit the activity of this key receptor. Given their efficacy in the subset of EGFR activating mutation-positive advanced NSCLC patients, gefitinib has been approved as first-line treatment in selected patients and the first-generation EGFR-TKIs have been approved as second- and third-line treatment in unselected NSCLCs. Furthermore, thanks to their tolerability and safety profile, these drugs have also been approved as maintenance therapy by FDA. Disappointingly, the use of these first-generation EGFR-TKIs has been limited by the emergence of different mechanisms of resistance, of which the most common is the occurrence of a secondary mutation in the target, and new strategies are needed to overcome such a problem. To date, the design of second-generation irreversible EGFR inhibitors has been suggested as a possible strategy to overcome this resistance. Unfortunately, EGFR-T790M is a common resistance mechanism to both reversible and, when amplified, irreversible EGFR-TKIs. The development of more potent and specific therapies against the gatekeeper mutation with the design of novel selective agents and the identification of new biomarkers to tailor the use of these targeting drugs are urgently needed. Hopefully, genetic studies will accelerate the transfer of basic research results to clinical practice and better define the characteristics of patients' selection for EGFR-TKIs treatment by identifying both genetically high-risk subgroup for drug-resistance or toxicity, and patients more likely to respond to these treatments.

ACKNOWLEDGEMENTS

This work was partially supported by: Associazione Italiana per la Ricerca sul Cancro (AIRC), Milan grant IG 8856.

REFERENCES

1. Govindan R, Page N, Morgensztern D, et al. Changing epidemiology of small-cell lung cancer in the United States over the last 30 years: analysis of the surveillance, epidemiologic, and end results database. J Clin Oncol 2006; 24(28):4539–44.
2. Scagliotti GV, Parikh P, von Pawel J, et al. Phase III study comparing cisplatin plus gemcitabine with cisplatin plus pemetrexed in chemotherapy-naive patients with advanced-stage non-small-cell lung cancer. J Clin Oncol 2008; 26(21):3543–51.
3. Sandler A, Gray R, Perry MC, et al. Paclitaxel-carboplatin alone or with bevacizumab for non-small-cell lung cancer. N Engl J Med 2006; 355(24):2542–50.
4. Siegel R, Naishadham D, Jemal A. Cancer Statistics 2012. CA Cancer J Clin 2012; (62):10–29.
5. Socinski MA, Crowell R, Hensing TE, et al. Treatment of non-small cell lung cancer, stage IV: ACCP evidence-based clinical practice guidelines (2nd edition). Chest 2007; 132(3 Suppl):277S–289S.
6. Chemotherapy in addition to supportive care improves survival in advanced non-small-cell lung cancer: a systematic review and meta-analysis of individual patient data from 16 randomized controlled trials. J Clin Oncol 2008; 26(28):4617–25.
7. Noble J, Ellis PM, Mackay JA, Evans WK. Second-line or subsequent systemic therapy for recurrent or progressive non-small cell lung cancer: a systematic review and practice guideline. J Thorac Oncol 2006; 1(9):1042–58.
8. Shepherd FA, Dancey J, Ramlau R, et al. Prospective randomized trial of docetaxel versus best supportive care in patients with non-small-cell lung cancer previously treated with platinum-based chemotherapy. J Clin Oncol 2000; 18(10):2095–103.
9. Tsuruo T. Molecular cancer therapeutics: recent progress and targets in drug resistance. Int Med 2003; 42(3):237–43.
10. Herbst RS, Heymach JV, Lippman SM. Lung cancer. N Engl J Med 2008; 359(13):1367–80.
11. Hoang T, Schiller JH. Advanced NSCLC: from cytotoxic systemic chemotherapy to molecularly targeted therapy. Expert Rev Anticanc 2002; 2(4):393–401.
12. Druker BJ, Talpaz M, Resta DJ, et al. Efficacy and safety of a specific inhibitor of the BCR-ABL tyrosine kinase in chronic myeloid leukemia. N Engl J Med 2001; 344(14):1031–7.
13. Hynes NE, Lane HA. ERBB receptors and cancer: the complexity of targeted inhibitors. Nat Rev Cancer 2005; 5(5):341–54.
14. Sibilia M, Kroismayr R, Lichtenberger BM, et al. The epidermal growth factor receptor: from development to tumorigenesis. Differentiation 2007; 75(9):770–87.
15. Miettinen PJ, Warburton D, Bu D, et al. Impaired lung branching morphogenesis in the absence of functional EGF receptor. Dev Biol. 1997; 186(2):224–36.
16. Luetteke NC, Qiu TH, Peiffer RL, et al. TGF alpha deficiency results in hair follicle and eye abnormalities in targeted and waved-1 mice. Cell 1993; 73(2):263–78.
17. Luetteke NC, Qiu TH, Fenton SE, et al. Targeted inactivation of the EGF and amphiregulin genes reveals distinct roles for EGF receptor ligands in mouse mammary gland development. Development 1999; 126(12):2739–50.
18. Yoshida T, Zhang G, Haura EB. Targeting epidermal growth factor receptor: central signaling kinase in lung cancer. Biochem Pharmacol 2010; 80(5):613–23.
19. Yarden Y, Sliwkowski MX. Untangling the ErbB signalling network. Nat Rev Mol Cell Bio 2001; 2(2):127–37.
20. Schlessinger J. Common and distinct elements in cellular signaling via EGF and FGF receptors. Science 2004; 306(5701):1506–7.
21. Schlessinger J. Ligand-induced, receptor-mediated dimerization and activation of EGF receptor. Cell 2002; 110(6):669–72.
22. Normanno N, De Luca A, Bianco C, et al. Epidermal growth factor receptor (EGFR) signaling in cancer. Gene 2006; 366(1):2–16.
23. Scaltriti M, Baselga J. The epidermal growth factor receptor pathway: a model for targeted therapy. Clin Cancer Res 2006; 12(18):5268–72.
24. Bjornsti M-A, Houghton PJ. The TOR pathway: a target for cancer therapy. Nat Rev Cancer 2004; 4(5):335–48.
25. Goswami A, Ranganathan P, Rangnekar VM. The phosphoinositide 3-kinase/Akt1/Par-4 axis: a cancer-selective therapeutic target. Cancer Res 2006; 66(6):2889–92.
26. Engelman JA, Jänne PA, Mermel C, et al. ErbB-3 mediates phosphoinositide 3-kinase activity in gefitinib-sensitive non-small cell lung cancer cell lines. P Natl Acad Sci USA 2005; 102(10):3788–93.
27. Mattoon DR, Lamothe B, Lax I, Schlessinger J. The docking protein Gab1 is the primary mediator of EGF-stimulated activation of the PI-3K/Akt cell survival pathway. BMC Biol 2004; 2:24.
28. Roberts PJ, Der CJ. Targeting the Raf-MEK-ERK mitogen-activated protein kinase cascade for the treatment of cancer. Oncogene 2007; 26(22):3291–310.
29. Yu H, Jove R. The STATs of cancer--new molecular targets come of age. Nat Rev Cancer 2004; 4(2):97–105.

30. Wang Y, Pennock S, Chen X, Wang Z. Endosomal signaling of epidermal growth factor receptor stimulates signal transduction pathways leading to cell survival. Mol Cell Biol 2002; 22(20):7279–90.

31. Hirsch FR, Varella-Garcia M, Bunn PA, et al. Epidermal growth factor receptor in non small-cell lung carcinomas: correlation between gene copy number and protein expression and impact on prognosis. J Clin Oncol 2003; 21(20):3798–807.

32. Suzuki S, Dobashi Y, Sakurai H, et al. Protein overexpression and gene amplification of epidermal growth factor receptor in nonsmall cell lung carcinomas. An immunohistochemical and fluorescence in situ hybridization study. Cancer 2005; 103(6):1265–73.

33. Sato M, Shames DS, Gazdar AF, Minna JD. A translational view of the molecular pathogenesis of lung cancer. J Thorach Oncol 2007; 2(4):327–43.

34. Shigematsu H, Lin L, Takahashi T, et al. Clinical and biological features associated with epidermal growth factor receptor gene mutations in lung cancers. J Natl Cancer I 2005; 97(5):339–46.

35. Hirsch FR, Varella-Garcia M, Cappuzzo F. Predictive value of EGFR and HER2 overexpression in advanced non-small-cell lung cancer. Oncogene 2009; 28 Suppl 1:S32–7.

36. Sharma SV, Settleman J. ErbBs in lung cancer. Exp Cell Res 2009; 315(4):557–71.

37. Weinstein IB, Joe A. Oncogene addiction. Cancer Res 2008; 68(9):3077–80; discussion 3080.

38. Cappuzzo F, Ligorio C, Jänne PA, et al. Prospective study of gefitinib in epidermal growth factor receptor fluorescence in situ hybridization-positive/phospho-Akt-positive or never smoker patients with advanced non-small-cell lung cancer: the ONCOBELL trial. J Clin Oncol 2007; 25(16):2248–55.

39. Fukuoka M, Yano S, Giaccone G, et al. Multi-institutional randomized phase II trial of gefitinib for previously treated patients with advanced non-small-cell lung cancer (The IDEAL 1 Trial) [corrected]. J Clin Oncol 2003; 21(12):2237–46.

40. Kris MG, Natale RB, Herbst RS, et al. Efficacy of gefitinib, an inhibitor of the epidermal growth factor receptor tyrosine kinase, in symptomatic patients with non-small cell lung cancer: a randomized trial. JAMA 2003; 290(16):2149–58.

41. Pérez-Soler R, Chachoua A, Hammond LA, et al. Determinants of tumor response and survival with erlotinib in patients with non-small cell lung cancer. J Clin Oncol 2004; 22(16):3238–47.

42. Cohen MH, Williams GA, Sridhara R, et al. United States Food and Drug Administration drug approval summary: gefitinib (ZD1839) (Iressa) tablets. Clin Cancer Res 2004; 10(4):1212–8.

43. Thatcher N, Chang A, Parikh P, et al. Gefitinib plus best supportive care in previously treated patients with refractory advanced non-small-cell lung cancer: results from a randomised, placebo-controlled, multicentre study (Iressa Survival Evaluation in Lung Cancer). Lancet 2005; 366(9496):1527–37.

44. Giaccone G, Herbst RS, Manegold C, et al. Gefitinib in combination with gemcitabine and cisplatin in advanced non-small-cell lung cancer: a phase III trial--INTACT 1. J Clin Oncol 2004; 22(5):777–84.

45. Herbst RS, Giaccone G, Schiller JH, et al. Gefitinib in combination with paclitaxel and carboplatin in advanced non-small-cell lung cancer: a phase III trial--INTACT 2. J Clin Oncol 2004; 22(5):785–94.

46. Crinò L, Cappuzzo F, Zatloukal P, et al. Gefitinib versus vinorelbine in chemotherapy-naive elderly patients with advanced non-small-cell lung cancer (INVITE): a randomized, phase II study. J Clin Oncol 2008; 26(26):4253–60.

47. Kim ES, Hirsh V, Mok T, et al. Gefitinib versus docetaxel in previously treated non-small-cell lung cancer (INTEREST): a randomised phase III trial. Lancet 2008; 372(9652):1809–18.

48. Shepherd FA, Rodrigues Pereira J, Ciuleanu T, et al. Erlotinib in previously treated non-small cell lung cancer. N Engl J Med 2005; 353(2):123–32.

49. Ciuleanu T, Stelmakh L, Cicenas S, et al. Efficacy and safety of erlotinib versus chemotherapy in second-line treatment of patients with advanced, non-small-cell lung cancer with poor prognosis (TITAN): a randomised multicentre, open-label, phase 3 study. Lancet Oncol 2012; 13(3):300–8.

50. Cappuzzo F, Ciuleanu T, Stelmakh L, et al. Erlotinib as maintenance treatment in advanced non-small-cell lung cancer: a multicentre, randomised, placebo-controlled phase 3 study. Lancet Oncol 2010; 11(6):521–9.

51. Herbst RS, Prager D, Hermann R, et al. TRIBUTE: a phase III trial of erlotinib hydrochloride (OSI-774) combined with carboplatin and paclitaxel chemotherapy in advanced non-small-cell lung cancer. J Clin Oncol 2005; 23(25):5892–9.

52. Gatzemeier U, Pluzanska A, Szczesna A, et al. Phase III study of erlotinib in combination with cisplatin and gemcitabine in advanced non-small-cell lung cancer: the Tarceva Lung Cancer Investigation Trial. J Clin Oncol 2007; 25(12):1545–52.

53. Lynch TJ, Bell DW, Sordella R, et al. Activating mutations in the epidermal growth factor receptor underlying responsiveness of non-small-cell lung cancer to gefitinib. N Engl J Med 2004; 350(21):2129–39.

54. Paez JG, Jänne PA, Lee JC, et al. EGFR mutations in lung cancer: correlation with clinical response to gefitinib therapy. Science 2004; 304(5676):1497–500.

55. Hirsch FR, Witta S. Biomarkers for prediction of sensitivity to EGFR inhibitors in non-small cell lung cancer. Curr Opin Oncol 2005;

17(2):118–22.

56. Hirsch FR, Varella-Garcia M, Bunn PA, et al. Molecular predictors of outcome with gefitinib in a phase III placebo-controlled study in advanced non-small-cell lung cancer. J Clin Oncol 2006; 24(31):5034–42.
57. Hirsch FR, Varella-Garcia M, Dziadziuszko R, et al. Fluorescence in situ hybridization subgroup analysis of TRIBUTE, a phase III trial of erlotinib plus carboplatin and paclitaxel in non-small cell lung cancer. Clin Cancer Res 2008; 14(19):6317–23.
58. Wellcome trust sanger institute: Catalogue of somatic mutations in cancer. Available on: http://www.sanger.ac.uk/perl/genetics/CGP/cosmic?action=gene&ln=EGFR
59. De Pas T, Toffalorio F, Manzotti M, et al. Activity of epidermal growth factor receptor-tyrosine kinase inhibitors in patients with non-small cell lung cancer harboring rare epidermal growth factor receptor mutations. J Thorach Oncol 2011; 6(11):1895–901.
60. Pao W, Miller V, Zakowski M, et al. EGF receptor gene mutations are common in lung cancers from “never smokers” and are associated with sensitivity of tumors to gefitinib and erlotinib. P Natl Acad Sci USA 2004; 101(36):13306–11.
61. Mok TS, Wu Y-L, Thongprasert S, et al. Gefitinib or carboplatin-paclitaxel in pulmonary adenocarcinoma. N Engl J Med 2009; 361(10):947–57.
62. Sharma SV, Bell DW, Settleman J, Haber DA. Epidermal growth factor receptor mutations in lung cancer. Nat Rev Cancer 2007; 7(3):169–81.
63. Eberhard DA, Johnson BE, Amler LC, et al. Mutations in the epidermal growth factor receptor and in KRAS are predictive and prognostic indicators in patients with non-small-cell lung cancer treated with chemotherapy alone and in combination with erlotinib. J Clin Oncol 2005; 23(25):5900–9.
64. Kim YT, Kim T-Y, Lee DS, et al. Molecular changes of epidermal growth factor receptor (EGFR) and KRAS and their impact on the clinical outcomes in surgically resected adenocarcinoma of the lung. Lung Cancer 2008; 59(1):111–8.
65. Marks JL, Broderick S, Zhou Q, et al. Prognostic and therapeutic implications of EGFR and KRAS mutations in resected lung adenocarcinoma. J Thorach Oncol 2008; 3(2):111–6.
66. Tomizawa Y, Iijima H, Sunaga N, et al. Clinicopathologic significance of the mutations of the epidermal growth factor receptor gene in patients with non-small cell lung cancer. Clin Cancer Res 2005; 11(19 Pt 1):6816–22.
67. Pao W, Miller VA. Epidermal growth factor receptor mutations, small-molecule kinase inhibitors, and non-small-cell lung cancer: current knowledge and future directions. J Clin Oncol 2005; 23(11):2556–68.
68. Fukuoka M, Wu Y-L, Thongprasert S, et al. Biomarker analyses and final overall survival results from a phase III, randomized, open-label, first-line study of gefitinib versus carboplatin/paclitaxel in clinically selected patients with advanced non-small-cell lung cancer in Asia (IPASS). J Clin Oncol 2011; 29(21):2866–74.
69. Hartmann JT, Haap M, Kopp H-G, Lipp H-P. Tyrosine kinase inhibitors - a review on pharmacology, metabolism and side effects. Curr Drug Metab 2009; 10(5):470–81.
70. Janne PA, Wang X, Socinski MA, et al. Randomized Phase II Trial of Erlotinib Alone or With Carboplatin and Paclitaxel in Patients Who Were Never or Light Former Smokers With Advanced Lung Adenocarcinoma: CALGB 30406 Trial. J Clin Oncol 2012; 30(17):2063–9.
71. Mitsudomi T, Morita S, Yatabe Y, et al. Gefitinib versus cisplatin plus docetaxel in patients with non-small-cell lung cancer harbouring mutations of the epidermal growth factor receptor (WJTOG3405): an open label, randomised phase 3 trial. Lancet Oncol 2010; 11(2):121–8.
72. Maemondo M, Inoue A, Kobayashi K, et al. Gefitinib or chemotherapy for non-small-cell lung cancer with mutated EGFR. N Engl J Med 2010; 362(25):2380–8.
73. Zhou C, Wu Y-L, Chen G, et al. Erlotinib versus chemotherapy as first-line treatment for patients with advanced EGFR mutation-positive non-small-cell lung cancer (OPTIMAL, CTONG-0802): a multicentre, open-label, randomised, phase 3 study. Lancet Oncol 2011; 12(8):735–42.
74. Rosell R, Carcereny E, Gervais R, et al. Erlotinib versus standard chemotherapy as first-line treatment for European patients with advanced EGFR mutation-positive non-small-cell lung cancer (EURTAC): a multicentre, open-label, randomised phase 3 trial. Lancet Oncol 2012; 13(3):239–46.
75. Han J-Y, Park K, Kim S-W, et al. First-SIGNAL: First-Line Single-Agent Iressa Versus Gemcitabine and Cisplatin Trial in Never-Smokers With Adenocarcinoma of the Lung. J Clin Oncol 2012; 30(10):1122–8.
76. Zhang L, Shenglin M, Song X, et al. Efficacy, tolerability, and biomarker analyses from a phase III, randomized, placebo-controlled, parallel group study of gefitinib as maintenance therapy in patients with locally advanced or metastatic non-small cell lung cancer (NSCLC; INFORM; C-TONG 0804). J Clin Oncol 2011; 29, suppl: abstract LBA7511.
77. Kobayashi S, Koizumi T, Agatsuma T, et al. A phase II trial of erlotinib in patients with EGFR wild-type advanced non-small-cell lung cancer. Cancer Chemother Pharmacol 2012; 69(5):1241-6.
78. Costa DB, Kobayashi S, Tenen DG, Huberman MS. Pooled analysis of the prospective trials of gefitinib monotherapy for EGFR-mutant non-small cell lung cancers. Lung Cancer 2007; 58(1):95–103.

79. Miller VA, Riely GJ, Zakowski MF, et al. Molecular Characteristics of Bronchioloalveolar Carcinoma and Adenocarcinoma, Bronchioloalveolar Carcinoma Subtype, Predict Response to Erlotinib. J Clin Oncol 2008; 26(9):1472–8.

80. Greulich H, Chen T-H, Feng W, et al. Oncogenic transformation by inhibitor-sensitive and -resistant EGFR mutants. PLoS Med 2005; 2(11):e313.

81. Stephens P, Hunter C, Bignell G, et al. Lung cancer: intragenic ERBB2 kinase mutations in tumors. Nature 2004; 431(7008):525–6.

82. Bell DW, Gore I, Okimoto RA, et al. Inherited susceptibility to lung cancer may be associated with the T790M drug resistance mutation in EGFR. Nat Genet 2005; 37(12):1315–6.

83. Shih J-Y, Gow C-H, Yang P-C. EGFR mutation conferring primary resistance to gefitinib in non-small-cell lung cancer. N Engl J Med 2005; 353(2):207–8.

84. Tibaldi C, Giovannetti E, Vasile E, et al. Inherited Germline T790M Mutation and Somatic Epidermal Growth Factor Receptor Mutations in Non-small. J Thorac Oncol 201; 6(2):395–6.

85. Godin-Heymann N, Bryant I, Rivera MN, et al. Oncogenic activity of epidermal growth factor receptor kinase mutant alleles is enhanced by the T790M drug resistance mutation. Cancer Res 2007; 67(15):7319–26.

86. Shimamura T, Lowell AM, Engelman JA, Shapiro GI. Epidermal growth factor receptors harboring kinase domain mutations associate with the heat shock protein 90 chaperone and are destabilized following exposure to geldanamycins. Cancer Res 2005; 65(14):6401–8.

87. Sawai A, Chandarlapaty S, Greulich H, et al. Inhibition of Hsp90 down-regulates mutant epidermal growth factor receptor (EGFR) expression and sensitizes EGFR mutant tumors to paclitaxel. Cancer Res 2008; 68(2):589–96.

88. Pao W, Wang TY, Riely GJ, et al. KRAS mutations and primary resistance of lung adenocarcinomas to gefitinib or erlotinib. PLoS Med 2005; 2(1):e17.

89. van Zandwijk N, Mathy A, Boerrigter L, et al. EGFR and KRAS mutations as criteria for treatment with tyrosine kinase inhibitors: retro- and prospective observations in non-small cell lung cancer. Ann Oncol 2007; 18(1):99–103.

90. Kranenburg O. The KRAS oncogene: past, present, and future. BBA-Rev 2005; 1756(2):81-2.

91. Riely GJ, Marks J, Pao W. KRAS mutations in non-small cell lung cancer. Proc Am Thorac Soc 2009; 6(2):201–5.

92. Subramanian J, Govindan R. Molecular genetics of lung cancer in people who have never smoked. Lancet Oncol 2008; 9(7):676–82.

93. Jackman DM, Yeap BY, Lindeman NI, et al. Phase II clinical trial of chemotherapy-naive patients > or = 70 years of age treated with erlotinib for advanced non-small-cell lung cancer. J Clin Oncol 2007; 25(7):760–6.

94. Kawano O, Sasaki H, Endo K, et al. PIK3CA mutation status in Japanese lung cancer patients. Lung Cancer 2006; 54(2):209–15.

95. Sun Y, Ren Y, Fang Z, et al. Lung adenocarcinoma from East Asian never-smokers is a disease largely defined by targetable oncogenic mutant kinases. J Clin Oncol 2010; 28(30):4616–20.

96. Ellis LM, Hicklin DJ. Resistance to Targeted Therapies: Refining Anticancer Therapy in the Era of Molecular Oncology. Clin Cancer Res 2009; 15(24):7471–8.

97. Cai D, Shames DS, Raso MG, et al. Steroid receptor coactivator-3 expression in lung cancer and its role in the regulation of cancer cell survival and proliferation. Cancer Res 2010; 70(16):6477–85.

98. Shaw AT, Yeap BY, Mino-Kenudson M, et al. Clinical features and outcome of patients with non-small-cell lung cancer who harbor EML4-ALK. J Clin Oncol 2009; 27(26):4247–53.

99. Frank NY, Schatton T, Frank MH. The therapeutic promise of the cancer stem cell concept. J Clin Invest 2010; 120(1):41–50.

100. Singh A, Settleman J. EMT, cancer stem cells and drug resistance: an emerging axis of evil in the war on cancer. Oncogene 2010; 29(34):4741–51.

101. Burris HA. Shortcomings of current therapies for non-small-cell lung cancer: unmet medical needs. Oncogene 2009; 28 Suppl 1:S4–13.

102. Jackman D, Pao W, Riely GJ, et al. Clinical definition of acquired resistance to epidermal growth factor receptor tyrosine kinase inhibitors in non-small-cell lung cancer. J Clin Oncol 2010; 28(2):357–60.

103. Costa DB, Halmos B, Kumar A, et al. BIM mediates EGFR tyrosine kinase inhibitor-induced apoptosis in lung cancers with oncogenic EGFR mutations. PLoS Med 2007; 4(10):1669–79; discussion 1680.

104. Balak MN, Gong Y, Riely GJ, et al. Novel D761Y and common secondary T790M mutations in epidermal growth factor receptor-mutant lung adenocarcinomas with acquired resistance to kinase inhibitors. Clin Cancer Res 2006; 12(21):6494–501.

105. Bean J, Riely GJ, Balak M, et al. Acquired resistance to epidermal growth factor receptor kinase inhibitors associated with a novel T854A mutation in a patient with EGFR-mutant lung adenocarcinoma. Clin Cancer Res 2008; 14(22):7519–25.

106. Pao W, Miller VA, Politi KA, et al. Acquired resistance of lung adenocarcinomas to gefitinib or erlotinib is associated with a second

mutation in the EGFR kinase domain. PLoS Med 2005; 2(3):e73.

107. Kobayashi S, Boggon TJ, Dayaram T, et al. EGFR mutation and resistance of non-small-cell lung cancer to gefitinib. N Engl J Med 2005; 352(8):786–92.

108. Kosaka T, Yatabe Y, Endoh H, et al. Analysis of epidermal growth factor receptor gene mutation in patients with non-small cell lung cancer and acquired resistance to gefitinib. Clin Cancer Res 2006; 12(19):5764–9.

109. Yun C-H, Mengwasser KE, Toms AV, et al. The T790M mutation in EGFR kinase causes drug resistance by increasing the affinity for ATP. P Natl Acad Sci USA 2008; 105(6):2070–5.

110. Maheswaran S, Sequist LV, Nagrath S, et al. Detection of mutations in EGFR in circulating lung-cancer cells. N Engl J Med 2008; 359(4):366–77.

111. Oxnard GR, Arcila ME, Sima CS, et al. Acquired resistance to EGFR tyrosine kinase inhibitors in EGFR-mutant lung cancer: distinct natural history of patients with tumors harboring the T790M mutation. Clin Cancer Res 2011; 17(6):1616–22.

112. Sequist LV, Waltman BA, Dias-Santagata D, et al. Genotypic and histological evolution of lung cancers acquiring resistance to EGFR inhibitors. Sci Transl Med 2011; 3(75):75ra26.

113. Engelman JA, Zejnullahu K, Mitsudomi T, et al. MET amplification leads to gefitinib resistance in lung cancer by activating ERBB3 signaling. Science 2007; 316(5827):1039–43.

114. Bean J, Brennan C, Shih J-Y, et al. MET amplification occurs with or without T790M mutations in EGFR mutant lung tumors with acquired resistance to gefitinib or erlotinib. P Natl Acad Sci USA 2007; 104(52):20932–7.

115. Turke AB, Zejnullahu K, Wu Y-L, et al. Preexistence and clonal selection of MET amplification in EGFR mutant NSCLC. Cancer Cell 2010; 17(1):77–88.

116. Toschi L, Jänne PA. Single-agent and combination therapeutic strategies to inhibit hepatocyte growth factor/MET signaling in cancer. Clin Cancer Res 2008; 14(19):5941–6.

117. Morgillo F, Kim W-Y, Kim ES, et al. Implication of the insulin-like growth factor-IR pathway in the resistance of non-small cell lung cancer cells to treatment with gefitinib. Clin Cancer Res 2007; 13(9):2795–803.

118. Guix M, Faber AC, Wang SE, et al. Acquired resistance to EGFR tyrosine kinase inhibitors in cancer cells is mediated by loss of IGF-binding proteins. J Clin Invest 2008; 118(7):2609–19.

119. Kwak EL, Sordella R, Bell DW, et al. Irreversible inhibitors of the EGF receptor may circumvent acquired resistance to gefitinib. P Natl Acad Sci USA 2005; 102(21):7665–70.

120. 120. Elkind NB, Szentpétery Z, Apáti A, et al. Multidrug transporter ABCG2 prevents tumor cell death induced by the epidermal growth factor receptor inhibitor Iressa (ZD1839, Gefitinib). Cancer Res 2005; 65(5):1770–7.

121. Engelman JA, Mukohara T, Zejnullahu K, et al. Allelic dilution obscures detection of a biologically significant resistance mutation in EGFR-amplified lung cancer. J Clin Invest 2006; 116(10):2695–706.

122. Yao Z, Fenoglio S, Gao DC, et al. TGF-beta IL-6 axis mediates selective and adaptive mechanisms of resistance to molecular targeted therapy in lung cancer. P Natl Acad Sci USA 2010; 107(35):15535–40.

123. Engelman JA, Zejnullahu K, Gale C-M, et al. PF00299804, an irreversible pan-ERBB inhibitor, is effective in lung cancer models with EGFR and ERBB2 mutations that are resistant to gefitinib. Cancer Res 2007; 67(24):11924–32.

124. Fry DW, Bridges AJ, Denny WA, et al. Specific, irreversible inactivation of the epidermal growth factor receptor and erbB2, by a new class of tyrosine kinase inhibitor. P Natl Acad Sci USA 1998; 95(20):12022–7.

125. Chiappori AA, Ellis PM, Hamm JT, et al. A phase I evaluation of oral CI-1033 in combination with paclitaxel and carboplatin as first-line chemotherapy in patients with advanced non-small cell lung cancer. J Thorac Oncol 2006; 1(9):1010–9.

126. Janne PA, von Pawel J, Cohen RB, et al. Multicenter, randomized, phase II trial of CI-1033, an irreversible pan-ERBB inhibitor, for previously treated advanced non-small-cell lung cancer. J Clin Oncol 2007; 25(25):3936-44.

127. Rabindran SK, Discafani CM, Rosfjord EC, et al. Antitumor activity of HKI-272, an orally active, irreversible inhibitor of the HER-2 tyrosine kinase. Cancer Res 2004; 64(11):3958–65.

128. Ji H, Zhao X, Yuza Y, et al. Epidermal growth factor receptor variant III mutations in lung tumorigenesis and sensitivity to tyrosine kinase inhibitors. P Natl Acad Sci USA 2006; 103(20):7817–22.

129. Minami Y, Shimamura T, Shah K, et al. The major lung cancer-derived mutants of ERBB2 are oncogenic and are associated with sensitivity to the irreversible EGFR/ERBB2 inhibitor HKI-272. Oncogene 2007; 26(34):5023–7.

130. Shimamura T, Ji H, Minami Y, et al. Non-small-cell lung cancer and Ba/F3 transformed cells harboring the ERBB2 G776insV_G/C mutation are sensitive to the dual-specific epidermal growth factor receptor and ERBB2 inhibitor HKI-272. Cancer Res 2006; 66(13):6487–91.

131. Sequist LV, Besse B, Lynch TJ, et al. Neratinib, an irreversible pan-ErbB receptor tyrosine kinase inhibitor: results of a phase II trial in patients with advanced non-small cell lung cancer. J Clin Oncol 2010; 28(18):3076–83.

132. Wong K-K, Fracasso PM, Bukowski RM, et al. A phase I study with neratinib (HKI-272), an irreversible pan ErbB receptor tyrosine

kinase inhibitor, in patients with solid tumors. Clin Cancer Res 2009; 15(7):2552–8.

133. Godin-Heymann N, Ulkus L, Brannigan BW, et al. The T790M “gatekeeper” mutation in EGFR mediates resistance to low concentrations of an irreversible EGFR inhibitor. Mol Cancer Ther 2008; 7(4):874–9.

134. Gonzales AJ, Hook KE, Althaus IW, et al. Antitumor activity and pharmacokinetic properties of PF-00299804, a second-generation irreversible pan-erbB receptor tyrosine kinase inhibitor. Mol Cancer Ther 2008; 7(7):1880–9.

135. Janne PA, Boss DS, Camidge DR, et al. Phase I dose-escalation study of the pan-HER inhibitor, PF-00299804, in patients with advanced malignant solid tumors. Clin Cancer Res 2011; 17(5): 1131-9.

136. Takahashi T, Boku N, Murakami H, et al. Phase I and pharmacokinetic study of dacomitinib (PF-00299804), an oral irreversible, small molecule inhibitor of human epidermal growth factor receptor-1, -2, and -4 tyrosine kinases, in Japanese patients with advanced solid tumors. Invest New Drugs 2012.

137. Campbell A, Reckamp KL, Camidge DR, et al. PF-00299804 (PF299) patient (pt)-reported outcomes (PROs) and efficacy in adenocarcinoma (adeno) and nonadeno non-small cell lung cancer (NSCLC): a phase (P) II trial in advanced NSCLC after failure of chemotherapy (CT) and erlotinib (E). J Clin Oncol 2010; 28, suppl: abstract 7596.

138. Park K, Heo DS, Cho B, et al. PF-00299804 (PF299) in Asian patients (pts) with non-small cell lung cancer (NSCLC) refractory to chemotherapy (CT) and erlotinib (E) or gefitinib (G): a phase (P) I/II study. J Clin Oncol, 2010; 28, suppl: abstract 7599.

139. Boyer MJ, Blackhall FH, Park K, et al. Efficacy and safety of PF299804 versus erlotinib: a global randomized phase 2 trial in patients with advanced non-small cell lung cancer (NSCLC) after failure of chemotherapy (CT). Oral presentation at: the 46th Annual Meeting of the American Society of Clinical Oncology, Chicago, IL, USA, June 4–8 (2010).

140. Boyer MJ, Janne PA, Mok T, et al. ARCHER: Dacomitinib (D; PF-00299804) versus erlotinib (E) for advanced (adv) non-small cell lung cancer (NSCLC) A randomized double-blind phase III study. J Clin Oncol 2012; 30, suppl; abstract TPS7615.

141. Kris MG, Mok T, Ou SH, et al. First-line dacomitinib (PF-00299804), an irreversible pan-HER tyrosine kinase inhibitor, for patients with EGFR-mutant lung cancers. J Clin Oncol, 2012; 30, suppl: abstract 7530.

142. Ruiz-Garcia A, Janne PA, Park K, et al. EGFR status and daily dose: Effect on tumor growth inhibition in cancer patients treated with dacomitinib (PF-00299804). J Clin Oncol 2012; 30, suppl: abstract e18093.

143. Li D, Ambrogio L, Shimamura T, et al. BIBW2992, an irreversible EGFR/HER2 inhibitor highly effective in preclinical lung cancer models. Oncogene 2008; 27(34):4702–11.

144. Yap TA, Vidal L, Adam J, et al. Phase I trial of the irreversible EGFR and HER2 kinase inhibitor BIBW 2992 in patients with advanced solid tumors. J Clin Oncol 2010; 28(25):3965–72.

145. Metro G, Crinò L. The LUX-Lung clinical trial program of afatinib for non-small-cell lung cancer. Expert Rev Anticancer Ther 2011; 11(5):673–82.

146. Murakami H, Tamura T, Takahashi T, et al. Phase I study of continuous afatinib (BIBW 2992) in patients with advanced non-small cell lung cancer after prior chemotherapy/erlotinib/gefitinib (LUX-Lung 4). Cancer Chemoth Pharm 2012; 69(4):891–9.

147. Atagi S, Katakami N, Hida T, et al. LUX-Lung 4: a phase II trial of afatinib (BIBW 2992) in advanced NSCLC patients previously treated with erlotinib or gefitinib Abstract associated with oral presentation at: the 14th Biennial World Conference on Lung Cancer, Amsterdam, Netherlands, July 3–7 (2011) [abstract O19.06].

148. Miller VA, Hirsh V, Cadranel J, et al. Afatinib versus placebo for patients with advanced, metastatic non-small-cell lung cancer after failure of erlotinib, gefitinib, or both, and one or two lines of chemotherapy (LUX-Lung 1): a phase 2b/3 randomised trial. Lancet Oncol 2012; 13(5):528–38.

149. Miller VA, Hirsh V, Cadranel J, et al. Subgroup analysis of LUX-Lung 1: a randomized phase III trial of afatinib (BIBW 2992) + best supportive care (BSC) versus placebo + BSC in patients with NSCLC failing 1–2 lines of chemotherapy and erlotinib or gefitinib. J Thorac Oncol 2010; 5, suppl: abstract LBPL3.

150. Yang JC-H, Shih J-Y, Su W-C, et al. Afatinib for patients with lung adenocarcinoma and epidermal growth factor receptor mutations (LUX-Lung 2): a phase 2 trial. Lancet Oncol 2012; 13(5):539–48.

151. Yang JC-H, Schuler MH, Yamamoto N, et al. LUX-Lung 3: a randomized, open-label, phase III study of afatinib versus pemetrexed and cisplatin as first-line treatment for patients with advanced adenocarcinoma of the lung harboring EGFR-activating mutations. J Clin Oncol 2012; 30, suppl: abstract LBA7500.

152. Yuza Y, Glatt KA, Jiang J, et al. Allele-dependent variation in the relative cellular potency of distinct EGFR inhibitors. Cancer Biol Ther 2007; 6(5):661–7.

153. Ercan D, Zejnullahu K, Yonesaka K, et al. Amplification of EGFR T790M causes resistance to an irreversible EGFR inhibitor. Oncogene 2010; 29(16):2346–56.

154. Zhou W, Ercan D, Chen L, et al. Novel mutant-selective EGFR kinase inhibitors against EGFR T790M. Nature 2009; 462(7276):1070–4.

155. Sakuma Y, Yamazaki Y, Nakamura Y, et al. WZ4002, a third-generation EGFR inhibitor, can overcome anoikis resistance in EGFR-mutant lung adenocarcinomas more efficiently than Src inhibitors. Lab Invest 2012; 92(3):371–83.

156. Ercan D, Xie T, Capelletti M, et al. Novel EGFR mutations that cause drug resistance to irreversible pyrimidine but not quinazoline based EGFR inhibitors. Oral presentation at AACR Annual Meeting 2012, Chicago [abstract 4832].

157. Walter AO, Tjin R, Haringsma H, et al. CO-1686, a novel mutant-selective EGFR inhibitor, overcomes T790M mediated resistance in Non-Small Cell Lung Cancer (NSCLC). AACR Annual Meeting 2012 [abstract 1791].

158. Shukuya T, Takahashi T, Tamiya A, et al. Gefitinib plus paclitaxel after failure of gefitinib in non-small cell lung cancer initially responding to gefitinib. Anti-Cancer Res 2009; 29(7):2747–51.

159. Goldman JW, Laux I, Chai F, et al. Phase 1 dose-escalation trial evaluating the combination of the selective MET (mesenchymal-epithelial transition factor) inhibitor tivantinib (ARQ 197) plus erlotinib. Cancer 2012 May 17. doi: 10.1002/cncr.27575. [Epub ahead of print]

160. Sequist LV, von Pawel J, Garmey EG, et al. Randomized phase II study of erlotinib plus tivantinib versus erlotinib plus placebo in previously treated non-small-cell lung cancer. J Clin Oncol 2011; 29(24):3307–15.

161. Weickhardt AJ, Price TJ, Chong G, et al. Dual Targeting of the Epidermal Growth Factor Receptor Using the Combination of Cetuximab and Erlotinib: Preclinical Evaluation and Results of the Phase II DUX Study in Chemotherapy-Refractory, Advanced Colorectal Cancer. J Clin Oncol 2012; 30(13):1505–12.

162. Janjigian YY, Azzoli CG, Krug LM, et al. Phase I/II trial of cetuximab and erlotinib in patients with lung adenocarcinoma and acquired resistance to erlotinib. Clin Cancer Res 2011; 17(8):2521–7.

163. Regales L, Gong Y, Shen R, et al. Dual targeting of EGFR can overcome a major drug resistance mutation in mouse models of EGFR mutant lung cancer. J Clin Invest 2009; 119(10):3000–10.

164. Janjigian YY, Groen HJ, Horn L, et al. Activity and tolerability of afatinib (BIBW 2992) and cetuximab in NSCLC patients with acquired resistance to erlotinib or gefitinib. J Clin Oncol 2011; 29, suppl: abstract 7525.

Chapter 4

EGFR-targeted therapy in NSCLC: role of germline polymorphisms in outcome and toxicity

Galvani E, Peters GJ & Giovannetti E.

FUTURE ONCOLOGY 2012

8:1015-29.

ABSTRACT

Conventional chemotherapeutic regimens have limited impact against most solid tumors and deal with significant toxicity. Over the last 10 years, novel anticancer treatments targeting specific molecules or genes involved in cancer progression have been developed to improve outcome and reduce side effects. In particular, the tyrosine kinase inhibitors gefitinib and erlotinib have been approved for the treatment of non-small-cell lung cancer. Their clinical activity has been related to different clinical and biological parameters, such as EGFR activating mutations. However, not all clinical outcomes, including tolerability, are explained, and the identification/validation of novel biomarkers is a viable area of research. Germline polymorphisms can be easily assessed in blood samples, and candidate polymorphisms in EGFR and ABCG2 have been correlated with outcome and toxicity in non-small-cell lung cancer patients treated with gefitinib or erlotinib. However, differences in study population and design resulted in several controversial findings, while the prognostic versus predictive role of the polymorphisms still needs to be validated within larger prospective studies. More studies on the relationship of the genotype with drug pharmacokinetics and mechanism of action are also warranted. These future studies, as well as further development and application of novel technologies to decipher genetic alterations, might contribute to the validation of selected polymorphisms as molecular markers predictive of drug activity and help in the selection of tyrosine kinase inhibitors best suited to the individual patient.

INTRODUCTION

Combined modality treatment, including surgery, radiation and chemotherapy, has reached an efficacy plateau against most solid tumors and is burdened by clinically relevant adverse effects [1–3]. The success of the ABL tyrosine kinase inhibitor imatinib for the treatment of chronic myeloid leukemia demonstrated the efficacy of targeting the key genetic lesions that promote proliferation of cancer cells [4]. From advances in understanding tumor biology and identification of several molecular targets, novel anticancer treatments have emerged during the last decade [5]. Through interaction with receptors, ligands, signaling molecules or genes that are pivotal in neoplastic growth and development, these new targeted drugs can inhibit proliferation of tumor cells, induce programmed cell death, inhibit angiogenesis or enhance antitumor immune response [6].

Protein kinases, including protein tyrosine kinases (PTKs), have been identified as targets because of their significantly different role in normal and cancerous cells. These phosphotransferases have a catalytic subunit that transfers the g-phosphate from nucleotide triphosphates (usually ATP) to amino acid residues in the substrate side chains of different proteins, resulting in conformational modifications influencing protein activity. Of the 518 protein kinases encoded in the human genome [7], 90 kinases belong to the group of PTKs. These enzymes are involved in the maintenance of cellular homeostasis and their activity is tightly regulated in normal cells. However, it has been well demonstrated that mutations or abnormal activation of PTKs lead to the development and progression of many cancers [8].

Non-small-cell lung cancer (NSCLC) represents the majority of human epithelial cancers and is frequently marked by functional activation of EGFR, suggesting the key biological role of this receptor in the amplification of cell growth and survival signaling [9,10]. Both monoclonal antibodies and small-molecule drugs have been demonstrated in the clinic to be effective in inhibiting the activity of PTKs.

The EGF receptor (EGFR) is overexpressed in 40–80% of cases, but the EGFR tyrosine kinase inhibitors (TKIs) gefitinib and erlotinib produce clinical responses in a small subgroup of NSCLC patients [11]. Conversely, EGFR amplification and activating mutations are associated with response to gefitinib [12] and erlotinib [13].

Although the introduction of these new agents has improved NSCLC treatment, oncologists are still facing relevant inter-individual variability in drug reactivity, toxicity and cancer outcomes, which might not only be caused by clinical and cancer molecular characteristics [14]. Thus, inherited genetic determinants may complement common clinical factors for the prediction of clinical outcome. These determinants are very appealing as predictive or prognostic markers, because they can be assessed in blood tissue and these analyses can be performed in the routine clinical setting, without the specific infrastructures needed for gene expression arrays of tumor specimens.

Inherited genetic polymorphisms, including single-nucleotide polymorphisms (SNPs) and variable numbers of tandem repeats, have been evaluated in several epidemiological studies as risk factors for NSCLC, mainly focusing on genes involved in the metabolism of xenobiotics [15]. By contrast, evaluation of the genetic polymorphisms or pharmacogenetics of EGFRtargeted therapy is a more recent research field.

The present review describes the main results achieved in this field and unravels the possible direction of future studies. Towards this aim, the authors reviewed the most important studies on genetic

polymorphisms correlated with drug activity or prognosis after EGFR-TKI treatment in NSCLC (Tables 1 & 2).

POLYMORPHISMS AFFECTING OUTCOME TO GEFITINIB

Gefitinib is an orally active, reversible EGFRTKI, and it has been used for treating advanced NSCLC with good tolerability and antitumor activity [16,17]. This drug has been approved for the treatment of patients with locally advanced or metastatic NSCLC after failure of at least one prior chemotherapy regimen [18,19]. Moreover, it is currently registered in most European countries as a first-line therapy for patients with EGFR activating mutations. This approval is based on the results of the IPASS study (Table 3), which showed superior progression-free survival (PFS), higher objective response rate, better tolerability and improvement in the quality-of-life benefits for gefitinib compared to carboplatin/paclitaxel doublet chemotherapy in patients selected according to their clinical characteristics in Asia [20,21]. In particular, PFS was significantly longer for gefitinib compared with standard chemotherapeutic regimens in patients harbouring EGFR-activating mutations. These results represent a significant step toward personalized medicine in NSCLC oncology.

Table 1. Functional germline polymorphisms affecting the outcome to the EGFR-TKIs gefitinib and erlotinib

Polymorphism	Location	Proposed functional effect
EGFR CA repeat	Chrom. 7, Intron 1	*EGFR* gene transcription declines with increasing number of *CA* repeats
EGFR R497K *A/G*	Chrom. 7, Exon 13	The substitution of Arginine by Lysine is associated with decreased EGFR activity
EGFR -216 *G/T*	Chrom. 7, Promoter	*T* allele associated with higher EGFR promoter activity
EGFR -191 *C/A*	Chrom 7, Exon 1	*A* allele associated with increased EGFR protein production
AKT1-SNP4	Chrom. 14, Exon 11	*A* allele associated with reduced *AKT1* mRNA
ABCG2 421 *C/A* (Q141K)	Chrom 4, Exon 5	*A* allele associated with reduced transport of TKIs
ABCG2 -15622 *C/T*	Chrom. 4, Promoter	*T* allele associated with lower ABCG2 expression
ABCG2 1143 *C/T*	Chrom. 4, Exon 4	*T* allele associated with lower ABCG2 expression
*CYP3A5*3*	Chrom. 7, Exon 7	*CYP3A5*3* variant associated with significant reduction in the protein and activity
*CYP3A4*1B*	Chrom. 7, Exon 7	*CYP3A4*1B* variant associated with two-fold higher promoter activity

However, other factors could be critical in the future of personalized targeted therapy, and these factors might play a key role in populations with a low frequency of somatic mutations. Furthermore, gefitinib also showed cytotoxic activity in NSCLC cells without EGFR activating mutations [22]. Finally, in the IPASS trial, gefitinib demonstrated a more favourable tolerability profile than chemotherapy, but there was still a large and unpredictable interindividual variability in toxicity [23]. Therefore, recent studies have focused on other potential markers to predict the responsiveness and toxicity to gefitinib, including germline polymorphisms.

EGFR POLYMORPHISMS

In order to understand the role of polymorphisms in the EGFR gene and in EGFR-related genes in the response and toxicity to EGFR-TKI therapy in NSCLC, several studies have been performed (Figure 1). In particular, most variants in the region that regulates the expression of the EGFR gene have been evaluated.

Table 2. Clinical studies on polymorphisms correlated with prognosis after gefitinib/erlotinib treatment

Study	Num. patients	Studied Polymorphisms	Effects	Ref.
Liu G, et al. 2008	92	EGFR: 216G/T,191C/A, Intr1, R497K	-*216G/T*:T allele is associated with longer PFS, increased SD/PR and risk of developing rash and diarrhea -*Intr1* homozygosis of short allele associated with longer PFS and OS	27
Ichiara T, et al. 2007	98	EGFR: 216G/T,191C/A, Intr1, mut, copy-num; KRAS: mut	-EGFR mut are associated with longer PFS and OS -short Intr1 increased OS in EGFR mutated patients	28
Gregorc V, et al. 2008	170	EGFR: 216G/T,191C/A	-G-C haplotype is associated with reduced RR	29
Han SW, et al. 2007	86	EGFR: Intr1, mut	-short Intr1 is associated with higher RR and increased TTP - EGFR mut are associated with longer OS	34
Ma F, et al. 2009	84	Whole gene based-tag SNP	-EGFR rs2293347GG(D994D) is associated with higher RR and longer PFS than GA and AA -short Intr1 is associated with higher RR	35
Dubey S, et al. 2006	157	EGFR: Intr1	-short Intr1 is associated with squamous cell histology -long Intr1 is associated with longer OS	36
Nie Q, et al. 2007	70	EGFR: Intr1, R497K	-short Intr1 is associated with higher EGFR expression, higher RR and longer PFS	37
Tiseo M, et al. 2008	58	EGFR: Intr1, mut, copy-num	-short Intr1 is associated with longer OS	38
Tiseo M, et al. 2010	91	EGFR: Intr1, mut, copy-num, expression; KRAS: mut; HER2: copy-num	-EGFR mut and copy-num are associated with higher RR -short Intr1 is associated with longer OS	39
Giovannetti E, et al. 2010	96	EGFR: 216G/T,191C/A, R497K, Intr1, mut; KRAS: mut; AKT1-SNP4	-EGFR mut are associated with higher RR, TTP and OS -216G/T, 191C/A and R497K are associated with higher risk of developing grade>1 diarrhea -AKT1-SNP4 A/A is associated with reduced TTP and OS	40
Liu G, et al. 2012	242	EGFR: 216G/T,191C/A, Intr1; ABCG2: 421C>A; AKT1-SNP4G>A	-long Intr1 is associated with reduced PFS -216T/T genotype is associated with higher risk of developing rash	41
Cappuzzo F, et al. 2004	106	Akt: activation; MAPK: activation	-p-Akt is associated with higher RR, DCR and TTP	44
Cappuzzo F, et al. 2007	42	EGFR: mut, copy-num; KRAS: mut; HER2: mut, copy-num; Akt: activation	-EGFR high copy-num is associated with higher RR, TTP and OS	45
Kim MJ, et al. 2012	310	AKT1: rs3803300, rs1130214, rs3730358, rs1130233, rs2494732	-rs3803300, rs1130214 and rs2494732 when combined are associated with worse OS and PFS	50
Lemos C, et al. 2011	94	ABCG2: 15622C/T, 1143C/T	-15622T/T and TT haplotype are associated with higher risk of developing grade 2/3 diarrhea	53
Han JY, et al. 2011	158	XRCC1: codon 399; ERCC1: codon 8092; RRMI: codon 2464	-XRCC1 399Arg/Arg is associated with higher RR and longer PFS than Gln allele -ERCC1 8092CA and RRMI 2464GG genotypes are associated with longer PFS	60
Huang CL, et al. 2009	52	EGFR: 216G/T,191C/A, R521K, Intr1	-homozygosis of short Intr1 is associated with higher risk of developing early grade 2/3 rash	62
Rudin CM, et al. 2008	43	EGFR: 216G/T,191C/A, 497G/A; CYP3A4*1B; CYP3A5*3; ABCG2: 421C/A, 34G/A, 15994G/A, 15622C>T, 16702G/A, 1143C/T	-15622C/T and 1143C/T: T allele is associated with lower ABCG2 expression -216G/T and 191C/A are associated with higher risk of developing diarrhea	63
Cusatis G, et al. 2006	124	ABCG2: 421C>A (Q141K)	-heterozygosis is associated with diarrhea	66
Brugger W, et al. 2011	889	EGFR: Intr1, mut, copy-num and expression; KRAS: mut	-EGFR mut are associated with longer PFS -KRAS mut are associated with reduced PFS	69
Hamada A, et al. 2012	50	ABCB1: 1236TT, 2677TT, 3435TT	-1236TT, 2677TT and 3435TT are associated with higher plasma concentration and risk of developing toxicity	72

Intr1, intron1; mut, mutations; copy-num, gene copy number.

Table 3. Gefitinib versus chemotherapy as first-line treatment fon NSCLC EGFR mutant patients

Study (Ref number)	Study Phase	Population	Treatment (num. of patients)	ORR (%)	Median PFS/TTP (months)	Median OS (months)
IPASS (Ref 21)	Phase III	EGFR mutation positive	Gefitinib (132)	71.2	9.5	21.6
			Carbo+Pac (129)	47.3 P<0.001	6.3 P<0.001	21.9 P=1.00
NEJSG002 (Ref 78)	Phase III	EGFR mutation positive	Gefitinib (115)	73.7	10.8	30.5
			Carbo+Pac (115)	30.7 P<0.001	5.4 P<0.001	23.6 P=0.31
WJTOG3405 (Ref 79)	Phase III	EGFR mutation positive	Gefitinib (88)	62.1	9.2	30.9
			Cis+Doc (89)	32.2 P<0.0001	6.3 P<0.0001	NA P=0.211

Carbo, Carboplatin; Pac, Paclitaxel; Cis, Cisplatin; Doc, Docetaxel.

The regulatory regions of EGFR are located within the 5´-flanking region and intron 1, and both the EGFR-191C/A and -216G/T polymorphisms lie in the transcriptional start site of the promoter region, wherein multiple nuclear regulatory affinity sites are located. The -191C/A polymorphism has been correlated with enhanced EGFR promoter gene expression and activity, while the AG variant, which leads to the substitution of an arginine with a lysine at codon 497 (R497K), has been associated with reduction of EGFR activity [24,25]. Similarly, the -216G/T genotype is located in the binding site for the transcription factor Sp1, and the T allele is associated with increased EGFR mRNA expression [26]. The -216G/T, -191C/A and R497K EGFR polymorphisms were evaluated in a study conducted in 92 Caucasian advanced NSCLC patients treated with gefitinib and the association of the -216G/T variant with longer PFS was reported.

The T allele was also associated with significantly higher rates of stable disease/ partial response ($p = 0.01$) and a significantly higher risk of treatment-related rash/diarrhea ($p = 0.004$) [27]. A recent study in 98 Japanese NSCLC patients treated with gefitinib screened for EGFR mutations and polymorphisms -216G/T and -191C/A reported the mutations as predictive factors of sensitivity to gefitinib, overall survival (OS) and PFS, but no correlation was found between polymorphisms and clinical outcome [28]. In another study, 175 Caucasian NSCLC patients treated with gefitinib were screened for the same EGFR polymorphisms, and a significantly lower response rate was observed in patients carrying the GC haplotype [29].

A highly polymorphic region is also located in the EGFR intron 1 as 14–21 CA repeats [30]. Shorter alleles of this CA-repeat polymorphism, which are less common in Asian populations, are correlated with enhanced EGFR transcription [31]. In particular, the longer allele 21 has been reported to induce an 80% decrease in the gene expression compared with the shorter allele 16 [32,33]. Most studies have reported a better response to gefitinib treatment in NSCLC patients harboring the short EGFR CA-repeat genotype [27–29,34–36]. Ichihara and colleagues studied the relationship between clinical outcome and several genetic factors, including the EGFR CA-repeat variant, in 98 Japanese NSCLC patients treated with gefitinib. In this analysis, among patients with EGFR activating mutations, individuals carrying the shorter CA alleles had a trend toward a significantly longer OS ($p = 0.13$) compared with those with the long alleles (defining long CA repeats as ≥19, or the sum of two alleles ≥39, and short CA repeats as <19, or the sum of two alleles <39) [28]. Another study focused on the correlation of clinical outcome after gefitinib treatment with EGFR

mutations and CA-repeat genotype in 86 Korean patients with advanced NSCLC. In this investigation, short CA was defined as the sum of both alleles ≤37, while long CA was defined as the sum of both alleles ≥38. In agreement with the previous study, EGFR activating mutations were associated with sensitivity to gefitinib and OS, and short CA-repeat status was also correlated with better response and longer time to progression [34]. In a subsequent study performed by Nie et al. in 70 Chinese NSCLC patients treated with gefitinib, a significantly higher response rate was associated with shorter CA-repeat status (defined as any allele ≤16). These patients also had higher EGFR expression and prolonged OS compared with those with long CA. No evidence of correlation with clinical outcome was reported for the R497K polymorphism or EGFR expression [37]. Shorter CA repeats (16 or less) were associated with significantly improved PFS and OS in another study in 92 Caucasian NSCLC patients who were treated with gefitinib [27]. Similarly, Tiseo et al. reported correlation of intron 1 EGFR (CA)16 status, including at least one (CA)16 allele, with survival in 91 Caucasian NSCLC patients treated with gefitinib [38]. However, in a second study performed by the same group, all the patients lacking the (CA)16 allele, except two EGFR-mutated patients (i.e., 18 out of the 76 evaluable patients), experienced rapid disease progression and shorter OS, suggesting a possible negative predictive value of (CA)16 allele absence in the response to gefitinib. No significant correlation was observed between (CA)n-repeat genotype and outcome [39].

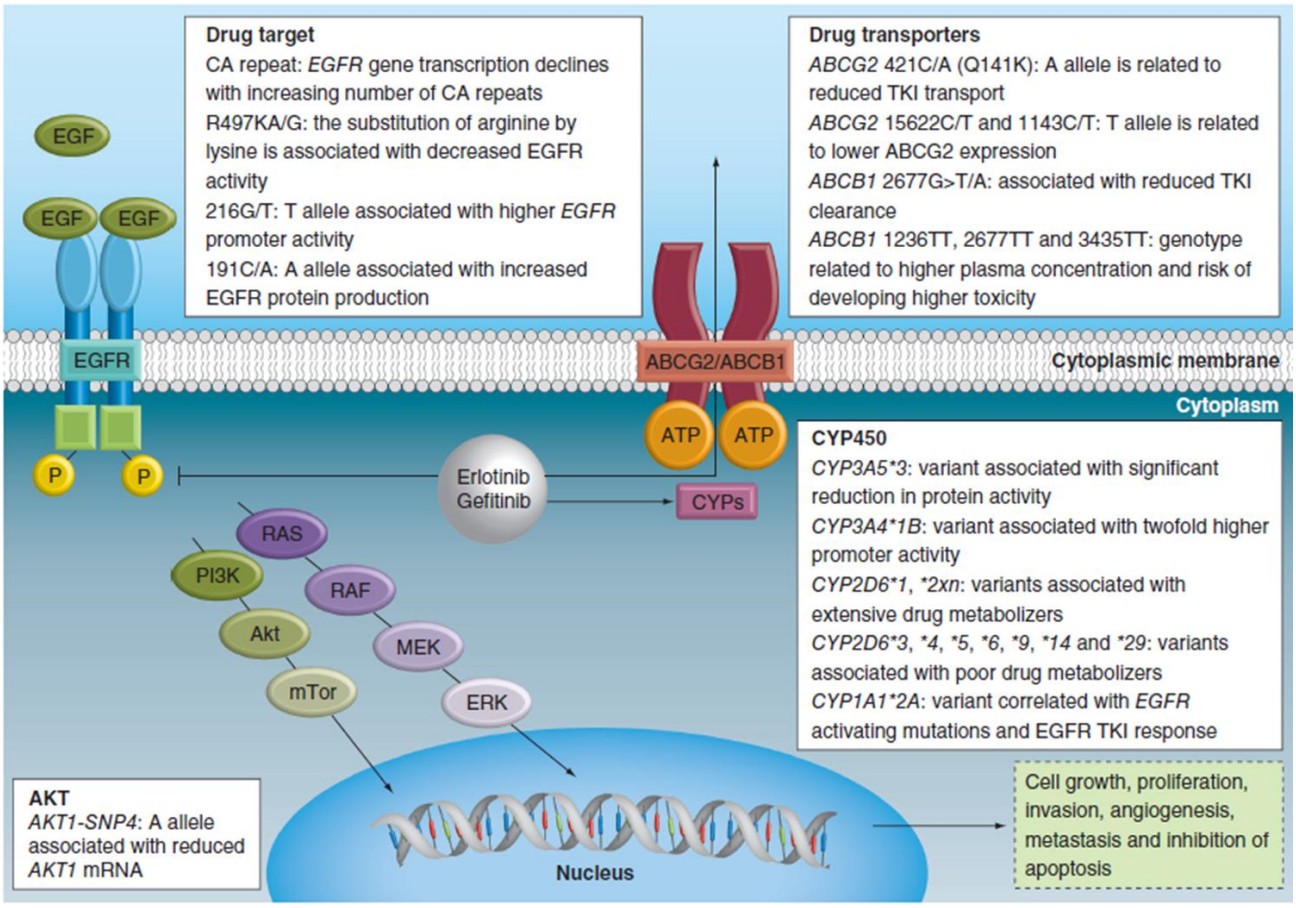

Figure 1. Some of the most relevant polymorphisms in key genes involved in pharmacokinetics and pharmacodynamics of EGF receptor tyrosine kinase inhibitors correlated with gefitinib and erlotinib response and toxicity in non-small-cell lung cancer patients. EGFR: EGF receptor; TKI: Tyrosine kinase inhibitor.

In the largest pharmacogenetic analysis in Caucasian NSCLC patients treated with gefitinib (n = 175), no

association of the EGFR intron 1 CA-repeat status with clinical outcome was observed, grouping patients both with combined CA-repeat length on both alleles of ≤35 versus >35, and a CA-repeat length on both alleles of <18 versus all other [29].

In agreement with the previous analysis, in the authors' study in 96 Caucasian NSCLC patients treated with gefitinib, it was observed that EGFR activating mutations were significantly associated with response, and longer time to progression and OS. By contrast, no correlation was found between EGFR intron 1 CA (for which patients were classified as S/S, L/L and S/L if the number of repeats was ≤16 on both alleles, >16 on both alleles and ≤16 on one allele and >16 on the other, respectively), -216G/T, -191C/A, and R497K polymorphisms and clinical outcome [40].

In order to investigate the correlation between different genotype variants in EGFR and therapeutic outcome and survival, a recent study used a whole-gene-based tag SNP approach in 84 Chinese NSCLC patients treated with gefitinib [35]. In this study, only the novel EGFR polymorphims rs2293347 (D994D) and intron 1 CA were associated with clinical response to the treatment. In particular, patients carrying the rs2293347 GG or shorter CA-repeat genotype (defined as ≤16 CA repeats) had more benefits from the treatment with gefitinib than those with the rs2293347 GA or AA or the longer CA-repeat variants. The rs2293347 GG genotype was also associated with a longer PFS compared with the rs2293347 GA or AA polymorphisms, whereas the combination of rs2293347 GG and shorter CA-repeat status showed the best clinical response.

The potential prognostic significance of EGFR intron 1 CA-repeat polymorphism was also evaluated in patients not treated with EGFR-TKIs. In particular, a recent study performed by Liu et al. reported a trend in significance for this polymorphism (hazard ratio [HR]: 1.7; $p = 0.07$]), whereby the longer alleles were associated with shorter PFS in a population of erlotinib-untreated patients. No other polymorphism was found to be as significantly prognostic for OS in the same study [41]. Conversely, the longer allele correlated with longer OS in a study performed in a US population (HR: 0.66; $p = 0.03$). On the basis of these results, the authors suggested that the allele length might predict the outcome in response to gefitinib [36]. Similar data were observed in a study of 30 pancreatic cancer patients; patients with a shorter sum of total CA repeats (<36) had significantly shorter median OS than patients with ≥36 repeats [42]. However, a more recent analysis performed by the same group in 135 pancreatic cancer patients revealed no correlation between EGFR intron 1 CA-repeat length and OS [43], suggesting that the prognostic role of this polymorphism might be related to a different tumor type.

AKT POLYMORPHISMS

Other potentially predictive polymorphisms include variations in the EGFR downstream signaling pathways, such as AKT1, as well as those in the DNA-repair genes and those of the genes encoding for the drug transporter ABCG2, which has been shown to be active in removing gefitinib from the cell. The serine/threonine kinase Akt is a central player in the PI3K oncogenic pathway, being involved in antiapoptotic as well as proliferative effects. Retrospective studies reported an improved response, disease control rate and time to progression in patients harboring phospho-Akt positive tumors, suggesting that basal Akt activation may be a favorable factor in gefitinib effectiveness [40,44]. In the ONCOBELL prospective trial, only the EGFR FISH, and not Akt immunohistochemistry, was reported as predictive for response to gefitinib [45]. An

oncogenic mutation in the AKT1 subunit involved in the stimulation of Akt signalling and induction of cellular transformation has recently been discovered. However, its rare incidence suggests that it may not play a role in NSCLC development or response to EGFRTKIs [46]. Different studies have reported the association of the haplotype including two functional polymorphisms (AKT1‐SNP3 and AKT1‐SNP4) with lower Akt protein levels in tissues from Caucasians, and with the lowest apoptotic response of Epstein–Barr virus-transformed lymphoblastoids to radiation [47,48]. Furthermore, in a recent study in 96 Caucasian patients, the authors observed a correlation between the AKT1-SNP4 A/A genotype and shorter OS. No other poor prognostic factors were found to potentially explain the short survival of patients carrying the AKT1-SNP4 A/A variant (n = 6) since their clinical and molecular characteristics were comparable to those of the other patients. Moreover, the AKT1-SNP4 polymorphism was found to be an independent predictive factor of progression and death risk at multivariate analysis [40]. A trial in esophageal cancer patients treated with fluoropyrimidines, platinum compounds and taxanes, but not with EGFR-TKIs, correlated other genetic polymorphisms in AKT1 with increased recurrence and significantly shorter overall survival. Similarly, a recent study in Korean NSCLC patients showed that other AKT1 polymorphisms could be used as prognostic markers for patients with early-stage NSCLC. These studies suggested that polymorphisms in the PI3K–AKT pathway might be prognostic and/or predictive factors of response to different drugs [49,50]. The authors' study recruited advanced NSCLC patients treated only with pemetrexed or carboplatin–pemetrexed regimens, in order to evaluate whether the AKT1-SNP4 genotype was a potential biomarker for drug activity prediction or prognostic factor. No correlation was found between the AKT1-SNP4 A/A variant and survival in these gefitinib-untreated patients, suggesting that this polymorphism is not a prognostic factor, whereas it might be a predictive factor of gefitinib activity. In agreement with the clinical results, a significant association between both AKT1 mRNA expression and gefitinib half maximal inhibitory concentrations was also observed in the authors' studies in NSCLC cells. However, these results have still to be validated in a larger cohort of patients, in prospective multicenter trials, as well as additional case-control studies.

ABCG2 & ABCB1 POLYMORPHISMS

A number of common ABCG2 polymorphisms affecting protein expression, function and localization have been described. ABCG2 is a member of the family of ATP-binding cassette transporters and its overexpression is frequently correlated with resistance toward several chemotherapeutic drugs, including anthracyclines, camptothecins and antifolates. Interactions between EGFRTKIs and ABCG2 have been recently suggested [51]. Of note, at clinically achievable concentrations (≤1 μM) gefitinib is a substrate of ABCG2, while higher drug concentrations (>1 μM) lead to the inhibition of the same transporter [52]. Therefore, gefitinib-resistance phenotypes, both in vitro and in vivo, might be affected by ABCG2 expression. Furthermore, ABCG2 is expressed mostly in the GI tract, where it participates in the extrusions of different xenobiotics, but might also play a key role in the absorption and elimination of gefitinib. In particular, the ABCG2 421C/A polymorphism, resulting in a glutamine-to-lysine amino acid change at position 141 (Q141K), has been correlated with the downregulation of ABCG2 and with increase in accumulation of both gefitinib and erlotinib [53]. However, no correlation between this polymorphism and ABCG2 protein expression, or with outcome after gefitinib treatment, was observed in a tissue microarray of 50 lung cancer

tissues [54].

DNA REPAIR GENES POLYMORPHISMS (ERCC1) & RRM1

It has been shown that SNPs in DNA repair genes modulate DNA repair capacity and may affect tumor response and prognosis. The ERCC1 enzyme plays a rate-limiting role in nucleotide excision repair and has been associated with cisplatin resistance [55]. Two common variants, -118C/T and -8092C/A, affect ERCC1 levels and are correlated with clinical outcomes in patients who receive platinum treatment [56,57]. Another key enzyme in DNA synthesis and repair is RRM1, which catalyzes the biosynthesis of deoxyribonucleotides from the corresponding ribonucleotides and is essential to the later stages of nucleotide excision repair [58]. RRM1 overexpression in lung tumors has been associated with resistance to platinum drugs and gemcitabine. Two polymorphisms located in the promoter region, -524C/T and -37C/A, have been linked with response to gemcitabine and cisplatin chemotherapy and survival in NSCLC patients [59]. Another DNA repair pathway is the XRCC1, which acts as a facilitator or coordinator in base excision repair. The XRCC1 399R/G is the most common variant; it occurs in the PARP-binding domain and may affect complex assembly or repair efficiency [60]. In a recent study in 158 never-smoker lung adenocarcinoma patients randomized to receive gefitinib or gemcitabine plus cisplatin as first-line therapy, the correlation between polymorphisms in DNA repair genes and clinical outcome was investigated. However, the XRCC1 399R/R variant, as well as the RRM1 2464G/G and ERCC1 8092C/A genotypes, were reported to be correlated with gefitinib response. These data suggested that having more of these genotypes may predict favorable prognosis for never-smoker lung adenocarcinoma [61].

POLYMORPHISMS AFFECTING TOXICITY INDUCED BY GEFITINIB

Several studies have evaluated the correlation between selected polymorphisms and toxicity induced by gefitinib [54]. Indeed, even if the specificity of gefitinib for its target results in a more favorable safety profile than most standard chemotherapy agents, treatment with this agent leads to the development of rash and diarrhea as specific major adverse effects. At present, little is known about the etiology of these effects, and there is a high interpatient variability that might be explained by the pharmacogenetic heterogeneity of patients [62]. A study in 52 NSCLC patients treated with gefitinib performed by Huang and colleagues analyzed the correlation between genetic factors and skin rash. In particular, patients were screened for EGFR intron 1 CA-repeat status as well as the EGFR SNPs -216G/T, -191C/A and R521K. Among these polymorphisms, only the intron 1 CA-repeat variant was correlated with grade 2/3 skin rash, observed in 21% of patients with L/L genotype (19–22 repeats), 31% with S/L genotype (15–18 repeats) and 71% with S/S genotype (<15 repeats) [63]. Of note, the early grade 2/3 rash was associated with tumor response but not with the number of CA repeats in the EGFR intron 1 ($p = 0.35$). No correlation was found with diarrhea for any of these polymorphisms. Another study reported the association of the EGFR 216 G/T variant with a significantly higher risk of both rash and diarrhea in 92 NSCLC patients treated with gefitinib [27]. Similar results were observed in the authors' study population of 96 NSCLC patients treated with gefitinib, in which grade >1 diarrhea was significantly more frequent in patients harboring the EGFR 191C/A and A/A variants, the EGFR 216G/G variant, and the R497K A/A variant [40]. These results might be explained by the pathophysiology of anti-EGFR-induced diarrhea, which is thought to result from excessive chloride secretion,

inducing secretory diarrhea. Therefore, diarrhea might result from the higher EGFR expression in the intestinal lumen associated with the EGFR promoter polymorphism variants, as suggested by Rudin et al. [64]. By contrast, EGFR ligand binding alterations were associated with the A allele in the R497K variant, resulting in reduced EGFR phosphorylation in colorectal cancer tissues. No differences were observed for EGFR mRNA expression in the same study [65]. However, the R497K polymorphism was also associated with decreased activation of c-Myc, whose activity is also downregulated by the major causative agent of secretory diarrhea, heat-stable enterotoxin from Escherichia coli [66]. A significant association of the ABCG2 421C/A variant with diarrhea was reported by Cusatis and colleagues in NSCLC patients treated with gefitinib [67]. In particular, only 12% of patients with the wild-type genotype of ABCG2 developed diarrhea, while the 44% of patients heterozygous for ABCG2 421C/A presented the adverse effect. The authors suggested that modulations in ATPase activity caused by the ABCG2 421C/A genotype, together with the reduced protein levels, might influence the oral absorption and/or the elimination of gefitinib, resulting in increased plasma concentrations in the steady state and causing the diarrhea. By contrast, no correlation was found between the ABCG2 421C/A variant and toxicity induced by gefitinib in a population of 94 Caucasian patients affected by NSCLC [54]. However, in the same population, the authors observed a correlation between moderate/severe diarrhea and the ABCG2 15622C/T polymorphism and the ABCG2 (1143C/T, -15622C/T) haplotype.

Finally, in a recent genome-wide association study (GWAS) of approximately 0.5 million SNPs in gefitinib-treated patients, comprising 80 interstitial lung disease (ILD) cases and 194 non-ILD controls from two studies, the authors reported that it was not possible to identify genetic associations between common sequence variations and diagnoses of ILD that could have clinical utility for prediction of ILD risk [68].

POLYMORPHISMS AFFECTING ERLOTINIB OUTCOME & TOXICITY

Erlotinib was the second EGFR-TKI inhibitor developed in the clinical setting and, similarly to gefitinib, it interacts with the ATP-binding site of the receptor in a reversible fashion. Erlotinib is approved for the treatment of NSCLC after failure of at least one prior chemotherapy regimen and in combination with gemcitabine for the first-line treatment of locally advanced, unresectable or metastatic pancreatic cancer. More recently, the US FDA has approved an expanded indication for erlotinib for the firstline maintenance treatment of locally advanced or metastatic NSCLC in patients whose disease has not progressed after four cycles of platinum‐based chemotherapy [101].

Several in vitro studies have reported a correlation between EGFR polymorphisms and erlotinib sensitivity. In particular, a combination of EGFR 216G/T and R497K polymorphisms was weakly associated with drug response in the panel of 60 human tumor cell lines established by the National Cancer Institute (NCI-60) [69], while shorter EGFR intron 1 length (sum <36) was associated with better response to erlotinib treatment in the 12 head and neck cancer cell lines [31] and the nine pancreatic cancer cell lines [42]. In a prospective analysis of the prognostic and predictive value of several biomarkers in the SATURN study, 889 advanced NSCLC patients were screened for EGFR expression, EGFR gene copy-number, EGFR and KRAS mutations, and EGFR CA-repeat length status. A profound predictive effect on PFS of erlotinib maintenance therapy relative to placebo was observed in the EGFR mutation-positive subgroup (HR: 0.10; p

< 0.001). Significant PFS benefits were also observed with erlotinib in the wild-type EGFR subgroup (HR: 0.78; p = 0.0185). No correlation was reported for EGFR protein expression, EGFR gene copy-number, KRAS mutation status, and EGFR CA polymorphisms, and PFS with erlotinib treatment and a negative prognostic role for erlotinib efficacy was associated with KRAS mutations [70]. In a double-blind, placebo-controlled trial of second-/third-line erlotinib in 242 advanced NSCLC patients EGFR 216G/T, EGFR 191C/A, ABCG2 421C/A and AKT1-SNP4 G/A genetic polymorphisms were evaluated. No correlation between these polymorphisms and erlotinib efficacy were reported, although the T/T genotype of EGFR 216 was correlated with the development of skin toxicity [41].

A few other data are available on the association between polymorphisms and erlotinibinduced toxicity, skin rash and diarrhea. An integrated analysis of genotypic/pharmacokinetic variability showed a strong association, independent from erlotinib plasma concentration, between diarrhea and the two linked EGFR promoter polymorphisms (-216G/T and -191C/A) in 80 NSCLC, head and neck, and ovarian cancer patients [64]. By contrast, skin rash was associated with intron 1 CA repeat polymorphism and erlotinib concentration (p = 0.044). In the same patients, the ABCG2 15622C/T and -1143C/T polymorphisms were associated with lower ABCG2 production and higher erlotinib concentration. At the multivariate analysis higher concentration levels of erlotinib were associated with a greater risk of grade ≥2 skin rash, with the odds of the rash increasing approximately 1.8-fold per 1 mg/dl increase in the trough level. In this analysis the ABCG2 1143C/T polymorphism was marginally associated with a lower risk of any grade skin rash (p = 0.086). The ABCG2 16,702G/A polymorphism also conferred a lower risk of any grade (p = 0.048) or high-grade (p = 0.050) rash, while no correlation was found for ABCG2 421C/A and diarrhea or skin rash.

Finally, the same study evaluated the common A to G transition within intron 3 of CYP3A5 (CYP3A5*3) as well as the common A to G transition in the 5´ regulatory region of CYP3A4 (CYP3A4*1B), which affected the activation (i.e., ifosphamide, tamoxifen and epipodophyllotoxins) or inactivation (i.e., paclitaxel, docetaxel and vinca alkaloids) of several anticancer agents [71]. Indeed, the primary role for the CYP enzyme system seems to be one of metabolism and detoxification of endogenous compounds after they have been taken in by mouth in the process of eating. Therefore, the CYP enzymes have high concentrations in the liver and small intestine, and are of particular importance when studying drug biotransformation and drug metabolism of oral compounds. The metabolism of both erlotinib and gefitinib is controlled by CYP3A4 and CYP3A5, and, therefore, inhibitors or inducers of these enzymes might affect clearance as well as systemic/tumor exposure. Of note, gefitinib is more susceptible than erlotinib to metabolism by these liver CYP proteins and this might explain the pharmacokinetic results that show higher oral clearance for gefitinib compared with erlotinib [72]. These data explain the achievement of a higher plasma erlotinib exposure despite the administration of a higher gefitinib daily dose compared with erlotinib (e.g., 250 vs 150 mg). However, other enzymes, such as CYP1A isozymes, may constitute an additional pathway in the hepatic/extrahepatic metabolism of both these EGFRTKIs, while CYP1A2 can metabolize erlotinib but not gefitinib [72]. Since all these CYPs are polymorphic, the distribution of specific variant CYP alleles might explain the different pharmacokinetics and activity of TKIs. However, the impact of several CYP polymorphisms on tailored in vivo treatment with TKIs largely remains to be elucidated. In the study by Rudin et al., CYP3A4 polymorphisms were slightly correlated with skin rash in patients treated with erlotinib [64]. Individuals with lower CYP3A4 expression (A/A) were more likely to develop rash than those with higher CYP3A4 levels (A/G

and G/G; p = 0.077). Similarly, the CYP3A5*3 G polymorphism was also marginally associated with grade ≥2 rash (p = 0.094, dominant model) and any-grade diarrhea (p = 0.062). These marginal associations warrant further studies on the role of CYP3A4 and CYP3A5 polymorphisms in determining the concentration levels and activity of erlotinib, as well as other TKIs. Regarding the latter point, a recent study in 50 Japanese NSCLC patients showed that erlotinib concentration at steady state in patients with the ABCB1 1236TT–2677TT–3435TT genotype was significantly higher compared with the levels detected in patients carrying the other genotypes. Furthermore, patients harbouring this genotype had a significantly higher risk of developing grade 2 toxicity, supporting future studies on polymorphisms that might play an important role in individual variations in plasma drug concentration and susceptibility to adverse events [73].

CONCLUSIONS

In recent years, several TKIs have been approved for cancer treatment, while numerous others are under investigation. In particular, gefitinib and erlotinib are rationally designed to target EGFR tyrosine kinase, the involvement of which in tumor development and progression has been demonstrated in different tumor types. These drugs have reached widespread clinical use in the subset of EGFR-mutated advanced NSCLC patients, but new biomarkers to tailor the use of these drugs are urgently needed. Furthermore, these drugs are used as palliative therapy and it is, therefore, relevant for patients that their quality of life is not reduced by the toxicity caused by this therapy. To date, it is not completely clear which patient characteristics are risk factors for EGFR-TKI-induced toxicity, and the large interindividual variability in toxic effects makes the identification of novel pharmacogenetic markers to screen patients an attractive prospect.

Germline polymorphisms are easy to assess and several polymorphic variants of EGFR and genes involved in anti-EGF agent activity, metabolism and transport have been studied as predictors of outcome and toxicity. Several studies have reported the correlation between short EGFR intron 1 CA repeats and clinical response to EGFR-TKI treatment in patients affected by NSCLC [27–29,34–36]. This variant was also associated with grade 2/3 skin rash, but controversial results were reported by other studies in which the role of polymorphisms in ABCG2 was suggested to predict gastrointestinal toxicity [54]. These controversial data might be clarified within future studies, which should evaluate the feasibility of sampling more accessible tissue (i.e., blood) compared to cancer specimens, showing whether germline and somatic genotypes of drug transporters, drug metabolism enzymes and drug targets are correlated with the gene expression or functional activity in the tumors. Moreover, most clinical observations need to be confirmed in larger populations, and there needs to be clinical validation of a more robust approach to genotyping of patients as the multiple-gene approach may overcome the limitations of the single-gene approach.

Hopefully, these studies will improve the transfer of basic research findings to the clinical setting and allow the selection of patients for EGFR-TKI treatment by identifying both subgroups at a genetically high risk for drug resistance or toxicity, and patients more likely to respond to these treatments. Indeed, since the identification of genetic markers predictive of clinical outcome is a potential key instrument for accurate patient stratification and personalized treatment, hopefully pharmacogenetics will become a strategic companion in the current clinical development of novel targeted anticancer agents.

FUTURE PERSPECTIVES

Novel approaches in pharmacogenetic studies

During the past decades, several studies based on DNA/RNA microarrays have tried to develop predictive signatures to decide the most suitable chemotherapy approach for specific types or subtypes of tumors. Conflicting results and difficulties in replicating the data led to a limited impact on clinical practice, mainly due to: i) lack of sufficiently powered clinical trials; ii) use of sample collection and data analysis methods that are not standardized; iii) intrinsic intratumor heterogeneity.

However, in the last few years, technical advancements in the development of rapid whole-genome studies have initiated a revolution in the field that could potentially change the pharmacogenomic approach to perzonalized treatment in the future. These techniques are represented mainly by massively parallel or next‐generation sequencing (NGS) and GWASs.

During recent decades, thanks to the introduction of advanced systems that may generate millions of short DNA reads (36–150 base pairs), the landscape of DNA sequencing has evolved from f irst-generation sequencing, which was based on DNA sequencing using dideoxynucleotide termination chemistry, to second-generation sequencing or NGS [74]. Noncoding regions of DNA/RNA, in addition to exons, can be analyzed at very high resolution in a short time by NGS with the possibility of identifying any chromosomal rearrangement and variations in copy-number. Furthermore, thanks to the progression in the development of whole-genome amplification, an insight into intratumor heterogeneity has become feasible by performing genetic studies even at the singlecell level [75]. Hopefully, with the diffusion of NGS methodologies in the next few years, we will develop an increasing knowledge of tumor biology.

GWASs are genetic studies that allow the simultaneous evaluation of many polymorphisms, especially common copy-number variations and SNPs, in order to identify existing correlations among any genetic variant and tumor features. In particular, the application of these types of studies in pharmacogenomics aims to find out any possible correlation between polymorphisms and drug response or toxicity. Of note, GWASs allow the investigation of the entire genome independently from preliminary information on chromosomal loci involvement in drug effects. The massive amount of SNPs analyzed with GWASs and the difficulty represented by the definition of real correlations are the limitations of this method, increasing the risk of a high rate of false-positive data; a massive number of samples is necessary to obtain a sufficient statistical power. A recent study has been published by University of Texas MD Anderson researchers (TX, USA), reporting a genome-wide scan of 307,260 polymorphisms in 327 NSCLC patients treated with cisplatin or carboplatin [76]. In this analysis, the rs1878022 variant, which is located within an intron of the gene CMKLR1, has been strongly correlated with shorter survival. The findings of this study were also validated in two other independent cohorts of 315 patients enrolled at the Mayo Clinic (USA) and 420 cases recruited in the Spanish Lung Cancer Group PLATAX clinical trials. Interestingly, the use of this unbiased non-candidate gene-driven approach led to the identification as strong predictive survival factor of a polymorphic variant within an intronic region of a platinum-unrelated gene.

In order to validate these pharmacogenetic findings and use them in the clinical setting, future genomic analysis should use validated and standardized methodology. Moreover, future analysis should be performed on larger cohorts of patients and/or utilize the sharing of data through common websites in order

to create ‘virtual multicentric pharmacogenetic trials’.

Clinical relevance

During recent decades, a number of important genetic determinants have been identified in different tumor types, including NSCLC. The FDA has approved a number of genetic tests and some pharmacogenetic markers have been included in drug labels [102]. However, the application of pharmacogenetic testing in primary care is not as common as predicted. This leads to questions regarding the clinical relevance of pharmacogenetic analyses and on future studies that should successfully bridge the gap from research to clinical practice.

Unfortunately, the clinical relevance of most of the polymorphisms described in the current literature remains controversial because of the exiguous number of (heterogeneous) patients screened, the lack of prospective studies designed to identify specific correlations between gene alterations and drug response or disease prognosis, and the strong variability in analytical analysis, as well as lack of quality controls among different studies.

The development of prospective clinical trials, in which patient treatments selected on the basis of conventional criteria are directly compared with patients given specific treatments suggested by genetic characteristics, might overcome these controversies and reduce the reluctance to transfer the novel knowledge into the clinical routine. Another obstacle to the successful clinical application of the new findings is the lack of association with the main pharmacokinetic/pharmacodynamic parameters as well as functional genomic analysis of the underlying mechanisms of drug sensitivity/resistance. The recent discovery of miRNA has improved our knowledge regarding the control of gene expression, and in the future it may help to clarify the role of the signaling pathways involved in lung cancer oncogenesis. Hopefully, growing evidence relating to miRNA may provide a clue to solve individual drug-resistance problems [77].

In conclusion, despite the intriguing findings of several studies, small sample sizes together with interethnic differences and the retrospective nature of most studies make it difficult to draw any clear conclusions regarding the role of most pharmacogenetic biomarkers in determining the clinical outcome or toxicity in gefitinib and erlotinib treatment. Hopefully, the accurate planning of new prospective trials, the increased knowledge of key mechanisms affecting drug distribution/activity and the use of novel technologies, including genome-wide approaches, may provide essential tools to improve the prospects of pharmacogenetic research, as well as to optimize currently available treatments in selected NSCLC patients.

REFERENCES

1. Galvani E, Peters GJ, Giovannetti E. Thymidylate synthase inhibitors for non-small cell lung cancer. Expert Opin Investig. Drug 20(10), 1343–1356 (2011).
2. Reck M, von Pawel J, Zatloukal P et al. Phase III trial of cisplatin plus gemcitabine with either placebo or bevacizumab as first-line therapy for nonsquamous non-small-cell lung cancer. J. Clin. Oncol. 27(8), 1227–1234 (2009).
3. Scagliotti GV, Parikh P, von Pawel J et al. Phase III study comparing cisplatin plus gemcitabine with cisplatin plus pemetrexed in chemotherapy-naive patients with advanced-stage non-small-cell lung cancer. J. Clin. Oncol. 26(21), 3543–3551 (2008).
4 Druker BJ, Talpaz M, Resta DJ et al. Efficacy and safety of a specific inhibitor of the BCR–ABL tyrosine kinase in chronic myeloid leukemia. N. Engl. J. Med. 344(14), 1031–1037 (2001).
5. Baselga J. Targeting tyrosine kinases in cancer: the second wave. Science 312(5777), 1175–1178 (2006).
6. Hoang T, Schiller JH. Advanced NSCLC: from cytotoxic systemic chemotherapy to molecularly targeted therapy. Expert Rev. Anticancer Ther. 2(4), 393–401 (2002).
7. Manning G, Whyte DB, Martinez R, Hunter T, Sudarsanam S. The protein kinase complement of the human genome. Science 298(5600), 1912–1934 (2002).
8. Hynes NE, Lane HA. ERBB receptors and cancer: the complexity of targeted inhibitors. Nat. Rev. Cancer 5(5), 341–354 (2005).
9. Suzuki S, Dobashi Y, Sakurai H, Nishikawa K, Hanawa M, Ooi A. Protein overexpression and gene amplification of epidermal growth factor receptor in nonsmall cell lung carcinomas. An immunohistochemical and fluorescence in situ hybridization study. Cancer 103(6), 1265–1273 (2005).
10. Hirsch FR, Varella-Garcia M, Bunn PA et al. Epidermal growth factor receptor in non-small-cell lung carcinomas: correlation between gene copy number and protein expression and impact on prognosis. J. Clin. Oncol. 21(20), 3798–3807 (2003).
11. Kris MG, Natale RB, Herbst RS et al. Efficacy of gefitinib, an inhibitor of the epidermal growth factor receptor tyrosine kinase, in symptomatic patients with non-small cell lung cancer: a randomized trial. JAMA 290(16), 2149–2158 (2003).
12. Lynch TJ, Bell DW, Sordella R et al. Activating mutations in the epidermal growth factor receptor underlying responsiveness of non-small-cell lung cancer to gefitinib. N. Engl. J. Med. 350(21), 2129–2139 (2004).
13. Tsao MS, Sakurada A, Cutz JC et al. Erlotinib in lung cancer – molecular and clinical predictors of outcome. N. Engl. J. Med. 353(2), 133–144 (2005).
14. Sharma SV, Bell DW, Settleman J, Haber DA. Epidermal growth factor receptor mutations in lung cancer. Nat. Rev. Cancer 7(3), 169–181 (2007).
15. Danesi R, De Braud F, Fogli S, Di Paolo A, Del Tacca M. Pharmacogenetic determinants of anti-cancer drug activity and toxicity. Trends Pharmacol. Sci. 22(8), 420–426 (2001).
16. Barker AJ, Gibson KH, Grundy W et al. Studies leading to the identification of ZD1839 (IRESSA): an orally active, selective epidermal growth factor receptor tyrosine kinase inhibitor targeted to the treatment of cancer. Bioorg. Med. Chem. Lett. 11(14), 1911–1914 (2001).
17. Normanno N, Maiello MR, De Luca A. Epidermal growth factor receptor tyrosine kinase inhibitors (EGFR-TKIs): simple drugs with a complex mechanism of action? J. Cell. Physiol. 194(1), 13–19 (2003).
18. Scagliotti GV, Selvaggi G, Novello S, Hirsch FR. The biology of epidermal growth factor receptor in lung cancer. Clin. Cancer Res. 10(12 Pt 2), 4227s–4232s (2004).
19. Kim ES, Hirsh V, Mok T et al. Gefitinib versus docetaxel in previously treated non-small-cell lung cancer (INTEREST): a randomised Phase III trial. Lancet 372(9652), 1809–1818 (2008).
20. Shepherd FA, Rodrigues Pereira J, Ciuleanu T et al. Erlotinib in previously treated non-small cell lung cancer. N. Engl. J. Med. 353(2), 123–132 (2005).
21. Mok TS, Wu YL, Thongprasert S et al. Gefitinib or carboplatin–paclitaxel in pulmonary adenocarcinoma. N. Engl. J. Med. 361(10), 947–957 (2009).
22. Helfrich BA, Raben D, Varella-Garcia M et al. Antitumor activity of the epidermal growth factor receptor (EGFR) tyrosine kinase inhibitor gefitinib (ZD1839, Iressa) in non-small cell lung cancer cell lines correlates with gene copy number and EGFR mutations but not EGFR protein levels. Clin. Cancer Res. 12(23), 7117–7125 (2006).
23. Hartmann JT, Haap M, Kopp HG, Lipp HP. Tyrosine kinase inhibitors – a review on pharmacology, metabolism and side effects. Curr. Drug Metab. 10(5), 470–481 (2009).
24. Nomura M, Shigematsu H, Li L et al. Polymorphisms, mutations, and amplification of the EGFR gene in non-small cell lung cancers. PLoS Med. 4(4), e125 (2007).
25. Moriai T, Kobrin MS, Hope C, Speck L, Korc M. A variant epidermal growth factor receptor exhibits altered type a transforming growth factor binding and transmembrane signaling. Proc. Natl Acad. Sci. USA 91(21), 10217–10221 (1994).

26. Liu W, Innocenti F, Wu MH et al. A functional common polymorphism in a Sp1 recognition site of the epidermal growth factor receptor gene promoter. Cancer Res. 65(1), 46–53 (2005).

27. Liu G, Gurubhagavatula S, Zhou W et al. Epidermal growth factor receptor polymorphisms and clinical outcomes in non-small-cell lung cancer patients treated with gefitinib. Pharmacogenomics J. 8(2), 129–138 (2008).

28. Ichihara S, Toyooka S, Fujiwara Y et al. The impact of epidermal growth factor receptor gene status on gefitinib-treated Japanese patients with non-small-cell lung cancer. Int. J. Cancer 120(6), 1239–1247 (2007).

29. Gregorc V, Hidalgo M, Spreafico A et al. Germline polymorphisms in EGFR and survival in patients with lung cancer receiving gefitinib. Clin. Pharmacol. Ther. 83(3), 477–484 (2008).

30. Gebhardt F, Bürger H, Brandt B. Modulation of EGFR gene transcription by secondary structures, a polymorphic repetitive sequence and mutations – a link between genetics and epigenetics. Histol. Histopathol. 15(3), 929–936 (2000).

31. Amador ML, Oppenheimer D, Perea S et al. An epidermal growth factor receptor intron 1 polymorphism mediates response to epidermal growth factor receptor inhibitors. Cancer Res. 64(24), 9139–9143 (2004).

32. Gebhardt F, Zänker KS, Brandt B. Modulation of epidermal growth factor receptor gene transcription by a polymorphic dinucleotide repeat in intron 1. J. Biol. Chem. 274(19), 13176–13180 (1999).

33. Buerger H, Gebhardt F, Schmidt H et al. Length and loss of heterozygosity of an intron 1 polymorphic sequence of egfr is related to cytogenetic alterations and epithelial growth factor receptor expression. Cancer Res. 60(4), 854–857 (2000).

34. Han SW, Jeon YK, Lee KH et al. Intron 1 CA dinucleotide repeat polymorphism and mutations of epidermal growth factor receptor and gefitinib responsiveness in non-small-cell lung cancer. Pharmacogenet. Genom. 17(5), 313–319 (2007).

35. Ma F, Sun T, Shi Y et al. Polymorphisms of EGFR predict clinical outcome in advanced non-small-cell lung cancer patients treated with gefitinib. Lung Cancer 66(1), 114–119 (2009).

36. Dubey S, Stephenson P, Levy DE et al. EGFR dinucleotide repeat polymorphism as a prognostic indicator in non-small cell lung cancer. J. Thorac. Oncol. 1(5), 406–412 (2006).

37. Nie Q, Wang Z, Zhang GC et al. The epidermal growth factor receptor intron1 (CA) n microsatellite polymorphism is a potential predictor of treatment outcome in patients with advanced lung cancer treated with gefitinib. Eur. J. Pharmacol. 570(1–3), 175–181 (2007).

38. Tiseo M, Capelletti M, De Palma G et al. Epidermal growth factor receptor intron-1 polymorphism predicts gefitinib outcome in advanced non-small cell lung cancer. J. Thorac. Oncol. 3(10), 1104–1111 (2008).

39. Tiseo M, Rossi G, Capelletti M et al. Predictors of gefitinib outcomes in advanced non-small cell lung cancer (NSCLC): study of a comprehensive panel of molecular markers. Lung Cancer 67(3), 355–360 (2010).

40. Giovannetti E, Zucali PA, Peters GJ et al. Association of polymorphisms in AKT1 and EGFR with clinical outcome and toxicity in non-small cell lung cancer patients treated with gefitinib. Mol. Cancer Ther. 9(3), 581–593 (2010).

41. Liu G, Cheng D, Ding K et al. Pharmacogenetic analysis of BR.21, a placebo-controlled randomized Phase III clinical trial of erlotinib in advanced non-small cell lung cancer. J. Thorac. Oncol. 7(2), 316–322 (2012).

42. Tzeng CWD, Frolov A, Frolova N et al. Pancreatic cancer epidermal growth factor receptor (EGFR) intron 1 polymorphism influences postoperative patient survival and in vitro erlotinib response. Ann. Surg. Oncol. 14(7), 2150–2158 (2007).

43. Frolov A, Liles JS, Kossenkov AV et al. Epidermal growth factor receptor (EGFR) intron 1 polymorphism and clinical outcome in pancreatic adenocarcinoma. Am. J. Surg. 200(3), 398–405 (2010).

44. Cappuzzo F, Magrini E, Ceresoli GL et al. Akt phosphorylation and gefitinib efficacy in patients with advanced non-small-cell lung cancer. J. Natl Cancer Inst. 96(15), 1133–1141 (2004).

45. Cappuzzo F, Ligorio C, Jänne PA et al. Prospective study of gefitinib in epidermal growth factor receptor fluorescence in situ hybridization-positive/phospho-Akt-positive or never smoker patients with advanced non-small-cell lung cancer: the ONCOBELL trial. J. Clin. Oncol. 25(16), 2248–2255 (2007).

46. Kim MS, Jeong EG, Yoo NJ, Lee SH. Mutational analysis of oncogenic AKT E17K mutation in common solid cancers and acute leukaemias. Br. J. Cancer 98(9), 1533–1535 (2008).

47. Harris SL, Gil G, Robins H et al. Detection of functional single-nucleotide polymorphisms that affect apoptosis. Proc. Natl Acad. Sci. USA 102(45), 16297–16302 (2005).

48. Emamian ES, Hall D, Birnbaum MJ, Karayiorgou M, Gogos JA. Convergent evidence for impaired AKT1–GSK3b signaling in schizophrenia. Nat. Genet. 36(2), 131–137 (2004).

49. Hildebrandt MAT, Yang H, Hung MC et al. Genetic variations in the PI3K/PTEN/AKT/mTOR pathway are associated with clinical outcomes in esophageal cancer patients treated with chemoradiotherapy. J. Clin. Oncol. 27(6), 857–871 (2009).

50. Kim MJ, Kang HG, Lee SY et al. AKT1 polymorphisms and survival of early stage non-small cell lung cancer. J. Surg. Oncol. 105(2), 167–174 (2012).

51. van Erp NP, Gelderblom H, Guchelaar HJ. Clinical pharmacokinetics of tyrosine kinase inhibitors. Cancer Treat. Rev. 35(8), 692–

706 (2012).

52. Lemos C, Jansen G, Peters GJ. Drug transporters: recent advances concerning BCRP and tyrosine kinase inhibitors. Br. J. Cancer 98(5), 857–862 (2008).
53. Li J, Cusatis G, Brahmer J et al. Association of variant ABCG2 and the pharmacokinetics of epidermal growth factor receptor tyrosine kinase inhibitors in cancer patients. Cancer Biol. Ther. 6(3), 432–438 (2007).
54. Lemos C, Giovannetti E, Zucali PA et al. Impact of ABCG2 polymorphisms on the clinical outcome and toxicity of gefitinib in non-small-cell lung cancer patients. Pharmacogenomics 12(2), 159–170 (2011).
55. Olaussen KA, Dunant A, Fouret P et al. DNA repair by ERCC1 in non-small-cell lung cancer and cisplatin-based adjuvant chemotherapy. N. Engl. J. Med. 355(10), 983–991 (2006).
56. Isla D, Sarries C, Rosell R et al. Single nucleotide polymorphisms and outcome in docetaxel–cisplatin-treated advanced non-small-cell lung cancer. Ann. Oncol. 15(8), 1194–1203 (2004).
57. Zhou W, Gurubhagavatula S, Liu G et al. Excision repair cross-complementation group 1 polymorphism predicts overall survival in advanced non-small cell lung cancer patients treated with platinum-based chemotherapy. Clin. Cancer Res. 10(15), 4939–4943 (2004).
58. Gazdar AF. DNA repair and survival in lung cancer – the two faces of Janus. N. Engl. J. Med. 356(8), 771–773 (2007).
59. Rosell R, Felip E, Taron M et al. Gene expression as a predictive marker of outcome in stage IIB–IIIA–IIIB non-small cell lung cancer after induction gemcitabine-based chemotherapy followed by resectional surgery. Clin. Cancer Res. 10(12 Pt 2), 4215s–4219s (2004).
60. Masson M, Niedergang C, Schreiber V, Muller S, Menissier-de Murcia J, de Murcia G. XRCC1 is specifically associated with poly(ADP-ribose) polymerase and negatively regulates its activity following DNA damage. Mol. Cell. Biol. 18(6), 3563–3571 (1998).
61. Han JY, Yoon KA, Park JH et al. DNA repair gene polymorphisms and benefit from gefitinib in never-smokers with lung adenocarcinoma. Cancer 117(14), 3201–3208 (2011).
62. Peréz-Soler R, Saltz L. Cutaneous adverse effects with HER1/EGFR-targeted agents: is there a silver lining? J. Clin. Oncol. 23(22), 5235–5246 (2005).
63. Huang CL, Yang CH, Yeh KH et al. EGFR intron 1 dinucleotide repeat polymorphism is associated with the occurrence of skin rash with gefitinib treatment. Lung Cancer 64(3), 346–351 (2009).
64. Rudin CM, Liu W, Desai A et al. Pharmacogenomic and pharmacokinetic determinants of erlotinib toxicity. J. Clin. Oncol. 26(7), 1119–1127 (2008).
65. Wang WS, Chen PM, Chiou TJ et al. Epidermal growth factor receptor R497K polymorphism is a favorable prognostic factor for patients with colorectal carcinoma. Clin. Cancer Res. 13(12), 3597–3604 (2007).
66. Pitari GM, Zingman LV, Hodgson DM et al. Bacterial enterotoxins are associated with resistance to colon cancer. Proc. Natl Acad. Sci. USA 100(5), 2695–2699 (2003).
67. Cusatis G, Gregorc V, Li J et al. Pharmacogenetics of ABCG2 and adverse reactions to gefitinib. J. Natl Cancer Inst. 98(23), 1739–1742 (2006).
68. Nyberg F, Barratt BJ, Mushiroda T et al. Interstitial lung disease in gefitinib-treated Japanese patients with non-small-cell lung cancer: genome-wide analysis of genetic data. Pharmacogenomics 12(7), 965–975 (2011).
69. Liu W, Wu X, Zhang W et al. Relationship of EGFR mutations, expression, amplification, and polymorphisms to epidermal growth factor receptor inhibitors in the NCI60 cell lines. Clin. Cancer Res. 13(22 Pt 1), 6788–6795 (2007).
70. Brugger W, Triller N, Blasinska-Morawiec M et al. Prospective molecular marker analyses of EGFR and KRAS from a randomized, placebo-controlled study of erlotinib maintenance therapy in advanced non-small cell lung cancer. J. Clin. Oncol. 29(31), 4113–4120 (2011).
71. Rodriguez-Antona C, Ingelman-Sundberg M. Cytochrome P450 pharmacogenetics and cancer. Oncogene 25(11), 1679–1691 (2006).
72. Li J, Zhao M, He P, Hidalgo M, Baker SD. Differential metabolism of gefitinib and erlotinib by human cytochrome P450 enzymes. Clin. Cancer Res. 13(12), 3731–3737 (2007).
73. Hamada A, Sasaki J, Saeki S et al. Association of ABCB1 polymorphisms with erlotinib pharmacokinetics and toxicity in Japanese patients with non-small-cell lung cancer. Pharmacogenomics 13(5), 615–624 (2012).
74. Metzker ML. Sequencing technologies – the next generation. Nat. Rev. Genet. 11(1), 31–46 (2010).
75. Navin N, Kendall J, Troge J et al. Tumour evolution inferred by single-cell sequencing. Nature 472(7341), 90–94 (2011).
76. Wu X, Ye Y, Rosell R et al. Genome-wide association study of survival in non-small cell lung cancer patients receiving platinumbased chemotherapy. J. Natl Cancer Inst. 103(10), 817–825 (2011).
77. Giovannetti E, Erozenci A, Smit J, Danesi R, Peters GJ. Molecular mechanisms underlying the role of microRNAs (miRNAs) in anticancer drug resistance and implications for clinical practice. Crit. Rev. Oncol. Hematol. 81(2), 103–122 (2012).

78. Maemondo M, Inoue A, Kobayashi K et al. Gefitinib or chemotherapy for non-small-cell lung cancer with mutated EGFR. N. Engl. J. Med. 362(25), 2380–2388 (2010).

79. Mitsudomi T, Morita S, Yatabe Y et al. Gefitinib versus cisplatin plus docetaxel in patients with non-small-cell lung cancer harbouring mutations of the epidermal growth factor receptor (WJTOG3405): an open label, randomised Phase 3 trial. Lancet Oncol. 11(2), 121–128 (2010).

Websites

101. National Cancer Institute at the NIH. FDA Approval for Erlotinib Hydrochloride. www.cancer.gov/cancertopics/druginfo/fda-erlotinib-hydrochloride

102. US FDA. Table of Pharmacogenomic Biomarkers in Drug Labels. www.fda.gov/Drugs/ScienceResearch/ResearchAreas/Pharmacogenetics/uc

Chapter 5

Molecular mechanisms underlying the role of microRNAs in resistance to EGFR-targeted agents and novel therapeutic strategies for treatment of NSCLC

Maftouh M, Avan A, Galvani E, Peters GJ & Giovannetti E.

CRITICAL REVIEWS IN ONCOGENESIS 2013

In Press.

ABSTRACT

Non-small-cell lung cancer (NSCLC) is one of the deadliest types of cancer. One explanation for this poor prognosis is the failure of most chemotherapeutic regimens, which prompted the development of new, rationally designed, targeted antitumor agents such as inhibitors of the epidermal growth factor receptor (EGFR) and downstream pathways. However, most of these targeted therapies also fail, and studies on the mechanisms underlying resistance towards targeted agents might provide critical findings for NSCLC research and treatment. Some of these studies showed that drug resistance can emerge not only from genetic aberrations, but also from epigenetic changes, including regulation of different signaling pathways by microRNAs (miRNAs), which act as key post-transcriptional regulators of gene expression. There is accumulating evidence that specific miRNAs correlated with drug sensitivity and can be used as prognostic markers in NSCLC. However, a greater knowledge of miRNAs might also provide novel insight in several drug-resistance mechanisms, and suggest their potential in novel therapeutic interventions, by sensitizing tumor cells to drug-induced apoptosis, as well as by inhibiting tumor proliferation and invasive capabilities. Therefore, this review highlights several recent and clinically relevant aspects of regulation of drug resistance by miRNA from the perspective of current anti-EGFR-targeted therapies in NSCLC.

1. DRUG RESISTANCE AND EMERGING ROLE OF MicroRNAs IN NSCLC

Despite the discovery of successful targeted therapies directed against specific alterations of oncogenic pathways, non-small-cell lung cancer (NSCLC) is the leading cause of cancer-related death with overall 5-year survival rate of about 15% and high recurrence rates [1]. The clinical success of the new biologically targeted agents has been limited by the evolution of acquired resistance, which leads to tumor relapse after initial response to therapy [2].

Resistance to the new biological compounds can be caused by a range of mechanisms, which are partially overlapping with the main factors involved in resistance towards conventional chemotherapy, such as increased drug elimination, decreased drug uptake, drug inactivation and alterations of drug targets [3]. Genetic changes, such as the occurrence of the secondary EGFR-T790M mutation or the amplification of c-Met, -account for about 70% of the resistant cases to the EGFR tyrosine kinase inhibitors (TKIs) gefitinib and erlotinib [4]. Recent data showed that drug resistance mechanisms can also be regulated by epigenetic modifications, including alterations in microRNAs (miRNAs or miR) [5].

MiRNAs are small (19-23 nucleotides, single strand), non-protein-coding, endogenous RNAs playing a pivotal role in regulation of gene expression at the post-transcriptional level [6]. The primary miRNA (pri-miRNA) is transcribed by RNA polymerase II, cleaved by Drosha RNase III endonuclease into the miRNA precursor (pre-miRNA), then transported from the nucleus to cytoplasm by Exportin-5 protein and further cleaved by Dicer into mature miRNA. These small RNAs, together with Argonaute (Ago) proteins, form the RNA-induced silencing complex (RISC) and bind to their target mRNA through partial complementarity, leading to inhibition of mRNA translation [7-10].

MiRNAs have been shown to regulate many biological processes, but they are also involved in the pathogenesis of several human diseases, including NSCLC. For instance, miR-15, miR-145, miR-34 and miR-7 regulate the expression of several key genes, such as Bcl-2, Myc, E2F1 and Ras, which modulate lung cancer cell proliferation, differentiation, and stem cells development [11].

Several studies showed that the expression of miRNAs is either up-regulated or down-regulated in lung tumors when compared with their normal counterparts, suggesting that miRNAs can contribute to oncogenesis by functioning as tumor suppressors or oncogenes, and that specific patterns of dysregulated miRNAs expression might be used as biomarkers in the early diagnosis of lung cancer [12]. For example, miR-21 is overexpressed in most tumor types, including NSCLC, and acts as an oncogene by targeting genes related to proliferation, cell death, and invasion, such as Apaf1, Faslg and RhoB, that play an important role in intrinsic/extrinsic apoptotic pathway and growth inhibition, respectively [9]. Finally, up-regulation of miR-21, which is further enhanced by activation of EGFR signaling pathway, plays a key role in lung carcinogenesis in never-smokers [13]. Defects in the miRNA biogenesis machinery might also be related to oncogenesis, and deletions in Dicer were described in K-Ras-induced lung cancer [14,15]

Moreover, miRNAs modulate signaling pathways triggered by growth factor receptors, including EGFR and c-Met, as well as the EGFR downstream pathways such as the Ras/ERK/Myc pathway, which represent the main targets of the targeted therapies commonly used in the clinical setting [16,17]. Therefore, in this review we provide an overview on the role of miRNAs in key oncogenic pathways, summarizing the main findings on the regulation of EGFR modulation of cell survival and proliferation, as well as important studies

on their potential role as biomarkers in NSCLC. The current status of research on miRNAs involved in resistance to the new targeted agents, focusing on anti-EGFR compounds is discussed as well as their possible role in drug resistance. Finally, we integrated the preclinical data with clinical evidences, showing how the study of miRNAs could help to predict the optimal treatment for different patients and provide novel therapeutic strategies for NSCLC treatment.

2. MicroRNAs REGULATING EGFR SIGNALING PATHWAY

Numerous reports suggested that several miRNAs play a critical role in the regulation of different signaling pathways and might be used as prognostic biomarkers, as well as possible modulators of the activity of new targeted agents, as summarized in the Table 1. A group of signaling proteins that has been identified as being significantly different between normal and cancerous cells are protein kinases, including tyrosine kinases (PTKs). These PTKs are involved in the maintenance of cellular homeostasis and their activity is tightly regulated in normal cells. However, when they are mutated or abnormally activated, they can become potent oncoproteins involved in the development and progression of many cancers [18]. Against this background, PTKs were identified as attractive targets for the development of anticancer drugs. In particular, the EGFR pathway has emerged as the major target for the inhibition of NSCLC progression, and EGFR-targeting drugs such as gefitinib and erlotinib are used in the clinical setting or being actively investigated in multiple clinical trials as a single agent or in combination with other agents. Mutations at position 858 (leucine-to-arginine substitution [L858R]) induce lung cancer in mouse models and make cells more sensitive to EGFR-TKIs, similar to other activating mutations in the first four exons (18 through 21) of the EGFR-TK domain [19,20].

However, EGFR and its downstream pathways can be regulated by several miRNAs. For example, Chou and colleagues demonstrated that miR-7 is an "oncomiR" which acts as a critical modulator of a regulatory network for EGFR signaling in lung cancer cells, where it downregulates the expression of several members of the EGFR signaling cascade [17]. The binding of c-Myc to the miR-7 promoter enhanced its activity, while ectopic miR-7 promoted cell growth and orthotopic tumor formation in nude mice. In these models, quantitative proteomic analysis revealed that miR-7 decreased levels of the Ets2 transcriptional repression factor ERF, which is a direct target of miR-7. Accordingly, the inhibition of miR-7 expression suppressed EGFR mRNA and protein expression in different lung cancer cell lines as well as the growth of the A549 lung adenocarcinoma cells [21,22].

More recently, computational approaches to miRNA target prediction and site functionality identified several candidate miRNAs that regulates EGFR and the following functional analyses in H3255, A549 and HCC827 cells, demonstrated that miR-542-5p directly suppressed the translation of EGFR mRNA, reducing cell proliferation and viability more strongly than miR-7 [23]. Interestingly, miR-542-5p binds to the 5'-UTR of the EGFR mRNA, whereas miR-7 interacts with the 3'-UTR. These results support the study of both these miRNAs as novel potential therapeutic targets in NSCLC.

Another recent study revealed that also miR-133b interacts with the 3'-UTR mRNA of EGFR, causing a significant inhibition of cell growth [24]. Transfection of miR-133b mimic or inhibitor molecules affected invasion, apoptosis induction and expression/phosphorylation of the downstream kinases ERK and Akt in the A549, PC9, H1975 and H1650 cell lines. Other targets beyond EGFR can also mediate these results, such

as Mcl-1 and Bcl-2, especially in non-EGFR addicted cells. However, miR-133b expression levels correlated with tumor stage as well as with the extent of lymph node involvement and visceral pleura or vessel invasion. Therefore the role of miR-133b as biomarker of tumor aggressive behavior is being investigated in future prospective studies.

Table 1. MicroRNAs involved in NSCLC sensitivity to EGFR-TKIs

miRNA	miRNA intracellular levels	Protein target	EGFR-TKIs	B/R	Related signaling cascade (s) and/or transcription factors	Ref
miRNA-21	Increased	PTEN, Spry1, Spry2, PDCD4, NFIB	N/A	B	MAPK, AP-1, NFIB, RASV12, ID-1	2, 46
miRNA-21, miRNA-23b	Increased	TKR	Erlotinib, Vandetanib	R	EGFR	2
miRNA-218	Increased	PXN	N/A	B	N/A	48
miRNA-221,	Increased	PTEN, TIMP3, TKI, p27	TRAIL	R	AKT pathway and metallopeptidases	49
miRNA-222	Decreased	EGF/MET	Gefitinib	R	EGFR/MET	16,36
miRNA-424	Decreased	N/A	Erlotinib Vandetanib	R	N/A	41
miRNA-328	Increased	PRKCA	N/A	B	N/A	50
miRNA-101	Increased	Zeste homolog 2 (EZH2)	N/A	B	N/A	51
miRNA-125a-5p	Decreased	Rock-1, IL16, CCL21, ERBB4, RhoG, MMP11, CCL4, VEGFB, MMP28, MMP14, ROCK1, ZEB2, Smad5, VEGFA, Smad2, MAPK1, 4CDH5, IGF2, CD14, MMP15, CCR7	N/A	B	CCR3-chemokine-mediated	52
miRNA-145	Decreased	c-Myc, Akt and ERK	Gefitinib	R	c-Myc/eIF4E pathway, EGFR	27,53
miRNA-7	Decreased	c-Myc, Ets2, AKt, ERK, RAf1	N/A	B	Ras/ERK/Myc EGFR	17,27
miRNA-34a, miRNA-199a/b	Decreased	Myc, SIRT1, MEK1, CDK4, CDK6	N/A	B	Axl receptor tyrosine kinase, P53, ELK1, ERK-MAPK	54,55
miRNA-125a-3p	Decreased	IGF2, CCL4 , Smad5, IL33, RAB13, RAPH1, MAPK1,NF1, ZEB2, RhoA, VEGFA	N/A	B	CCR5 receptor	52
miRNA-126	Increased	Akt and ERK	Gefitinib	R	EGFL7 and VEGF-A	27,30
miRNA-128	Decreased	TKI	Gefitinib	R	EGFR	41
miRNA-214	Increased	PTEN	Gefitinib	R	PTEN/AKT	33

B, biomarker; R, resistance; N/A, not available.

Several studies also evaluated the modulation of the main downstream mediators of EGFR, but only a few investigated their impact on EGFR-TKIs activity. In particular, miR-205 was described as a new oncosuppressor gene in breast cancer because of its ability to down-modulate both Akt and HER3 receptor. The reintroduction of miR-205 in SKBr3 cells inhibited their clonogenic potential and increased the responsiveness to both gefitinib and lapatinib, abrogating the HER3-mediated resistance and restoring a potent proapoptotic activity [25]. Conversely, miR-26a enhanced lung cancer cell metastasis potential via modulation of metastasis-related gene expression, and activation of Akt pathway by PTEN suppression, suggesting that miR-26a might be a potential therapeutic candidate in patients with metastatic lung cancer [26].

The activation of both Akt and ERK is also regulated by miR-126, whose overexpression has been

shown to inhibit NSCLC cells proliferation. Additionally, forced expression of this miRNA significantly enhanced the cytotoxicity of gefitinib in the lung cancer cells H460 and A549 [27]. More recently, bioinformatics and functional studies demonstrated that EGF-like domain 7 (EGFL7) is a target of miR-126, which can inhibit A549 cells proliferation in vitro and inhibit tumor growth in vivo by targeting EGFL7 [28]. Similarly, miR-126 might alter lung cancer cells phenotype by inhibiting adhesion, migration, and invasion and the effects on invasion through regulation of Crk [29]. However, miR-126 has also been related to angiogenesis and regulation of VEGF-A, and univariate and multivariate analyses in two studies in resected stage I to IIIA NSCLC patients demonstrated its role as a significant negative prognostic factor [30, 31]. Thus, further studies to understand the main biological functions of miR-126 and explore its possible clinical relevance in NSCLC patients treated with EGFR-TKIs are warranted.

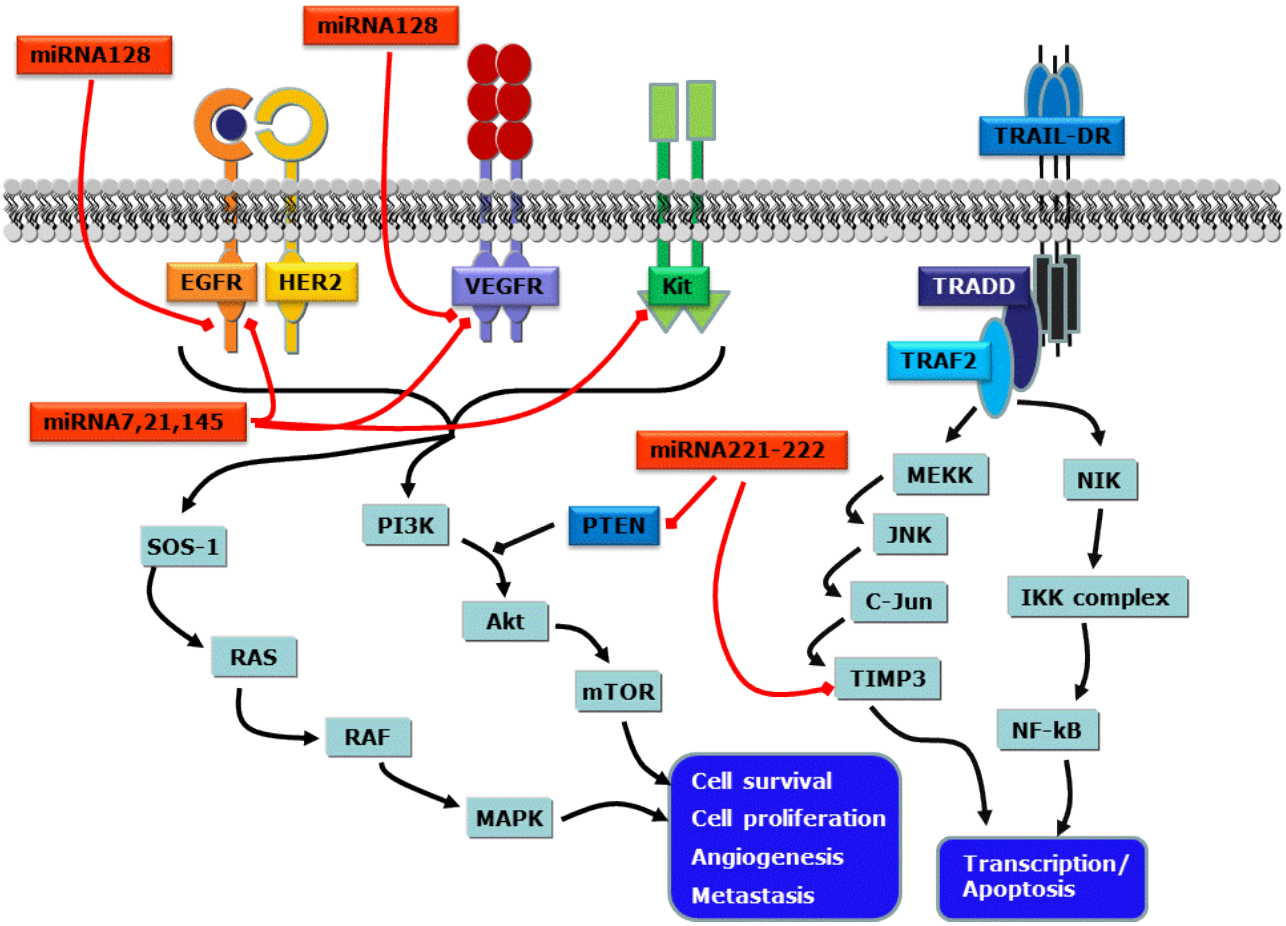

Figure 1. MicroRNAs regulating EGFR signaling cascade and related pathways (VEGFR, c-KIT, and TRAIL) in NSCLC.

3. ROLE OF MicroRNAs IN THE RESISTANCE TO EGFR-TKIs

NSCLC patients who have activating mutations of EGFR derive clinical benefit from treatment with gefitinib and erlotinib, but these therapeutic weapons are ultimately limited by the occurrence of mutations or alternative molecular mechanisms conferring drug resistance.

Some preliminary studies in NSCLC cell lines, evaluating miRNA associated with TKIs resistance in vitro, reported that increased levels of miR-21, miR-23a, miR-23b, and miR-29 were associated with resistance in three sunitinib-resistant variants of H1703 cells, while decreased miR-424 levels were

indicative of increased resistance to both erlotinib and vandetanib [2,32]. More recently, studies in the established gefitinib resistant cell line HCC827/GR, showed a significant up-regulation of miR-214. This study also showed that miR-214 and PTEN were inversely expressed, while knockdown of miR-214 altered the expression of PTEN and p-Akt, re-sensitizing HCC827/GR to gefitinib [33] The inhibition of miR-214 has been also correlated with decreased apoptosis in the lung adenocarcinoma cells A549 [22]. Moreover, miR-424 is among the significantly altered angiogenesis-related miRs in NSCLC tissues whereas the expression of miR-29 family (29a, 29b, and 29c) is inversely correlated to DNA methyltransferase DNMT3A and -3B in lung cancer tissues [31]. Thus, the enforced expression of miR-29s in lung cancer cell lines restores normal patterns of DNA methylation, inducing re-expression of methylation-silenced tumor suppressor genes, such as FHIT and WWOX [34].

The sensitivity to erlotinib can also be predicted by 13-gene miRNA signatures, identified using expression data of 8 NSCLC cell lines, which are separated in sensitive (H3255, H1650, H358 and PC9) and resistant (A549, UKY-29, H460 and H1975) according to apoptosis induction after 48 hours treatment [35]. Ontological annotation of these miRNAs (miR-140-3p, miR-628-5p, miR-518f, miR-636, miR-301a, miR-34c, miR-224, miR-197, miR-205, miR135b, miR-200b, miR-200c, and miR-141) and their potential targets revealed enrichment in the components of epithelial-to-mesenchymal transition (EMT), including Wnt pathway, which may explain the ability of this signature to separate primary from metastatic lung tumor samples. Interestingly, treatment with TGFβ1 modulated the expression of these miRNAs and EMT proteins, such as the transcription factor ZEB1, modulating cell migration. Therefore, Bryant and colleagues hypothesized that the tumor microenvironment might elicit TGFβ1 and trigger a miRNA expression pattern that induces resistance to anti-EGFR therapies and favor EMT of tumor cells and invasive behavior.

MET protein expression and phosphorylation have been associated with both primary and acquired resistance to EGFR-TKI therapy in NSCLC patients [36]. A pivotal study was performed which was focused on miR-30b, miR-30c, miR-221 and miR-222, which are regulated by both EGFR and MET, and miR-103 and miR-203, which are regulated by MET only. This study showed that gefitinib treatment triggers programmed cell death through the downregulation of miR-30b, miR-30c, miR-221 and miR-222 and the consequent upregulation of APAF-1 and BIM in gefitinib-sensitive HCC827 and PC9 cells. Conversely, gefitinib treatment did not decrease miR-30b, miR-30c, miR-221 and miR-222 expression in gefitinib-resistant Calu-1, A549 and HCC827/GR cells as a result of MET overexpression. Therefore, EGFR inhibition alone in cells overexpressing MET is not sufficient to induce the downregulation of these miRNAs and, accordingly, cell death. However, gefitinib-resistance was overcome by MET inhibitors, which downregulated miR-30b, miR-30c, miR-221 and miR-222 and sensitized NSCLCs to gefitinib. Gefitinib-resistance was also reversed by anti–miR-221 and anti–miR-30c, which strongly increased gefitinib sensitivity in vitro and in xenograft mouse models in vivo, suggesting that the modulation of specific miRNAs could have therapeutic applications to sensitize lung tumors to TKI therapy [16].

All these findings are stimulating more research to validate the role of miRNAs, in order to translate these results to the clinical setting, as legitimate tools to predict treatment response to EGFR inhibitors or NSCLC prognosis [2].

Multiple studies reported that the deregulation of several miRNAs, such as miR155, let7a-2, miR-21 and

miR-146, correlated with outcome in NSCLC patients [37-40]. However, only few data are available on the correlation of miRNAs expression with NSCLC patients' outcome after treatment with EGFR inhibitors. Since allelic loss in chromosome 3p is one of the most frequent and earliest genetic events in lung carcinogenesis, Weiss and colleagues investigated whether the loss of miR-128b correlated with response to targeted EGFR inhibition, since miR-128b is located on chromosome 3p, and is a putative regulator of EGFR [41]. Fifty-eight NSCLC tumor samples were analyzed and loss of miR-128b expression was frequently observed and associated with increased sensitivity to gefitinib via overexpression of EGFR. Another study showed a significant association between EGFR mutation status and miR-21 expression [13] but these data were not confirmed in a large number of NSCLC samples evaluated by Voortman and colleagues [40]. In tumor specimens from 639 IALT patients, the expression of miR-21, miR-29b, miR-34a/b/c, miR-155, and let-7a did not show any predictive relation with outcome, of cisplatin-based adjuvant chemotherapy. Similar studies, in large homogeneous populations, are needed to clarify the role of the above-mentioned miRNAs in resistance towards EGFR inhibitors. Furthermore, new technologies, such as next-generation sequencing, may provide useful tools to understand the role of miRNAs as effective biomarkers in the prediction of drug activity/resistance and outcome in specific clinical settings.

4. CONCLUSIONS AND FUTURE PERSPECTIVES

The availability of EGFR targeted agents has become an invaluable resource in the treatment of NSCLC, and the approval of gefitinib and erlotinib as first-line treatment of advanced NSCLC patients with EGFR activating mutations represents a milestone toward personalized medicine in medical oncology. However, most of these patients inevitably relapse due to the emergence of acquired resistance [4]. The challenge of tumor drug resistance to EGFR-TKIs makes multiple areas of research a priority, including assessment of novel biomarkers and possible targets that might prevent or suppress the proliferative, invasive and resistant behavior of lung cancer cells.

The understanding of the role exerted by specific miRNAs in the initiation and progression of lung cancer is exponentially increasing, but the knowledge about miRNAs affecting EGFR-TKIs resistance is still at an early stage. From previous studies on the role of miRNAs in resistance to conventional chemotherapy it is evident that, as with previous studies on gene profiling, most emerging miRNA signatures are not fully overlapping [42]. These difference might be explained by the type of specimens (frozen vs paraffin-embedded, micro- vs non-microdissected), experimental platforms used (quantitative PCR versus different miRNA array or in situ hybridization systems), tumor histology types, stage, regimens, small sample size, ethnic differences in the populations, lack of multivariate analysis and correction for multiple testing. In this regard, a general consensus is needed on the techniques and controls to be used and larger series of studies should be performed on paired neoplastic and normal tissues for NSCLC patients. Furthermore, the association of pathobiological with clinical information is warranted for the proper validation of specific miRNAs as new biomarkers.

The high stability of miRNAs in formalin-fixed or laser-microdissected tissues, and their expression levels, which can be directly measured also in blood, will increase their potential to contribute as diagnostic tool in lung cancer and, eventually, to identify responders and non-responders patients [43, 44].

An improved knowledge of the functions exerted by specific miRNAs in EGFR signaling pathways and

the precise identification of their key targets relevant to the resistance to EGFR-TKIs will also be instrumental for the development of miRNA-based therapeutics. Since miRNAs have the potential to modulate a cohort of gene networks, they might become therapeutically relevant in a “one-hit multitarget” context. The possibility to use miRNA agonists or antagonists, in order to restore/inhibit the function of down-regulated onco-suppressive miRNAs or upregulated oncogenic miRNAs, respectively, has been already successfully demonstrated in experimental tumor models. However, before translating experimental research advances into clinical practice, important issues mainly related to the development of new approaches for the in vivo delivery of miRNA-modulating molecules need to be addressed [45].

Hopefully, in the near future, the expression profiles of specific miRNAs could provide information about resistance of individual tumors to anti-EGFR treatments before starting therapy, whereas, the modulation of the expression of specific miRNAs before and during treatment might offer a new tool to overcome drug resistance and thereby improve the clinical outcome of NSCLC patients.

ACKNOWLEDGEMENTS

This work was supported by grants from the Netherlands Organization for Scientific Research (NWO, Veni grant, Elisa Giovannetti), AIRC-Marie Curie (International Fellowship, Elisa Giovannetti), CCA-VICI foundation (grant#2012-5-07, Amir Avan, Godefridus J. Peters, Elisa Giovannetti), FIRC grant (Fellowship for abroad, Elena Galvani).

REFERENCES

1. Siegel R, Naishadham D, Jemal A. Cancer statistics, 2012. CA Cancer J Clin. 2012;62:10-29.
2. Allen KE, Weiss GJ. Resistance may not be futile: microRNA biomarkers for chemoresistance and potential therapeutics. Mol Cancer Ther. 2010;9:3126-3136.
3. Broxterman HJ, Gotink KJ, Verheul HM. Understanding the causes of multidrug resistance in cancer: a comparison of doxorubicin and sunitinib. Drug Resist Updat. 2009;12:114–26.
4. Galvani E, Peters GJ, Giovannetti E. EGF receptor-targeted therapy in non-small-cell lung cancer: role of germline polymorphisms in outcome and toxicity. Future Oncol. 2012;8:1015-29.
5. Fojo T. Multiple paths to a drug resistance phenotype: mutations, translocations, deletions and amplification of coding genes or promoter promoter regions, epigenetic changes and microRNAs. Drug Resist Updat. 2007;10:59–67.
6. He L, Hannon GJ. microRNAs. small RNAs with a big role in gene regulation. Nature. 2004;5:522–31.
7. Cho WC. OncomiRs: The discovery and progress of microRNAs in cancers. Mol Cancer. 2007;6:60.
8. Esquela-Kerscher A, Slack FJ. Oncomirs: microRNAs with a role in cancer. Nat Rev Cancer. 2006;6:259-269.
9. Hatley ME, Patrick DM, Garcia MR, Richardson JA, Bassel-Duby R, van Rooij E, et al. Modulation of K-Ras-Dependent Lung Tumorigenesis by MicroRNA-21. Cancer Cell. 2010;18:282-293.
10. Pillai RS, Artus CG, Filipowicz W. Tethering of human Ago proteins to mRNA mimics the miRNA-mediated repression of protein synthesis. RNA. 2004;10:1518-1525.
11. Du L, Pertsemlidis A. microRNAs and lung cancer: tumors and 22-mers. 2010;29:109-122.
12. Croce CM. Causes and consequences of microRNA dysregulation in cancer. Nat Rev Genet. 2009;10:704-714.
13. Seike M, Goto A, Okano T, Bowman ED, Schetter AJ, Horikawa I, et al. MiRNA21 is an EGFR-regulated anti-apoptotic factor in lung cancer in never-smokers. Proc Natl Acad Sci U S A. 2009;106:12085-12090.
14. Kumar MS, Lu J, Mercer KL, Golub TR, Jacks T. Impaired microRNA processing enhances cellular transformation and tumorigenesis. Nat Genet. 2007;39:673-677.
15. Merritt WM, Lin YG, Han LY, Kamat AA, Spannuth WA, Schmandt R, et al. Dicer, Drosha, and outcomes in patients with ovarian cancer. N Engl J Med. 2008;359:2641-2650.
16. Garofalo M, Romano G, Di Leva G, Nuovo G, Jeon YJ, Ngankeu A, et al. EGFR and MET receptor tyrosine kinase-altered microRNA expression induces tumorigenesis and gefitinib resistance in lung cancers. Nat Med. 2011;18:74-82.
17. Chou YT, Lin HH, Lien YC, Wang YH, Hong CF, Kao YR, et al. EGFR promotes lung tumorigenesis by activating miRNA7 through a Ras/ERK/Myc pathway that targets the Ets2 transcriptional repressor ERF. Cancer Res. 2010;70:8822-8831.
18. Passetti F, Ferreira CG, Costa FF. The impact of microRNAs and alternative splicing in pharmacogenomics. Pharmacogenomics J. 2009;9:1-13.
19. Rosell R, Moran T, Queralt C, Porta R, Cardenal F, Camps C, et al. Screening for epidermal growth factor receptor mutations in lung cancer. N Engl J Med. 2009;361:958-967.
20. Lin PY, Yu SL and Yang PC. MicroRNA in lung cancer. Br J Cancer. 2010;103:1144-8.
21. Webster RJ, Giles KM, Price KJ, Zhang PM, Mattick JS, Leedman PJ. Regulation of epidermal growth factor receptor signaling in human cancer cells by microRNA-7. J Biol Chem. 2009; 284:5731-5741.
22. Cheng AM, Byrom MW, Shelton J, Ford LP. Antisense inhibition of human miRNAs and indications for an involvement of miRNA in cell growth and apoptosis. Nucleic Acids Research. 2005;33:1290-97.
23. Yamaguchi G, Takanashi M, Tanaka M, Fujita K, Ohira T, Kuroda M, et al. Isolation of miRNAs that target EGFR mRNA in human lung cancer. Biochem Biophys Res Commun. 2012;420:411-6.
24. Liu L, Shao X, Gao W, Zhang Z, Liu P, Wang R, et al. MicroRNA-133b Inhibits the Growth of Non-small Cell Lung Cancer by Targeting the Epidermal Growth Factor Receptor. FEBS J. 2012;doi: 10.1111/j.1742-4658.
25. Iorio MV, Casalini P, Piovan C, Di Leva G, Merlo A, Triulzi T, et al. microRNA-205 regulates HER3 in human breast cancer. Cancer Res. 2009;69:2195-200.
26. Liu B, Wu X, Liu B, Wang C, Liu Y, Zhou Q, et al. MiR-26a enhances metastasis potential of lung cancer cells via AKT pathway by targeting PTEN. Biochim Biophys Acta. 2012;1822:1692-1704.
27. Zhong M, Ma X, Sun C, Chen L. MicroRNAs reduce tumor growth and contribute to enhance cytotoxicity induced by gefitinib in non-small cell lung cancer. Chem Biol Interact. 2010;184:431-438.
28. Sun Y, Bai Y, Zhang F, Wang Y, Guo Y, Guo L. miRNA126 inhibits non-small cell lung cancer cells proliferation by targeting EGFL7. Biochem Biophys Res Commun. 2010;391:1483-1489.
29. Crawford M, Brawner E, Batte K, Yu L, Hunter MG, Otterson GA, et al. MicroRNA-126 inhibits invasion in non-small cell lung

carcinoma cell lines. Biochem Biophys Res Commun. 2008;373:607-12.

30. Donnem T, Lonvik K, Eklo K, Berg T, Sorbye SW, Al-Shibli K, et al. Independent and tissue-specific prognostic impact of miRNA126 in nonsmall cell lung cancer: Coexpression with vascular endothelial growth factor-A predicts poor survival. Cancer. 2011;117:3193-3200.
31. Donnem T, Fenton CG, Lonvik K, Berg T, Eklo K, Andersen S, et al. MicroRNA signatures in tumor tissue related to angiogenesis in non-small cell lung cancer. PLoS One. 2012;7:e29671.
32. Nelson K, Sima C, Edwards D, Weiss G. microRNA biomarkers associated with sunitinib resistance in non-small cell lung cancer. Proceedings of the 101st Annual Meeting of the American Association for Cancer Research, 2010 Apr 17-21, Washington, DC. Philadelphia: AACR, 2010. Abstract nr. 3048.
33. Wang YS, Wang YH, Xia HP, Zhou SW, Schmid-Bindert G, Zhou CC. MicroRNA-214 regulates the acquired resistance to gefitinib via the PTEN/AKT pathway in EGFR-mutant cell lines. Asian Pac J Cancer Prev. 2012;13:255-60.
34. Fabbri M, Garzon R, Cimmino A, Liu Z, Zanesi N, Callegari E, et al. MicroRNA-29 family reverts aberrant methylation in lung cancer by targeting DNA methyltransferases 3A and 3B. Proc Natl Acad Sci U S A. 2007;104:15805-10.
35. Bryant JL, Britson J, Balko JM, Willian M, Timmons R, Frolov A, et al. A microRNA gene expression signature predicts response to erlotinib in epithelial cancer cell lines and targets EMT. Br J Cancer. 2012;106:148-56.
36. Zucali PA, Ruiz MG, Giovannetti E, Destro A, Varella-Garcia M, Floor K, et al. Role of cMET expression in non-small-cell lung cancer patients treated with EGFR tyrosine kinase inhibitors. Ann Oncol. 2008;19:1605-12.
37. Markou A, Tsaroucha EG, Kaklamanis L, Fotinou M, Georgoulias V, Lianidou ES. Prognostic value of mature microRNA-21 and microRNA-205 overexpression in non-small cell lung cancer by quantitative real-time RT-PCR. Clin Chem. 2008;54:1696-704.
38. Raponi M, Dossey L, Jatkoe T, Wu X, Chen G, Fan H, et al. MicroRNA classifiers for predicting prognosis of squamous cell lung cancer. Cancer Res. 2009;69:5776-83.
39. Patnaik SK, Kannisto E, Knudsen S, Yendamuri S. Evaluation of microRNA expression profiles that may predict recurrence of localized stage I non-small cell lung cancer after surgical resection. Cancer Res. 2010;70:36-45.
40. Voortman J, Goto A, Mendiboure J, Sohn JJ, Schetter AJ, Saito M, et al. MicroRNA expression and clinical outcomes in patients treated with adjuvant chemotherapy after complete resection of non-small cell lung carcinoma. Cancer Res. 2010;70:8288-98.
41. Weiss GJ, Bemis LT, Nakajima E, Sugita M, Birks DK, Robinson WA, et al. EGFR regulation by microRNA in lung cancer: correlation with clinical response and survival to gefitinib and EGFR expression in cell lines. Ann Oncol. 2008;19:1053-1059.
42. Giovannetti E, Erozenci A, Smit J, Danesi R, Peters GJ. Molecular mechanisms underlying the role of microRNAs (miRNAs) in anticancer drug resistance and implications for clinical practice. Crit Rev Oncol Hematol. 2012;81:103-22.
43. Funel N, Giovannetti E, Pollina LE, del Chiaro M, Mosca F, Boggi U, et al. Critical role of laser microdissection for genetic, epigenetic and proteomic analyses in pancreatic cancer. Expert Rev Mol Diagn. 2011;11:695-701.
44. Hu Z, Chen X, Zhao Y, Tian T, Jin G, Shu Y, et al. Serum microRNA signatures identified in a genome-wide serum microRNA expression profiling predict survival of non-small-cell lung cancer. J Clin Oncol. 2010;28:1721-6.
45. Gandellini P, Profumo V, Folini M, Zaffaroni N. MicroRNAs as new therapeutic targets and tools in cancer. Expert Opin Ther Targets. 2011;15:265-79.
46. Fujita S, Ito T, Mizutani T, Minoguchi S, Yamamichi N, Sakurai K. miRNA21 Gene expression triggered by AP-1 is sustained through feedback mechanism. J Mol Biol. 2008;378,492-504.
47. Sarkar FH, Li Y, Wang Z, Kong D, Ali S. Implication of microRNAs in drug resistance for designing novel cancer therapy. Drug Resist Upda. 2010;13:57-66.
48. Wu DW, Cheng YW, Wang J, Chen CY, Lee H. Paxillin predicts survival and relapse in non-small cell lung cancer by microRNA-218 targeting. Cancer Res. 2010;70:10392-10401.
49. Garofalo M, Di Leva G, Romano G, Nuovo G, Suh SS, Ngankeu A, et al. miRNA221&222 regulate TRAIL resistance and enhance tumorigenicity through PTEN and TIMP3 downregulation. Cancer Cell. 2009;16:498-509.
50. Arora S, Ranade AR, Tran NL, Nasser S, Sridhar S, Korn RL, et al. MicroRNA-328 is associated with (non-small) cell lung cancer (NSCLC) brain metastasis and mediates NSCLC migration. Int J Cancer. 2011;129:2621-2631.
51. Zhang JG, Guo JF, Liu DL, Liu Q, Wang JJ. MicroRNA-101 Exerts Tumor-Suppressive Functions in Non-small Cell Lung Cancer through Directly Targeting Enhancer of Zeste Homolog 2. J Thorac Oncol. 2011;6:671-678.
52. Jiang L, Huang Q, Zhang S, Zhang Q, Chang J, Qiu X, et al. Hsa-miRNA125a-3p and hsa-miRNA125a-5p are downregulated in non-small cell lung cancer and have inverse effects on invasion and migration of lung cancer cells. BMC Cancer. 2010;10:318.
53. Chen Z, Zeng H, Guo Y, Liu P, Pan H, Deng A, et al. miRNA-145 inhibits non-small cell lung cancer cell proliferation by targeting c-Myc. J Exp Clin Cancer Res. 2010;29:151.
54. Mudduluru G, Ceppi P, Kumarswamy R, Scagliotti GV, Papotti M, Allgayer H. Regulation of Axl receptor tyrosine kinase expression by miRNA34a and miRNA199a/b in solid cancer. Oncogene. 2011;30:2888-2899.

55. Wang Z, Chen Z, Gao Y, Li N, Li B, Tan F, et al. DNA hypermethylation of microRNA-34b/c has prognostic value for stage I non-small cell lung cancer. Cancer Biol Ther. 2011;11:490-496.

Chapter 6

Irreversible Inhibition of EGFR Activity by 3-Aminopropanamides

Carmi C, Galvani E, Vacondio F, Rivara S, Lodola A, Russo S, Aiello S, Bordi F, Costantino G, Cavazzoni A, Alfieri RR, Ardizzoni A, Petronini PG & Mor M.

JOURNAL OF MEDICINAL CHEMISTRY 2012

55(5):2251-64.

ABSTRACT

Irreversible EGFR inhibitors contain a reactive warhead which covalently interacts with a conserved cysteine residue in the kinase domain. The acrylamide fragment, a commonly employed warhead, effectively alkylates Cys797 of EGFR, but its reactivity can cause rapid metabolic deactivation or nonspecific reactions with off-targets. We describe here a new series of irreversible inhibitors containing a 3-aminopropanamide linked in position 6 to 4-anilinoquinazoline or 4-anilinoquinoline-3-carbonitrile driving portions. Some of these compounds proved as efficient as their acrylamide analogs in inhibiting EGFR-TK autophosphorylation in A549 lung cancer cells. Moreover, several 3-aminopropanamides suppressed proliferation of gefitinib-resistant H1975 cells, harboring the T790M mutation in EGFR, at significantly lower concentrations than did gefitinib. A prototypical compound, N-(4-(3-bromoanilino)quinazolin-6-yl)-3-(dimethylamino)propanamide (**5**), did not show covalent binding to cell-free EGFR-TK in a fluorescence assay, while it underwent selective activation in the intracellular environment, releasing an acrylamide derivative which can react with thiol groups.

INTRODUCTION

The epidermal growth factor receptor (EGFR, ErbB1) is a member of the ErbB family of receptor tyrosine kinases (RTKs), also including ErbB2/HER2, ErbB3/HER3, and ErbB4/HER4 [1,2]. Upon ligand binding, EGFR forms homo- or heterodimers with other members of the ErbB family and undergoes autophosphorylation of specific tyrosine residues in its intracellular domain. This event activates a series of downstream signals and regulates biological processes such as cell proliferation, apoptosis, angiogenesis and differentiation [3,4]. Deregulation of EGFR signaling has been observed in many human cancers, including lung, head and neck, colorectal, ovarian, breast and bladder cancers and it has been associated with more aggressive disease and poorer clinical outcome [5-7]. In this light, inhibitors targeting the EGFR have been extensively investigated and employed as anti-tumor agents.

The EGFR inhibitors **1** (gefitinib, Figure 1) and 4-(3-ethynylanilino)-6,7-bis(2-methoxyethoxy)quinazoline (erlotinib, Figure 1), and the EGFR/erbB2 inhibitor **2** (lapatinib, Figure 1) belong to the chemical class of 4-anilinoquinazolines, designed to bind the ATP binding pocket of the kinase domain of the target [8-10]. Although **1** is effective in the treatment of non-small cell lung cancer (NSCLC) in patients having activating mutations within the EGFR tyrosine kinase domain, accumulating clinical experience indicates that most patients develop resistance after repeated treatments [11,12]. In half of NSCLC cases, resistance was associated with the emergence of a single amino acid substitution in the catalytic domain of EGFR: conversion of the gatekeeper threonine 790 with methionine (T790M) [12-15].

Covalent alkylation of a cysteine residue (Cys797), positioned at the entrance of the ATP binding site, was the additional mechanism of second-generation irreversible EGFR inhibitors, which had been shown to overcome resistance to gefitinib [16-20]. Several inhibitors of this class, such as N-(4-(3-chloro-4-fluoroanilino)-7-(3-morpholinopropoxy)quinazolin-6-yl)acrylamide (CI-1033, canertinib, Figure 1) [21], N-(4-(3-chloro-4-fluoroanilino)-7-(tetrahydrofuran-3-yloxy)quinolin-6-yl)-4-(dimethylamino)but-2-enamide (BIBW-2992, Figure 1) [22], and N-(4-(3-chloro-4-(pyridin-2-ylmethoxy)anilino)-3-cyano-7-ethoxyquinolin-6-yl)-4-(dimethylamino)but-2-enamide (HKI-272, neratinib, Figure 1) [23], have progressed to clinical investigation in patients that initially responded to **1** and subsequently relapsed [24]. EGFR irreversible covalent inhibitors are characterized by a heterocyclic core structure (driving portion) carrying at a proper position an electrophilic functionality (warhead) that covalently interacts with the specific cysteine residue in the target protein [25-29]. The ability of the warhead to covalently interact with nucleophiles is responsible for the advantages of EGFR irreversible inhibitors over conventional ATP-competitive ones: i) overcoming secondary resistance [19], ii) selectivity for ErbB-family TK [30], iii) long lasting effect [16]. On the other hand, the intrinsic reactivity of the warhead is also associated with augmented metabolic degradation and toxicity, due to reactions with non-target proteins [31,32]. Systematic analysis of cysteine residues present in the nucleotide binding site of kinases had recently shown that combination of a driving portion and an electrophilic warhead could also be applied in a more general way to target different cysteines in different kinases [33]. To this aim, the availability of a panel of cysteine-reactive groups with different reactivity could be beneficial for the development of new drug-like inhibitors.

Recently, our group has reported a systematic exploration of the role and reactivity of warheads for EGFR-TK inhibition by introducing different cysteine-trap portions on an 4-anilinoquinazoline recognition

scaffold [34]. Compounds with different functional groups that were less reactive towards bionucleophiles (such as glutathione) than the reference acrylamide **3** [16] (PD168393, Table 1), proved efficient in irreversibly inhibiting EGFR autophosphorylation.

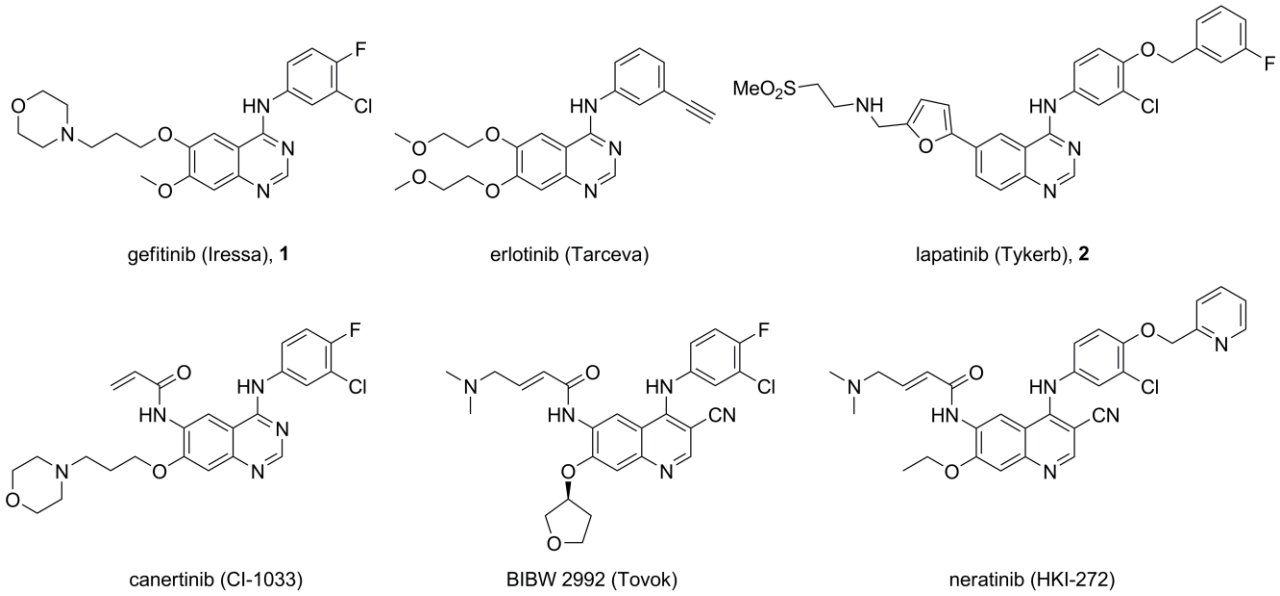

Figure 1. Chemical structures of reversible and irreversible EGFR inhibitors.

In our ongoing search for functional groups that are able to covalently interact with cysteine residues of EGFR, we focused on a new chemical entity containing a 3-aminopropanamide moiety [35-37]. Aryl β-aminoethyl ketones (Mannich bases) have been described as irreversible inhibitors of enzymes having a crucial cysteine residue in the active site or at regulatory positions [38-40]. These compounds possess a particular profile of reactivity, being non-reactive directly, but able to covalently modify their biological target after bioconversion via β-elimination to the corresponding α,β-unsaturated carbonyl compound. Maresso and co-workers reported aryl β-aminoethyl ketones as irreversible inhibitors of the bacterial enzyme sortase, a target for the development of antibacterial therapeutics [38]. They demonstrated through mass spectrometry and X-ray analysis that enzyme inhibition proceeds via a reactive olefin intermediate, generated in-situ by amine elimination, which forms a covalent adduct with a specific cysteine residue within the protein active site. Aryl β-aminoethyl ketones have also been reported as inhibitors of intracellular kinases, such as Janus kinase 3 (Jak3), interleukin-2 inducible tyrosine kinase (ITK) and Bruton's tyrosine kinase (BTK) [42], as well as weak EGFR tyrosine kinase inhibitors in enzymatic assay [41-43]. Recently, β-aminolactones have also been described as novel anticancer agents, endowed with high oral bioavailability in rats. β-Aminolactone derivatives can undergo retro-Michael addition reaction to generate the parent α-methylenelactones that interact with nucleophilic sites on biological macromolecules [44]. In principle, masking the acrylamide warhead of irreversible inhibitors should reduce the risk of covalent interactions with off-targets, due to limited systemic exposure. Of course, this would result in a specific advantage only if the anti-proliferative potency and efficacy of masked agents is equivalent or similar to those of corresponding compounds having a free acrylamide fragment.

In the present study, we describe the synthesis and biological evaluation of new EGFR-TK inhibitors

containing a 3-aminopropanamide side chain linked to a 4-anilinoquinazoline (**5-9** A-series, and **11-13** B-series in Table 1) or 4-anilinoquinoline-3-carbonitrile (**15-17**, and **19-21**, C- and D-series, respectively, in Table 1) driving portion. Reference acrylamide derivatives for each series were also prepared (**3**, **10**, **14**, and **18**, Table 1).

The new compounds were tested as EGFR tyrosine kinase inhibitors in enzyme-based and cell-based assays. Antiproliferative activity of the new compounds was also investigated in the gefitinib-resistant H1975 NSCLC cell line, harboring the T790M mutation. Moreover, for the most active agents, effects on mutated (T790M) EGFR autophosphorylation and on ErbB2 tyrosine kinase activity were evaluated. We hypothesized that the observed long-lasting effect on EGFR autophosphorylation was the result of an irreversible covalent interaction between the 3-aminopropanamide side chain and Cys797 within the active site of the enzyme. To evaluate this hypothesis, we performed a series of in vitro chemical stability assays; reactivity studies in the presence of thiol nucleophiles, and reactivity studies toward EGFR tyrosine kinase. Pharmacological data and reactivity study results were combined and evaluated in order to identify new irreversible EGFR inhibitors with lower intrinsic reactivity and optimized efficacy/toxicity profile compared to those of the other cysteine-reactive species described to date.

Table 1. EGFR tyrosine kinase and autophosphorylation inhibition in A549 cells. Viability inhibition of H1975 gefitinib-resistant cell line.

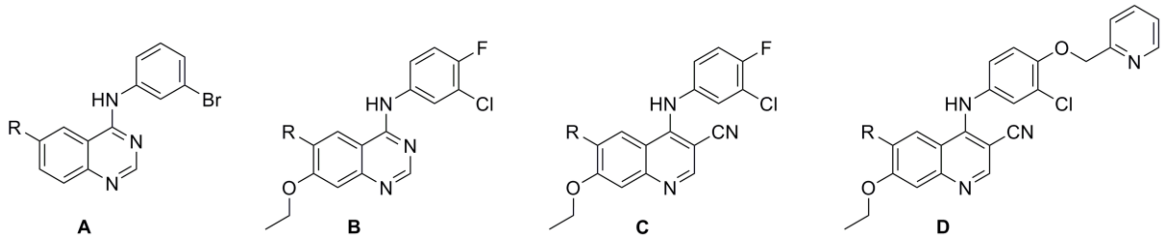

Compd	Series	R	kinase assay[a]	autophosphorylation assay (A549)[b]		H1975 cell line[c]
			IC_{50} (nM)	% inhibition 1 µM		IC_{50} (µM)
				1 h	8 h	
3	A	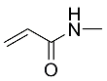	1.69 ± 0.16[d]	98 ± 1.8	86 ± 0.4	0.61 ± 0.05[d]
4	A	H_2N-	n.d.	91 ± 5.9	0.0 ± 0.1	19.5 ± 2.46[d]
5	A	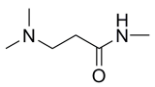	0.28 ± 0.07	97 ± 1.4	89 ± 1.0	3.69 ± 1.10
6	A	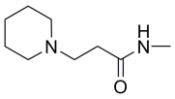	0.27 ± 0.04	95 ± 2.6	93 ± 4.0	6.67 ± 0.75
7	A	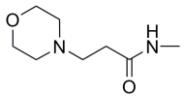	0.51 ± 0.06	98 ± 1.8	91 ± 5.4	> 20
8	A	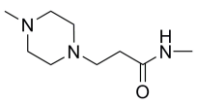	0.23 ± 0.07	99 ± 0.5	79 ± 11	14.3 ± 2.23

9	A	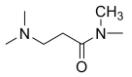	17.4 ± 1.62	47 ± 8.8	10 ± 3.3	13.6 ± 1.66
10	B	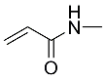	0.18 ± 0.04	96 ± 4.0	99 ± 0.6	1.62 ± 0.45
11	B	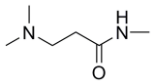	0.27 ± 0.05	98 ±1.1	100 ±0.3	2.21 ± 0.69
12	B	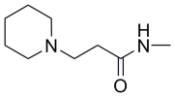	0.51 ± 0.06	98 ± 1.6	92 ±3.7	1.61 ± 0.07
13	B	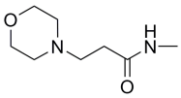	0.29 ± 0.06	97 ± 2.3	97 ± 0.4	2.11 ± 0.63
14	C	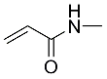	1.46 ± 0.37	92 ± 4.4	33 ±11	3.57 ± 1.04
15	C	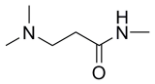	0.68 ± 0.11	88 ± 2.8	67 ± 8.6	2.37 ± 0.15
16	C	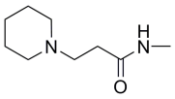	2.21 ± 0.37	96 ± 5.8	82 ± 3.6	2.73 ± 0.28
17	C	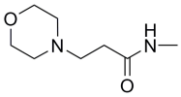	2.02 ± 0.44	86 ± 5.2	48 ± 7.4	3.93 ± 0.95
18	D	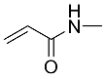	50.7 ± 1.33	100 ± 0.3	83 ± 7.9	0.63 ± 0.13
19	D	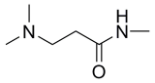	12.5 ± 0.88	61 ± 5.2	59 ± 11	2.03 ± 0.42
20	D	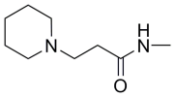	24.8 ± 3.88	71 ± 2.1	58 ± 3.2	0.71 ± 0.14
21	D	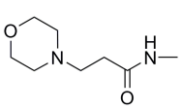	37.5 ± 8.99	48 ± 3.3	39 ± 9.5	2.76 ± 0.41

[a] Concentration to inhibit by 50% EGFR-wt tyrosine kinase activity. IC_{50} values were measured by the phosphorylation of a peptide substrate using time-resolved fluorometry (see Experimental Section). Mean values of three independent experiments ± SEM are reported. [b] Inhibition of EGFR autophosphorylation was measured in A549 intact cells by Western blot analysis. Percent inhibition at 1 μM concentration was measured immediately after and 8 h after removal of the compound from the medium (1 h incubation). Mean values of at least two independent experiments ± SEM are reported. [c] Concentration to inhibit by 50% the proliferation of NSCLC H1975. The cell proliferation was determined by the MTT assay, after 72 h of incubation with compounds (0.1–20 μM). Mean values of three independent experiments ± SEM are reported. [d] Data from Ref. 34.

CHEMISTRY

Compounds of series A (**5-9**) of Table 1 were synthesized by coupling their precursor amines (**4** or **26**) with the proper carboxylic acid and substituting the terminal chlorine with various amines, as described in Scheme 1. The 6-amino-4-(3-bromoanilino)quinazoline **4** was prepared in three steps from 5-nitroanthranilonitrile 22 as previously described (Scheme 1) [45,46]. Condensation of 4 with 3-chloropropionyl chloride gave the 3-chloropropanamide intermediate **27a**, which underwent substitution with

the proper amine to obtain the secondary 3-aminopropanamides **5-9**. Alternatively, 6-aminoquinazoline **4** was converted to its N-methyl analogue **26** [47] by carbamoylation with ethyl chloroformate in pyridine followed by reduction of the resulting carbamate **25** with sodium bis(2-methoxyethoxy)aluminum hydride (Red-Al). The N-methylaminoquinazoline **26** thus generated was first condensed with 3-chloropropionyl chloride to **27b**, and then substituted with dimethylamine to obtain the tertiary 3-aminopropanamide derivative **9** (Scheme1).

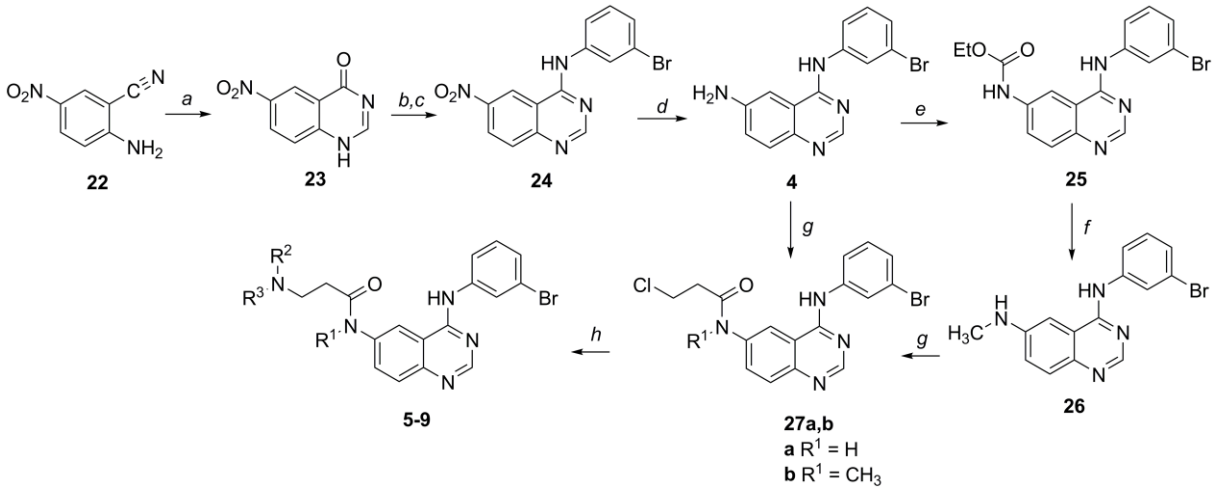

Scheme 1. Synthesis of compounds 4-9. Reagents and conditions: (a) H_2SO_4, formic acid, reflux; (b) $SOCl_2$, dioxane, reflux; (c) 3-bromoaniline, *i*-PrOH, 60 °C; (d) Fe, AcOH, EtOH/H_2O, reflux; (e) ClCOOEt, anhydrous pyridine, 0 °C to rt; (f) Red-Al, THF, rt; (g) $ClCH_2CH_2COCl$, THF, 50 °C; (h) R^2R^3NH, KI, abs EtOH, reflux.

4-(3-Chloro-4-fluoroanilino)-7-ethoxyquinazolino compounds of series B (**10-13**) of Table 1 were synthesized as described in Scheme 2. 6-Aminoquinazoline intermediate **34** [48] was obtained following a slightly modified procedure [49] from 4-chloroanthranilic acid **28**. Briefly, cyclization of **28** with formamidine acetate followed by nitration gave a mixture of isomers from which pure **30** was obtained after recrystallization from acetic acid. The 7-chlorine group was substituted with sodium ethoxide and the resulting 7-ethoxy derivative **31** was first chlorinated by heating in phosphorus oxychloride then substituted with 3-chloro-4-fluoroaniline to obtain the intermediate **33**. Reduction of the nitro group of **33** with iron and acetic acid gave the 6-aminoquinazoline **34**. The 6-acrylamide derivative 10 was then obtained from **34** with acryloyl chloride in the presence of N,N-diisopropylethylamine (DIPEA). Finally, 3-aminopropanamides **11-13** were synthesized from **34** by reaction with 3-chloropropionyl chloride to **35** and then substituting the chlorine with the proper secondary amine (Scheme 2).

4-Anilinoquinoline-3-carbonitriles of series C and D (**14-17** and **18-21**, respectively) of Table 1 were synthesized as described in Scheme 3. The key N-(4-chloro-3-cyano-7-ethoxyquinolin-6-yl)acetamide intermediate **40** was synthesized in 6 steps from 2-amino-5-nitrophenol **36**, as previously reported [50]. The quinoline intermediate 40 was reacted with the proper aniline (to **41a** and **41b**) and deacetylated in aqueous hydrochloric acid to amines **42a** [51] and **42b** [52]. Aniline derivative **45** was synthesized by reaction of 4-amino-2-chlorophenol **44** and picolyl chloride in the presence of benzaldehyde as described in Scheme 3 [53]. The acrylamides **14** and **18** were subsequently synthesized from amine precursors, **42a** and **42b** respectively, with acryloyl chloride in the presence of a base (DIPEA). The 3-aminopropanamides **15-17** and **19-21** were synthesized in two steps from amines **42** by condensation with 3-chloropropionyl chloride and

substitution with a secondary amine (Scheme 3).

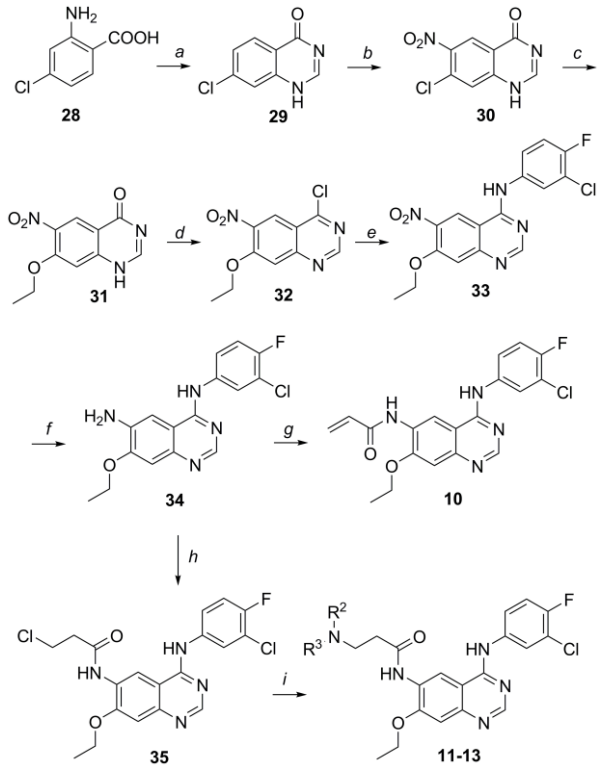

Scheme 2: **Synthesis of compounds 10-13.** Reagents and conditions: (a) Formamidine acetate, 2-methoxyethanol, 130 °C; (b) H_2SO_4, HNO_3, 100 °C; (c) NaOEt, anhydrous EtOH, reflux; (d) $POCl_3$, reflux; (e) 3-chloro-4-fluoroaniline, *i*-PrOH, reflux; (f) Fe, AcOH, EtOH/H_2O, reflux; (g) acryloyl chloride, DIPEA, DMF, 0 °C to 50 °C; (h) $ClCH_2CH_2COCl$, 50 °C; (i) R^2R^3NH, KI, abs EtOH, reflux.

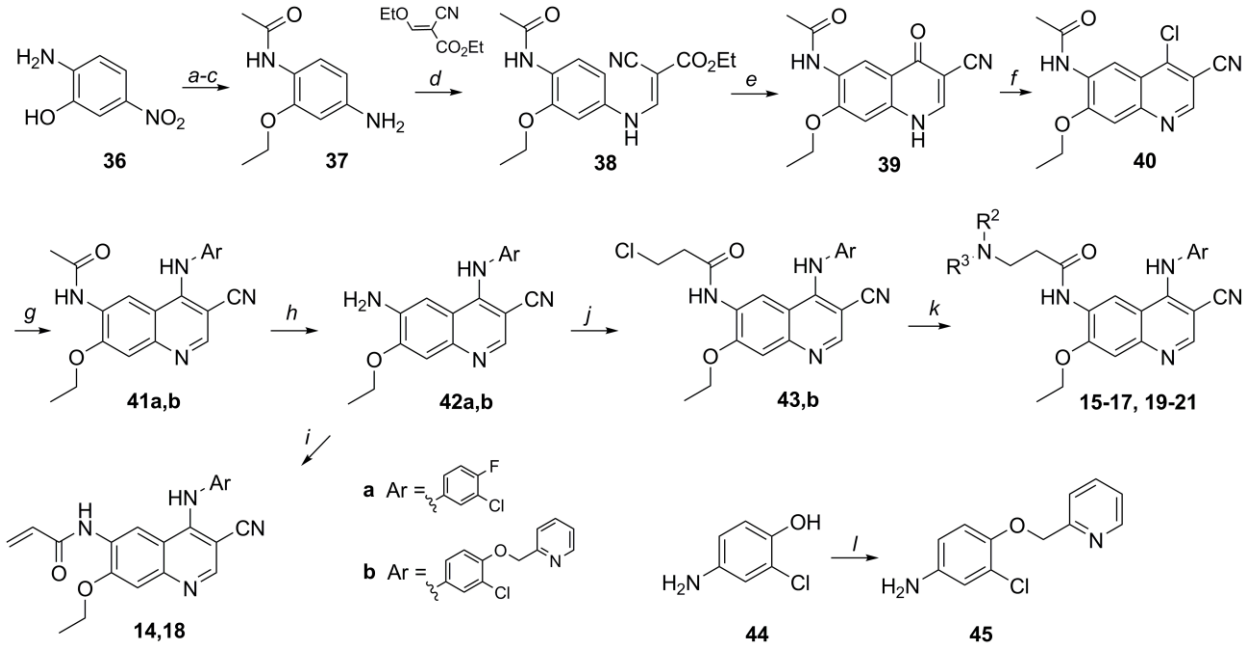

Scheme 3: **Synthesis of compounds 14-21.** Reagents and conditions: (a) Ac_2O, AcOH, 60 °C; (b) EtBr, DMF, K_2CO_3, 60 °C; (c) H_2, Pd/C, THF, rt; (d) toluene, 90 °C; (e) Dowterm, 250 °C; (f) $POCl_3$, diglyme, 100 °C; (g) 3-chloro-4-fluoroaniline or **45**, pyridine hydrochloride, *i*-PrOH, reflux; (h) HCl, reflux; (i) acryloyl chloride, DIPEA, DMF, 0 °C to 50 °C; (j) $ClCH_2CH_2COCl$, THF, 50 °C; (k) R^2R^3NH, KI, abs EtOH, reflux; (l) PhCHO, K_2CO_3, picolyl chloride hydrochloride, DMF, 50 °C.

RESULTS AND DISCUSSION

Kinase and Cellular Inhibitory Activities

Compounds **3-21** (Table 1) were evaluated in enzyme-based and cell-based assays for their ability to inhibit EGFR tyrosine-kinase activity. Their inhibitor potency on human EGFR in a cell-free environment was measured on the phosphorylation of a peptide substrate, using time-resolved fluorometry (see Experimental Section). In these conditions, the reference compound 3 had an IC_{50} of 1.7 nM [34]. Within the series of quinazoline derivatives with the same driving portion as **3** (series A in Table 1), substitution of the acrylamide warhead with a substituted 3-aminopropanamide (**5-8**) produced a generalized increase in inhibitor potency, with IC_{50} values in the subnanomolar range. These values are likely to result from a complex inhibition mechanism, including reversible competition with ATP and covalent interaction with EGFR in different proportions for different compounds. We therefore consider these values as rough measures of the relative propensity to interact with the target. Methylation of the amide nitrogen of **5** to the tertiary amide **9** notably reduced EGFR-TK inhibition potency (IC_{50} 17 nM). B-series quinazoline compounds **10-13**, carrying 4-(4-fluoro-3-chloroanilino) and 7-ethoxy substituents, did not show significant changes in kinase inhibition potencies when the electrophilic warhead (**10**) was replaced with 3-dimethylamino- (**11**), 3-piperidino- (**12**) or 3-morpholinopropanamide (**13**), all compounds having subnanomolar IC_{50}s. Considering the two series of quinoline-3-carbonitriles C and D, compounds **14-17** (C-series) were only slightly less potent in inhibiting EGFR-TK compared to the parent B-series quinazoline derivatives, while compounds **17-21** (D-series), carrying a 3-chloro-4-(3-fluorobenzyloxy)anilino substituent at position 4 similar to that of the EGFR/erbB2 inhibitor 2 (Figure 1), were up to 60-fold less potent than the A- and B-series quinazolines. In view of the similarity between the D-series compounds (Table 1) and the EGFR/erbB2 inhibitor **2**, the effect of **19** and **20** was also evaluated on erbB2-TK. Compound **2** is a slowly reversible, non-covalent inhibitor of tyrosine kinase that binds the enzyme in an inactive-like conformation, thus reducing the rate of inhibitor dissociation enabling prolonged actions in biological systems [10]. Results of enzyme-based assay for ErbB2 inhibition by time-resolved fluorometry were compared to that of the 3-dimethylaminopropanamide **5**, belonging to the A-series of quinazoline compounds (Supporting Information, Table S2). As expected, while **5** did not inhibit ErbB2 up to 10 μM concentration, compounds **19** and **20** showed IC_{50} values for erbB2 tyrosine kinase inhibition in the submicromolar range (IC_{50} = 0.97 and 0.98 μM, respectively). These data show that the 3-aminopropanamide is well tolerated at both the EGFR and erbB2 binding sites of the quinazoline/quinoline-3-carbonitrile driver portions.

The ability of the compounds to inhibit EGFR autophosphorylation was investigated in the A549 human lung cancer cell line by Western blotting. Percent inhibitions at 1 μM concentration are reported in Table 1. Results were compared to those observed for the reference compounds **3** and **4**, recognized as irreversible and reversible EGFR inhibitors, respectively. A549 cells, which express wild type EGFR, were treated for 1 h with inhibitor and then washed with drug-free medium. The degree of EGFR autophosphorylation was measured either immediately after or 8 h after removal of the inhibitor [16]. As previously reported, 80% or greater EGFR inhibition 8 h after removal of the inhibitor from the medium were considered a sign of irreversible inhibition [54]. Within the A-series of 4-anilinoquinazolines, the irreversible acrylamide **3** showed 86% inhibition after the 8-h washout. Substitution of the reactive acrylamide warhead with 3-dimethylamino-

(**5**), 3-piperidino- (**6**) or 3-morpholinopropanamide (**7**) gave similar results on EGFR autophosphorylation, both immediately after and 8 h after washout, with inhibition of EGFR autophosphorylation over 95% and in the range 89-93% at 1 h and 8 h, respectively. The 4-methylpiperazine analogue **8** strongly inhibited EGFR autophosphorylation after 1 h (> 99% inhibition), while it showed a slightly decrease in inhibitory activity 8 h after removal from the medium (79% inhibition). The tertiary amide **9** poorly inhibited EGFR (47% inhibition at 1 h) with only 10% residual inhibition 8 h after treatment, probably because of reduced affinity at the recognition site. As expected, the 6-amino derivative **4** completely inhibited EGFR activity after 1 h treatment and did not show any inhibitory effect 8 h after its removal from the medium.

We further introduced the 3-aminopropanamido fragment on quinazoline or quinoline-3-carbonitrile scaffolds with 3-chloro-4-fluoro substitution on the 4-aniline ring and a 7-ethoxy group on the heterocyclic nucleus (B- and C-series, Table 1) since previous work had suggested that this substitution pattern led to optimal activity [25,51]. The acrylamide derivative **10**, belonging to the B-series of quinazolines, completely inhibited EGFR autophosphorylation 1 h and 8 h after treatment at 1 μM concentration (96% and 99% inhibition, respectively). Substitution of the electrophilic warhead of **10** with a 3-aminopropanamide side chain led to compounds **11** (dimethylamino), **12** (piperidino), and **13** (morpholino) which gave EGFR percents inhibition at 1 h and 8 h after removal from the medium between 92 and 100%. In the C-series of compounds, the acrylamide **14** proved efficient in inhibiting EGFR at 1 μM concentration after 1 h treatment (92% inhibition), but produced only partial inhibition 8 h after wash-out (33% inhibition). This unexpected behavior may be due to the reduced solubility of compound **14** in the reaction medium (data not shown). In fact, among 3-aminopropanamides **15-17**, only the piperidino derivative **16** gave complete and irreversible EGFR inhibition (92% and 82% inhibition 1 h and 8 h after removal from the medium, respectively), while dimethylamino (**15**) and morpholino (**17**) compounds inhibited EGFR at 1 h, but produced only a partial, yet significant, irreversible inhibition 8 h after treatment, as demonstrated by 67% and 48% inhibition of autophosphorylation, respectively.

Partial inhibition of EGFR autophosphorylation in A459 cells was also shown by the other series of quinoline-3-carbonitrile derivatives (D-series, **19-21**). In this series, the acrylamide **18** was quite effective as an irreversible inhibitor of EGFR (100% and 83% inhibition at 1 h and 8 h after treatment, respectively), while 3-dimethylamino- (**19**), 3-piperidino- (**20**) and 3-morpholinopropanamide (**21**) produced incomplete EGFR inhibition after 1 h treatment at 1 μM concentration (inhibitions between 48% and 71%) with only partial inhibition 8 h after removal from the medium (**19**, 59% inhibition; **20**, 58% inhibition; and **21**, 39% inhibition at 8 h).

Activity on Gefitinib-Resistant H1975 Cells

Compounds **5-21** were evaluated for their ability to inhibit the growth of the gefitinib-resistant H1975 NSCLC cell line harboring the T790M mutation, by MTT assay. Results were compared with those of the reference compounds **1**, **3** and **4** in the same assay. As reported in Table 1, the 3-dimethylaminopropanamide **5** showed the best antiproliferative activity on H1975 cells within the A-series of quinazoline compounds with IC_{50} of 3.7 μM, being 2 times more potent than **1** (IC_{50} of 8.3 μM) [34] and 5 fold more active than **4** (IC_{50} of 19.5 μM) [34]. Substitution of the dimethylamino group with a piperidine made compound **6** equally potent to **1** (IC_{50} of 6.7 μM), while 3-morpholinopropanamide **7**, 3-(4-

methylpiperazino)propanamide **8**, and 3-(dimethylamino)-N-methylpropanamide **9** gave IC_{50} values over 13 μM. B-series 3-aminoamides **11-13** proved 3-4 times more effective than **1** in inhibiting H1975 proliferation and showed IC_{50}s between 1.6 and 2.2 μM, in the same range of the corresponding irreversible acrylamide **10** (IC_{50} of 1.6 μM). Compounds characterized by a quinoline-3-carbonitrile driving portion (C- and D-series) were more potent than **1** in inhibiting H1975 cell proliferation. In particular, 3-aminopropanamides **15-17** (C-series) showed IC_{50} values between 2.4 and 4.0 μM comparable to that of the corresponding acrylamide derivative **14**. Finally, D-series quinoline-3-carbonitrile **19-21** gave similar results, with the compounds displaying IC_{50} values in the low micromolar or submicromolar range. The 3-piperidinopropanamide derivative **20** showed the most potent antiproliferative effect on H1975 cells within the all series of 3-aminopropanamide derivatives (IC_{50} of 0.7 μM). In particular this compound was 11 fold more potent than **1** in the same test.

We further examined the ability of compounds **5** and **20** to inhibit EGFR autophosphorylation in the NSCLC cell line H1975 harboring the T790M mutation on EGFR. Results of Western blot analysis are shown in Figure 2. The compounds produced dose-dependent inhibition of EGFR autophosphorylation indicating that the 3-aminopropanamide side chain had a positive effect on EGFR-T790M inhibition (compound **1** had marginal activity on EGFR in H1975 cells up to 10 μM) [34]. In particular, quinazoline derivative **5** showed IC_{50} of 0.07 μM, and the potent antiproliferative quinoline-3-carbonitrile derivative **20** had IC_{50} of 0.15 μM. No correlation was found between enzyme activities and the ability of these compounds to inhibit the growth of the H1975 cell line and neither between wild-type EGFR and T790M-mutated EGFR autophosphorylation inhibition. However, this was not an unexpected result, as factors other than EGFR-TK inhibiting potency (e.g. cell permeability of our compounds) may account for the results observed.

Reactivity Studies

Compound **5**, carrying a 3-dimethylaminopropanamidic side chain at position 6 on a 4-(3-bromoanilino)quinazoline nucleus, was chosen as the prototype of the new series and tested for its chemical (buffered solutions at pH 7.4 and pH 9.0) and biological (80% v/v rat plasma) stability, as well as for its reactivity against low-molecular weight thiol nucleophiles. Results were compared to those obtained for the acrylamide **3** (Tables 2 and 3).

Both compounds **3** and **5** were stable at pH 7.4, with percentages of remaining compound over 97% after 24 h incubation at 37 °C in buffer (Table 2). Under alkaline pH conditions (pH 9.0), while **3** was stable over the entire incubation time, 77% of intact 3-aminopropanamide 5 was recovered, with acrylamide **3** (19%) and amine **4** (4%) as the major degradation products. (see Supporting Information, Figure S1 for details). In the presence of rat plasma, compound **5** showed high stability, while only 22% of acrylamide **3** was detected after 24 h incubation. Reactivity of compounds **3** and **5** against thiol nucleophiles was evaluated according to literature procedures [55,56]. While for the acrylamide derivative **3** significant formation of conjugates was detected in the presence of cysteamine, glutathione (GSH), and N-acetylcysteine (NAC) (Table 3 and Supporting Information, Figure S2), compound **5** gave no measurable adducts with thiol derivatives up to 24 h of incubation.

Intracellular concentrations of **5**, **3** and **4** were measured by HPLC-ESI-MS in A549 lung cancer cells

under the condition of the EGFR autophosphorylation assay, i.e. immediately after or 8 h after incubation for 1 h with the compound at 1 μM (see Experimental Section and Supporting Information, Table S1) [57]. Both **4** and **5** were detected in the intracellular extracts after incubation (0.105 ± 0.010 and 0.050 ± 0.010 nmol/mg prot, respectively), while their levels dropped below the limit of detection (LOD) of the LC-MS method when measured 8 h after incubation. Intracellular concentrations of **3** were below the limit of detection both 1h and 8 h after incubation. This result is probably due to the reactivity of the acrylamide group in **3**, interacting covalently with cellular components.

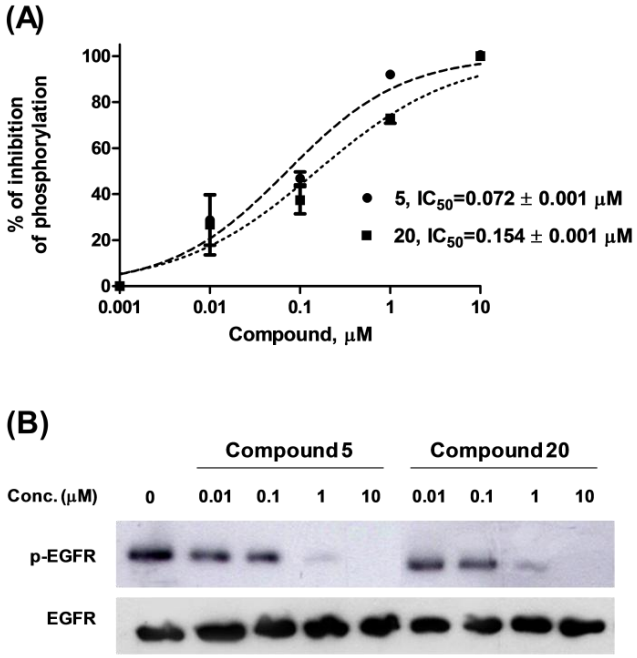

Figure 2. Effect of compounds 5 and 20 on EGFR autophosphorylation in H1975 cell line harboring the T790M mutation. (A) Percent of inhibition of EGFR autophosphorylation for compounds **5** (●) and **20** (■) on H1975 cells. Results are reported as mean ± SD of three independent experiments. (B) Representative Western blot analysis for EGFR inhibition by **5** and **20**. Analysis was done using monoclonal antibodies directed to p-Tyr1068 (see Experimental Section). Total EGFR is shown as loading control.

Reactivity of **5** was also tested in the presence of purified EGFR-TK by a fluorescence-based assay for evaluation of irreversible kinase inhibition [58,59]. Fluorescent molecules are very sensitive to solvent polarity and dipolar perturbation from their environments [60,61]. Moreover, reversible interactions [62], such as solvation, hydrogen bonding, charge transfer and redox, as well as irreversible interactions [63], such as Michael addition of thiols to electron-deficient alkenes, significantly influence fluorescent spectra of fluorophores. In particular, quinazoline and quinoline fluorophores had been shown to significantly enhance fluorescence emission after covalent reaction with Cys797 of EGFR-TK [58]. Thus, the 3-aminopropanamide **5** was added to a buffered solution containing EGFR-TK (see Experimental Section and Figure 3A for details), samples were excited at 390 nm and fluorescence emission at 420 nm was monitored over time. Results were compared to those of the irreversible **3** and the reversible N-(4-(3-bromoanilino)quinazolin-6-yl)acetamide **46** (Figure 3B) [64]. Upon addition of **3** to EGFR-TK, covalent bond formation with cysteine sulfhydryl group resulted in a time-dependent saturable increase in emission intensity at 420 nm, whereas a significantly lower fluorescence change was observed over 50 min when the reversible 6-acetyl compound

46 or the 3-aminopropanamide **5** were added to EGFR-TK. This result suggests that **5** did not covalently react with EGFR under these experimental conditions, behaving more like the acetamide derivative than like the acrylamide one.

Table 2. In vitro stability studies on compounds 3 and 5.

Conditions	% Remaining Compound (1 µM, 24 h)[a]	
	3	**5**
pH 7.4	102.3 ± 3.1	97.5 ± 0.1
pH 9.0	105.2 ± 3.7	77.0 ± 0.8
80% v/v rat plasma	21.8 ± 7.4	98.7 ± 4.6

[a] Percentage of parent compound detected by LC-UV and LC-ESI-MS after incubation for the indicated time at 37 °C (see Experimental Section). Mean ± SD, n = 3.

Finally, compounds **5** and **3** were tested for their reactivity in A549 cell lysate. The formation of conjugates with cysteine added in molar excess (2 mM) was evaluated in cell lysate by LC-HR-MS employing a LTQ-Orbitrap mass analyzer [56]. Compound **3** quickly reacted with the thiol derivative to form the corresponding cysteine conjugate (data not shown). When compound **5** was added to the cell lysate containing cysteine, a peak corresponding to the acrylamide derivative **3** was detected after 1 h ([M + H]+ = 369.03, tR = 8.87; Figure 4A), as well as a peak corresponding to the adduct of cysteine to the acrylamide fragment ($[M + H]^+$ = 490.05, t_R = 6.61 min; Figure 4B). After 1 h of incubation, 25.5% of starting acrylamide **3** had been converted to the corresponding cysteine conjugate, compared to a 1.1% conversion observed for **5**. The concentration of cysteine conjugate doubled for both **3** and **5** at the second time point (t = 4 h), being 54.4% (**3**) and 2.0% (**5**) of starting concentrations, respectively. The unique identity of the conjugate formed by compounds **3** and **5** with cysteine was further confirmed by high resolution mass spectra (Supporting Information, Figure S4). On the other hand, the effect of acrylamide released by the 3-aminopropionamide derivative can be enhanced by higher persistence of the prodrug **5**, which has detectable intracellular levels in A549 cells 1h after incubation (see above).

Table 3. In vitro reactivity studies on compounds **3** and **5**.

Conditions	% Remaining Compound (1 µM, 1 h)[a]	
	3	**5**
DTT	100.0 ± 2.3	99.2 ± 8.1
GSH	63.8 ± 1.9	101.4 ± 2.8
NAC	85.6 ± 3.1	100.4 ± 2.1
cysteamine	20.1 ± 0.4	100.0 ± 1.1

[a] Percentage of parent compound detected by LC-UV and LC-ESI-MS after incubation in the presence of LMW thiols (2 mM) for the indicated time at pH 7.4, 37 °C (see Experimental Section). Mean ± SD, n = 3.

Evidence for Irreversible Binding to EGFR

Mannich bases are versatile synthetic intermediates used in various transformations to prepare Michael acceptors via elimination of the amino moiety [65]. As reported in the literature, aryl β-aminoethyl ketones can irreversibly inhibit enzymes by covalent interaction with cysteine residues after bioconversion to the corresponding α,β-unsaturated carbonyl compound [38-40]. The new 3-aminopropanamides, characterized by a quinazoline (**5-7** and **11-13**) or quinoline-3-carbonitrile (**15-17** and **19-21**) driving portion, showed inhibition of EGFR autophosphorylation in A549 cells after 1 h incubation at 1 μM concentration and the effect generally persisted up to 8 h after removal of the compounds from the reaction medium (Table 1). In principle, the long-lasting effect observed on EGFR autophosphorylation could be ascribed to different phenomena: i) accumulation of the inhibitor in cells, as previously demonstrated for some reversible quinazolines [66]; ii) conversion of the competitive inhibitor into an irreversible one at the active site of the enzyme (mechanism-based inhibition), as described for other β-aminocarbonyl compounds [38]; iii) generation of the corresponding reactive acrylamide, as described for aryl β-aminoethyl ketones that have potential application as prodrugs of unsaturated ketones [67].

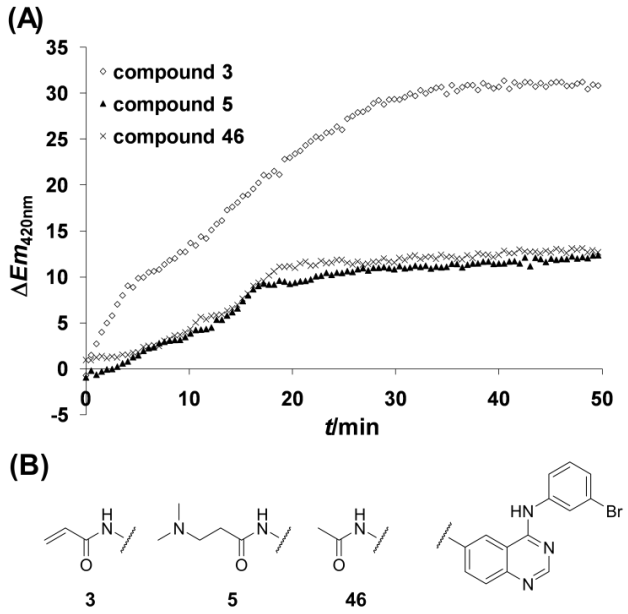

Figure 3. Fluorescence–based assay for irreversible kinase inhibition. (A) Compounds **3**, **5**, and **46** (1 μM) were added to purified EGFR-TK (0.5 μM) in the presence of ATP (1 mM) and fluorescence emission was monitored at 420 nm in real time over 50 min (excitation 390 nm); $\Delta Em_{420nm} = Em_{Compd+EGFR\ solution} - Em_{Compd\ solution} - Em_{EGFR\ solution}$. (B) Chemical structures of compounds **3**, **5**, and **46**.

As previously described, some reversible quinazoline EGFR inhibitors are sequestered in cells generating false positive results in the autophosphorylation assay based on the 8-h washout protocol [54,66]. As an example, the fully reversible compound **1**, which is strongly sequestered in cells, produced 46.4 ± 6.7% inhibition of EGFR autophosphorylation (A459 cells) at 1 μM concentration 8 h after removal from the medium. We therefore first tested if the long-lasting inhibition observed for the new 3-aminopropamides of Table 1 could be explained by their accumulation in cells. The absence of a detectable amount of **5** in A549 cells after the 8 h period, and the presence of **1** in the same conditions, suggested that **5** is not accumulated in the A549 cell line [57]. Moreover, data from fluorescence-based assay for irreversible enzyme inhibition

(Figure 3) ruled out direct interaction between the 3-aminopropanamide **5** and purified EGFR-TK in the chosen time period. On the other hand, reactivity studies on **5** indicated that the compound regenerated significant amounts of the acrylamide **3** only in the presence of cell lysate (Figure 4) while it did not under cell-free conditions (Tables 2 and 3). The results demonstrate that **5** can act as prodrug of **3** releasing the acrylamide fragment in the intracellular environment of A549 cells.

In principle, activation of 3-aminopropanamides to acrylamides in the intracellular environment could be affected by the nature of the heterocyclic nucleus (i.e. quinazoline or quinoline-3-carbonitrile), since a specific enzymatic transformation is likely to occur. However, the similar behaviour of quinazolines (A- and B-series) and quinoline-3-carbonitriles (C- and D-series) on EGFR autophosphorylation at 8 h, as well as previous data on in vivo activity of Mannich bases (see Introduction), suggest that activation of the β-aminocarbonyl fragment to a Michael acceptor is a rather general process. In this context, masking the electrophilic warhead may provide some improvements in the pharmacokinetic or pharmacodynamic profile of anti-proliferative agents. Although not a conclusive evidence of specific advantages, the observation that some 3-aminopropionamide derivatives in the aninlinoquinazoline and cianoquinoline series showed inhibition potencies on H1975 cell lines close to those of the corresponding acrylamides encourages futher evaluation of the biological properties of these compounds.

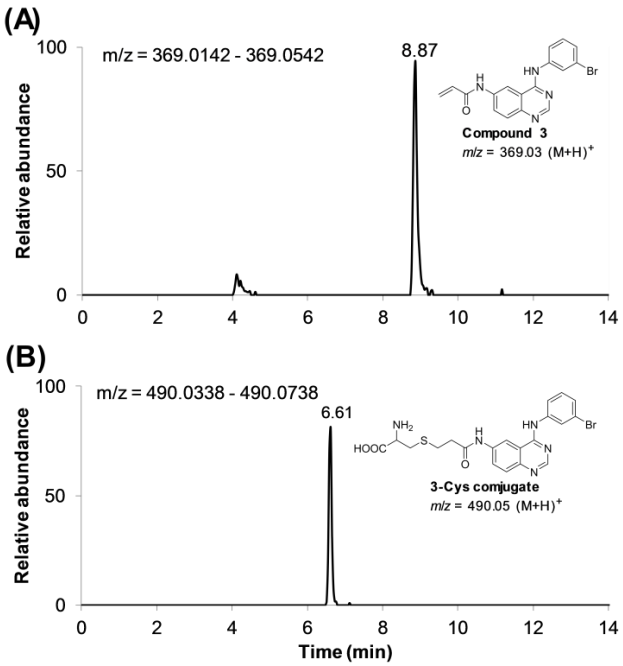

Figure 4. HPLC-HRMS extracted ion chromatograms of A549 cell lysate after 1 h incubation in the presence of compound 5 (10 μM) and cysteine (2 mM). (A) The formed acrylamide derivative (*m*/*z* = 369.03 $(M+H)^+$; t_R = 8.81 min). (B) The acrylamide-cysteine conjugate (*m*/*z* = 490.03 $(M+H)^+$; t_R = 6.61 min).

CONCLUSIONS

We report here a new series of EGFR inhibitors containing a 3-aminopropanamide linked to a 4-anilinoquinazoline (**5-7** and **11-13**) or 4-anilinoquinoline-3-carbonitrile (**15-17** and **19-21**) nucleus. The newly synthesized 3-aminopropanamides proved efficient in inhibiting EGFR-TK activity, showing a long-lasting effect on the enzyme autophosphorylation in A549 lung cancer cells. Notably, several 3-aminopropanamides

suppressed proliferation of gefitinib-resistant NSCLC cells (H1975) at significantly lower concentration than **1**. Furthermore, compounds **5** and **20** blocked mutated (T790M) EGFR-TK activity on the resistant cellular model.

Finally, a combined approach, based on i) in vitro chemical stability assays, ii) reactivity studies in the presence of thiol nucleophiles, and iii) reactivity studies toward EGFR tyrosine kinase and in the presence of cell lysate, showed that 3-dimethylaminopropanamide **5** acts as prodrug, releasing the acrylamide derivative **3** in the intracellular environment, although it is stable in other conditions.

In conclusion, these findings expand the chemical diversity of irreversible inhibitors of EGFR, and similar strategies might be applied to the design of compounds able to form a covalent bond with a peripheral cysteine residue within a biological target.

EXPERIMENTAL SECTION

Reagents were obtained from commercial suppliers and used without further purification. Solvents were purified and stored according to standard procedures. Anhydrous reactions were conducted under a positive pressure of dry N_2. Reactions were monitored by TLC, on Kieselgel 60 F 254 (DC-Alufolien, Merck). Final compounds and intermediates were purified by flash chromatography (SiO_2 60, 40-63 μm). Microwave reactions were conducted using a CEM Discover Synthesis Unit (CEM Corp., Matthews, NC). Melting points were not corrected and were determined with a Gallenkamp melting point apparatus. The ^{1}H NMR spectra were recorded on a Bruker 300 MHz Avance or on a Bruker 400 MHz Avance spectrometer; chemical shifts (δ scale) are reported in parts per million (ppm) relative to the central peak of the solvent. ^{1}H NMR spectra are reported in the following order: multiplicity, approximate coupling constant (*J* value) in hertz (Hz) and number of protons; signals were characterized as s (singlet), d (doublet), dd (doublet of doublets), t (triplet), dt (doublet of triplets), q (quartet), m (multiplet) br s (broad signal). Mass spectra were recorded using an API 150 EX instrument (AB/SCIEX, Toronto, Canada). Compounds **1** [68], **3** [54], and **4** [69] were synthesized according to literature methods. The final compounds were analyzed on ThermoQuest (Italia) FlashEA 1112 Elemental Analyzer, for C, H and N. Analyses were within ± 0.4% of the theoretical values (Supporting Information, Table S3). All tested compounds were > 95% pure by elemental analysis.

N-(4-(3-Bromoanilino)quinazolin-6-yl)-3-(dimethylamino)propanamide (**5**). A 33% v/v solution of dimethylamine in absolute EtOH (0.8 mL, 4.46 mmol) was added over 15 min to a stirred suspension of 3-chloropropanamide **27a** (145 mg, 0.36 mmol) and KI (42 mg, 0.25 mmol) in absolute EtOH (10 mL) and the resulting mixture was refluxed for 8 h. After cooling to 0 °C, the mixture was basified with KOH pellets (0.74 g) and stirred for 1 h at 0 °C. The solvent was evaporated under reduced pressure and the solid residue was dissolved with EtOAc and washed with brine. The organic phase was dried, the solvent evaporated, and the residue purified by silica gel chromatography (CH_2Cl_2/MeOH, 99:1 to 70:30) to give **5** as pale yellow solid (86%): mp (EtOAc/*n*-hexane) 170-172 °C; MS (APCI) *m/z* 414.4, 416.4; ^{1}H NMR (CD_3OD, 300 MHz) δ 2.35 (s, 6H), 2.65 (t, *J* = 6.5 Hz, 2H), 2.78 (t, *J* = 6.5 Hz, 2H), 7.29-7.31 (m, 2H), 7.74 (m, 3H), 8.12 (br s, 1H), 8.53 (s, 1H), 8.66 (br s, 1H). Anal. ($C_{19}H_{20}BrN_5O$) C, H, N.

N-(4-(3-Bromoanilino)quinazolin-6-yl)-3-piperidin-1-ylpropanamide (**6**).

N-(4-(3-Bromoanilino)quinazolin-6-yl)-3-chloropropanamide **27a** was reacted with anhydrous piperidine according to the procedure described for compound **5**. The product was purified by silica gel chromatography (CH_2Cl_2/MeOH, 95:5) to give **6** as a white solid (78%): mp (Et_2O) 184-186 °C; MS (APCI) *m/z* 454.1, 456.2; ^{1}H NMR (DMSO-d6, 300 MHz) δ 1.61 (m, 2H), 1.74-1.82 (m, 10H), 2.68-2.73 (m, 2H), 7.18-7.32 (m, 3H), 7.67 (d, *J* = 6.8 Hz, 1H), 7.83 (d, *J* = 8.8 Hz, 1H), 7.97 (s, 1H), 8.08 (s, 1H), 8.71 (s, 1H), 8.89 (s, 1H), 12.04 (s, 1H). Anal. ($C_{22}H_{24}BrN_5O\cdot 3/4H2O$) C, H, N.

N-(4-(3-Bromoanilino)quinazolin-6-yl)-3-morpholino-1-ylpropanamide (**7**).

N-(4-(3-Bromoanilino)quinazolin-6-yl)-3-chloropropanamide **27a** was reacted with morpholine according to the procedure described for compound **5**. The product was purified by silica gel chromatography (CH_2Cl_2/MeOH, 95:5) to give **7** as a yellow solid (70%): mp (Et_2O/*n*-hexane) 196-198 °C; MS (APCI) *m/z* 456.2, 458.4; ^{1}H NMR ($CDCl_3$, 300 MHz) δ 2.59-2.77 (m, 8H), 3.89 (m, 4H), 7.17-7.25 (m, 3H), 7.62 (d, *J* = 7.4 Hz, 1H), 7.76 (d, *J* = 8.9 Hz, 1H), 7.90 (s, 1H), 8.16 (bs, 1H), 8.67 (s, 1H), 8.93 (d, *J* = 1.9 Hz, 1H), 11.40 (s, 1H). Anal. ($C_{21}H_{22}BrN_5O_2\cdot 1/3H2O$) C, H, N.

N-(4-(3-Bromoanilino)quinazolin-6-yl)-3-(4-methylpiperazin-1-yl)propanamide (**8**).

N-(4-(3-Bromoanilino)quinazolin-6-yl)-3-chloropropanamide **27a** was reacted with N-methylpiperazine according to the procedure described for compound **5**. The product was purified by silica gel chromatography (CH_2Cl_2/MeOH, 95:5) to give **8** as a white solid (77%): mp (Et_2O) 196 °C; MS (APCI) *m/z* 469.3, 471.3; ^{1}H NMR ($CDCl_3$, 300 MHz) δ 2.33 (s, 3H), 2.42-2.49 (m, 12H), 6.94-7.07 (m, 3H), 7.44-7.51 (m, 2H), 7.58 (s, 1H), 8.50 (s, 1H), 8.68 (m, 1H), 8.88 (s, 1H), 11.55 (s, 1H). Anal. ($C_{22}H_{25}BrN_6O\cdot 1/2H2O$) C, H, N.

N-(4-(3-Bromophenylamino)quinazolin-6-yl)-3-(dimethylamino)-N-methylpropanamide (**9**).

N-(4-(3-Bromophenylamino)quinazolin-6-yl)-3-chloro-N-methylpropanamide **27b** was reacted with dimethylamine according to the procedure described for compound 5. Silica gel chromatography purification (CH_2Cl_2/MeOH, 98:2 to 90:10) afforded **9** as a white solid (68%): mp (CH_2Cl_2/*n*-hexane) 169-172 °C; MS (APCI) *m/z* 430.4, 431.4, 432.4; ^{1}H NMR (CD_3OD, 300 MHz) δ 2.14 (s, 6H), 2.39 (br s, 2H), 2.67 (br s, 2H), 3.40 (s, 3H), 7.34 (m, 2H), 7.79 (m, 1H), 7.85 (dd, *J* = 8.6, 2.3 Hz, 1H), 7.93 (d, *J* = 8.0 Hz, 1H), 8.17 (s, 1H), 8.42 (s, 1H), 8.66 (s, 1H). Anal. ($C_{20}H_{22}BrN_5O$) C, H, N.

N-(4-(3-Chloro-4-fluoroanilino)-7-ethoxyquinazolin-6-yl)acrylamide (**10**).

Acryloyl chloride (25 µL, 0.3 mmol) in anhydrous THF (0.5 mL) was added dropwise to a solution of 6-aminoquinazoline **34** (100 mg, 0.3 mmol) and N,N-diisopropylethylamine (DIPEA) (52 µL, 0.3 mmol) in anhydrous DMF (2.5 mL) at 0 °C. The reaction mixture was stirred for 1 h, then the solvent was removed under reduced pressure and the residue was purified by silica gel chromatography (CH_2Cl_2/MeOH, 95:5) to afford **10** as a white solid (25%): mp (EtOH/H_2O) 228.5-230 °C; MS (APCI) *m/z* 387.3, 389.3; ^{1}H NMR (Acetone-d6, 400 MHz) δ 1.52 (t, *J* = 6.9 Hz, 3H), 4.35 (q, *J* = 6.9 Hz, 2H), 5.83 (dd, *J* = 10.1, 1.7 Hz, 1H), 6.45 (dd, *J* = 16.8, 1.7 Hz, 1H), 6.70 (dd, *J* = 16.8, 10.1 Hz, 1H), 7.29 (s, 1H), 7.32 (t, *J* = 9.0 Hz, 1H), 7.86 (ddd, *J* = 9.0, 4.1, 2.8 Hz, 1H),

8.25 (dd, *J* = 6.8, 2.6 Hz, 1H), 8.57 (s, 1H), 9.04 (s, 1H). Anal. ($C_{19}H_{16}ClFN_4O_2$) C, H, N.

N-(4-(3-Chloro-4-fluoroanilino)-7-ethoxyquinazolin-6-yl)-3-(dimethylamino)propanamide (**11**). 3-Chloropropanamide **35** was reacted with dimethylamine according to the procedure described for compound **5**. The product was purified by silica gel chromatography (AcOEt/MeOH, 99:1 to 85:15) to obtain **11** as a white solid (85%): mp (EtOH/H_2O) 182-183 °C; MS (APCI) *m/z* 432.5, 434.3; ^{1}H NMR (CD_3OD, 300 MHz) δ 1.54 (t, *J* = 7.0 Hz, 3H), 2.37 (s, 6H), 2.69 (m, 4H), 4.26 (q, *J* = 7.0 Hz, 2H), 7.11 (s, 1H), 7.21 (t, *J* = 9.0 Hz, 1H), 7.62 (ddd, *J* = 9.0, 4.1, 2.7 Hz, 1H), 7.95 (dd, *J* = 6.7, 2.6 Hz, 1H), 8.41 (s, 1H), 8.83 (s, 1H); Anal. ($C_{21}H_{23}ClFN_5O_2 \cdot 2/3H_2O$) C, H, N.

N-(4-(3-Chloro-4-fluoroanilino)-7-ethoxyquinazolin-6-yl)-3-(piperidin-1-yl)propanamide (**12**). 3-Chloropropanamide **35** was reacted with anhydrous piperidine according to the procedure described for compound **5**. The product was purified by silica gel chromatography (AcOEt/MeOH, 99:1 to 93:7) to give **12** as a white solid (60%): mp (EtOH/H_2O) 106.5-108 °C; MS (APCI) *m/z* 472.2, 474.2; ^{1}H NMR (DMSO-d6, 400 MHz) δ 1.54 (t, *J* = 6.9 Hz, 5H), 1.68 (4H, m), 2.56 (s, 4H), 2.75 (m, 4H), 4.38 (q, *J* = 6.9 Hz, 2H), 7.22 (s, 1H), 7.25 (t, *J* = 8.9 Hz, 1H), 7.65 (ddd, *J* = 9.0, 3.7, 2.8 Hz, 1H), 7.99 (dd, *J* = 6.6, 2.5 Hz, 1H), 8.47 (s, 1H), 8.83 (s, 1H); Anal. ($C_{24}H_{27}ClFN_5O_2 \cdot H_2O$) C, H, N.

N-(4-(3-Chloro-4-fluorophenylamino)-7-ethoxyquinazolin-6-yl)-3-morpholinopropanamide (**13**). 3-Chloropropanamide **35** was reacted with morpholine according to the procedure described for compound **5**. The product was purified by silica gel chromatography (AcOEt/MeOH, 99:1 to 96:4) to obtain **13** as a light yellow solid (96%): mp (EtOH/H_2O) 108-110 °C; MS (APCI) 474.0, 476.3 °C; ^{1}H NMR (DMSO-d6, 400 MHz) δ 1.54 (t, *J* = 7.0 Hz, 3H), 2.60 (m, 4H), 2.74 (t, *J* = 6.0, 2H), 2.81 (t, *J* = 5.8 Hz, 2H), 3.77 (t, *J* = 4.6 Hz, 4H), 4.37-4.41 (m, 2H), 7.18-7.26 (m, 2H), 7.63-7.65 (m, 1H), 7.97-7.99 (m, 1H), 8.46 (d, *J* = 2.9 Hz, 1H), 8.83 (d, *J* = 4.7 Hz, 1H); Anal. ($C_{23}H_{25}ClFN_5O_3 \cdot 2/3H2O$) C, H, N.

N-(4-(3-Chloro-4-fluoroanilino)-3-cyano-7-ethoxyquinolin-6-yl)acrylamide (**14**). The product was obtained by coupling the amino intermediate **42a** with acryloyl chloride as described for compound **10**. Silica gel chromatography purification (EtOAc/*n*-hexane, 60:40) afforded 14 (40%) as a white solid: mp (EtOH/H_2O) > 230 °C; MS (APCI) *m/z* 411.0; ^{1}H NMR (DMSO-d6, 300MHz) δ 1.48 (t, *J* = 6.9 Hz, 3H), 4.33 (q, *J* = 6.9 Hz, 2H), 5.81 (d, *J* = 10.7 Hz, 1H), 6.29 (d, *J* = 16.5 Hz, 1H), 6.77 (dd, *J* = 16.5, 9.7 Hz, 1H), 7.25 (m, 1H), 7.41 (m, 3H), 8.53 (s, 1H), 8.98 (s, 1H), 9.60 (s, 1H), 9.75 (br s, 1H); Anal. ($C_{21}H_{16}ClFN_4O_2 \cdot 1/2H2O$) C, H, N.

N-(4-(3-Chloro-4-fluoroanilino)-3-cyano-7-ethoxyquinolin-6-yl)-3-(dimethylamino)propanamide (**15**). 3-Chloropropanamide **43a** was reacted with dimethylamine according to the procedure described for compound **5**. Silica gel chromatography (CH_2Cl_2/MeOH, 99:1 to 97:3) gave **15** as a light yellow solid (69%): mp (EtOH) 168-171 °C; 1H NMR (DMSO-d6, 300 MHz) δ 1.48 (t, *J* = 7.0 Hz, 3H), 2.29 (s, 6H), 2.57 (m, 4H), 4.32 (q, *J* = 7.0 Hz, 2H), 7.19 (m, 1H), 7.40 (m, 3H), 8.54 (s, 1H),

9.06 (s, 1H), 9.68 (br s, 1H), 10.98 (s, 1H); Anal. ($C_{23}H_{23}ClFN_5O_2 \cdot H_2O$) C, H, N.

N-(4-(3-Chloro-4-fluoroanilino)-3-cyano-7-ethoxyquinolin-6-yl)-3-(piperidin-1-yl)propanamide (**16**). 3-Chloropropanamide **43a** was reacted with piperidine according to the procedure described for compound **5**. Silica gel chromatography (CH_2Cl_2/MeOH, 96:4) gave **16** as a white solid (45%): mp (EtOH) 180-184 °C; MS (APCI) *m/z* 496.4, 497.3, 499.4; ^{1}H NMR (DMSO-d6, 400 MHz) δ 1.46 (t, *J* = 7.0 Hz, 3H); 1.49 (m, 2H), 1.56 (m, 4H), 2.44 (m, 4H), 2.60 (s, 4H), 4.39 (t, *J* = 7.0 Hz, 2H), 7.22 (m, 1H), 7.41 (m, 3H), 8.54 (s, 1H), 8.97 (s, 1H), 9.68 (br s, 1H), 10.24 (s, 1H); Anal. ($C_{26}H_{27}ClFN_5O_2 \cdot 1/2C_2H_6O$) C, H, N.

N-(4-(3-Chloro-4-fluoroanilino)-3-cyano-7-ethoxyquinolin-6-yl)-3-morpholinopropanamide (**17**). 3-Chloropropanamide **43a** was reacted with morpholine according to the procedure described for compound **5**. Silica gel chromatography (CH_2Cl_2/MeOH, 98:2) afforded **17** as a white solid (52%): mp (EtOH/H_2O) 195-198 °C; MS (APCI) *m/z* 498.3, 499.2, 500.3; ^{1}H NMR (DMSO-d6, 400 MHz) δ 1.45 (t, *J* = 7.0 Hz, 3H), 2.46 (m, 4H), 2.63 (m, 4H), 3.62 (t, *J* = 4.2 Hz, 4H), 4.36 (q, *J* = 7.1 Hz, 2H), 7.20 (br s, 1H), 7.39 (m, 3H), 8.53 (br s, 1H), 8.94 (s, 1H), 9.69 (br s, 1H), 9.89 (s,1H); Anal. ($C_{25}H_{25}ClFN_5O_3 \cdot 1/2C_2H_6O$) C, H, N.

N-(4-(3-Chloro-4-(pyridin-2-ylmethoxy)anilino)-3-cyano-7-ethoxyquinolin-6-yl)acrylamide (**18**). The product was obtained by coupling the amino intermediate **42b** with acrylic acid as described for compound **10**. Silica gel chromatography purification (CH_2Cl_2/MeOH, 98:2) gave **18** as a white solid (35%): mp (EtOH/H_2O) > 230 °C; MS (APCI) *m/z* 500.1; ^{1}H NMR (DMSO-d6, 300MHz) δ 1.53 (t, *J* = 6.9 Hz, 3H), 4.39 (q, *J* = 6.9 Hz, 2H), 5.32 (s, 2H); 5.79 (dd, *J* = 10.1, 1.9 Hz, 1H), 6.39 (dd, *J* = 16.9, 1.9 Hz, 1H), 6.68 (dd, *J* = 16.9, 10.1 Hz, 1H), 7.30 (m, 3H), 7.41 (s, 1H), 7.48 (d, *J* = 2.3 Hz, 1H), 7.68 (d, *J* = 7.8 Hz, 1H), 7.87 (td, *J* = 7.8, 1.8 Hz, 1H), 8.50 (s, 1H), 8.60 (d, *J* = 4.5 Hz, 1H), 9.05 (s, 2H), 9.16 (s, 1H); Anal. ($C_{27}H_{22}ClN_5O_3$) C, H, N.

N-(4-(3-Chloro-4-(pyridin-2-ylmethoxy)anilino)-3-cyano-7-ethoxyquinolin-6-yl)-3-(dimethylamino)propanamide (**19**). 3-Chloropropanamide **43b** was reacted with dimethylamine according to the procedure described for compound **5**. Silica gel chromatography (CH_2Cl_2/MeOH, 99:1 to 90:10) gave **19** as a white solid (73%): mp (EtOH) 235-237 °C; MS (APCI) *m/z* 545.4, 547.3, 502.7, 500.2; ^{1}H NMR (DMSO-d6, 300 MHz) δ 2.29 (s, 6H), 2.54-2.61 (m, 4H), 4.31 (q, *J* = 7.0 Hz, 2H), 5.28 (s, 2H), 7.17 (dd, *J* = 7.7, 1.7 Hz, 1H), 7.25 (d, *J* = 8.8 Hz, 1H), 7.38-7.40 (m, 3H), 7.59 (d, *J* = 7.9 Hz, 1H), 7.88 (dt, *J* = 7.7, 1.7 Hz, 1H), 8.47 (s, 1H), 8.60 (d, *J* = 4.0 Hz, 1H), 9.06 (s, 1H), 9.58 (br s, 1H), 10.92 (br s, 1H); Anal. ($C_{29}H_{29}ClN_6O_3 \cdot 1/2H_2O$) C, H, N.

N-(4-(3-Chloro-4-(pyridin-2-ylmethoxy)anilino)-3-cyano-7-ethoxyquinolin-6-yl)-3-(piperidin-1-yl)propanamide (**20**). 3-Chloropropanamide **43b** was reacted with piperidine according to the procedure described for compound **5**. Silica gel chromatography (CH_2Cl_2/MeOH, 97:3 to 95:5) gave **20** as a light yellow solid (69%): mp (EtOH) 190-193 °C; MS (APCI) *m/z* 585.2, 587.5, 588.5; ^{1}H NMR (DMSO-d6,

400 MHz) δ 1.45 (t, *J* = 6.8 Hz, 3H), 1.50 (m, 2H), 1.56 (m, 4H), 2.44 (m, 4H), 2.60 (s, 4H), 4.36 (q, *J* = 7.0 Hz, 2H), 5.28 (s, 2H), 7.18 (d, *J* = 8.2 Hz, 1H), 7.25 (d, *J* = 8.4 Hz, 1H), 7.39 (m, 3H), 7.58 (d, *J* = 7.2 Hz, 1H), 7.88 (t, *J* = 7.3 Hz, 1H), 8.47 (s, 1H), 8.60 (d, *J* = 4.3 Hz, 1H), 8.95 (s, 1H), 9.59 (s, 1H), 10.21 (s, 1H); Anal. ($C_{32}H_{33}ClN_6O_3 \cdot 3/2H_2O$) C, H, N.

N-(4-(3-Chloro-4-(pyridin-2-ylmethoxy)anilino)-3-cyano-7-ethoxyquinolin-6-yl)-3-morpholinopropanamide (**21**). 3-Chloropropanamide **43b** was reacted with morpholine according to the procedure described for compound **5**. Silica gel chromatography (CH_2Cl_2/MeOH, 99:1 to 97:3) gave **21** as a light yellow solid (74%): mp (EtOH) 224-228 °C; MS (APCI) *m/z* 587.3, 589.5; ^{1}H NMR ($CDCl_3$, 400 MHz) δ 1.49 (t, *J* = 6.9 Hz, 3H), 2.55 (m, 4H), 2.67 (m, 4H), 3.77 (s, 4H), 4.30 (q, *J* = 6.8 Hz, 2H), 5.19 (s, 2H), 6.72 (s, 2H), 7.61 (d, *J* = 7.8 Hz, 2H), 7.75 (t, *J* = 7.7 Hz, 1H), 8.16 (s, 1H), 8.32 (s, 1H), 8.58 (d, *J* = 4.4 Hz, 1H), 9.19 (s,1H), 10.08 (s,1H); Anal. ($C_{31}H_{31}ClN_6O_4$) C, H, N.

In vitro Stability and Reactivity assays.

Chemical (pH 7.4; pH 9.0) and rat plasma stability was investigated at 37 °C according to procedures reported previously [70] (See Supporting Information for details). Reactivity of **5** and **3** towards cysteamine, N-acetylcysteine (NAC), dithiothreitol (DTT) and reduced glutathione (GSH) was evaluated adding a freshly-prepared thiol solution (2 mM) to PBS pH 7.4 containing the test compound (1 μM). Formation of conjugates with LMW thiols after 1 h of incubation at 37 °C was measured by HPLC-UV and HPLC-ESI-MS. Reactivity of compounds **5** and **3** in A549 cell lysate was tested in the presence of cysteine, to trap thiol-reactive compounds. A549 cells were seeded at 1,000,000 cells/dish (66 cm^2); after two days, cells were lysed mechanically by freeze/thaw method. Stock solutions (1 mM) of **3** and **5** were prepared in DMSO immediately before use and 3 μL of this solution (or 3 μL of DMSO in controls) were added to 297 μL of cell lysate, where 2 mM cysteine had been previously added. Incubations were carried out at 37 °C. At stated time points (t = 0, 1, and 4 h) aliquots were sampled, a double volume of acetonitrile was added, centrifuged (4 °C, 10,000 g, 10 min) and directly analyzed by LC-HRMS employing a LTQ-Orbitrap mass analyzer, working in positive ion mode (PIM). (See Supporting Information for details).

Determination of intracellular concentrations

A549 Cells were plated at 1,000,000 cells/dish (25 cm^2) density. After 24 h, test compounds (**3**-**5**) were added to the medium (final concentration: 1 μM; final DMSO concentration: 0.1%). Cells were incubated for 1 h at 37 °C and tested either immediately after or 8 h after removal of the compound from the extracellular medium by washing the cells for three times with 1 mL aliquots of fresh medium. Compounds were then extracted from cells with absolute EtOH (1.1 mL at 4 °C), cell extracts were centrifuged (4 °C, 10,000 g, 5 min) and collected. A fixed volume of ethanolic extract was evaporated to dryness, dissolved in HPLC eluent and injected into the LC/MS system. Calibration curves were built in the concentration range 5 μM-50 nM for compounds **3-5** (limit of quantification, LOQ = 50 nM; limit of detection, LOD = 20 nM). Cell proteins were quantified after solubilization in NaOH 0.5 N (2 mL/25 cm^2 dish) by the Bradford method [71].

Analytical Method

A linear gradient elution was set up to evaluate in the same chromatographic run the disappearance of compounds **3**, **5** and the formation of corresponding degradation products. An Agilent 1100 HPLC gradient system (Agilent Technologies, Santa Clara, CA, USA) with a RP-C18 Supelco Discovery (Supelco, Bellefonte, PA, USA), 5 µm, 150 x 4.6 mm i.d. column and an AB/SCIEX API 150-EX single quadrupole mass spectrometer equipped with an ESI ion source acquiring in positive ion mode were employed. (See Supporting Information for details).

Real-time detection of covalent bond formation in microtiter plates

The assay was carried out in black 384-well small-volume plates, and fluorescence emission was measured over time by using a multilabel plate reader (Victor, PerkinElmer), as previously described [58]. EGFR-TK was purchased from Sigma-Aldrich. Sample wells were excited at 390 nm and the changing emission intensity was monitored at 420 nm. The reaction was monitored immediately after combining equal volumes (7 µL) of EGFR-TK (0.5 µM) in buffer (50 mM Hepes, 200 mM NaCl, 0.05% Triton-X100, pH 7.4) containing ATP (1 mM) and inhibitor (1 µM, 0.2% DMSO) solution in each well. Data were reported as ΔEm_{420nm}, calculated as difference in emission intensity between samples (inhibitor + EGFR) and controls (inhibitor in buffer solution, and EGFR in buffer solution).

Kinase assay

Evaluation of the effects of compounds on the kinase activity of human EGFR was performed by measuring the phosphorylation of the substrate Ulight-CAGAGAIETDKEYYTVKD (JAK1) using a human recombinant enzyme expressed in insect cells [72] and the LANCE detection method [73], employing the Cerep EGFR kinase assay [74] as previously described [34].

Cell culture

The human NSCLC cell lines A549 and H1975 were cultured as recommended. Medium was supplemented with L-glutamine (2 mmol/L) and fetal calf serum (FCS) (10%) and cells were maintained under standard cell culture conditions at 37 °C in a water-saturated atmosphere of 5% CO_2 in air. A549 cell line was from the American Type Culture Collection (Manassas, VA, USA) and H1975 was kindly provided by Dr E. Giovannetti (Department of Medical Oncology, VU University Medical Center, Amsterdam, The Netherlands).

Antibodies and reagents

Medium was from Euroclone, FBS was purchased from Gibco-BRL (Grand Island, NY, USA). Monoclonal anti-EGFR and polyclonal anti-phospho-EGFR (Tyr1068) antibodies were from Cell Signaling Technology (Beverly, MA, USA). Horseradish peroxidase-conjugated (HRP) secondary antibodies were from Pierce. The enhanced chemiluminescence system (ECL) was from Millipore (Millipore, MA, USA). Reagents for electrophoresis and blotting analysis were obtained from, respectively, BIO-RAD Laboratories and Millipore.

Western blot analysis

Procedures for protein extraction, solubilization, and protein analysis by 1-D PAGE are described elsewhere [75]. 40-50 µg proteins from lysates were resolved by 7.5% SDS-PAGE and transferred to PVDF membranes (Millipore). The membranes were then incubated with primary antibody, washed and then incubated with HRP-anti-rabbit antibody. Immunoreactive bands were visualized using an enhanced chemiluminescence system.

Autophosphorylation assay

Inhibition of EGFR autophosphorylation was determined as previously described using specific anti-phosphotyrosine and anti-total EGFR antibodies by Western blot analysis [34].

Cell growth inhibition

Cell viability was assessed after 3 days of treatment by tetrazolium dye [3-(4,5-dimethylthiazol-2-yl)-2,5-diphenyltetrazolium bromide (MTT), Sigma, Dorset, UK] assay as previously described [75]. Representative results of at least three independent experiments were used for evaluation of dose-response curves, calculated from experimental points using Graph Pad Prism5 software. The concentration that inhibits 50% (IC_{50}) (e.g., the point at which viability is 50%) was extrapolated from the dose-response curves.

ACKNOWLEDGEMENTS

Grant support for this work was from the Ministero della Salute (Programma straordinario di ricerca oncologica 2006), Regione Emilia Romagna, AIRC (Associazione Italiana per la Ricerca sul Cancro), Associazione Chiara Tassoni, Parma, and Associazione Davide Rodella, Montichiari BS. We thank Prof. Prisco Mirandola (Department of Anatomy, Pharmacology and Forensic Medicine at the University of Parma) for support in the fluorescence-based kinase assay.

REFERENCES

1. Yarden Y; Sliwknowski MX. Untangling the ErbB signaling network. *Nat. Rev. Mol. Cell. Biol.* 2001, *2*, 127–137.
2. Hynes NE; Lane HA. ErbB receptors and cancer: the complexity of targeted inhibitors. *Nat. Rev. Cancer* 2005, *5*, 341–354.
3. Schlessinger J. Cell signaling by receptor tyrosine kinases. *Cell*. 2000, *103*, 211–225.
4. Olayioye MA; Neve RM; Lane HA; Hynes NE. The ErbB signaling network: receptor heterodimerization in development and cancer. *EMBO J.* 2000, *19*, 3159–3167.
5. Mendelson J; Balsega J. Epidermal growth factor receptor targeting in cancer. *Semin. Oncol.* 2006, *33*, 369–385.
6. Salomon DS; Brandt R; Ciardello F; Normanno N. Epidermal growth factor-related peptides and their receptors in human malignancies. *Crit. Rev. Oncol. Hematol.*, 1995, *19*, 183–232.
7. Teman S; Kawaguchi H; El-Naggar AK; et al. Epidermal growth factor receptor copy number alterations correlate with poor clinical outcome in patients with head and neck squamous cancer. *J. Clin. Oncol.* 2007, *25*, 2164–2170.
8. Barker AJ; Gibson KH; Grundy W; Godfrey AA; et al. Studies leading to the identification of ZD1839 (Iressa): an orally active, selective epidermal growth factor receptor tyrosine kinase inhibitor targeted to the treatment of cancer. *Bioorg. Med. Chem. Lett.* 2001, *11*, 1911–1914.
9. Moyer JD; Barbacci EG; Iwata KK; et al. Induction of apoptosis and cell cycle arrest by CP-358,774, an inhibitor of epidermal growth factor receptor tyrosine kinase. *Caner Res.* 1997, *57*, 4838–4848.
10. Wood ER; Truesdale AT; McDonald OB; et al. A unique structure for epidermal growth factor receptor bound to GW572016 (lapatinib): relationships among protein conformation, inhibitor off-rate, and receptor activity in tumor cells. *Cancer Res.* 2004, *64*, 6652–6659.
11. Lynch TJ; Bell DW; Sordella R; et al. Activating mutations in the epidermal growth factor receptor underlying responsiveness of non-small-cell lung cancer to gefitinib. *N. Engl. J. Med.* 2004, *350*, 2129–2139.
12. Kobayashi S; Boggon TJ; Dayaram T; et al. EGFR mutation and resistance of non-small-cell lung cancer to gefitinib. *N. Engl. J. Med.* 2005, *352*, 786–792.
13. Pao W; Miller VA; Politi KA; et al. *KRAS* mutations and primary resistance of lung adenocarcinomas to gefitinib or erlotinib. *PLoS Med* 2005, *2*, e17.
14. Engelman JA; Jänne PA. Mechanisms of acquired resistance to epidermal growth factor receptor tyrosine kinase inhibitors in non-small cell lung cancer. *Clin. Cancer Res.* 2008, *14*, 2895–2899.
15. Yun CH; Mengwasser KE; Toms AV; et al. The T790M mutation in EGFR kinase causes drug resistance by increasing the affinity for ATP. *Proc. Natl. Acad. Sci. U.S.A.* 2008, *105*, 2070–2075.
16. Fry DW; Bridges AJ; Denny WA; et al. Specific, irreversible inactivation of the epidermal growth factor receptor and erbB2, by a new class of tyrosine kinase inhibitor. *Proc. Natl. Acad. Sci. U.S.A.* 1998, *95*, 12022–12027.
17. Blair JA; Rauh D; Kung C; et al. Structure-guided development of affinity probes for tyrosine kinases using chemical genetics. *Nature Chem. Biol.* 2007, *3*, 229–238.
18. Kwak EL; Sordella R; Bell DW; et al. Irreversible inhibitors of the EGF receptor may circumvent acquired resistance to gefitinib. *Proc. Natl. Acad. Sci. U.S.A.* 2005, *102*, 7665–7670.
19. Carter TA; Wodicka LM; Shah NP; et al. Inhibition of drug-resistant mutants of ABL, KIT, and EGF receptor kinases. *Proc. Natl. Acad. Sci. U.S.A.* 2005, *102*, 11011–11016.
20. Godin-Heymann N; Ulkus L; Brannigan BW; et al. The T790M “gatekeeper” mutation in EGFR mediates resistance to low concentration of an irreversible EGFR inhibitor. *Mol. Cancer Ther.* 2008, *7*, 874–879.Slichenmyer WJ; Elliott WL; Fry DW. CI-1033, a pan-erbB tyrosine kinase inhibitor. *Semin. Oncol.* 2001, *28*, 80–85.
22. Minkovsky N; Berezov A. BIBW-2992, a dual receptor tyrosine kinase inhibitor for the treatment of solid tumours. *Curr. Opin. Invest. Drugs* 2008, *9*, 1336–1346.
23. Rabindran SK; Discafani CM; Rosfjord EC; et al. Antitumor activity of HKI-272, an orally active, irreversible inhibitor of the Her-2 tyrosine kinase. *Cancer Res.* 2004, *64*, 3958–3965.
24. Singh J; Petter RC; Kluge AF. Targeted covalent drugs of the kinase family. *Curr. Opin. Chem. Biol.* 2010, *14*, 475–480.
25. sTsou HR; Mamuya N; Johnson BD; et al. 6-Substituted-4-(3-bromophenylamino)quinazolines as putative irreversible inhibitors of the epidermal growth factor receptor (EGFR) and human epidermal growth factor receptor (HER-2) tyrosine kinases with enhanced antitumor activity. *J. Med. Chem.* 2001, *44*, 2719–2734.
26. Smaill JB; Showalter HDH; Zhou H; et al. Tyrosine kinase inhibitors. 18. 6-Substituted 4-anilinoquinazolines and 4-anilinopyrido[3,4-d]pyrimidines as soluble, irreversible inhibitors of the Epidermal Growth Factor Receptor. *J. Med. Chem.* 2001, *44*, 429–440.
27. Mishani E; Abourbeh G; Jacobson O; et al. High-affinity Epidermal Growth Factor Receptor (EGFR) irreversible inhibitors with

diminished chemical reactivities as Positron Emission Tomography (PET)-imaging agent candidates of EGFR overexpressing tumors. *J. Med. Chem.* 2005, *48*, 5337–5348.

28. Carmi C; Lodola A; Rivara S; et al. Epidermal growth factor receptor irreversible inhibitors: Chemical exploration of the cysteine-trap portion. *Mini Rev. Med. Chem.* 2011, *11*, 1019–1030.
29. Zhou W; Ercan D; Chen L; et al. Novel mutant-selective EGFR kinase inhibitors against EGFR T790M. *Nature*, 2009, *462*, 1070–1074.
30. Garuti L; Roberti M; Bottegoni G. Irreversible protein kinase inhibitors. *Curr. Med. Chem.* 2011, *18*, 2981–2994.
31. Jänne PA; von Pawel J; Cohen RB; Crino, et al. Multicenter, randomized, phase II trial of CI-1033, an irreversible pan-ERBB inhibitor, for previously treated advanced non small-cell lung cancer. *J. Clin. Oncol.* 2007, *25*, 3936–3944.
32. Besse B; Eaton KD; Soria JC; et al. Neratinib (HKI-272), an irreversible pan-ErbB receptor tyrosine kinase inhibitor: preliminary results of a phase 2 trial in patients with advanced non-small cell lung cancer. *Eur. J. Cancer* 2008, *Suppl. 6*, 64.
33. Leproult E; Barluenga S; Moras D; et al. Cysteine mapping in conformationally distinct kinase nucleotide binding sites: Application to the design of selective covalent inhibitors. *J. Med. Chem.* 2011, *54*, 1347–1355.
34. Carmi C; Cavazzoni A; Vezzosi S; et al. Novel irreversible epidermal growth factor receptor inhibitors by chemical modulation of the cysteine-trap portion. *J. Med. Chem.* 2010, *53*, 2038–2050.
35. Carmi C; Cavazzoni A; Zuliani V; et al. 5-Benzylidene-hydantoins as new EGFR inhibitors with antiproliferative activity. *Bioorg. Med. Chem. Lett.* 2006, *16*, 4021–4025.
36. Zuliani V; Carmi C; Rivara M; et al. 5-Benzylidene-hydantoins: Synthesis and antiproliferative activity on A549 lung cancer cell line. *Eur. J. Med. Chem.* 2009, *44*, 3471–3479.
37. Cavazzoni A; Alfieri RR; Carmi C; et al. Dual mechanisms of action of the 5-benzylidene-hydantoin UPR1024 on lung cancer cell lines. *Mol. Cancer Ther.* 2008, *7*, 361–370.
38. Maresso AW; Wu R; Kern JW; et al. Activation of inhibitors of sortase triggers irreversible modification of the active site. *J. Biol. Chem.* 2007, *282*, 23129–23139.
39. Wenzel NI; Chavain N; Wang Y; et al. Antimalarial versus cytotoxic properties of dual drugs derived from 4-aminoquinolines and Mannich bases: Interaction with DNA. *J. Med. Chem.* 2010, *53*, 3214–3226.
40. Hwang JY; Arnold LA; Zhu F; et al. Improvement of pharmacological properties of irreversible thyroid receptor coactivator binding inhibitors. *J. Med. Chem.* 2009, *52*, 3892–3901.
41. Brown GR; Bamford AM; Bowyer J; et al. Naphthyl ketones: A new class of Janus kinase 3 inhibitors. *Bioorg. Med. Chem. Lett.* 2000, *10*, 575–579.
42. Flynn GA; Lee SA; Faris M; et al. Intracellular kinase inhibitors. PCT Int. Appl. WO2007/136790, 2007.
43. Traxler P; Trinks U; Buchdunger E; et al. [(Alkylamino)methyl]acrylophenones: Potent and selective inhibitors of the epidermal growth factor receptor protein tyrosine kinase. *J. Med. Chem.* 1995, *38*, 2441–2448.
44. Neelakantan S; Nasim S; Guzman ML; et al. Aminopartenolides as novel anti-leukemic agents: Discovery of the NF-κB inhibitor, DMAPT (LC-1). *Bioorg. Med. Chem. Lett.* 2009, *19*, 4346–4349.
45. Rewcastle GW; Denny WA; Bridges AJ; et al. Tyrosine kinase inhibitors: synthesis and structure-activity relationships for 4-[(phenylmethyl)amino]- and 4-[(phenylamino)quinazolines as potent adenosine 5'-triphosphate binding site inhibitors of the tyrosine kinase domain of the epidermal growth factor receptor. *J. Med. Chem.* 1995, *38*, 3482–3487.
46. Roth GA; Tai JJ. A new synthesis of aryl substituted quinazolin-4(1*H*)-ones. *J. Heterocycl. Chem.* 1996, *33*, 2051–2053.
47. Domarkas J; Dudouit F; Williams C; et al. The combi-targeting concept: Synthesis of stable nitrosoureas designed to inhibit the epidermal growth factor receptor (EGFR). *J. Med. Chem.* 2006, *49*, 3544–3552.
48. Tang PC; Li X; Wang B; et al. 6-Amino quinazoline or 3-cyano quinoline derivatives, preparation methods and pharmaceutical uses thereof. PCT Int. Appl. WO2011/029265, 2011.
49. Wissner A; Fraser HL; Ingalls CL; et al. Dual irreversible kinase inhibitors: Quinazoline-based inhibitors incorporating two independent reactive centers with each targeting different cysteine residues in the kinase domains of EGFR and VEGFR-2. *Bioorg. Med. Chem.* 2007, *15*, 3635–3648.
50. Tsou HR; Overbeek-Klumpers EG; Hallett WA; et al. Optimization of 6,7-disubstituted-4-(arylamino)quinoline-3-carbonitriles as orally active, irreversible inhibitors of human epidermal growth factor receptor-2 kinase activity. *J. Med. Chem.* 2005, *48*, 1107–1131.
51. Wissner A; Overbeek E; Reich MF; et al. Synthesis and structure-activity relationships of 6,7-disubstituted 4-anilinoquinoline-3-carbonitriles. The design of an orally active, irreversible inhibitor of the tyrosine kinase activity of the epidermal growth factor receptor (EGFR) and the human epidermal growth factor receptor-2 (HER-2). *J. Med. Chem.* 2003, *46*, 49–63.
52. Chew W; Cheal GK; Lunetta JF. Methods of synthesizing substituted 3-cyanoquinolines and intermediates thereof. PCT Int. Appl. WO2006/127207, 2006.

53. Barlaam BC; Ducray R; Kettle JG. Pyrazolopyrimidine compounds as antitumor agents. PCT Int. Appl. WO2006/064196, 2006.

54. Smaill JB; Palmer BD; Rewcastle GW; et al. Tyrosine kinase inhibitors. 15. 4-(Phenylamino)quinazoline and 4-(phenylamino)pyrido[d]pyrimidine acrylamides as irreversible inhibitors of the ATP binding site of the Epidermal Growth Factor Receptor. *J. Med. Chem.* 1999, *42*, 1803–1815.

55. Böhme A; Thaens D; Paschke A; et al. Kinetic glutathione chemoassay to quantify thiol reactivity of organic electrophiles: application to alpha,beta-unsaturated ketones, acrylates, and propiolates. *Chem Res Toxicol.* 2009, *22*, 742–750.

56. Oballa RM; Truchon JF; Bayly CI; et al. A generally applicable method for assessing the electrophilicity and reactivity of diverse nitrile-containing compounds. *Bioorg. Med. Chem. Lett.* 2007, *17*, 998–1002.

57. Galetti M; Alfieri RR; Cavazzoni A; et al. Functional characterization of gefitinib uptake in non-small cell lung cancer cell lines. *Biochem Pharmacol.* 2010, *80*, 179–187.

58. Külter S; Simard JR; Rode HB; et al. Characterization of irreversible kinase inhibitors by direct detecting covalent bond formation: A tool for dissecting kinase drug resistance. *ChemBioChem* 2010, *11*, 2557–2566.

59. Sos ML; Rode HB; Heynck S; et al. Chemogenomic profiling provides insights into the limited activity of irreversible EGFR inhibitors in tumor cells expressing the T790M EGFR resistance mutation. *Cancer Res.* 2010, *70*, 868–874.

60. Prendergast FG; Meyer M; Carlson GL; et al. Synthesis, spectral properties, and use of 6-acryloyl-2-dimethylaminonaphthalene (Acrylodan). A thiol-selective, polarity-sensitive fluorescent probe. *J. Biol. Chem.* 1983, *258*, 7541–7544.

61. Weber G; Farris FJ. Synthesis and spectral properties of a hydrophobic fluorescent probe: 6-propionyl-2-(dimethylamino)naphthalene. *Biochemistry* 1979, *18*, 3075–3078.

62. de Silva AP; Gunaratne HQN; Gunnlaugsson T; et al. Signaling recognition events with fluorescent sensors and switches. *Chem. Rev.* 1997, *97*, 1515–1566.

63. de Silva AP; Gunaratne HQN; Gunnlaugsson T. Fluorescent PET (Photoinducer Electron Tranfer) reagentsfor thiols. *Tetraherdron Lett.* 1998, *39*, 5077–5080.

64. Rauh D; Simard JR; Getlik M. Fluorescently or spin-labeled kinases for rapid screening and identification of novel kinase inhibitor scaffolds, and drug discovery uses. PCT Int. Appl. WO2010009886, 2010.

65. Arend M; Westermann B; Risch N. Modern variants of the Mannich reaction. *Angew. Chem. Int. Ed.* 1998, *37*, 1044–1070.

66. Bridges AJ; Zhou H; Cody DR; et al. Tyrosine kinase inhibitors. 8. An unusually steep structure−activity relationship for analogues of 4-(3-bromoanilino)-6,7-dimethoxyquinazoline (PD 153035), a potent inhibitor of the epidermal growth factor receptor. *J. Med. Chem.* 1996, *39*, 267–276.

67. Simplício AL; Clancy JM; Gilmer JF. Beta-aminoketones as prodrugs with pH-controlled activation. *Int. J. Pharm.* 2007, *336*, 208–214.

68. Gilday JP; David M. Process for the preparation of 4- (3'-chloro-4'-fluoroanilino) -7-methoxy-6- (3-morpholinopropoxy) quinazoline. PCT Int. Appl.WO2004/024703, 2004.

69. Rewcastle GW; Denny WA; Bridges AJ; et al. Tyrosine kinase inhibitors: synthesis and structure-activity relationships for 4-[(phenylmethyl)amino]- and 4-[(phenylamino)quinazolines as potent adenosine 5'-triphosphate binding site inhibitors of the tyrosine kinase domain of the epidermal growth factor receptor. *J. Med. Chem.* 1995, *38*, 3482–3487.

70. Vacondio F; Silva C; Lodola A; et al. Biphenyl-3-yl alkylcarbamates as fatty acid amide hydrolase (FAAH) inhibitors: Steric effects of *N*-alkyl chain on rat plasma and liver stability. *Eur. J. Med. Chem.* 2011, *46*, 4466–4473.

71. Bradford MM. A rapid and sensitive method for the quantitation of microgram quantities of protein utilizing the principle of protein-dye binding. *Anal. Biochem.* 1976, *72*, 248–254.

72. Weber W; Bertics PJ; Gill GN. Immunoaffinity purification of the epidermal growth factor receptor. Stoichiometry of binding and kinetics of self-phosphorylation. *J Biol Chem.* 1984, *259*, 14631–14636.

73. Olive DM. Quantitative methods for the analysis of protein phosphorylation in drug development. *Expert Rev. Proteomics* 2004, *1*, 327–341.

74. www.cerep.fr.

75. Cavazzoni A; Petronini PG; Galetti M; et al. Dose-dependent effect of FHIT-inducible expression in Calu-1 lung cancer cell line. *Oncogene* 2004, *23*, 8439–8446.

Chapter 7

Molecular mechanisms underlying the antitumor activity of 3-aminopropanamide Irreversible Inhibitors of the EGFR in NSCLC

Galvani E, Giovannetti E, Saccani F, Cavazzoni A, Leon GL, Dekker H, Alfieri RR, Carmi C, Mor M, Ardizzoni A, Petronini PG & Peters GJ.

NEOPLASIA 2013

In press.

ABSTRACT

Overcoming the emergence of acquired resistance to clinically approved epidermal growth factor receptor (EGFR) inhibitors is a major challenge in the treatment of advanced non-small cell lung cancer (NSCLC). The aim of this study was to investigate the effects of a series of novel compounds affecting viability of NSCLC NCI-H1975 cells (carrying the EGFR-T790M mutation). The inhibition of the autophosphorylation of EGFR occurred at nanomolar concentrations and both UPR1282 and UPR1268 caused a significant induction of apoptosis. Targeting of EGFR and downstream pathways was confirmed by a peptide substrate array, which highlighted the inhibition of other kinases involved in NSCLC cell aggressive behavior. Accordingly, the drugs inhibited migration (about 30% vs. control), which could be in part explained also by the increase of E-cadherin expression. Additionally, we observed a contraction of the volume of H1975 spheroids, associated with the reduction of the cancer stem-like cells hallmark CD133. The activity of UPR1282 was retained in H1975 xenograft models where it determined tumor shrinkage ($P<0.05$) and resulted well tolerated compared to carnetinib. Of note, the kinase activity profile of UPR1282 on xenograft tumor tissues showed overlapping results with respect to the activity in H1975 cells, unraveling the inhibition of kinases involved in pivotal proliferation and invasive signaling pathways. In conclusion, UPR1282 and UPR1268 are effective against various processes involved in malignancy transformation and progression and may be promising compounds for the future treatment of gefitinib-resistant NSCLCs.

INTRODUCTION

Non-small cell lung cancer (NSCLC) represents the majority of human epithelial cancers [1]. About 10% of NSCLCs is marked by functional activation of crucial “driver” oncoproteins with a pivotal dependency on growth factors and their receptors [2]. The epidermal growth factor receptor (EGFR) is a member of the ErbB family of receptor tyrosine kinases. These receptors are commonly expressed in different tissues of epithelial, mesenchymal and neural origin and their pivotal role in normal individual development has been largely investigated. The involvement of EGFR in the regulation of important tumorigenic processes, such as proliferation, apoptosis, angiogenesis, and invasion has also been demonstrated for different tumor types [3]. Furthermore, activated ErbB receptors stimulate several intracellular signaling pathways including the phosphatidylinositol 3-kinase (PI3K)/Akt/mammalian target of rapamycin (mTOR) and the Ras/Raf/mitogen-activated protein kinase (MAPK) pathways which have been demonstrated to play a key role in the control of numerous fundamental cellular processes. Along with its ligands (e.g. EGF, TGF-α, neuregulins) EGFR is often overexpressed and negatively correlated with prognosis in various tumor types, including NSCLC. In particular, the EGFR overexpression has been observed in 40-80% of NSCLC cases and multiple mutations of such receptor have been described and correlated with malignancy “oncogene-addiction” [3]. Taken together these findings identified EGFR as an ideal target for cancer therapy [4]. Small-molecule EGFR tyrosine kinase inhibitors (TKIs), such as gefitinib and erlotinib, have been approved as first line treatment in selected NSCLC patients, as well as second/third-line treatment or maintenance therapy in unselected patients [3]. The clinical response to TKIs is correlated with activating EGFR mutations, predominantly the common in-frame deletions of the exon 19 (delE746-A750) and the missense point mutation L858R. These aberrations are currently used as biomarkers to select patients more likely to benefit from EGFR-TKIs as first-line treatment [5]. Unfortunately, after a progression-free period of about 10 months, most of the EGFR-TKIs responsive patients inevitably relapse. The acquired resistance to first-generation EGFR-TKIs can be caused by multiple mechanisms, including the secondary EGFR point-mutation T790M which accounts for ~50% of the cases [6,7]. The amplification of the receptor for the hepatocyte growth factor (c-Met) was also described as important mechanism of acquired resistance to gefitinib or erlotinib being observed in 20% of the cases [8]. The coexistence of the T790M mutation with c-Met amplification was rarely described [9].

A covalent interaction between EGFR-TKIs with a cysteine residue located at the entrance of the EGFR ATP-binding cleft (Cys797) was described as a possible mechanism to bypass the T790M-related resistance to gefitinib. Several second-generation irreversible inhibitors have been developed [10-13], and many compounds, such as canertinib [14], afatinib [15], neratinib [16], and dacomitinib [17], progressed to clinical investigation, with mixed results. Therefore acquired resistance against first-line EGFR inhibitors so far remains one of the major challenges for NSCLC treatment and the identification of new molecules targeting EGFR-T790M mutants is warranted.

Furthermore, other factors might lay the foundation of drug resistance and novel compounds should be evaluated for their abilities to overcome also these emerging mechanisms. Recent studies reported the epithelial-to-mesenchymal transition (EMT) as a pivotal mechanism involved in the resistance of cancer cells against conventional therapeutics [18,19]. The EMT process results from a number of dramatic cellular and molecular changes, including dissolution of adherent junctions, reorganization of the cytoskeleton, loss of

cell polarity, induction of pro-mesenchymal gene expression, and migration through basement membranes and tissues. Several studies reported the reduction of the expression of the epithelial cell junction protein E-cadherin as key biomarker of EMT in the development of resistance to EGFR inhibition in lung cancer [20]. Importantly, the EMT is also involved in the acquisition of tumor stem-like cell phenotype characterized by high potential of self-renewal in vitro and tumorigenicity in vivo [21].

We recently developed a new series of irreversible EGFR inhibitors containing a 3-aminopropanamide fragment. The cytotoxicity of these compounds was previously tested in vitro in NSCLC H1975 cells [22]. Importantly, these molecules inhibited cell growth at considerably lower concentrations than gefitinib, showing irreversible inhibition of EGFR autophosphorylation, in spite of the lack of a cysteine-trapping warhead [22]. These compounds, while chemically stable in the extracellular environment, proved to be able to release an acrylamide derivative by retro-Michael degradation of the 3-aminopropanamide fragment in the intra-cellular environment. In principle, replacing the reactive acrylamide group of typical second-generation EGFR inhibitors by a chemically-stable and basic aminopropanamide should confer both pharmaceutical (increased stability, water solubility, bioavailability) and therapeutic (lower propensity to give non-specific adducts with biological tissues) advantages. On the other hand, the ability of these pro-covalent inhibitors to exert anti-proliferative activity on tumor cells can depend on the specific intra-cellular environment, and must therefore be thoroughly examined. In particular, we investigated the activity of the 4-(3-Chloro-4-fluoroanilino)-7-ethoxyquinazolino derivative UPR1282 and the 4-Anilinoquinoline-3-carbonitriles derivative UPR1268 (Fig. 1A) in both in vitro and in vivo models derived from the established gefitinib-resistant NSCLC H1975 cell line, which harbors the EGFR-T790M mutation. Other pancreatic and lung cancer cell lines were included in this investigation to compare and understand their effects in diseases where EGFR inhibitors have demonstrated to be active.

MATERIALS AND METHODS

Drugs & chemicals

The synthesis of UPR1282 and UPR1268 has previously been described by Carmi et al [22]. Gefitinib was a generous gift from AstraZeneca (Macclesfield, UK). The drugs were dissolved in DMSO at the stock concentration of 10 mM and then diluted for the experiments in culture medium before use. RPMI medium, fetal bovine serum (FBS), penicillin (50 IU/ml) and streptomycin (50 µg/ml) were from Gibco (Gaithersburg, MD). All other chemicals were purchased from Sigma-Aldrich (Zwijndrecht, The Netherlands).

Cell culture

The human NSCLC cell lines NCI-H1975 (H1975), Calu-1 and A549, and the pancreatic ductal adenocarcinoma (PDAC) cell lines PANC-1 and MIA PaCa-2 were purchased from ATCC (Manassas, VA), and cultured as recommended. Cells were maintained as monolayers in RPMI 1640 (containing 2mM L-glutamine) supplemented with 10% heat-inactivated FBS and 1% streptomycin and penicillin in a 37 °C water-saturated atmosphere of 5% CO_2 in air in 75 cm2 tissue culture flasks (Costar, Cambridge, MA). The cell lines were tested for their authentication by PCR profiling using short tandem repeats (STR), which was performed by BaseClear (Leiden, The Netherlands) in August 2011.

Cell Growth Inhibition

Cell growth inhibition was assessed by sulforhodamine B (SRB) assay according to the NCI protocol with slight modifications [23]. The pure compounds were initially dissolved in DMSO and tested in triplicates in the range 0.01–20 μM. The treatment was started on day 1 after plating, and cells were exposed to drugs for 72 h. The control wells were exposed to 0.1% DMSO. After 72 h treatment, 25 μl of ice-cold 50% (w/v) trichloroacetic acid were added to each well for 60 min at 4°C. Then the SRB assay was performed, as described previously [24]. The optical density (OD) of each well was measured at 540 nm by TiterTek Multiskan MCC/340 (Flow Laboratories, Inc, Rockville, Maryland) 96-wells plate reader. Values were corrected for background OD from wells containing medium only supplemented with 0.1% DMSO. The inhibition of cell viability was calculated with respect to control DMSO treated cells based on the difference in OD at the beginning (day 0) and after 72 h of treatment (day 3), according to the NCI protocol [23]. The 50% growth inhibitory concentration (IC_{50}) was expressed as the concentration inhibiting 50% of the growth of drug treated cells relative to the DMSO only-treated ones, and calculated by non-linear least squares curve fitting (GraphPad PRISM, Intuitive Software for Science, San Diego, CA). Microscopic pictures of H1975 cells exposed to 0.1% DMSO, or UPR1282 and UPR1268 at their IC_{50}s were taken immediately before (time-zero) and after 72 h of treatment by Leica DFC345 FX microscope (Leica Microsystems, Wetzlar, Germany).

Analysis of Apoptosis with AnnexinV Staining and Mitochondrial Membrane Potential.

For the AnnexinV staining H1975 cells were plated at the density of $2x10^5$ cells/well in 6 wells plates. After 24 h 1 μM gefitinib, or UPR1282 and UPR1268 at their respective IC_{50}s were added and cells were then incubated for 24 h. DMSO 0.1% was added to the control wells. Cells were then trypsinized, harvested, transferred to test tubes (12×75mm) and centrifuged at 1200 rpm for 10 min. The pellets were resuspended in 100 μl of ice-cold binding buffer (0.1 M Hepes/NaOH (pH 7.4) 1.4 M NaCl, 25 μM $CaCl_2$). Annexin staining was performed according to the manufacturer`s protocol (Annexin V-FITC apoptosis detection Kit I, Becton Dickinson, San José, CA), with minor modifications as previously described [25]. Cells were stained with both 5 μl Annexin V-FITC and 5 μl propidium iodide (PI) and incubated for 15 min at RT in the dark before adding 400 μl of binding buffer to each tube. Samples were then analyzed by flow cytometry in FACSCalibur Flow Cytometer (Becton Dickinson, San José, CA, USA) and the results were processed using FacsDiva 6.0 software (Becton Dickinson). A total of 10,000 events were collected using excitation/emission wavelengths of 488/525 and 488/675 nm for Annexin V and PI, respectively.

For the analysis of the mitochondrial membrane potential, H1975 cells treated as described above, were harvested and transferred to flow cytometer's tubes and incubated in PBS supplemented with 40 nM DiOC6 (Sigma) for 20 min at 37ºC in the dark. Then cells were washed with PBS and the samples analyzed with the FACSCalibur Flow Cytometer and the FacsDiva 6.0 software. A total of 10,000 events were acquired and living cells were defined by size (Forward Scatter - FSC) and granularity (Side Scatter - SSC).

Genetic characterization of cancer cells.

DNA was isolated from 10^6 cells per cell line, using the miniDNA-kit (Qiagen, Hilden, Germany). DNA yields and purity were checked at 260-280 nm with NanoDrop®-1000-Detector (NanoDrop-Technologies,

Wilmington, USA). Nested PCR to amplify EGFR (exons 18-21) and K-Ras (exon 1-2) and sequencing of PCR products on an ABI-3100 genetic analyzer (Applied Biosystems, Foster City, CA) was performed as described previously [24]. The AKT1-SNP4 G/A (dbSNP-ID:rs1130233) polymorphism was studied using a Taqman®-probes-based assay with specific primers and probes obtained from Applied Biosystems (C_7489835_10). The PCR reactions were performed using 20 ng DNA diluted in 5.94 µl DNAse-RNAse free water, with 6.25 µl of TaqMan Universal PCR Master Mix and 0.31 µl of the mix, including the primers and probes, in a total volume of 12.5 µl. After thermal cycling, the 7500HT instrument determined the allelic content of each sample in the plate by reading the generated fluorescence, using the SDS-2.0 software.

Quantitative real-time RT-PCR.

Total RNA was isolated using the TRI REAGENT LS (Invitrogen, Carlsbad, CA). One µg RNA was retro-transcribed using the DyNAmo cDNA Synthesis Kit (Thermo Scientific, Vantaa, Finland), according to the manufacturers' instructions. Primers and probes to specifically amplify CD133 and E-cadherin were obtained from Applied Biosystems Assay-on-Demand Gene expression products (Hs00901885_m1, Hs01023894_m1). The quantitative real-time PCR was performed in a 25 µl reaction volume containing TaqMan Universal master mix (Applied Biosystems). All reactions were performed in triplicate using the ABI-PRISM 7500 sequence detection system instrument (Applied Biosystems). Samples were amplified using the following thermal profile: 50°C for 2 min, 95°C for 10 minutes, 40 cycles of denaturation at 95°C for 15 sec followed by annealing and extension at 60°C for 1 min. A validation experiment was performed to demonstrate that the efficiencies of the targets (E-cadherin and CD133) and reference (beta-actin) gene amplifications were approximately equal, using a standard curve method with several dilutions of the cDNA sample from untreated control H1975 cells. An ideal slope should be -3.32; the values of the slopes of cDNA calibrator relative to threshold cycle (CT) for the target genes revealed PCR efficiencies above 95%. Amplifications were normalized to beta-actin (TaqMan® B-actin Detection Reagents part number 401846). The fold change was calculated by the $\Delta\Delta$CT method and results were plotted as $2^{-\Delta\Delta CT}$.

Western blot.

After 1 h of exposure to 0.1% DMSO or different concentrations of gefitinib (0.01 to 10 µM), UPR1282 and UPR1268 (both from 0.001 to 10 µM), H1975 cells were stimulated for 5 min with EGF 50 µg/ml and then lysed by RIPA buffer supplemented with protease and phosphatase inhibitor cocktails. Procedures for protein extraction, solubilization, and protein analysis by 1-D PAGE are described elsewhere [26]. Samples of 40-50 µg of proteins were resolved by 10% SDS-PAGE and transferred to PVDF membranes. The following antibodies were used (Bioké, Leiden, The Netherlands): polyclonal anti-phospho-EGFR (Tyr1068) (1:1000 in 1:1 solution of Rockland-Rockland inc., Philadelphia, PA with PBS-T (PBS supplemented with 0.05% Tween-20)), monoclonal anti-EGFR (1:1000), polyclonal anti-phospho-Akt (Ser473) (1:1000), monoclonal anti-Akt (1:1000), polyclonal anti-phospho-p44/42 (Thr202/Tyr204) (1:1000) and monoclonal anti-p44/42 (1:1000). As secondary antibodies, goat-a-mouse-InfraRedDye (1:10,000, 800CW; #926-32210 and 680CW; #926-32220, Westburg, Leusden, The Netherlands) or goat-a-rabbit-InfraRedDye (1:10,000, 800CW; #926-32211 and 680CW; #926-32221) were used. As a loading control, expression of beta-actin was determined using an antibody against beta-actin in stripped membranes (1:10,000, Millipore Bioscience

Research Agents, Temecula, CA). Fluorescent proteins were detected by an Odyssey Infrared Imager (LI-COR Biosciences, Lincoln, NE), at 84 µm resolution, 0 mm offset, using high quality settings.

Peptide substrate array.

To evaluate modulation of kinase activity by gefitinib, canertinib and UPR1282 in H1975 cells and tissues from xenograft models, we profiled lysates from the cells and the tumors by using a kinase peptide substrate array (PamChip®, PamGene International, 's-Hertogenbosch, The Netherlands) as previously described [27]. This array contains 144 peptides consisting of 15 amino-acids including a tyrosine, usually in the middle of the peptide. The 13 COOH-terminal amino-acids of each peptide correspond to known or putative phosphorylation sites in a variety of human proteins. The samples were lysed for 20 min at 4° C by M-PER containing phosphatase and protease inhibitors (Thermo Scientific, Rockford, IL, USA). Lysates were centrifuged for 15 min at 10,000 g; the supernatant was collected and stored at -80 °C. Forty µl control sample mix for the kinase activity array was subsequently prepared by using reaction buffer containing 1×ABL buffer (Westburg, Leusden, The Netherlands), 100 µM ATP (Sigma-Aldrich), fluorescein-labeled antibody PY20 (Exalpha, Maynard, MA, USA), 5 µg (lysate) protein, and DMSO. Kinases inhibition was measured by the addition of 25 µM gefitinib, 25 µM canertinib or 25 µM UPR1282 (final drug concentrations; DMSO concentration in all samples, 2.5%). After blocking the arrays with 2% BSA and subsequent loading of the sample mix onto the arrays, incubation (at 30°C) was started for 60 cycles using a PamStation®12 instrument. Repeated fluorescent imaging of each array was performed with a 12-bit CCD camera, monitoring fluorescence intensities in real time. Spot intensity at each time-point was quantified (and corrected for local background), and the resulting time-resolved curves were fit to calculate the initial phosphorylation rate (V_{ini}) using specific kinetic algorithms and appropriate statistical methods, by Bionavigator software version 5.1 (PamGene International).

In vitro migration assay (Wound healing assay).

Migration was evaluated using the LeicaDMI300B migration station (Leica Microsystems GmbH, Wetzlar, Germany) integrated with the Scratch Assay 6.1 software (Digital Cell Imaging Labs, Keerbergen, Belgium). Thirty thousand H1975 cells/well were plated onto 96-well plates and after 24 h artificial wound tracks were created by scraping with a specific scratcher within the confluent monolayers. After removal of the detached cells by gently washing with PBS, the medium was replaced and the cells were exposed to 0.1% DMSO, 1 µM gefitinib, or UPR1282 and UPR1268 at their respective IC_{50}s. The ability of the cells to migrate into the wound area was assessed by comparing the pixels of the wound tracks in the images taken at the beginning of the exposure (time 0), with those taken after 4, 6, 8 and 24 h [28].

Activity on H1975-derived tumor spheres.

A subpopulation of lung cancer stem-like cells were isolated by culturing $1.5x10^4$ H1975 cells/well in serum free insulin-transferrin-selenium (1:1000, Gibco, Invitrogen) supplemented DMEM/F12+GlutaMAX-I (1:1), in 24-well ultra-low adherent plates (Corning Incorporated, NY, USA), according to the manufacturers' protocol, as previously described [28]. The spheroids were generated for 20-25 days, and then harvested for the growth inhibition studies in 96-well plates, as well as for RNA isolation. After checking their growth and

stability, H1975 spheroids were treated with 0.1% DMSO, 1 μM gefitinib, as well as UPR1282 or UPR1268 at their IC_{50}s. Each well was scanned at 0, 24, 48 and 72 h of treatment. The effects of the drugs were evaluated in term of changes in the volume and in the total number of spheroids using the inverted phase contrast microscope LeicaDMI300B integrated with the Universal Grab 6.3 software (Digital Cell Imaging Labs, Keerbergen, Belgium). The volume of the spheroids (V) was calculated as volume of spheres having as diameter the average of the maximum and minimum diameters ($D = (Dmax + Dmin)/2$; $V = 4/3\pi (D/2)^3$) obtained from the pictures by measurement with ImageJ software (ImageJ 1.45s, Wayne Rasband-National Institutes of Health, Bethesda, Maryland, USA).

Tumor xenografts.

All experiments involving animals were performed in accordance with Guiding Principles in the Care and Use of Animals (DL116/92). Twenty-four Balb/c-Nude female mice (Charles River Laboratories, Calco, Italy) were housed in a protected unit for immunodeficient animals with 12-hour light/dark cycles and provided with sterilized food and water ad libitum. At the time of xenograft experiments, mice were 7 weeks old and weighted about 20 g. Two hundreds μl of matrigel (BD Biosciences) and sterile PBS (1:1) containing 1×10^7 H1975 cells, were subcutaneously injected on the right flank of each mouse (using a 1 ml syringe, needle G25). The injected cells generated a solid tumor localized in correspondence of injection site. When tumor volume reached an average size of 150-200 mm^3, one month after injection, animals were randomized into four groups and treated for 25 days. At the end of the treatment, mice were euthanized by cervical dislocation and tumors collected and stored at -80°C until used for peptide kinase array or formalin fixed for hematoxylin-eosin staining or immunohystochemistry.

Treatment and tumor measurement.

Gefitinib, canertinib and UPR1282 were orally administered, 5 days/week, at the dosage of 25 mg/Kg in 1% Tween 80, while the animals in the control group received oral gavage of vehicle alone.

Tumor xenografts were measured twice a week and tumor volume was calculated using the formula: $(\text{length} \times \text{width}^2)/2$. Final data are expressed as percentage of volume increase: tumor volume/pre-treatment tumor volume × 100.

Sections of formalin-fixed, paraffin-embedded xenograft tumors were stained with hematoxylin and eosin for initial histopathologic examination to confirm the presence of NSCLC cells. This is a widely used, two-stage stain for cells in which hematoxylin is followed by a counterstain of red eosin so that the nuclei stain a deep blue-black and the cytoplasm stains pink. This staining allows the detection of focally multinucleated cells and mitotic figures within the tumors.

Immunohistochemistry.

Tumor tissue sections were constructed using tissue biopsies obtained from 3 mice from the different groups included in recipient paraffin blocks. Before staining with the monoclonal antibody from the EGFR pharmDx™ Kit, the slides were deparaffinized using xylene, and rehydrated in alcohol, as described previously [29]. Negative controls were obtained by replacement of primary antibody with buffer (PBS 1X). EGFR staining was evaluated using a four-tier system including the analysis of both the number of positive

cells and the staining intensity. All slides were reviewed by two independent observers who also evaluated the amount of tissue loss, background staining and overall interpretability before the formal EGFR reactivity evaluation. Neoplastic cells were always uniformly stained and positivity assessment was made by counting at least 2000 tumor representative cells.

Statistical analysis.

All experiments were performed in triplicate and repeated at least twice. Data were expressed as mean values ± S.D. and analyzed using the two-tailed Student's t-test or ANOVA followed by the Bonferroni's multiple comparison test, using Prism 5.0 (GraphPad Software). The level of significance was set at $P<0.05$.

RESULTS

Anti-proliferative and cytotoxic effects.

The novel UPR1282 and UPR1268 compounds (Fig. 1A) were evaluated in comparison to the first-generation EGFR-TKI gefitinib for their ability to inhibit the growth and viability of different cell lines, including the gefitinib-resistant H1975 cell line harboring the T790M mutation (Table 1). The 4-(3-Chloro-4-fluoroanilino)-7-ethoxyquinazolino derivative UPR1282 was significantly more active in comparison with gefitinib in the three tested NSCLC cell lines. In particular, UPR1282 was 9-fold more effective than gefitinib in inhibiting H1975 proliferation, but only 2-fold in the NSCLC cell lines A549 and Calu-1. Because of the approval of the EGFR-TKI erlotinib in combination with gemcitabine [30], for the treatment of advanced PDAC, we also evaluated the biological activity of our compounds in PDAC cells. Our molecules were as active as gefitinib in inhibiting the proliferation of both PANC-1 and MIA PaCa-2 cells. Moreover, a 16-fold difference compared to gefitinib was observed with UPR1268 in H1975 cells. This compound was also 9-fold and 2-fold more effective than gefitinib in reducing A549 and Calu-1 cells viability, respectively. Furthermore, in the PDAC cells MIA PaCa-2, the same compound showed a 5-6 fold increase in potency with respect to the first-generation EGFR-TKI. The inhibition of H1975 cells proliferation was detected also microscopically after exposure of the cells to UPR1282 and UPR1268 at their IC_{50}s.

Apoptosis was investigated as potential mechanism of cell death induced by these compounds using cytofluorimetric analysis of Annexin V staining and mitochondrial membrane potential. One micro-molar gefitinib was chosen as treatment of reference as it is the concentration more commonly used in the preclinical setting to reflect the mean blood concentration reached in NSCLC patients treated with the inhibitor. In apoptotic cells, the membrane phospholipid phosphatidylserine (PS) is translocated from the inner to the outer leaflet of the plasma membrane, thereby exposing PS to the external cellular environment. Annexin V labeled with the FITC fluorescent tag was used with flow cytometry to measure this event. Moreover, since Annexin V staining precedes the loss of membrane integrity which accompanies the later stages of cell death resulting from either apoptotic or necrotic processes, we used the staining with Annexin V-FITC in conjunction with a live/dead dye such as PI to allow the identification of early apoptotic cells (PI negative, Annexin V-FITC positive) from late-apoptotic/dead cells (PI positive, Annexin V-FITC positive). The 24 h treatment with the novel molecules increased both events, as illustrated in the Figure 1B. In particular, IC_{50} concentrations of UPR1282 and UPR1268 increased the early apoptosis from 3.9 to 16.0 and 10.8%, and the late apoptosis from 4.4 to 9.6 and 12.2%, respectively. Mitochondrial damage was assessed

biochemically by measuring $DiOC_6$, a cationic dye that is released when the mitochondrial membrane potential is damaged. As shown by the representative histograms of cytofluorometric analysis in the Figure 1C, a clear decrease in the binding of DiOC6 was observed in H1975 cells treated for 24 h with UPR1282 and UPR1268, as described above. Conversely, no differences were observed in cells treated with gefitinib compared to control cells which were exposed to 0.1% DMSO (Fig. 1B-C).

Table 1: Human cancer cell lines characteristics and sensitivity to EGFR-TKIs

Cell line	Histology	EGFR status	K-Ras status	AKT1 SNP4	Gefitinib IC_{50} µM	UPR1282 IC_{50} µM	UPR1268 IC_{50} µM
H1975 (NSCLC)	Adenocarcinoma	L858R T790M	WT	GG	11.7±1.3	1.2±0.5*	0.6±0.1*
A549 (NSCLC)	Adenocarcinoma	WT	Mut (G12S)	GA	6.4±0.8	3.4±0.3*	0.7±0.1*
Calu-1 (NSCLC)	Squamous cell Carcinoma	WT	Mut (G12C)	GG	19.3±1.2	8.6±0.2*	8.0±0.5*
PANC-1 (PDAC)	Epithelioid carcinoma	WT	Mut (G12D)	AA	7.6±0.4	7.7±1.1	5.6±0.1*
MIA PaCa-2 (PDAC)	Carcinoma	WT	Mut (G12C)	AA	14.1±0.2	11.6±0.3*	2.4±0.1*

NOTE: Data on determinants of gefitinib sensitivity in NSCLC cell lines have been published by Giovannetti et al. [24]. Mut, Mutation; Wt, wild-type; NSCLC, non-small cell lung cancer; PDAC, pancreatic ductal adenocarcinoma. *P<0.05 with respect to gefitinib treatment.

Inhibition of EGFR authophosphorylation and downstream signaling pathways.

In order to get further insights into the mechanism of action of the new compounds compared to gefitinib, we investigated their effect on crucial phosphorylation pathways (Fig. 2). A concentration-dependent inhibition of EGFR autophosphorylation in H1975 cells was observed after exposure to both UPR1282 and UPR1268, with IC_{50} of 0.08 and 0.15 µM, respectively. A complete inhibition of EGFR phosphorylation was reached by both UPR compounds at the highest tested concentration (10 µM). As consequence of the inhibition of the receptor, both our novel compounds affected the phosphorylation of the downstream signaling molecules p-Akt and p-p44/42, while gefitinib had a marginal effect on p-Akt at 10 µM. Furthermore, we investigated alterations of core signaling pathways after exposure to UPR1282, in comparison with gefitinib and canertinib, using a recently established high-throughput kinase array [27].

In the same experimental conditions, gefitinib only slightly reduced EGFR autophosphorylation at 10 µM. In cell lysates, kinase activity profiling was performed in the absence and presence of 25 µM gefitinib, canertinib or UPR1282. Data of V_{ini} in treated cells were compared to the DMSO-treated ones and a total of 28, 43 and 21 kinases, linked to many peptide substrates, were identified with a percentage of inhibition over the 66.6%, caused by gefitinib, canertinib and UPR1282, including 9 common targets (Table 2). Importantly, EGFR, ErbB2 and ErbB4 inhibition was observed as consequence of each treatment.

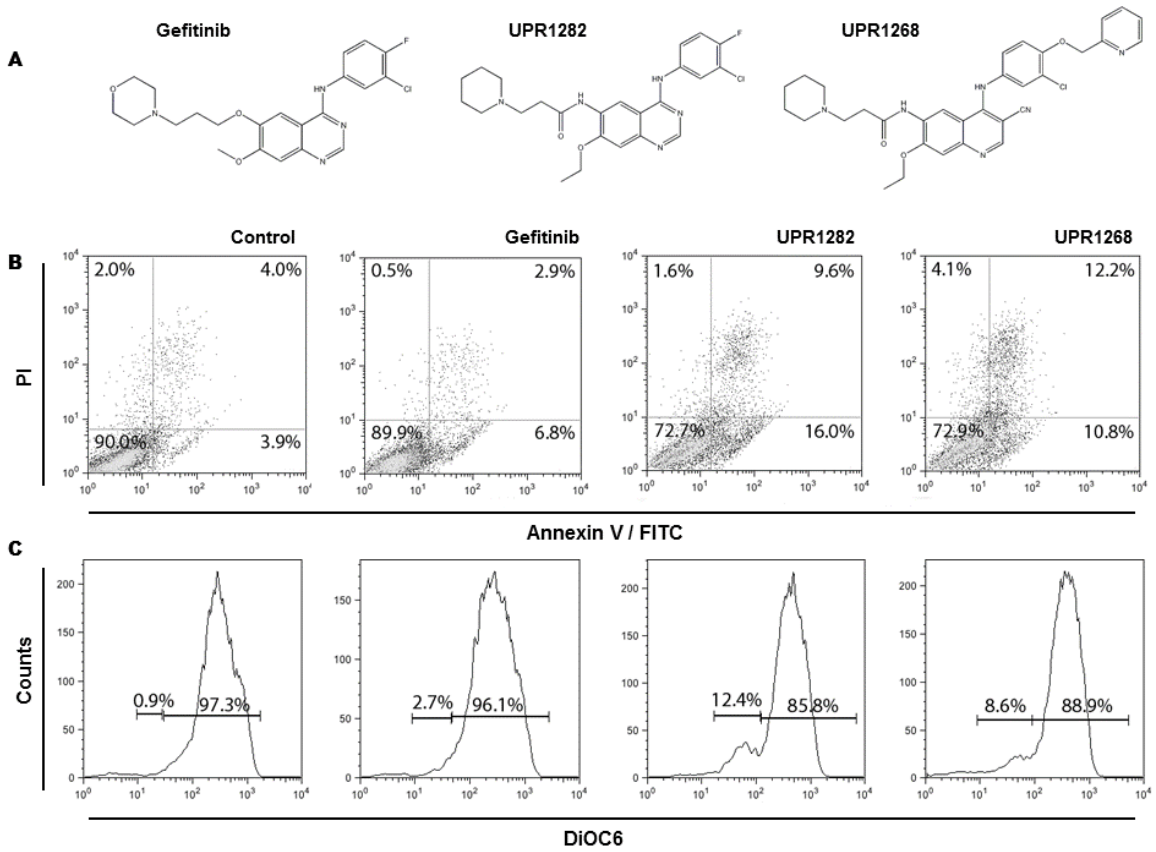

Figure 1. Molecular structure and apoptosis induction of EGFR-TKIs in H1975 cells. (A) Molecular structure of gefitinib, UPR1282 and UPR1268. **(B)** AnnexinV staining: $2x10^5$ H1975 cells/well were treated for 24 h with 0.1% DMSO, 1 µM gefitinib or UPR1282/UPR1268 at their respective IC_{50}s. Cells were then stained with AnnexinV-FITC and PI and samples were analyzed by flow cytometry using excitation/emission wavelengths of 488/525 and 488/675 nm for AnnexinV and PI, respectively. **(C)** Mitochondrial membrane potential: $2x10^5$ H1975 cells/well were treated for 24 h with 0.1% DMSO, 1 µM gefitinib or UPR1282/UPR1268 at their respective IC_{50}s, and then incubated with 40 nM DiOC6. The samples were analyzed with the Flow Cytometer and living cells were defined by size (FSC) and granularity (SSC).

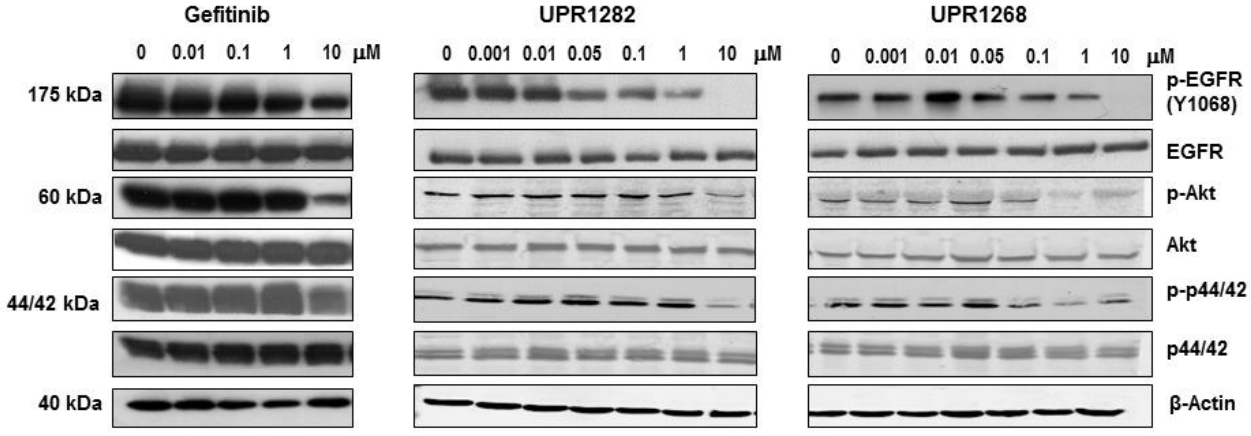

Figure 2. EGFR and downstream pathways phosphorylation analysis by Western blot. $1x10^6$ H1975 cells/well were plated in 6-well plates and after 24 h were exposed for 1 h to 0.01 to 10 µM gefitinib, 0.001 to 10 µM of both UPR1282 and UPR1268, or 0.1 % DMSO (control). Stimulation with EGF 50 µg/ml for 5 minutes was performed before protein extraction. Samples of 40-50 µg of proteins were resolved by 10% SDS-PAGE and transferred to PVDF membranes. Fluorescent proteins were detected and analyzed by Odyssey Infrared Imager at 84 µm resolution, 0 mm offset, using high quality settings. The immunoblot of gefitinib activity in H1975 cells has been previously published by Carmi et al., J Med Chem 2010 (10).

Table 2: Kinase activity profiles of gefitinib, canertinib and UPR1282 in H1975 cells

Peptides	Gef	Can	UPR	Peptides	Gef	Can	UPR	Peptides	Gef	Can	UPR
ANXA1_14_26		X		FAK2_572_584	X			PRGR_545_557	X		
ANXA2_17_29	X	X		FES_706_718		X		PRGR_786_798	X		
B3AT_39_51			X	FGFR3_641_653		X	X	RASA1_453_465	X	X	X
PGFRB_1014_1028		X		JAK1_1015_1027		X		RBL2_99_111	X	X	
CALM_95_107	X	X	X	JAK2_563_577		X		RON_1346_1358	X	X	
CBL_693_705		X		K2C6B_53_65	X	X	X	RON_1353_1365		X	
CD3Z_116_128		X		K2C8_425_437		X	X	STAT1_694_706	X	X	
CD3Z_146_158		X		KSYK_518_530	X			STAT4_714_726	X	X	
CDK2_8_20		X		LCK_387_399		X		TNNT1_2_14	X		X
DCX_109_121	X	X	X	MK01_180_192		X	X	TYRO3_679_691	X	X	
EGFR_1190_1202		X	X	MK10_216_228	X	X	X	VGFR1_1046_1058	X	X	
EGFR_862_874	X			MK14_173_185		X		VGFR1_1162_1174		X	
EPHA4_589_601		X	X	NTRK1_489_501	X	X	X	VGFR1_1235_1247	X	X	
EPHB1_771_783		X		NTRK2_509_521	X	X	X	VGFR2_1046_1058		X	
EPHB4_583_595	X		X	ODPAT_291_303	X	X	X	VGFR2_1052_1064	X	X	
EPOR_361_373		X	X	PP2AB_297_309	X			VGFR2_1168_1180	X		X
ERBB2_870_882	X			PECA1_706_718		X		VGFR2_1207_1219	X	X	X
ERBB4_1181_1193		X		PERI_458_470	X		X	VGFR3_1061_1073	X	X	
ERBB4_1277_1289		X		PLCG1_1246_1258		X					
FAK1_569_581			X	PLCG1_776_788		X					

Gef, gefitinib; Can, canertinib; UPR, UPR1282; X, % of kinase inhibition > than 66.6% in comparison with untreated H1975 cells. The acronyms refer to peptides/proteins from http://www.expasy.org/uniprot/

EMT and inhibition of cellular migration.

Accumulating evidence suggests a critical role of EMT in epithelial cancer progression, invasion and metastasis. Cell features, including cell-cell and cell-matrix interactions, are highly affected by EMT and loss of intracellular cohesion, together with the disruption of extracellular matrix and modifications of the cytoskeleton, have been related to increased cell motility and invasiveness [31]. The family of cadherins comprises molecules which are involved in cell-cell adhesion, and their deregulation may result in EMT and cell motility. Recent studies demonstrated the correlations between cell-cell contact and cytoplasmic signaling pathways activation or inhibition [32]. Wnt signaling has emerged as critical pathway in lung tumorigenesis via the beta-catenin-mediated transcription of zinc-finger proteins such as Slug and Snail, which expression is inversely correlated with E-cadherin transcription [33]. Destruction of E-cadherin by RTK/Ras was demonstrated to cause release of beta-catenin from disassembled junctions between epithelial cells and promote cell transformation [34]. Thus, E-cadherin was first investigated by RT-PCR as molecule related to cellular migration. While gefitinib did not affect the level of E-cadherin mRNA in H1975 cells, the exposure to the novel irreversible inhibitors significantly increased its gene expression when compared to DMSO-treated cells (Fig. 3A). Furthermore, to explore whether UPR1282 and UPR1268 affect cell migration, a scratch motility assay was performed in H1975 cells. Both molecules significantly reduced cell migration in comparison to the control, while gefitinib did not result in any effect (Fig. 3B-C).

Volume reduction of H1975-derived tumor spheres.

Results from earlier studies illustrated that the sensitivity of two-dimensional monolayer cell cultures to anticancer drugs is different from that obtained in three-dimensional culture models [35]. Furthermore, the cancer stem cells (CSCs) theory prompted to the re-examination of established views of tumor initiation, progression and therapeutic resistance [36]. Recently, the use of serum-free medium has been reported to select cell populations harboring CSC-like characteristics, including self-renewal and differentiation into

heterogeneous lineages of cancer cells [37]. This experimental approach represents the best strategy so far to obtain the expansion of the tumorigenic cell subpopulation. Furthermore, recent studies unraveled the importance of CSC CD133-positive cells in tumorigenicity and chemoresistance of lung cancer [38]. Thus, in order to determine whether three-dimensional systems, enriched with CSC-like properties, could be affected by our compounds, we developed tumor spheres from H1975 cells which, after 20-25 days of culture, reached a size of approximately 400-500 μm in diameter (Fig. 4A). We evaluated then by RT-PCR the level of CD133 mRNA as marker of stemness, comparing adherent cells versus tumor spheres. In agreement with previous studies, a significantly higher expression of CD133 mRNA was observed in tumor spheres when compared to adherent cells (Fig. 4B). When treated with gefitinib or the novel TKIs, the total number of H1975-spheroids was not affected. However, the treatment with the novel inhibitors significantly reduced tumor spheres volume when compared to the time zero of treatment (Fig. 4C-D). In contrast, gefitinib treatment did not affect the growth of these three-dimensional spheroidal systems (data not shown). Furthermore, the exposure of tumor spheres to UPR1282 and UPR1268 significantly reduced CD133 gene expression (Fig. 4E), while the treatment with gefitinib did not cause any change in CD133 mRNA when compared to DMSO-only treated spheroids (data not shown).

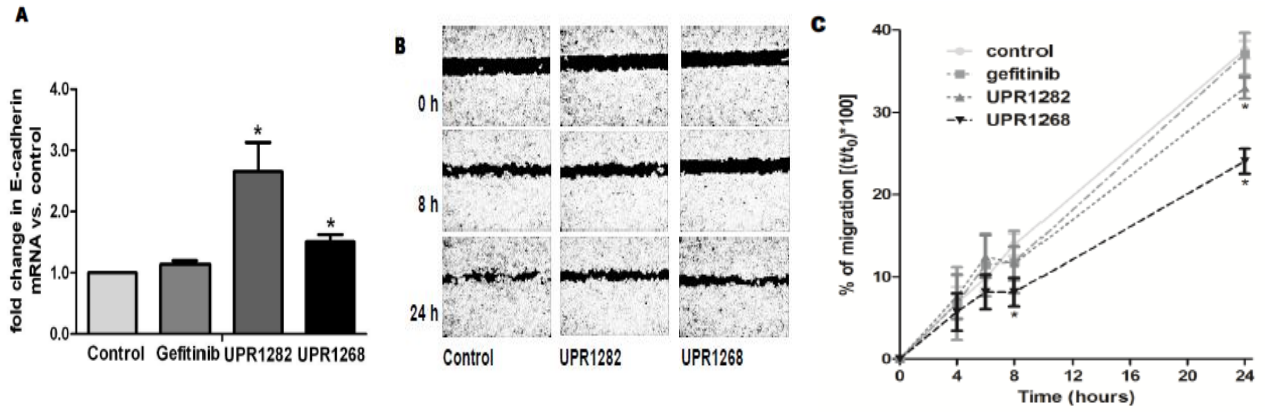

Figure 3. Effects of EGFR-TKIs on H1975 cells migration. (A) E-cadherin evaluation by quantitative RT-PCR after exposure of H1975 cells to 1 μM gefitinib, or UPR1282 and UPR1268 to their respective IC_{50}s for 24 h. **(B)** Representative pictures of the wound tracks (created 24 h after plating $3x10^5$ H1975 cells/well) in time with different treatments. The control is represented by cells exposed to 0.1% DMSO. **(C)** Comparison of the effect of the different treatments on the percentage of cell migration. After 24 h since plating, cells were treated with 0.1% DMSO, 1 μM gefitinib, 1.2 μM UPR1282 or 0.6 μM UPR1268. The wound areas were measured after 0, 4, 6, 8 and 24 h of treatment. The percentages of migration are referred to the time 0 measurements and represent the averages of 4 replicates repeated in 3 independent experiments.

Tumor shrinkage in H1975-xenograft model and signaling pathways inhibition in tumor tissue.

To evaluate the potential of our compounds in vivo, we tested the effects of UPR1282 in comparison with gefitinib and canertinib (H1975 IC_{50}=2.4 μM) in H1975-derived xenografts. When tumors were well established and reached an average volume of 150-200 mm^3 the mice were randomized into four treatment groups receiving gefitinib, canertinib, UPR1282 or vehicle. The treatment with either canertinib or UPR1282 caused tumor shrinkage, while gefitinib did not affect tumor growth in comparison to the control group (Fig. 5A). Of note, canertinib significantly inhibited tumor growth after 21 days of treatment. However, this shrinkage was accompanied by a significant reduction of animal body weight compared to untreated animals

as well as to mice treated with UPR1282 (Fig. 5B). Immunohistochemistry was then performed on 3 tumor tissues per group and EGFR was evaluated as marker to confirm the origin of the tumor from our human lung cancer cells (Fig. 5C). In order to evaluate the activity of our novel drug in tumor tissues, we performed an additional kinase activity profiling in tissue lysates, in absence or presence of 25 µM UPR1282.

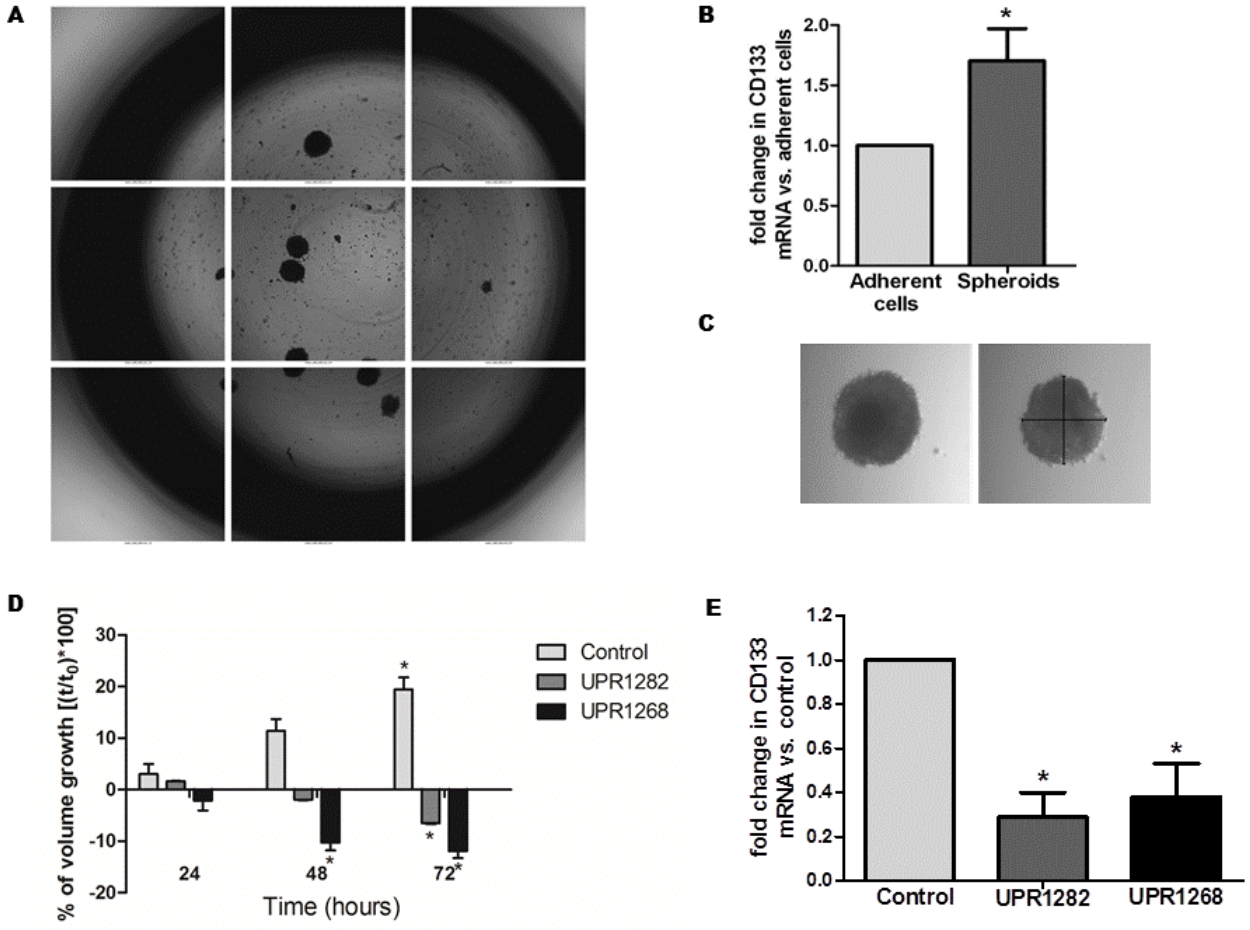

Figure 4. Effects of EGFR-TKIs on H1975 grown as spheroids. (A) Composite representative picture of an experimental well containing several spheroids. **(B)** Comparison of CD133 mRNA by quantitative RT-PCR in H1975 adherent cells versus tumor spheres. The fold change of CD133 mRNA in spheroids was calculated using the 2^(-ΔΔCt) method relatively to adherent cells, used as control. **(C)** Representative image of diameters measurement in the evaluation of spheroids volume. **(D)** After 20-25 days H1975 spheroids were treated with 1 µM gefitinib as well as with UPR1282 and UPR1268 at their IC_{50}s. The volume of the spheroids was measured at 24, 48 and 72 h treatment and normalized to the volume of the spheroids at time zero treatment. **(E)** CD133 evaluation by quantitative PCR after exposure of tumor spheres to 1 µM gefitinib or to UPR1282 and UPR1268 at their IC_{50}s for 24 h.

Data of V_{ini} in treated lysates from H1975 xenograft specimens, which according to hematoxylin-eosin staining in figure 5C contained more than 80% of tumor cells, were compared to data obtained from the treatment of H1975 cells lysate. This array identified a strong percentage of inhibition (i.e., over the 66.6%) of 17 and 21 kinases in tissue and cell lysates, respectively, including 7 common targets (Fig. 5D). Importantly, EGFR inhibition by UPR1282 was confirmed by the peptide substrates array in both tissue and cells, confirming its powerful activity on this target.

DISCUSSION AND CONCLUSIONS

The present study demonstrates the activity of novel EGFR irreversible inhibitors against tumor cells, including in vitro and in vivo models of EGFR-T790M NSCLC. Moreover, we evaluated several molecular mechanisms underlying the abilities of these novel compounds to effectively antagonize NSCLC aggressive and invasive behaviour.

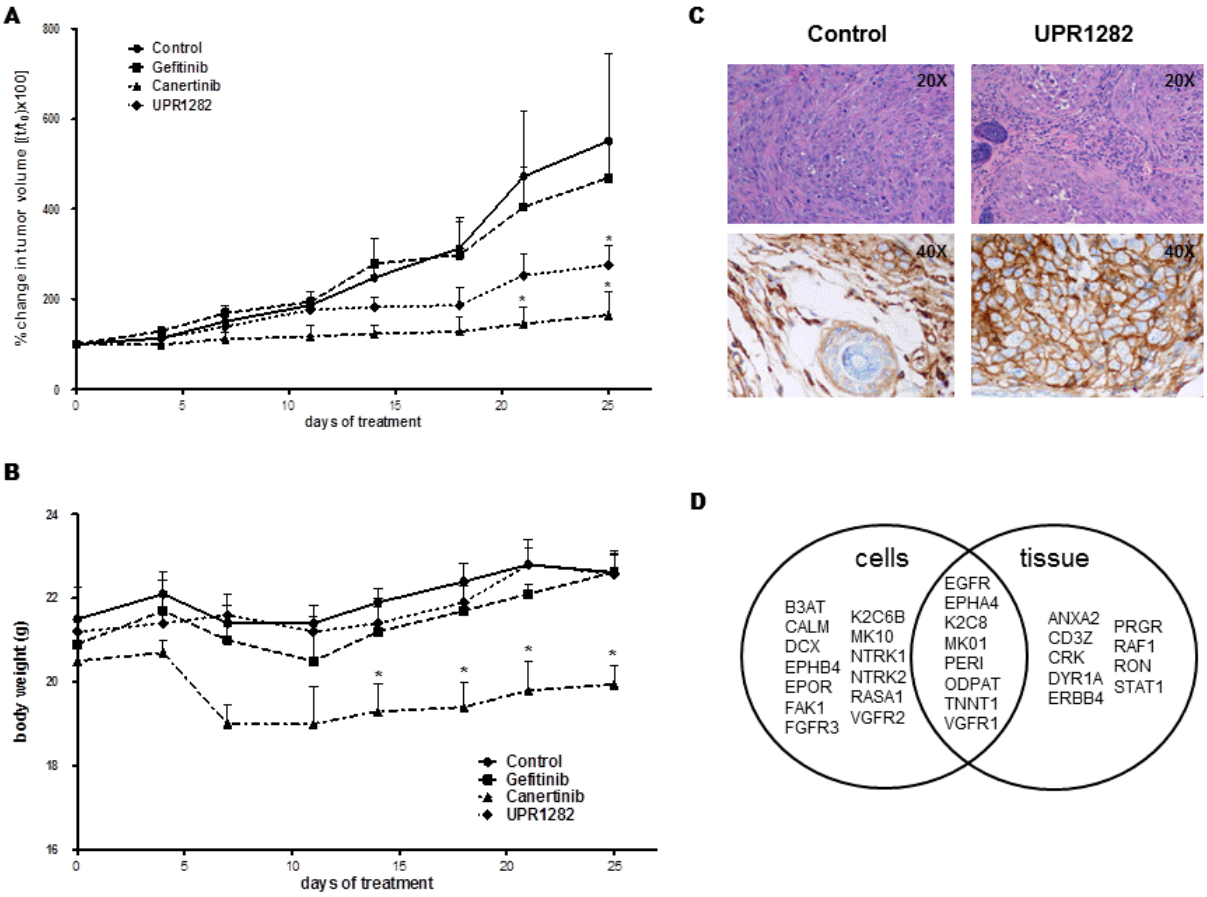

Figure 5. Effects of EGFR-TKIs in xenograft models. **(A)** Effect of treatments with reversible and irreversible TKIs on tumor growth in a human NSCLC xenograft model. H1975 cells were suspended in a matrigel and sterile PBS (1:1) and implanted s.c. (right flank) on female BALB/c-Nude mice. Tumors were allowed to growth for one month, and the treatments started when they reached an average volume of 150-200 mm^3. Vehicle, gefitinib, canertinib or UPR1282 were administered orally five days per week, at the dosage of 25 mg/Kg, for all the duration of the study. Data are expressed as percentage of change in tumor volume ± SEM. **(B)** Effect of the chronic treatment of mice with vehicle, gefitinib, canertinib or UPR1282 administered orally five days per week, at the dosage of 25 mg/Kg on animal body weight. Data are expressed as percentage of change in tumor volume ± SEM. **(C)** Representative tumor xenografts staining with haematoxilin and eosin and immunohistochemistry for EGFR of tissues from xenografts from control and UPR1282-treated groups. **(D)** Venn Diagram of kinase profiles obtained from cells and tissue lysates treated with 25 µM UPR1282. After loading of the sample mix onto the arrays, incubation (at 30°C) was started for 60 cycles utilizing a PamStation®12 instrument. Repeated fluorescent imaging of each array was performed to monitor fluorescence intensities in real time. Spot intensity was quantified and the resulting time-resolved curves were fit to calculate the initial phosphorylation rate (V_{ini}) using specific kinetic algorithms and appropriate statistical methods. Kinases which were identified to be inhibited more than 66.6% compared to DMSO-treated lysates of both cells and tissues are plotted in the Venn diagram.

Molecular targeting of EGFR with the first-generation reversible TKIs gefitinib and erlotinib is now an established therapeutic option in advanced NSCLC patients who harbor activating mutations of the receptor

[39]. However, the emerging acquired resistance together with the low survival benefit prompt further studies to improve this therapeutic approach. The necessity to overcome the resistance due to the T790M secondary mutation of EGFR led to the development of several second-generation irreversible TKIs of this target [3]. We recently synthesized a series of novel 3-aminopropanamide compounds which demonstrated to be active against H1975 NSCLC cells harboring the EGFR-T790M mutation by irreversible binding to the receptor following intra-cellular activation to a cysteine-trapping chemical species [22]. The present study demonstrates that the two most promising compounds inhibit cell proliferation and induce apoptosis in different NSCLC cell lines at significantly lower concentration than gefitinib. Since the EGFR-TKI erlotinib has been approved for the treatment of advanced PDAC in combination with gemcitabine [30], we also evaluated the new molecules in PANC-1 and MIA PaCa-2 cells.

In these cell lines both our compounds were as active as gefitinib or even more active than the first-generation EGFR-TKI. However, the very slight increase in survival obtained with the use of erlotinib [40], and the recent success of multicombinatorial approaches with conventional cytotoxic drugs reduce the impact of EGFR-TKIs in the treatment of PDAC [41].

As expected on the basis of their anti-EGFR activity, the main downstream mediators of the EGFR signal transduction pathways (p-Akt and p-p44/42) were also affected by our novel compounds. However, despite EGFR inhibition was already detectable by Western blot in the nano-molar range of concentrations, the downstream signaling molecules were slightly inhibited at 1 µM, particularly by UPR1268, and more clearly at the highest used concentration (10 µM) for both the inhibitors. Furthermore, using a commercially available 144-peptide array, we detected other tyrosine kinases affected by UPR1282. The restricted subset of the peptides spotted on the array, together with the limited specificity and the use of lysates which cannot reproduce subcellular compartmentalization and protein docking or scaffolding represent the main interdictions of this study [42]. However, several additional tyrosine kinases were identified which were significantly inhibited by UPR1282, including the fibroblast growth factor receptor 3 (FGFR3), whose upregulation has been correlated to radioresistance in squamous cell carcinoma [43]. Of note, EphB4 and the focal adhesion kinase 1 (FAK1), which are both involved in the neoplastic transformation process, were also inhibited by UPR1282 in H1975 cells [44,45]. Additionally, the treatment of the cell lysates with UPR1282 also inhibited c-Met, which amplification represents the second cause of acquired resistance to the treatment with EGFR-TKIs. In particular, the activity of the receptor was reduced of around 53% by UPR1282. Importantly, many kinases, including the previously mentioned, had relevant (although not always below the 66.6% threshold) levels of inhibition in both H1975 cell line and xenografts exposed to UPR1282. These results potentially extend the use of UPR1282 to the treatment of NSCLCs which harbor mechanisms of resistance different than the EGFR-T790M mutation.

The invasive and metastastic capacity of tumor cells constitute two pivotal mechanisms of malignant tumor development. The poor prognosis of lung cancer is related to strong metastasis potential, which is directly correlated with EMT [33]. The transformation of epithelial cells to motile, invasive and migratory mesenchymal cells is the major feature of such process. Cell adhesion and detachment are regulated by interactions between cell–cell and cell–extracellular matrix (ECM) which coordinate the invasive mechanism [46]. Several classes of proteins participate to invasive cancer phenotype. Recent studies reported the loss of function of the cadherin adhesion complex, and in particular E-cadherin, as hallmark of EMT which leads

to increased proliferation, invasiveness and metastasis [47]. Thus, we investigated whether the exposure to UPR1282 or UPR1268 might affect E-cadherin gene expression. While treatment with gefitinib did not affect the level of mRNA coding for E-cadherin in H1975 cells, a significant increase in its gene expression was observed after exposure to our novel compounds. Furthermore, since recent studies demonstrated that EGF modifies cell–ECM adhesion [48], we tested whether our compounds might affect migration of EGFR-T790M H1975 cells. Differently from what observed after exposure to gefitinib, the novel 3-aminopropanamide compounds significantly reduced cell migration after few hours of treatment, as detected by the wound-healing assay. Such reduction in cell motility agrees with previous evidence on FAK inhibition and increased E-cadherin gene expression.

Accumulating evidence suggests that specific sub-populations of cancer cells within the bulk of tumors undergo different degree of EMT, and this process has been related with the acquisition of stem cell-like characteristics. Both EMT and stemness are implicated in the pathogenesis and chemoresistance of heterogeneous malignant tumors [21,49]. Treatment strategies for the elimination of cancer, therefore, need to consider the presence of CSCs. Sphere assay has proven to be an excellent technique to isolate CSCs and several studies demonstrated that the three-dimensional aggregates can contain different cell proliferation and metabolic gradients, such as an outer rim of viable and actively proliferating cells and an inner necrotic region [35]. Thus, after generating tumor spheres which overexpress the stem/initiating-cell marker CD133, we explored whether our novel EGFR-TKIs affected spheroids growth. Conversely to gefitinib, both the 3-aminopropanamide derivatives significantly reduced tumor spheres dimensions. Furthermore, we demonstrated that the level of CD133 mRNA was reduced after exposure to UPR1282 and UPR1268 [37,50].

The evaluation of the activity of UPR1282 was also extended to xenograft models of EGFR-T790M NSCLC. The chronic administration of UPR1282 in athymic mice was well tolerated and produced significant inhibition of tumor growth, which might result from inhibition of both EGFR and downstream kinases activity. Of note, while tumor shrinkage induced by canertinib treatment was accompanied by significant toxicity, UPR1282 did not induce significant loss of body weight and toxicity even after a prolonged treatment. This might be, at least in part, related to the masking of acrylamide warhead which results in reduced risk of covalent interaction with off-target molecules [22].

In conclusion, our 3-aminopropanamide irreversible EGFR-TKIs seem very promising anticancer agents by attacking different key mechanisms involved in the resistance of NSCLC cells to the first-generation EGFR-TKIs gefitinib and erlotinib, including the EMT process. These data should prompt future trials that will give the ultimate proof of the utility of these novel anticancer agents for the treatment of lung cancer.

ACKNOWLEDGEMENTS

This work was supported by: Associazione Italiana per la Ricerca sul Cancro (AIRC), Milan grant IG 8856 (Andrea Ardizzoni); the Netherlands Organization for Scientific Research (NWO, Veni grant, Elisa Giovannetti); AIRC-Marie Curie (International Fellowship, Elisa Giovannetti); FIRC grant (Fellowship for abroad; E. Galvani).

REFERENCES

1. Govindan R, Page N, Morgensztern D, *et al.*. J. Changing epidemiology of small-cell lung cancer in the United States over the last 30 years: analysis of the surveillance, epidemiologic, and end results database. J Clin Oncol 2006; 24(28):4539-44.
2. Hoang T, Schiller JH. Advanced NSCLC: from cytotoxic systemic chemotherapy to molecularly targeted therapy. Expert Rev Anticancer Ther 2002; 2(4):393-401.
3. Galvani E, Alfieri R, Giovannetti E *et al.*. Epidermal Growth Factor Receptor Tyrosine Kinase Inhibitors: current status and future perspectives in the development of novel irreversible inhibitors for the treatment of mutant non-small cell lung cancer. Curr Pharm Des 2013; 19(5):818-832..
4. Olayioye MA, Neve RM, Lane HA, *et al.*. The ErbB signaling network : receptor heterodimerization in development and cancer. EMBO Journal 2000; 19(13):3159-3167.
5. Ciardiello F, Tortora G. EGFR antagonists in cancer treatment. New Engl J Med 2008; 358(11):1160-74.
6. Pao W, Miller V a, Politi K a, *et al.*. Acquired resistance of lung adenocarcinomas to gefitinib or erlotinib is associated with a second mutation in the EGFR kinase domain. PLoS Med 2005; 2(3):e73.
7. Suda K, Onozato R, Yatabe Y, *et al.*. EGFR T790M Mutation A double role in lung cancer cell survival? J Thorac Oncol 2009; 4(1):1-4.
8. Engelman JA, Zejnullahu K, Mitsudomi T, *et al.*. MET amplification leads to gefitinib resistance in lung cancer by activating ERBB3 signaling. Science 2007; 316(5827): 1039-43.
9. Bean J, Brennan C, Shih J-Y, *et al.*. MET amplification occurs with or without T790M mutations in EGFR mutant lung tumors with acquired resistance to gefitinib or erlotinib. P Natl Acad Sci USA 2007; 104(52): 20932-7
10. Carmi C, Cavazzoni A, Vezzosi S, *et al.*. Novel irreversible epidermal growth factor receptor inhibitors by chemical modulation of the cysteine-trap portion. J Med Chem 2010; 53(5):2038-50.
11. Wu C-H, Coumar MS, Chu C-Y, *et al.*. Design and synthesis of tetrahydropyridothieno[2,3-d]pyrimidine scaffold based epidermal growth factor receptor (EGFR) kinase inhibitors: the role of side chain chirality and Michael acceptor group for maximal potency. J Med Chem 2010; 53(20):7316-26.
12. Cha MY, Lee K-O, Kim JW, *et al.*.Discovery of a novel Her-1/Her-2 dual tyrosine kinase inhibitor for the treatment of Her-1 selective inhibitor-resistant non-small cell lung cancer. J Med Chem 2009; 52(21):6880-8.
13. Ding K, Zhang L, Xu S, *et al.*. Design, Synthesis and Biological Evaluation of Novel Conformationally Constrained Inhibitors Targeting Epidermal Growth Factor Receptor T790M mutant. J Med Chem 2012; 55(6):2711-23..
14. Smaill JB, Rewcastle GW, Loo J a, *et al.*. Tyrosine kinase inhibitors. 17. Irreversible inhibitors of the epidermal growth factor receptor: 4-(phenylamino)quinazoline- and 4-(phenylamino)pyrido[3,2-d]pyrimidine-6-acrylamides bearing additional solubilizing functions. J Med Chem 2000; 43(7):1380-97.
15. Li D, Ambrogio L, Shimamura T, *et al.*. BIBW2992, an irreversible EGFR/HER2 inhibitor highly effective in preclinical lung cancer models. Oncogene 2008; 27(34):4702-11.
16. Wissner A, Overbeek E, Reich MF, *et al.*. Synthesis and structure-activity relationships of 6,7-disubstituted 4-anilinoquinoline-3-carbonitriles. J Med Chem 2003; 46(1):49-63.
17. Gonzales AJ, Hook KE, Althaus IW, *et al.*. Antitumor activity and pharmacokinetic properties of PF-00299804, a second-generation irreversible pan-erbB receptor tyrosine kinase inhibitor. Mol Cancer Ther 2008; 7(7):1880-9.
18. Wang Z, Li Y, Kong D, *et al.*. Acquisition of epithelial-mesenchymal transition phenotype of gemcitabine-resistant pancreatic cancer cells is linked with activation of the notch signaling pathway. Cancer Res 2009; 69(6):2400-7.
19. Kajiyama H, Shibata K, Terauchi M, *et al.*. Chemoresistance to paclitaxel induces epithelial-mesenchymal transition and enhances metastatic potential for epithelial ovarian carcinoma cells. Int J Oncol 2007; 31(2):277-83.
20. Rho JK, Choi YJ, Lee JK, *et al.*. Epithelial to mesenchymal transition derived from repeated exposure to gefitinib determines the sensitivity to EGFR inhibitors in A549, a non-small cell lung cancer cell line. Lung cancer 2009; 63(2):219-26.
21. Jung M-J, Rho J-K, Kim Y-M, *et al.*. Upregulation of CXCR4 is functionally crucial for maintenance of stemness in drug-resistant non-small cell lung cancer cells. Oncogene 2012; 1-13.
22. Carmi C, Galvani E, Vacondio F, *et al.*. Irreversible Inhibition of Epidermal Growth Factor Receptor Activity by 3-Aminopropanamides. J Med Chem 2012.
23. Skehan P, Storeng R, Scudiero D, *et al.*. New colorimetric cytotoxicity assay for anticancer-drug screening. J Nat Cancer In 1990; 82(13):1107-12.
24. Giovannetti E, Zucali P a, Peters GJ, *et al.*. Association of polymorphisms in AKT1 and EGFR with clinical outcome and toxicity in non-small cell lung cancer patients treated with gefitinib. Mol Cancer Ther 2010; 9(3):581-93.
25. Giovannetti E, Zucali P a, Assaraf YG, *et al.*. Preclinical emergence of vandetanib as a potent antitumour agent in mesothelioma: molecular mechanisms underlying its synergistic interaction with pemetrexed and carboplatin. British J Cancer 2011; 105(10):1542-53.
26. Alfieri RR, Galetti M, Tramonti S, *et al.*. Metabolism of the EGFR tyrosin kinase inhibitor gefitinib by cytochrome P450 1A1 enzyme in EGFR-wild type non small cell lung cancer cell lines. Mol Cancer 2011; 10:143.
27. Giovannetti E, Labots M, Dekker H, *et al.*. Molecular mechanisms and modulation of key pathways underlying the synergistic interaction of sorafenib with erlotinib in non-small-cell-lung cancer (NSCLC) cells. Curr Pharm Des 2013;19(5):927-939.
28. Avan A, Crea F, Paolicchi E, *et al.*. Molecular mechanisms involved in the synergistic interaction of the EZH2 inhibitor 3 deazaneplanocin A (DZNeP) with gemcitabine in pancreatic cancer cells. Mol Cancer Ther 2012; 11(8):1735-46.
29. Funel N, Vasile E, Del Chiaro M, *et al.*. Correlation of basal EGFR expression with pancreatic cancer grading but not with clinical outcome after gemcitabine-based treatment. Ann Oncol. 2011; 22(2):482-4.
30. Moore MJ, Goldstein D, Hamm J, *et al.*. Erlotinib plus gemcitabine compared with gemcitabine alone in patients with advanced

pancreatic cancer: a phase III trial of the National Cancer Institute of Canada Clinical Trials Group. J Clin Oncol 2007; 25(15):1960-6.
31. Voulgari A, Pintzas A. Epithelial-mesenchymal transition in cancer metastasis: mechanisms, markers and strategies to overcome drug resistance in the clinic. Biochimica et biophysica acta 2009; 1796(2):75-90.
32. Wheelock MJ, Shintani Y, Maeda M *et al.*. Cadherin switching. J Cell Sci 200; 121(Pt 6):727-35.
33. Dasari V, Gallup M, Lemjabbar H, *et al.*. Epithelial-mesenchymal transition in lung cancer: is tobacco the “smoking gun”? Am J Resp Cell Mol 2006; 35(1):3-9.
34. Chen Y-T, Gallup M, Nikulina K, *et al.*. Cigarette smoke induces epidermal growth factor receptor-dependent redistribution of apical MUC1 and junctional beta-catenin in polarized human airway epithelial cells. Am J Pathol 2010; 177(3):1255-64.
35. Padrón JM, van der Wilt CL, Smid K, *et al.*. The multilayered postconfluent cell culture as a model for drug screening. Crit Rev Oncol Hemat 2000; 36(2-3):141-57.
36. Reya T, Morrison SJ, Clarke MF, *et al.*. Stem cells, cancer, and cancer stem cells. Nature 2001; 414(6859):105-11.
37. Eramo a, Haas TL, De Maria R. Lung cancer stem cells: tools and targets to fight lung cancer. Oncogene 2010; 29(33):4625-35
38. Bertolini G, Roz L, Perego P, *et al.*. Highly tumorigenic lung cancer CD133+ cells display stem-like features and are spared by cisplatin treatment. P Natl Acad Sci USA 2009; 106(38):16281-6
39. Lynch TJ, Bell DW, Sordella R, *et al.*. Activating Mutations in the Epidermal Growth Factor Receptor Underlying Responsiveness of Non–Small-Cell Lung Cancer to Gefitinib. N Engl J Med 2004; 350(21):2129-2139.
40. Miksad RA, Schnipper L, Goldstein M. Does a statistically significant survival benefit of erlotinib plus gemcitabine for advanced pancreatic cancer translate into clinical significance and value? J Clin Oncol 2007; 25(28):4506-7; author reply 4508.
41. Conroy T, Desseigne F, Ychou M, *et al.*. FOLFIRINOX versus gemcitabine for metastatic pancreatic cancer. N Engl J Med 2011; 364(19):1817-25.
42. Piersma SR, Labots M, Verheul HMW, *et al.*. Strategies for kinome profiling in cancer and potential clinical applications: chemical proteomics and array-based methods. Anal Bioanal Chem 2010; 397(8):3163-71.
43. Uzawa K, Ishigami T, Fushimi K, *et al.*. Targeting fibroblast growth factor receptor 3 enhances radiosensitivity in human squamous cancer cells. Oncogene 2011; 30(43):4447-52.
44. Nakamoto M, Bergemann AD. Diverse roles for the Eph family of receptor tyrosine kinases in carcinogenesis. Microsc Res Techniq 2002; 59(1):58-67.
45. Infusino GA, Jacobson JR. Endothelial FAK as a therapeutic target in disease. Microvasc Res 2012; 83(1):89-96.
46. Forest V, Campos L, Vergnon J-M, *et al.*. Characterization of the focal adhesion complex in human non-small cell lung cancer cell lines. Anticancer Res 2005; 25(6B):4135-9.
47. Xiao D, He J. Epithelial mesenchymal transition and lung cancer. J Thorac Disease 2010; 2(3):154-9.
48. Fonseca FL a, Azzalis L a, Feder D, *et al.*. Adhesion molecules affected by treatment of lung cancer cells with epidermal growth factor. Lung 2011; 189(5):383-9.
49. Thomson S, Buck E, Petti F, *et al.*. Epithelial to mesenchymal transition is a determinant of sensitivity of non-small-cell lung carcinoma cell lines and xenografts to epidermal growth factor receptor inhibition. Cancer Res 2005; 65(20):9455-62.
50. Tirino V, Camerlingo R, Franco R, *et al.*. The role of CD133 in the identification and characterisation of tumour-initiating cells in non-small-cell lung cancer. Eur J Cardio-Thorac 2009; 36(3):446-53.

Chapter 8

Molecular mechanisms and modulation of key pathways underlying the synergistic interaction of sorafenib with erlotinib in NSCLC cells

Giovannetti E, Labots M, Dekker H, Galvani E, Lind JSW, Sciarrillo R, Honeywell R, Smit EF, Verheul HM & Peters GJ.

CURRENT PHARMACEUTICAL DESIGN 2013

19(5):927-939.

ABSTRACT

Combination of drugs with different targets is a logical approach to overcome multilevel cross-stimulation among key pathways in NSCLC progression such as EGFR, K-Ras and VEGFR. The sorafenib-erlotinib combination showed clinical activity and acceptable safety. Therefore, we evaluated mechanisms underlying sorafenib-erlotinib interaction in seven NSCLC cell lines selected for their heterogeneous pattern of EGFR and Raf-kinase-inhibitor protein (RKIP) expression, and EGFR/K-Ras mutations. Pharmacologic interaction was studied using MTT/SRB assays and the combination index (CI) method, while effects on EGFR, Erk1/2 and Akt phosphorylation, cell cycle and apoptosis were studied with western-blot, ELISA, and flow cytometry. Intracellular drug concentrations were measured with LC-MS/MS, whereas kinase activity profiles were generated on tyrosine kinase peptide substrate arrays.

Synergism was detected in all cell lines, with CIs<0.6 in K-Ras mutated A549, SW1573 and H460, as well as in H1975 (EGFR-T790M) cells. Sorafenib slowed cell cycle progression and induced apoptosis, which was significantly increased in the combination. Moreover, sorafenib reduced Akt/ERK phosphorylation in erlotinib-resistant cells, associated with significant RKIP up-regulation. No direct drug interaction was detected by LC-MS/MS measurement, while lysates from A549 and H1975 cells exposed to erlotinib+sorafenib showed a significant inhibition in the phosphorylation of 16 overlapping peptides, including sites from RAF, VEGFR2, PDGFR, CDK2 and SRC, suggesting new markers to identify NSCLC patients who are likely to respond to this treatment.

In conclusion, several mechanisms, including apoptosis-induction, modulation of expression/phosphorylation of RKIP and crucial kinases contribute to erlotinib-sorafenib synergistic interaction and should be evaluated in future trials for the rational development of this combination in NSCLC.

INTRODUCTION

Lung cancer is the leading cause of cancer related mortality worldwide. The majority of patients present with locally advanced (stage IIIB) or metastatic (stage IV) non-small cell lung cancer (NSCLC) for which no curative treatment is currently available. The standard first-line treatment for unselected patients is a platinum-based doublet chemotherapy regimen. However, conventional regimens have limited impact, with (a) 1-year survival rate of 35-45% [1].

Studies on the molecular basis of NSCLC have enabled the development of new, rationally designed, targeted antitumor agents [2]. In particular, the epidermal growth factor receptor (EGFR) pathway was recognized as part of a complex signal-transduction network central to critical processes in lung cancer progression. Indeed, the EGFR tyrosin kinase inhibitors (TKIs) gefitinib and erlotinib have been accepted as standard of treatment for patients with EGFR activating mutations [3,4]. However, the majority of patients with NSCLC acquire resistant disease or present with intrinsically resistant disease to EGFR-TKIs.

K-Ras mutations are present in one third of NSCLCs and are responsible for the constitutional activation of the proliferation signaling through the RAS/RAF/mitogen-activated protein kinase kinase (MEK)/extracellular signal-regulated kinase (ERK) pathway, associated with poor prognosis and poor response to EGFR-TKIs [5,6]. The development of new strategies against the Ras pathway represents therefore an important focus for pharmacotherapy.

To date, a clinical effective inhibitor of this pathway is sorafenib, which is an orally available, bi-aryl urea compound [7], approved for the treatment of metastatic renal cell carcinoma and hepatocellular carcinoma [8,9]. Although it was initially developed as a Raf kinase inhibitor (for C-RAF and B-RAF, both the wild-type and activated V600E mutant), it has been shown to have activity against many receptor tyrosine kinases involved in tumorigenesis and angiogenesis, including platelet derived growth factor receptor (PDGFR) α and β, RET, Flt-3, c-Kit, p38a, and vascular endothelial growth factor receptor (VEGFR) 2 and 3 [10].

Several studies demonstrated a clear interplay between EGFR and VEGFR pathways, and VEGF-A upregulation was associated with resistance to anti-EGFR treatment [11-15]. Therefore, the blockade of these pathways could provide an effective anticancer strategy, and a recent preclinical study showed a synergistic antitumor effect of the erlotinib-sorafenib combination in lung and colorectal cancer cell lines and xenografts [16].

Moreover, our multicenter, single arm, prospective phase II study established the safety and tolerability of combining sorafenib and erlotinib in chemotherapy-naïve patients with NSCLC, showing promising clinical activity [17]. The combination of erlotinib and sorafenib was also feasible as first-line treatment in unselected elderly patients with advanced NSCLC, and was associated with a higher 1-year survival rate than the combination of sorafenib and gemcitabine [18]. Similar results were reported in NSCLC patients who received one or two prior chemotherapy regimens for metastatic disease [19], and a recent randomized phase II trial of sorafenib and erlotinib versus erlotinib alone demonstrated that both regimens were tolerable, with a survival advantage for (the) sorafenib/erlotinib combination in the subgroup of patients with EGFR wild type or EGFR FISH-negative tumors [20].

One potential explanation for this finding may be that EGFR wild type tumors are more dependent on other signaling pathways, including VEGFR, Raf, PDGFR, which are inhibited by sorafenib. Conversely, K-

Ras did not seem to be a useful predictive biomarker in that trial, whereas our report on the efficacy of sorafenib alone in ten chemotherapy-pretreated patients harbouring K-Ras mutations showed very good results, with three partial remissions and three minimal responses [21]. However, another recent study showed no correlation of both K-Ras and EGFR mutations with response or survival [22]. This study, as well as a feasibility study on a serial of dynamic contrast-enhanced computed tomography to correlate tumor blood flow with treatment outcome [23], suggested that a combination of vascular flow/permeability imaging and circulating factors measured at various time points might yield a “composite biomarker” to predict those patients who will gain clinical benefit or that can be used to monitor therapeutic response.

From the main difficulties encountered in novel drug development, we have learned that targeted therapy should not be given to all patients irrespective of their characteristics, but preferably to individuals presenting the molecular target of the therapy and in whom this target is crucial for cancer cell survival [24]. Therefore, future trials on combination of agents targeting EGFR and the Ras pathways should use careful patient selection based on well-characterized and validated predictive markers.

In particular, preclinical studies deciphering mechanisms of pharmacological interaction as well as potential markers of drug activity are urgently needed. Toward this end, the present study evaluated the molecular and cellular characteristics underlying the synergistic cytotoxicity observed between erlotinib and sorafenib through an extensive in vitro assessment of their pharmacologic activities. We observed a potent synergistic interaction against eight human NSCLC cell lines with differential EGFR and K-Ras status. Several factors including apoptosis induction, modulation of expression and phosphorylation of critical determinants of drug activity, contributed to this synergistic interaction. Kinase activity profiles in absence and presence of erlotinib, sorafenib and the combination were also studied in tumor samples from NSCLC patients. Future development and validation of tumor tissue profiling might lead to the selection of individual patients for targeted treatment.

MATERIALS & METHODS

Drugs & chemicals

Erlotinib (Tarceva®, OSI-774, N-(3-ethynylphenyl)-6,7-bis(2-methoxyethoxy)-4-quinazolinamine) was a gift from Roche Pharmaceuticals (Mannheim, Germany), while sorafenib (Nevaxar®, BAY 43-90064, [4-[[4-chloro-3-(trifluoromethyl)phenyl]carbamoylamino]phenoxy]-N-methyl-pyridine-2-carboxamide) was a gift from Bayer (Leverkusen, Germany). The drugs were dissolved in DMSO and diluted in culture medium before use. RPMI and DMEM media, fetal bovine serum (FBS), penicillin and streptomycin were from Gibco (Gaithersburg, MD). All other chemicals were from Sigma-Aldrich (St. Louis, MO).

Cell lines

Cell lines were maintained as monolayer cultures in RPMI or DMEM (containing 2 mM L-glutamine) supplemented with 10% heat-inactivated FBS, penicillin (50 IU/ml) and streptomycin (50 µg/ml). The human NSCLC cell lines NCI-H460 (H460), NCI-H1703 (H1703), NCI-H292 (H292), NCI-H3255 (H3255) and NCI-H1975 (H1975) were cultured in RPMI, while A549 and SW1573 cells were cultured in DMEM. Cells were grown in 75 cm^2 flasks (Costar, Cambridge, MA), at 37°C in 5% CO_2 and 95% air, and harvested with trypsin-EDTA when they were in exponential growth.

Analysis of mutations and polymorphisms in determinants of drug activity

The NSCLC cells used in this study have been previously characterized for EGFR and K-Ras mutations [25]. Furthermore, we evaluated genetic variations that may influence erlotinib and sorafenib sensitivity/metabolism, such as the rs#1130233, rs#776746 polymorphisms in AKT1 and CYP3A5 genes, respectively. DNA yields and purity were checked at 260-280 nm with NanoDrop®-1000-Detector (NanoDrop-Technologies, Wilmington, USA). All polymorphisms were evaluated with PCR reactions performed with 20 ng of DNA with Taqman®-probes-based assays using the ABIPRISM-7500HT instrument (Applied Biosystems), as described previously [26].

Cytotoxicity assays

To evaluate the cytotoxic activity of single drugs, the cell growth inhibitory effect of erlotinib and sorafenib (0.01-50 µM, 72-hour exposure) was studied using MTT and SRB assays in 96 wells plates (Greiner Bio-One, Alphen a/d Rijn, The Netherlands). For this purpose cells were plated at 10^4 cells/well and growth inhibition was expressed as the percentage of control (vehicle-treated cells) absorbance (corrected for absorbance before drug addition). The 50% inhibitory concentration of cell growth (IC_{50}) was calculated by non-linear least squares curve fitting (GraphPad PRISM, Intuitive Software for Science, San Diego, CA).

Drug combination studies

Combination studies were focused on simultaneous treatment, testing at least six different concentrations, in a constant ratio calculated with respect to drug IC_{50}s. The cytotoxicity of the combination was compared with the cytotoxicity of each drug alone using the combination index (CI), where CI<0.9, CI=0.9-1.1, and CI>1.1 indicated synergistic, additive and antagonistic effects, respectively. Data analysis was carried out using CalcuSyn software version 2.0 (Biosoft, Oxford, UK). Since we considered growth inhibition lower than 50% as no relevant, CI values at fraction affected (FA) of 0.5, 0.75 and 0.9 were averaged for each experiment, and this value was used to calculate the mean between experiments.

Cell cycle analysis

Cell cycle modulation induced by treatments at IC_{50}s for 72 hours was studied by propidium iodide staining and flow cytometry analysis, using a FACScan (Becton Dickinson, San José, CA). Data analysis was carried out with CELLQuest (Becton Dickinson), while cell cycle distribution was determined using Modfit software (Verity Software, Topsham, ME).

Evaluation of apoptosis

Erlotinib, sorafenib and their combination(s) were also characterized for their ability to induce apoptosis, which was detected after 72-hour drug exposure. Cell death was measured by evaluating the sub-G1 region of the previous FACS analysis, and by fluorescence microscopy analysis with bisbenzimide staining [27]. Two hundred cells from randomly chosen microscopic fields were counted, and the apoptotic index was calculated as the percentage ratio between the number of cells displaying apoptotic features and the number of counted cells.

Real-time RT-PCR

To compare the possible influence of gene expression profile on drug sensitivity, we selected cells characterized by heterogeneous patterns of EGFR expression [28]. However, the basal expression of EGFR (NM_005228.3), was also assessed in this study, as well as the expression of Raf kinase inhibitor protein (RKIP, NM_002567) before and after treatments, in order to evaluate the effect of 72-hour treatment with IC50 levels of erlotinib, sorafenib and their combination on this gene, which is an inhibitor of Raf-mediated activation of mitogen-activated protein (MAP) kinase (MEK)-MAP kinase and is considered as an important tumor suppressor and modulator of tumor chemoresistance [29]. Furthermore, since our previous studies showed that EGFR-TKIs affected E2F-1 [28], we also evaluated the expression of E2F-1 (NM_005225.2) mRNA. RNA was extracted using the QiaAmp RNA mini-Kit (Qiagen, San Diego, CA), and reverse transcribed. Forward and reverse primers and probes were designed with Primer Express (Applied Biosystems) on the basis of RKIP gene sequence, while primers and probes for EGFR and E2F-1 were obtained from Applied Biosystems Assay-on-Demand Gene expression products [30].

Amplification data were normalized to β-actin, and quantification of gene expression was performed using standard curves obtained with dilutions of cDNA from Quantitative-PCR Human-Reference Total-RNA (Stratagene, La Jolla, CA).

EGFR, ERK1/2 and Akt phosphorylation assays

To study the effect of drug treatments on the activation of EGFR, as well as of ERK1/2 and Akt, cells were exposed to IC_{50}s of erlotinib, sorafenib and erlotinib-sorafenib combination and stimulated with EGF (10 ng/ml), as previously described [28]. After protein extraction from cell pellets, EGFR phosphorylation at the tyrosine residue at position 1173 (EGFR [pY1173]), dual-phosphorylation of ERK2 at threonine 185 and tyrosine 187 (ERK2 [pTpY185/187]) and ERK1 at threonine 202 and tyrosine 204 (ERK1 [pTpY202/204]) and Akt phosphorylation at serine residue 473 (Akt [pS473]), were evaluated with specific ELISA assays (BioSource International, Camarillo, CA), and normalized respectively to the total EGFR, ERK1/2 and Akt and protein content [31].

ELISA measurement of VEGF levels

Measurement of VEGF levels in medium was performed after exposing 1×10^5 cells to IC_{50} concentrations of the drugs, alone or in combination. Samples of the medium (200µL) were taken after 24 hours, centrifuged for 20 minutes at 1000g and VEGF levels were measured using a specific kit (R&D diagnostics, Minneapolis, USA). A calibration line was included in each plate.

Liquid chromatography–mass spectrometry (LC-MS/MS) measurement of erlotinib and sorafenib

Intracellular concentrations of erlotinib and sorafenib were quantified from cell pellets collected after 72 hours of treatment with IC_{50} levels of the drugs, alone or in combination, using a validated liquid chromatography/tandem mass spectrometry (LC-MS/MS) assay [32]. Chromatography was conducted using a Dionex Ultimate 3000 system coupled with an Applied Biosciences SCIEX API 3000 mass spectrometer for detection. Data acquisition and integration was carried out with the software Analyst version 1.42, from

Applied Biosciences, in combination with Dionex chromeleon LC modules, version 6.8, controlled by Dionex Mass link version 2.0 software.

Peptide substrate array

To evaluate modulation of kinase activity by erlotinib and sorafenib in the A549 and H1975 cells, we have profiled lysates of these cell lines by using a kinase peptide substrate array (PamChip®, PamGene International, 's-Hertogenbosch, The Netherlands). This array contains 144 peptides consisting of 15 amino-acids including a tyrosine, usually in the middle of the peptide. The 13 COOH-terminal amino-acids of each peptide correspond to known or putative phosphorylation sites in a variety of human proteins. The cells were lysed using M-PER containing phosphatase and protease inhibitors (Thermo Scientific, Rockford, IL, USA) during incubation on ice for 20 min. Lysates were centrifuged for 15 minutes at 10000 g; the supernatant was collected and stored at -80 °C. Forty µl control sample mix for the kinase activity array was subsequently prepared by using reaction buffer containing 1× ABL buffer (Westburg, Leusden, The Netherlands), 100 µM adenosine triphosphate (ATP; Sigma-Aldrich), fluorescein-labeled antibody PY20 (Exalpha, Maynard, MA, USA), 7.5 µg (lysate) protein, and DMSO. Inhibition samples were prepared by the subsequent addition of 20 µM erlotinib, 25 µM sorafenib or the combination of 20 µM erlotinib with 12.5 µM sorafenib [final drug concentrations; DMSO concentration in all samples 2.5%]. After blocking the arrays with 2% BSA and subsequent loading of the sample mix onto the arrays in triplicate, incubation (at 30 °C) was started for 60 cycles utilizing a PamStation®12 instrument during which the sample mix is pumped up and down through the array once per minute. Repeated fluorescent imaging of each array was performed with a 12-bit CCD camera, monitoring fluorescence intensities in real time. Spot intensity at each time point was quantified (and corrected for local background), and the resulting time-resolved curves were fit to calculate the initial phosphorylation rate (V_{ini}) using specific kinetic algorithms and appropriate statistical methods, using Bionavigator software version 5.1 (PamGene International, 's-Hertogenbosch, The Netherlands).

Tumor samples from NSCLC patients

Additional analyses were performed in lysates from 2 NSCLC patient-derived tumor tissues, in order to evaluate the possible utility of this platform for ex vivo kinase activity profiling. Both patients had metastatic NSCLC and, after their informed consent, tumor tissue for kinase activity profiling was obtained during diagnostic procedures performed to determine standard treatment for these patients. Patient#1 underwent excision of a pulmonary metastasis to perform mutation analysis for additional targeted treatment options after chemotherapy. Haematoxylin and eosin (H&E) staining revealed a tumor cells content of about 70% in this specimen. The mutational analysis detected a G12D mutation in K-RAS exon 1, while no mutations were detected in EGFR exons 19, 20 and 21. Patient#2 underwent needle biopsy of a liver metastasis, and H&E staining of this biopsy revealed a content of tumor cells of about 60%. The EGFR exon 20 harboured an in-frame duplication of codon 771-773 as well as a V769L mutation, while no mutation were found in EGFR exons 19 and 21, and in K-RAS exon 1. The lysates from patient-derived tumor tissues were prepared by adding M-PER to 10 µm cryoslides containing >50% tumor cells, as described [33].

Western blot

To validate the possible role of the proteins containing the phosphorylated peptides emerging from the kinase activity profiling analyses, we performed Western blot analysis in our panel of NSCLC cells. Total lysates were prepared in buffer containing 50 mM Tris (pH 7.6), 20% (v/v) glycerol, 5 mM DTT, 0.5% (v/v) NP-40, and 4.0% (v/v) of a protease inhibitor cocktail. Lysates were sonicated and centrifuged. The protein-containing supernatant was collected and protein content was determined using a Bradford assay (Bio-Rad, Hertfordshire, UK). In each lane of a minigel system (Bio-Rad) 30 µg of proteins were loaded. The following monoclonal antibodies were used: anti-phospho-CDK2 (Tyr15) 1:1000, anti-CDK2 1:1000, anti-phospho-SRC (1:500, Tyr416), anti-SRC 1:1000 (all from Cell Signaling Technology Inc, Danvers, MA). Moreover because our previous results we also studied E2F-1 protein expression with the monoclonal anti-E2F-1 (1:100, Santa Cruz Biotechnologies, Santa Cruz, CA). As secondary antibodies, horseradish peroxidase-conjugated anti-rabbit or anti-mouse (1:2000, DakoCytomation, Glostrup, Denmark) were used. As a loading control expression of β-actin was determined using an antibody against β-actin (1:10000, Chemicon International, Temecula, CA).

Erlotinib, sorafenib and their combination, at IC_{50}s, were also studied for their ability to modulate protein expression of these possible surrogate markers of drug activity. After 2-hour exposure, cell pellets were collected and lysed, and 30 µg of proteins were loaded and separated on a 10% SDS-PAGE gel, followed by blotting onto a nitrocellulose membrane. The membrane was pre-incubated in blocking buffer (0.5% milk powder, 0.5% BSA in TBS-T (10 mM Tris-HCl pH 8.0, 0.15 M NaCl, 0.05% Tween-20)) for 1 hour, while the primary antibodies were added overnight, at 4°C. After washing in TBS-T, the blots were incubated for 1 hour with anti-rabbit and anti-mouse horseradish peroxidase-labelled secondary antibodies (1:2000, DakoCytomation). Antibody binding was detected using enhanced chemoluminescence, with the VersaDoc 3000 instrument (Bio-Rad).

Statistical analysis

All experiments were performed in triplicate and repeated at least twice. Data were expressed as mean values ± S.E. and analysed by Student's t-test or ANOVA followed by the Tukey's multiple comparison test. The Pearson/Spearman correlation and regression analysis were used to demonstrate the relationship between gene expression profile and chemosensitivity. The level of significance was $P<0.05$.

RESULTS

Genetic background of the human NSCLC cell lines

Genomic DNA and RNA extracted from the NSCLC cells were used to detect mutations, polymorphisms and mRNA expression levels of genes potentially affecting drug activity, as depicted in Table 1.

Growth inhibition studies and correlation with genetic background

A dose-dependent inhibition of tumor cell growth was observed with both erlotinib and sorafenib in all the seven NSCLC cell lines, with less than 50% of these cells still growing after exposure at the highest concentration (Table 1). The IC_{50} values for erlotinib ranged from 0.10±0.02 (H3255 cells) to 20.12±2.21 µM

(H1975 cells), while sorafenib displayed similar growth inhibitory activity in most cells, with an IC_{50} range between 0.82±0.13 and 2.07±0.64 μM, in SW1573 and H1975 cells, respectively.

The H3255 cells, carrying the EGFR activating mutation L858R, were the most sensitive cells, whereas H1975, harbouring the L858R/T790M EGFR mutation, and the H460 cells, harbouring the G61H mutation in K-Ras, were the least sensitive cells to erlotinib.

In this panel of NSCLC cells a significant inverse correlation was found between sorafenib IC_{50} values and mRNA levels of RKIP (R2=0.64, P=0.03). In contrast, no relationship was found between candidate polymorphisms or EGFR expression and chemosensitivity.

Table 1. Sensitivity to erlotinib and sorafenib and genetic characterization of NSCLC cell lines

	A549	SW1573	H460	H292	H1703	H1975	H3255
IC_{50} (μM)							
Erlotinib	2.88±0.35	6.36±1.00	10.17±0.79	0.50±0.17	9.01±1.80	20.12±2.21	0.10±0.02
Sorafenib	1.10±0.22	0.82±0.13	0.94±0.27	0.88±0.22	0.96±0.17	2.07±0.64	1.12±0.23
Mutations							
EGFR	*Wt*	*Wt*	*Wt*	*Wt*	*Wt*	*Mut(T790M)*	*Mut(L858R)*
k-Ras	*Mut(G12S)*	*Mut(G12C)*	*Mut(Q61H)*	*Wt*	*Wt*	*Wt*	*Wt*
Polymorphisms							
rs#1130233	*GA*	*GG*	*GA*	*GA*	*GG*	*GG*	*GG*
rs#776746	*GG*	*GG*	*GG*	*GG*	*GG*	*GG*	*GG*
Expression[a]							
EGFR	684.45	57.93	79.50	456.71	95.28	45.23	25.12
RKIP	12.35	22.12	18.90	15.24	13.20	4.58	8.93

[a]Mean mRNA expression values calculated in comparison with standard curves and with respect to the respective expression values of the housekeeping gene beta-actin, SE are less than 20%. Data were reported with 2 decimals, given the accuracy of the method used.

Pharmacological interaction

Since the CI method recommends a ratio of concentrations at which drugs are equipotent, combination studies were performed using fixed ratios with IC_{50} values for erlotinib and sorafenib in all the NSCLC cells. Representative growth inhibition curves for A549 cells are shown in Fig.1A. Multiple drug-effect analysis revealed synergistic/additive effects at the more relevant FA values (≥50%). The average CI values for all the combinations in the seven NSCLC cell lines are summarized in Fig.1B. To explore the mechanisms underlying these synergistic drug interactions, we performed several biochemical analyses, as detailed below. Cell cycle and apoptosis studies were performed in 6 cell lines (A549, SW1573, H460, H292, H3255 and H1975), while PCR, ELISA, Western blot, LC-MS/MS, and peptide arrays were performed on A549 and H1975 cells.

Cell cycle perturbations and induction of apoptosis

Flow cytometric DNA analysis was performed to evaluate the effect of erlotinib, sorafenib and their combination on cell cycle distribution and to determine whether or not their cell cycle alterations might provide clues to optimise drug scheduling. Both targeted agents were able to affect the cell cycle parameters of the NSCLC cell lines (Table 2). In particular, both erlotinib and sorafenib caused a 1.2-1.4-fold increase in the population of cells in the G1-phase. The treatment with the erlotinib/sorafenib combination resulted in a

similar increase in the percentage of cells in the G1-phase. Conversely, after erlotinib, sorafenib and their combination, we observed slight variations of the S-phase and a reduction of the G2/M-phase cell population, which was most pronounced in H3255 cells (e.g., 3.3-fold).

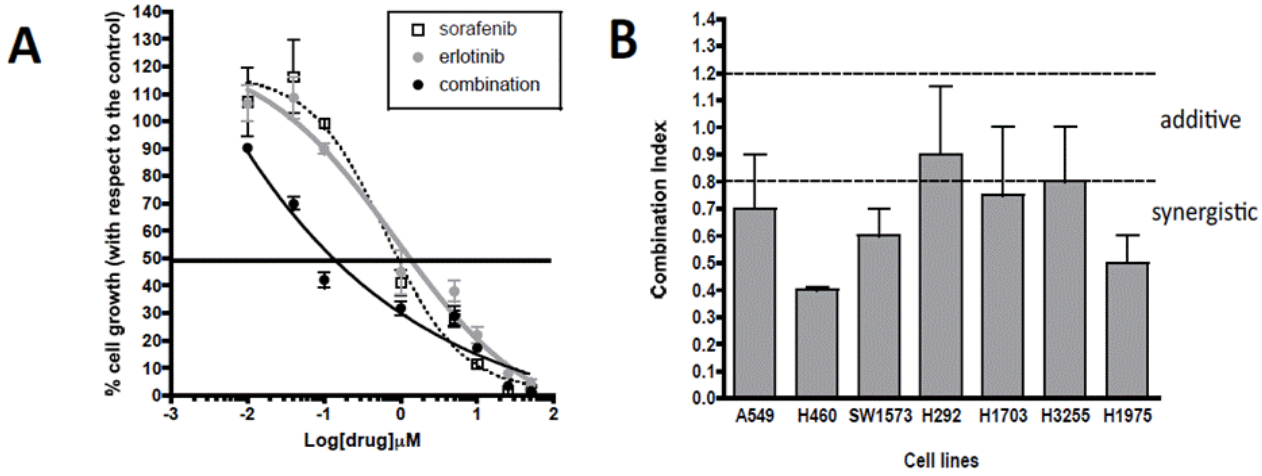

Figure 1. Cytotoxicity and pharmacological interaction of erlotinib and sorafenib. (A) Representative curves of growth inhibitory effects of erlotinib, sorafenib, and their simultaneous 72-hour exposure. **(B)**, Mean CI values of erlotinib-sorafenib combination in the panel of NSCLC cells. CI values at FA of 0.5, 0.75 and 0.9 were averaged for each experiment, and this value was used to calculate the mean between experiments, as described in the Materials and Methods section. Points and columns, mean values obtained from three independent experiments; bars, SE.

All treatments induced cell death, as shown by the presence of a cell population with sub-G1 DNA content in the FACS analysis. Similar results were observed by fluorescence microscopy analysis after bisbenzimide staining (Figure 2). Cells exposed to erlotinib, sorafenib and their combinations, at the IC50s, presented typical apoptotic morphology with cell shrinkage, nuclear condensation and fragmentation, and rupture into apoptotic bodies. Erlotinib slightly increased AI with respect to controls in A549, SW1573, H460 and H1975 cells, while higher AI values were observed in the more sensitive cell lines (6.5% and 14.2% in H292 and H3255 cells, respectively). Sorafenib induced more apoptosis than erlotinib, with AI values ranging from 6.5% to 15.6% in H1975 and H292 cells, respectively. The combinations of the two drugs additionally increased the AI, up to 28.0% in H3255 cells, with a significant induction of apoptosis when compared with both controls and erlotinib-treated cells in all cell lines.

Modulation of EGFR, ERK1/2 and Akt phosphorylation detected by ELISA

As expected, erlotinib induced a significant suppression of EGF-induced phosphorylation of EGFR at the tyrosine residue pY1173 in all the NSCLC cell lines, with percentages of reduction of EGFR phosphorylated protein ranging from -17.9 to -39.6% with respect to controls, in H1975 and A549 cells, respectively.

Conversely, sorafenib minimally affected pY1173-EGFR levels, varying from -5.6% to -6.2% in A549 and H1975 cells, respectively, while drug combinations reduced the phosphorylation status of EGFR, but to a lower extent than erlotinib alone.

EGFR signaling is transduced mainly through the Akt and ERK1/2 kinase pathways, and we investigated their phosphorylation status to determine their activity after drug treatment. Erlotinib and sorafenib resulted in an inhibition of pERK1/2 and pAkt in all the NSCLC cells. In particular, in both A549 and H1975 cells

pERK1/2 levels were potently (>50%) downregulated by sorafenib, while a lower degree of inhibition (about 25%) was detected after exposure to erlotinib. The drug combination cause a reduction of pERK1/2 more pronounced than the one observed with erlotinib or sorafenib alone in A549 cells (Fig. 3A), while drug combinations reduced the phosphorylation status of pERK1/2, to a similar extent than sorafenib alone in H1975 cells. Akt phosphorylation at the serine residue pS473 was significantly decreased (>50%) by erlotinib in A549 cells, whereas the inhibition was less efficient (about 30%) in H1975 cells. Akt phosphorylation was additionally reduced by the simultaneous combination of erlotinib and sorafenib, with a degree of inhibition up to -70.6% and -54.2 in A549 and H1975 cells, respectively.

Table 2. Cell cycle modulation and apoptotic index

Cells	Treatment[a]	G1 phase (%)	S phase (%)	G2/M phase (%)	Sub-G1 phase (%)
A549	Control	59.9±2.4	21.1±1.4	18.9±1.4	1.2±0.2
	Erlotinib	69.2±2.0	18.2±1.5	12.5±2.3	4.5±0.5*
	Sorafenib	67.9±4.3	20.1±3.2	12.0±1.5	11.1±1.5*
	Combination	67.5±5.0	21.3±3.6	11.2±1.6	18.6±2.2**
SW1573	Control	47.2±4.0	24.6±2.3	28.2±1.9	0.8±0.2
	Erlotinib	55.0±6.6	23.1±9.0	21.9±2.2	4.8±1.0*
	Sorafenib	45.5±1.8	23.5±2.3	31.0±4.1	16.3±2.1*
	Combination	50.2±3.9	24.2±4.7	25.8±1.8	20.2±3.0**
H460	Control	41.8±3.0	25.0±2.0	33.2±1.3	1.3±0.3
	Erlotinib	57.7±3.2	19.2±3.7	23.1±3.7	3.5±1.0*
	Sorafenib	51.7±3.7	25.0±1.9	23.3±2.8	12.2±1.8*
	Combination	61.0±3.9	20.1±2.4	18.9±1.8	21.9±3.1**
H292	Control	46.8±2.2	24.7±2.2	28.5±4.4	1.0±0.3
	Erlotinib	62.7±6.1	19.7±1.9	17.6±5.0	6.5±1.0*
	Sorafenib	55.2±3.9	23.5±1.8	21.3±3.6	13.6±2.7*
	Combination	54.3±2.5	25.7±1.3	20.0±3.9	18.2±2.4**
H3255	Control	64.2±2.5	22.8±0.6	13.0±1.4	1.2±0.3
	Erlotinib	75.9±6.4	18.7±1.2	5.4±1.3	14.2±2.7*
	Sorafenib	72.2±4.3	19.1±1.9	8.7±2.5	10.6±0.5*
	Combination	78.2±7.7	17.5±1.9	4.4±0.3	25.8±2.4**
H1975	Control	48.1±2.1	21.7±2.3	30.2±0.6	1.5±0.3
	Erlotinib	56.0±1.7	20.2±2.2	23.8±2.5	4.5±0.6*
	Sorafenib	55.8±3.2	18.3±0.9	25.9±2.7	6.1±0.5*
	Combination	57.8±1.7	19.0±3.8	23.2±2.0	20.6±3.7**

*p<0.05 with respect to control cells, **p<0.05 with respect to pemetrexed-treated cells

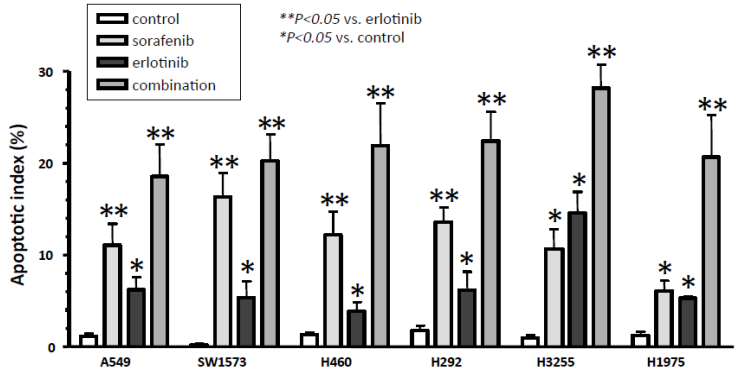

Figure 2. Apoptotic index of erlotinib, sorafenib and their combination. The apoptotic index was calculated as the percentage of cells displaying apoptotic features compared to the number of counted cells. Points and columns, mean values obtained from three independent experiments; bars, SE. *****Significantly different from controls (*P*<0.05); ******Significantly different from erlotinib (*P*<0.05)

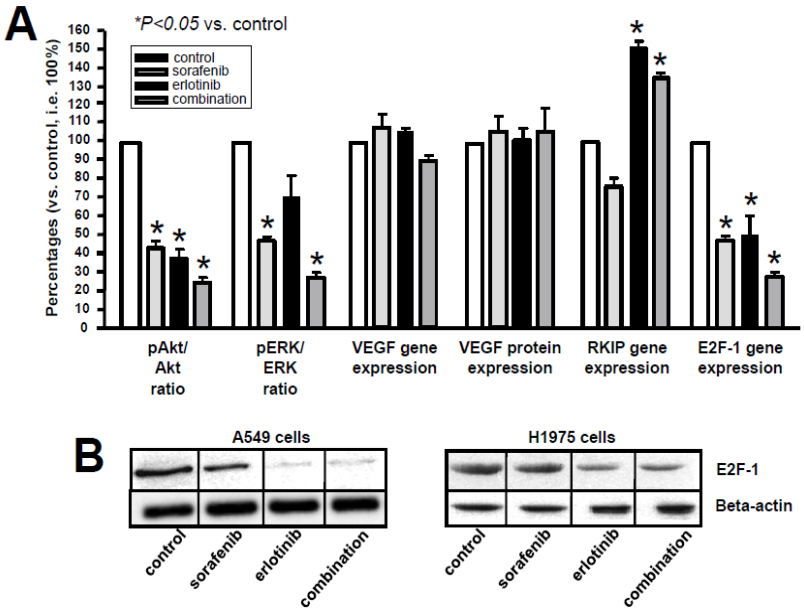

Figure 3. Effects of erlotinib, sorafenib and their combination on phosphorylation of ERK1/2 and Akt, VEGF mRNA and protein, and RKIP mRNA expression. (A) Mean expression values of activated (ratio of phosphorylated compared to total) ERK and Akt, VEGF mRNA and protein, RKIP and *E2F-1* mRNA. **(B)** Representative blot of at least two independent western blotting analyses of E2F-1 protein expression performed as described in the Material and Methods, in A549 *(Bottom right panels)* and H1975 cells *(Bottom left panels).* Points and columns, mean values obtained from three independent experiments; bars, SE. *****Significantly different from controls ($P<0.05$); ******Significantly different from erlotinib ($P<0.05$)

Modulation of VEGF expression

Since erlotinib and sorafenib have been reported to have an impact on plasma VEGF levels, we evaluated the expression of VEGF levels in both cells and culture medium. However, sorafenib minimally affected VEGF mRNA levels and VEGF secretion into the medium in A549 and H1975 cells. Similarly, erlotinib and erlotinib-sorafenib combination hardly modulated VEGF in both A549 and H1975 cells (Fig.3A).

Modulation of RKIP and E2F-1 expression

To gain further insight into the molecular mechanisms underlying drug interaction, we examined alterations in the expression of RKIP, which is a key regulator of the RAS/RAF pathway, and E2F-1, which is an important nuclear target.

A549 and H1975 cells treated with erlotinib had a 1.5-fold and 2.4-fold increase in RKIP expression, respectively. In contrast, sorafenib slightly decreased RKIP levels in both cell lines. However, the erlotinib/sorafenib combination, not only prevented the sorafenib-induced decrease, but significantly increased RKIP mRNA expression, up to +67% and +40% in H1975 and A549 cells, respectively (Fig.3A).

Erlotinib, sorafenib and their combination significantly reduced E2F-1 mRNA in both A549 and H1975 cells, with expression levels of about 40-50% compared to untreated cells. Similarly, the erlotinib/sorafenib combination induced a significant decrease in E2F-1, with values ranging from -64 to -73% in H1975 and A549 cells, respectively (Fig.3A). E2F-1 expression was also studied at the protein level using Western blot analysis in both A549 and H1975 cells (Fig.3B). This analysis revealed a reduction in both erlotinib and erlotinib-sorafenib-treated cells, with barely detectable levels observed in protein extracts isolated from A549 cells exposed to erlotinib-sorafenib combination.

Peptide substrate arrays

Assuming that responses to tyrosine kinase inhibitors depend on specific receptor and protein signaling activities, kinase activity profiling is a promising approach to identify new potential markers and targets for

treatment. Therefore, we used high-throughput tyrosine kinase peptide substrate arrays for the identification of novel peptide substrate kinases or substrate kinases that were inhibited by erlotinib, sorafenib and their combination. In cell lysates, kinase activity profiling has been performed in absence and presence of 20 µM erlotinib, 25 µM sorafenib and their combination (20 µM erlotinib, 12.5 µM sorafenib). Data of Vini in treated cells were compared by t-test versus untreated cells. Using Bonferroni correction, we observed in the A549 extracts a total of 11 and 13 peptide substrates significantly inhibited by erlotinib and sorafenib, respectively, including 10 common targets. These peptides were also inhibited by the drug combination, which additionally inhibited other 14 peptides (Table 3). Similar results were observed in the H1975 cells (Table 3), and the Venn diagram (Fig. 4A) shows the common peptides which were inhibited in both cell lines.

With the aid of the KEGG and REACTOME databases, we were able to construct a provisional signal transduction scheme of some of the key kinases in NSCLC, including several kinases annotated as being able to phosphorylate the peptides emerging from the previous analyses (Figure 4B). This scheme showed kinase activity on peptides corresponding with phosphorylation site sequences from the Human Epidermal Growth Factor Receptor 2 (ERBB2), platelet-derived growth factor receptor beta (PDGFRB), vascular endothelial growth factor (VEGFR1), Fibroblast growth factor receptor 2 and 3 (FGFR2, FGFR3), and hepatocyte growth factor receptor (MET). In addition, we found associated downstream inhibition of Ras/MAPK pathways, focal adhesion kinase (FAK), and SRC kinase (correlated with LCK, and ZAP70) signaling (Fig.4B). Further studies are planned to validate these kinases also as potential druggable targets in erlotinib/sorafenib resistant cells. However, to evaluate some of our most interesting results we performed western blot analyses of CDK2 and SRC, showing a significant reduction of phosphorylation for both these kinases after exposure to erlotinib, sorafenib and their combination (Fig.4C). Finally, peptide substrate array-based kinase activity profiling was also performed using tumor tissue lysates of patients with NSCLC. These tumor tissues were already characterized within genetic analyses, and one tumor harboured the K-Ras G12D mutation, while the other carried EGFR exon 20 mutations.

The studies with the peptide substrate array demonstrated the feasibility of kinase profiling in patients' tissues even when obtained by needle biopsy. However, the number of kinases significantly inhibited by erlotinib and sorafenib (i.e., 0 in patient#1, and 17 in patient#2) was lower than in the cells, and only 3 of these inhibited kinases (EFS, RASA1 and SRC8) were also significantly inhibited by erlotinib and sorafenib in the cells. These results suggest that these peptide array studies did not reveal response predictive profiles of kinase inhibition for the tested compounds in the two tumor samples from patients. However, further retrospective and prospective clinical studies are needed to demonstrate the capacity of this technique for the prediction of response to tyrosine kinase inhibitors.

LC-MS/MS measurement of erlotinib and sorafenib

Previous clinical trials reported significantly decreased steady-state plasma levels of the EGFR inhibitors erlotinib and gefinitib by the coadministration of sorafenib. Since the mechanism of this possible drug interaction is unclear, we tested the concentration of these drugs in cell pellets and medium and we evaluated whether sorafenib or erlotinib affected each other intracellular drug accumulation. However, no direct drug interaction was detected by LC-MS/MS measurement, and drug concentrations after exposure to

erlotinib or sorafenib alone were identical to concentrations detected after drug combination (data not shown).

DISCUSSION

In the present study we demonstrated that the interaction between erlotinib and sorafenib was highly synergistic in NSCLC cells. These findings are of importance since erlotinib is already registered for treatment of NSCLC, while sorafenib might be a promising agent to improve the effect of erlotinib in patients with NSCLC, possibly as a more effective regimen in resistant tumors, such as in patients with K-Ras or EGFR exon-20 resistant mutations. The synergistic activity of sorafenib was indeed detected in A549, H460 and SW1573 cells, harbouring K-Ras mutations, as well as in the H1975 cells, harbouring EGFR T790M mutation, at concentrations similar to those achieved in clinical trials [17].

Table 3. PamChip tyrosin containing peptides significantly inhibited by erlotinib, sorafenib and their combination

Peptides inhibited by							
	In the A549 cells				In the H1975 cells		
*P**	erlotinib/sorafenib combination	erl	sor	*P**	erlotinib/sorafenib combination	erl	sor
3,5E-06	EPHA1_774_786_LDDFDGTYETQGG	X	X	*1,8E-06*	EFS_246_258_GGTDEGIYDVPLL	X	X
1,3E-05	ANXA1_14_26_IENEEQEYVQTVK	X	X	*6,6E-06*	ENOG_37_49_SGASTGIYEALEL	X	X
2,1E-05	EFS_246_258_GGTDEGIYDVPLL	X	X	*6,6E-06*	EPHA7_607_619_TYIDPETYEDPNR		X
2,5E-05	MK07_211_223_AEHQYFMTEYVAT			*8,6E-06*	FRK_380_392_KVDNEDIYESRHE	X	X
2,6E-05	PAXI_24_36_FLSEETPYSYPTG	X	X	*1,0E-05*	EPHA1_774_786_LDDFDGTYETQGG	X	X
4,4E-05	ENOG_37_49_SGASTGIYEALEL	X	X	*1,2E-05*	RAF1_332_344_PRGQRDSSYYWEI		
4,9E-05	LCK_387_399_RLIEDNEYTAREG			*1,7E-05*	P85A_600_612_NENTEDQYSLVED	X	X
6,5E-05	PLCG1_764_776_IGTAEPDYGALYE			*2,6E-05*	CDK2_8_20_EKIGEGTYGVVYK		X
7,5E-05	NCF1_313_325_QRSRKRLSQDAYR			*4,1E-05*	RASA1_453_465_TVDGKEIYNTIRR		X
0,00010	PGFRB_572_584_VSSDGHEYIYVDP			*4,3E-05*	PGFRB_572_584_VSSDGHEYIYVDP	X	
0,00012	PGFRB_1014_1028_PNEGDNDYIIPLPDP		X	*5,0E-05*	EPHA2_765_777_EDDPEATYTTSGG	X	X
0,00012	PAXI_111_123_VGEEEHVYSFPNK	X	X	*5,8E-05*	EPOR_419_431_ASAASFEYTILDP		
0,00012	RON_1346_1358_SALLGDHYVQLPA		X	*7,7E-05*	PECA1_706_718_KKDTETVYSEVRK	X	
0,00013	VGFR1_1326_1338_DYNSVVLYSTPPI			*0,00012*	FES_706_718_REEADGVYAASGG	X	
0,00015	EPHA7_607_619_TYIDPETYEDPNR	X	X	*0,00012*	ART_004_EAIYAAPFAKKKXC_EAIYAAPFAKKK		X
0,00015	ZAP70_485_497_ALGADDSYYTARS			*0,00012*	PGFRB_1002_1014_LDTSSVLYTAVQP		
0,00018	FES_706_718_REEADGVYAASGG	X	X	*0,00013*	PAXI_24_36_FLSEETPYSYPTG		X
0,00019	EPHB1_771_783_DDTSDPTYTSSLG	X	X	*0,00013*	PAXI_111_123_VGEEEHVYSFPNK		
0,00021	RASA1_453_465_TVDGKEIYNTIRR			*0,00014*	SRC8_CHICK_492_504_YQAEENTYDEYEN		X
0,00027	MET_1227_1239_RDMYDKEYYSVHN		X	*0,00015*	CTNB1_79_91_VADIDGQYAMTRA		
0,00027	RAF1_332_344_PRGQRDSSYYWEI			*0,00015*	EPHB1_771_783_DDTSDPTYTSSLG	X	
0,00027	EPOR_419_431_ASAASFEYTILDP			*0,00017*	FGFR2_762_774_TLTTNEEYLDLSQ	X	X
0,00028	FGFR3_753_765_TVTSTDEYLDLSA			*0,00017*	PDPK1_2_14_ARTTSQLYDAVPI		
0,00028	LAT_249_261_EEGAPDYENLQEL			*0,00024*	PLCG1_764_776_IGTAEPDYGALYE		
0,00029	CDK2_8_20_EKIGEGTYGVVYK	X	X	*0,00025*	SRC8_CHICK_476_488_EYEPETVYEVAGA	X	
0,00032	SRC8_CHICK_476_488_EYEPETVYEVAGA	X		*0,00027*	DCX_109_121_GIVYAVSSDRFRS		
0,00033	ART_004_EAIYAAPFAKKKXC_EAIYAAPFAKKK			*0,00027*	VGFR1_1326_1338_DYNSVVLYSTPPI		
0,00034	ERBB2_870_882_LDIDETEYHADGG						

**P* was calculated with respect to control cells, using t-test. Only values below the Bonferroni corrected P (<0.000347) are reported in this list. Erl, erlotinib; sor, sorafenib.

During the last decade novel anticancer treatments have emerged from advances in understanding of tumor biology, and identification of a number of key molecular targets in cancer signaling [24]. However, the multilevel cross-stimulation among the targets of these new agents along several pathways of signal transduction involved in neoplastic events allows other pathways to act as salvage mechanisms for cancer cells [34]. To overcome this problem one strategy might be to fine-tune the right mixture of drugs that target specific molecules. Therefore, drug combination treatment strategies should be explored in preclinical settings for the development of more effective combination treatment regimens.

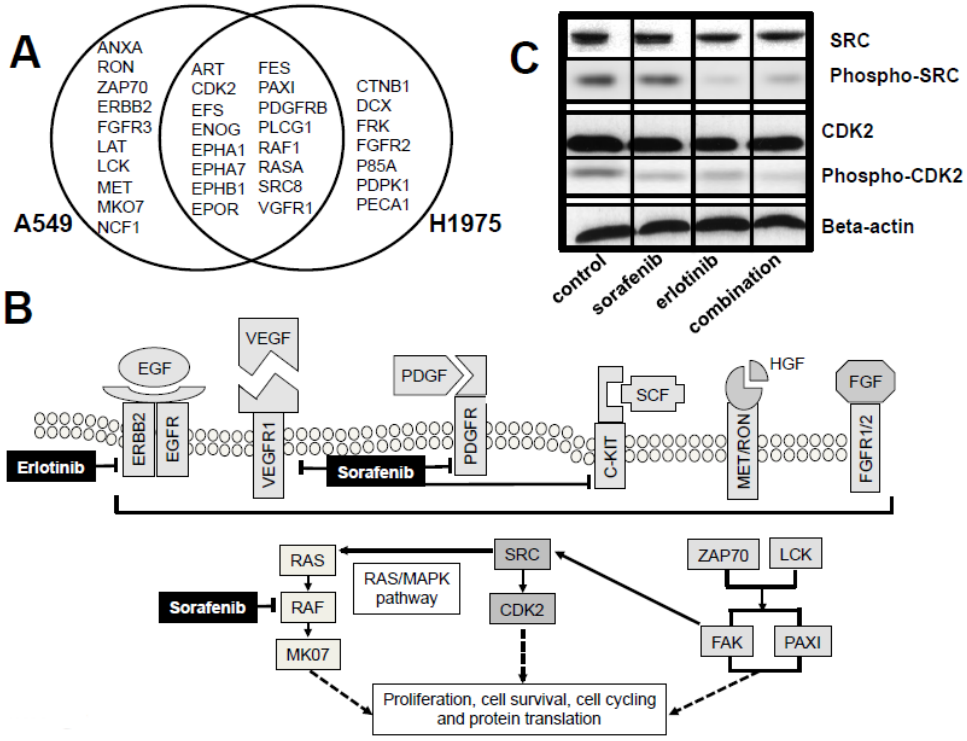

Figure 4. Analysis of emerging targets of erlotinib-sorafenib combination from the Pamchip array. (A) Overlap analysis of kinases significantly inhibited by erlotinib-sorafenib in A549 and H1975 cells. **(B)** Signal transduction scheme of several key kinases in NSCLC, including kinases annotated as being able to phosphorylate the peptides emerging from the previous Pamchip array analyses. **(C)** Representative blots of at least two independent western blotting analyses performed as described in the Material and Methods, in A549 cells.

By targeting the EGFR- and RAF- dependent cancer cell proliferation and the VEGFR-2-dependent tumor angiogenesis pathways, the combination of erlotinib with sorafenib offers the potential advantage of blocking key pathways in different cell types, namely cell proliferation in the tumor and angiogenesis in endothelial cells. Several studies demonstrated that NSCLC is characterized by dysregulation of molecular mechanisms involved in cell proliferation and angiogenesis [35]. NSCLC has one of the highest EGFR levels among solid tumors, K-Ras mutations are detected in more than 30% of NSCLC samples [36], and most studies showed that an increased VEGF expression is a poor prognostic factor in lung cancer patients [37]. Therefore, combination of small molecule inhibitors that target these factors, such as the erlotinib-sorafenib combination, may be very useful for NSCLC treatment.

In a recent study a strong synergism of erlotinib and sorafenib was found in colorectal and lung cancer cells, associated by a marked inhibition of MEK signal and in vitro migration in the H1299 NSCLC cells [11]. Similar synergistic effects were observed in in vitro studies on cetuximab-sorafenib combination, as well as

in H1299 xenografts [11], while another study provided evidences that sorafenib can inhibit the growth of the gefitinib/erlotinib/vandetanib-resistant variant of Calu-3 NSCLC cells, which showed a significant increase in the levels of activated Akt, MAPK and surviving [16]. However, our findings are novel because they show that the synergistic interaction seems to be mediated by several other mechanisms, which enhanced both the sensitivity to erlotinib and to sorafenib, and should be further evaluated as potential predictive biomarkers for the future clinical development of this or similar combinations.

The main downstream mediators of the EGFR signal transduction pathway were affected by the sorafenib-erlotinib combination, which significantly reduced both ERK and Akt phosphorylation. These data fit with the synergistic interaction suggesting that combinations of specific signal transduction inhibitors targeting different steps of EGFR-PI3K pathways may be a successful strategy. There are several genetic and laboratory studies suggesting that the MAPK and PI3K-Akt pathways are vital to the growth and survival of cancer cells, and inhibitors targeting these pathways are entering the clinic at a rapid pace [38-39]. Moreover, since phospho-Akt downregulation correlated with the enhancement of drug-induced apoptosis and antitumor activity in lung cancer cells [28], the reduction of activated-Akt may explain the increased apoptosis found in the erlotinib-sorafenib combination.

The erlotinib-sorafenib combination was also able to reduce the mRNA and protein expression of E2F-1. These results may be related to the nuclear effects of EGFR-TKIs, which influence the activity of some cell cycle proteins and transcription factors, including E2F-1 [40], This effect might be exerted directly or via down-regulation of cyclin D1 [41-42]. However, the Ras/MAPK/ERK dependent pathway is also implicated in the modulation of the expression of the cyclin D1 gene, and cyclin D1 down-regulation results in E2F-1 inhibition [42]. E2F-1 belongs to the p53-Rb pathway and acts as a growth-promoting factor associated with adverse prognosis in NSCLC [43]. Since adenovirus-mediated E2F-1 gene transfer in NSCLC cells induces cell growth arrest and apoptosis [44], we might hypothesize that E2F-1 inhibition caused by the erlotinib-sorafenib combination plays an important role in the synergistic inhibition of cell growth and apoptosis observed in our NSCLC cells. Moreover, the Rb-E2F-1 pathway contributes to the expression of VEGF receptors [45], suggesting that a reduction in the amount of E2F-1 mediated by the erlotinib-sorafenib combination might also affect the expression of genes involved in other aspects of tumor growth and progression, such as angiogenesis.

Circulating VEGF levels have attracted considerable interest as a potential pharmacodynamic marker of VEGFR-2 inhibition, and recent studies reported that sorafenib significantly increased plasma levels of VEGF [23, 46]. Although our in vitro models cannot represent the complexity of the interaction of tumor cells with the tumor neovasculature, sorafenib alone and in combination with erlotinib did not significantly affect VEGF mRNA expression nor VEGF secretion into the medium in our NSCLC cells, reflecting the slight non-significant increase in plasma VEGF during 21 days of treatment in patients treated with erlotinib-sorafenib combination [47].

In addition to the effects on EGFR cytoplasmatic and nuclear signaling pathways, the present study also shows that erlotinib interfered with the activity of other key determinants of sorafenib, such RKIP, which was significantly correlated with sorafenib sensitivity in our panel of NSCLC cells. The increased expression of RKIP after erlotinib treatment could be explained by the reduced nuclear factor κB (NF-κB) activation caused by EGFR inhibition [48]. Activation of NF-κB requires the phosphorylation and degradation of IKB, which

allows NF-κB to translocate into the nucleus. Yeung and colleagues demonstrated that RKIP dephosphorylated IKB, leading to inhibition of NF-κB activation [49]. Therefore, the reduced NF-κB activation and enhancement of IKB phosphorylation may cause a compensatory increase of RKIP expression, facilitating sorafenib activity.

After the analysis of several candidate biomarkers, we also evaluated whether a commercially available 144-peptide array might be useful to detect other tyrosine kinases that can be inhibited by the erlotinib-sorafenib combination and might represent new potential interesting druggable targets. The main limitations of this study included 1) the limited subset of the peptides spotted on the array, 2) the limited specificity, since for the majority of kinases it is difficult to have a single peptide substrate that is specific to a single kinase, and 3) the fact that cell lysates cannot reproduce subcellular compartmentalization and protein docking or scaffolding [50]. However, we were able to identify a list of tyrosine kinase peptide substrates which were significantly inhibited by erlotinib and sorafenib, respectively, including several common targets. In agreement with the synergistic interaction, these peptides were also inhibited by the drug combination, which additionally inhibited other 11 common peptides in the two studied cell lines. A validation of some of these results was obtained by subsequent western blot analysis of two of the kinases that can phosphorylate these peptides and constitute appealing targets as central nodes of the signaling pathways involved in NSCLC proliferation, SRC and CDK2 [51-52]. Finally, we were able to find modulation of kinase activity of a few kinases in tumor tissues, supporting further ex vivo studies. In particular, detection of key deregulated signaling pathways may pave the way for novel therapeutics design and appropriate therapy selection in individual patients. However, since DNA and microRNA samples are easier to be collected and stored than frozen tumor-biopsy samples, the data from these protein-array studies should be integrated with the results of novel pharmaco/epigenetic analyses [53-54].

CONCLUSIONS

The present study characterizes several molecular mechanisms and determinants involved in the synergistic interaction of erlotinib and sorafenib against NSCLC cells, focusing on cells harbouring K-Ras and EGFR T790M mutations. Sorafenib reduced ERK and Akt phosphorylation, which was additionally reduced by drug combination, and favoured apoptosis induction. Erlotinib and sorafenib significantly reduced E2F-1 expression, while erlotinib and the combination increased RKIP expression, favouring sorafenib activity. The modulation of all these determinants influences the cytotoxicity of this combination and, although the extrapolation of in vitro data to the clinical setting should be considered with caution, these results may have implications for the rational development of chemotherapeutic regimes including erlotinib and sorafenib or other emerging multikinase inhibitor of angiogenic, stromal and oncogenic kinases, such as regorafenib [55].

ACKNOWLEDGEMENTS

This work was partially supported by grants from the Netherlands Organization for Scientific Research (NWO-VENI grant, Elisa Giovannetti), and AIRC-Marie Curie International Fellowship (Elisa Giovannetti). We would like to thank Rob Ruijtenbeek (Pamgene International B.V, Inc.), who provided initial technical support to conduct this project.

REFERENCES

1. Azzoli CG, Temin S, Aliff T, et al. 2011 Focused Update of 2009 American Society of Clinical Oncology Clinical Practice Guideline Update on Chemotherapy for Stage IV Non-Small-Cell Lung Cancer. J Clin Oncol 2011; 29: 3825-31.
2. Dorans K. Outpacing cancer. Nat Med. 2009;15:718-22.
3. Sequist LV, Martins RG, Spigel D, et al. First-line gefitinib in patients with advanced non-small-cell lung cancer harboring somatic EGFR mutations. J Clin Oncol. 2008;26:2442-9.
4. Erlotinib versus standard chemotherapy as first-line treatment for European patients with advanced EGFR mutation-positive non-small-cell lung cancer (EURTAC): a multicentre, open-label, randomised phase 3 trial. Rosell R, Carcereny E, Gervais R, et al. Lancet Oncol 2012;13:239-46.
5. Scoccianti C, Vesin A, Martel G, et al. Prognostic value of TP53, KRAS and EGFR mutations in Non-Small Cell Lung Cancer: EUELC cohort. Eur Respir J. 2012 Jan 20. [Epub ahead of print]
6. Roberts PJ, Stinchcombe TE, Der CJ, Socinski MA. Personalized medicine in non-small-cell lung cancer: is KRAS a useful marker in selecting patients for epidermal growth factor receptor-targeted therapy? J Clin Oncol. 2010;28:4769-77.
7. Adnane L, Trail PA, Taylor I, Wilhelm SM. Sorafenib (BAY 43-9006, Nexavar), a dual-action inhibitor that targets RAF/MEK/ERK pathway in tumor cells and tyrosine kinases VEGFR/PDGFR in tumor vasculature. Methods Enzymol. 2006;407:597-612.
8. Escudier B, Eisen T, Stadler WM, et al. Sorafenib in advanced clear-cell renal-cell carcinoma. N Engl J Med. 2007;356:125-34.
9. Llovet JM, Ricci S, Mazzaferro V, et al. Sorafenib in advanced hepatocellular carcinoma. N Engl J Med. 2008;359:378-90.
10. Wilhelm SM, Carter C, Tang L, et al. BAY 43-9006 exhibits broad-spectrum oral antitumor activity and targets the RAF/MEK/ERK pathway and receptor tyrosine kinases involved in tumor progression and angiogenesis. Cancer Res 2004;64:7099-109.
11. Martinelli E, Troiani T, Morgillo F, et al. Synergistic antitumor activity of sorafenib in combination with epidermal growth factor receptor inhibitors in colorectal and lung cancer cells. Clin Cancer Res. 2010;16:4990-5001.
12. Viloria-Petit A, Crombet T, Jothy S, et al. Acquired resistance to the antitumor effect of epidermal growth factor receptor-blocking antibodies in vivo: a role for altered tumor angiogenesis. Cancer Res 2001;61:5090-101.
13. Ciardiello F, Bianco R, Caputo R, et al. Antitumor activity of ZD6474, a vascular endothelial growth factor receptor tyrosine kinase inhibitor, in human cancer cells with acquired resistance to antiepidermal growth factor receptor therapy. Clin Cancer Res 2004;10:784-93.
14. Tortora G, Ciardiello F, Gasparini G. Combined targeting of EGFR-dependent and VEGF-dependent pathways: rationale, preclinical studies and clinical applications. Nat Clin Pract Oncol 2008;5:521–30.
15. Naumov GN, Nilsson MB, Cascone T, et al. Combined vascular endothelial growth factor receptor and epidermal growth factor receptor (EGFR) blockade inhibits tumor growth in xenograft models of EGFR inhibitor resistance. Clin Cancer Res 2009;15:3484-94.
16. Morgillo F, Martinelli E, Troiani T, Orditura M, De Vita F, Ciardiello F. Antitumor activity of sorafenib in human cancer cell lines with acquired resistance to EGFR and VEGFR tyrosine kinase inhibitors. PLoS One. 2011;6:e28841.
17. Lind JS, Dingemans AM, Groen HJ, et al. A multicenter phase II study of erlotinib and sorafenib in chemotherapy-naive patients with advanced non-small cell lung cancer. Clin Cancer Res. 2010;16:3078-87.
18. Gridelli C, Morgillo F, Favaretto A, et al. Sorafenib in combination with erlotinib or with gemcitabine in elderly patients with advanced non-small-cell lung cancer: a randomized phase II study. Ann Oncol. 2011;22:1528-34.
19. Cho B, Kim S, Heo DS, et al. A multicenter phase II study of sorafenib in combination with erlotinib in patients with advanced non-small cell lung cancer (NSCLC) J Clin Oncol 2010;28:7s
20. Spigel DR, Burris HA 3rd, Greco FA, et al. Randomized, double-blind, placebo-controlled, phase II trial of sorafenib and erlotinib or erlotinib alone in previously treated advanced non-small-cell lung cancer. J Clin Oncol. 2011;29:2582-9.
21. Smit EF, Dingemans AM, Thunnissen FB, Hochstenbach MM, van Suylen RJ, Postmus PE. Sorafenib in patients with advanced non-small cell lung cancer that harbor K-ras mutations: a brief report. J Thorac Oncol. 2010;5:719-20.
22. Lind JS, Meijerink MR, Dingemans AM, et al. Dynamic contrast-enhanced CT in patients treated with sorafenib and erlotinib for non-small cell lung cancer: a new method of monitoring treatment? Eur Radiol. 2010;20:2890-8.
23. Kelly RJ, Rajan A, Force J, et al. Evaluation of KRAS mutations, angiogenic biomarkers, and DCE-MRI in patients with advanced non-small-cell lung cancer receiving sorafenib. Clin Cancer Res. 2011 Mar 1;17(5):1190-9.
24. Bates SE, Amiri-Kordestani L, Giaccone G. Drug development: portals of discovery. Clin Cancer Res. 2012;18:23-32.
25. Giovannetti E, Zucali PA, et al. Association of polymorphisms in AKT1 and EGFR with clinical outcome and toxicity in non-small cell lung cancer patients treated with gefitinib. Mol Cancer Ther. 2010;9:581-93.
26. Tibaldi C, Giovannetti E, Tiseo M, et al. Correlation of cytidine deaminase polymorphisms and activity with clinical outcome in gemcitabine-/platinum-treated advanced non-small-cell lung cancer patients. Ann Oncol. 2012;23:670-7.
27. Granchi C, Roy S, Giacomelli C, et al. Discovery of N-hydroxyindole-based inhibitors of human lactate dehydrogenase isoform A (LDH-A) as starvation agents against cancer cells. J Med Chem. 2011;54:1599-612.
28. Giovannetti E, Lemos C, Tekle C, et al. Molecular mechanisms underlying the synergistic interaction of erlotinib, an epidermal growth factor receptor tyrosine kinase inhibitor, with the multitargeted antifolate pemetrexed in non-small-cell lung cancer cells. Mol Pharmacol. 2008;73:1290-300
29. Al-Mulla F, Bitar MS, Feng J, Park S, Yeung KC. A new model for raf kinase inhibitory protein induced chemotherapeutic resistance. PLoS One. 2012;7:e29532.
30. Giovannetti E, Mey V, Loni L, et al. Cytotoxic activity of gemcitabine and correlation with expression profile of drug-related genes in human lymphoid cells. Pharmacol Res. 2007;55:343-9.
31. Bianco C, Giovannetti E, Ciardiello F, et al. Synergistic antitumor activity of ZD6474, an inhibitor of vascular endothelial growth factor receptor and epidermal growth factor receptor signaling, with gemcitabine and ionizing radiation against pancreatic cancer.

Clin Cancer Res. 2006;12:7099-107.
32. Honeywell R, Yarzadah K, Giovannetti E, et al. Simple and selective method for the determination of various tyrosine kinase inhibitors used in the clinical setting by liquid chromatography tandem mass spectrometry. J Chromatogr B Analyt Technol Biomed Life Sci. 2010;878:1059-68.
33. Labots M, Gotink KJ, Dekker H, et al. Measurement of kinase activity in cancer cell lines and tumor tissue using a tyrosine kinase peptide substrate array. Proceedings Annual Meeting American Association Cancer Research 2012
34. Garraway LA, Jänne PA. Circumventing Cancer Drug Resistance in the Era of Personalized Medicine. Cancer Discov 2012 [Epub ahead of print]
35. Giovannetti E, Honeywell R, Hanauske AR, et al. Pharmacological aspects of the enzastaurin-pemetrexed combination in non-small cell lung cancer (NSCLC). Curr Drug Targets. 2010;11:12-28.
36. Chowdhuri SR, Xi L, Pham TH, et al. EGFR and KRAS mutation analysis in cytologic samples of lung adenocarcinoma enabled by laser capture microdissection. Mod Pathol. 2012;25:548-55.
37. Farhat FS, Tfayli A, Fakhruddin N, et al. Expression, prognostic and predictive impact of VEGF and bFGF in non-small cell lung cancer. Crit Rev Oncol Hematol. 2012 Apr 9. [Epub ahead of print]
38. Schubbert S, Shannon K, Bollag G. Hyperactive Ras in developmental disorders and cancer. Nat Rev Cancer 2007;7:295-308.
39. Engelman JA. Targeting PI3K signalling in cancer: opportunities, challenges and limitations. Nat Rev Cancer 2009;9:550-62.
40. Lo HW, Hung MC. Nuclear EGFR signalling network in cancers: linking EGFR pathway to cell cycle progression, nitric oxide pathway and patient survival. Br J Cancer 2006;94:184-8.
41. Kobayashi S, Shimamura T, Monti S, et al. Transcriptional profiling identifies cyclin D1 as a critical downstream effector of mutant epidermal growth factor receptor signaling. Cancer Res 2006;66:11389-98.
42. Suenaga M, Yamaguchi A, Soda H, et al Antiproliferative effects of gefitinib are associated with suppression of E2F-1 expression and telomerase activity. Anticancer Res 2006;26:3387-91.
43. Gorgoulis VG, Zacharatos P, Mariatos G, et al. Transcription factor E2F-1 acts as a growth-promoting factor and is associated with adverse prognosis in non-small cell lung carcinomas. J Pathol. 2002;198:142-56.
44. Kuhn H, Liebers U, Gessner C, et al. Adenovirus-mediated E2F-1 gene transfer in non small-cell lung cancer induces cell growth arrest and apoptosis. Eur Respir J. 2002;20:703-9.
45. Pillai S, Kovacs M, Chellappan S. Regulation of vascular endothelial growth factor receptors by Rb and E2F1: role of acetylation. Cancer Res 2010;70:4931-40.
46. Raut CP, Boucher Y, Duda DG, et al. Effects of sorafenib on intra-tumoral interstitial fluid pressure and circulating biomarkers in patients with refractory sarcomas (NCI protocol 6948). PLoS One 2012;7:e26331.
47. Vroling L, Lind JS, de Haas RR, et al. CD133+ circulating haematopoietic progenitor cells predict for response to sorafenib plus erlotinib in non-small cell lung cancer patients. Br J Cancer 2010;102:268-75.
48. Li Y, Sarkar FH. Inhibition of nuclear factor kappaB activation in PC3 cells by genistein is mediated via Akt signaling pathway. Clin Cancer Res 2002;8:2369-77.
49. Yeung KC, Rose DW, Dhillon AS, et al. Raf kinase inhibitor protein interacts with NFkappaB-inducing kinase and TAK1 and inhibits NF-kappaB activation. Mol Cell Biol 2001;21:7207-17.
50. Piersma SR, Labots M, Verheul HM, Jiménez CR. Strategies for kinome profiling in cancer and potential clinical applications: chemical proteomics and array-based methods. Anal Bioanal Chem 2010;397:3163-71.
51. Giaccone G, Zucali PA. Src as a potential therapeutic target in non-small-cell lung cancer. Ann Oncol. 2008;19:1219-23.
52. Cai D, Latham VM Jr, Zhang X, Shapiro GI. Combined depletion of cell cycle and transcriptional cyclin-dependent kinase activities induces apoptosis in cancer cells. Cancer Res 2006;66:9270-80.
53. Danesi R, Altavilla G, Giovannetti E, Rosell R. Pharmacogenomics of gemcitabine in non-small-cell lung cancer and other solid tumors. Pharmacogenomics. 2009;10:69-80.
54. Giovannetti E, Erozenci A, Smit J, Danesi R, Peters GJ. Crit Rev Oncol Hematol. 2012;81:103-22.
55. Mross K, Frost A, Steinbild S, et al. A Phase I Dose-Escalation Study of Regorafenib (BAY 73-4506), an Inhibitor of Oncogenic, Angiogenic, and Stromal Kinases, in Patients with Advanced Solid Tumors. Clin Cancer Res. 2012;18:2658-67.

Chapter 9

Metabolism of the EGFR-TKI gefitinib by cytochrome P450-1A1 enzyme in EGFR wild-type NSCLC cell lines

Alfieri RR, Galetti M, Tramonti S, Andreoli R, Mozzoni P, Cavazzoni A, Bonelli MA, Fumarola C, La Monica S, Galvani E, De Palma G, Mutti A, Mor M, Tiseo M, Mari E, Ardizzoni A & Petronini PG.

MOLECULAR CANCER 2011

10:143.

ABSTRACT

Background: Gefitinib is a tyrosine kinase inhibitor (TKI) of the epidermal growth factor receptor (EGFR) especially effective in tumors with activating EGFR gene mutations while EGFR wild-type non-small cell lung cancer (NSCLC) patients at present do not benefit from this treatment. The primary site of gefitinib metabolism is the liver nevertheless tumor cell metabolism can significantly affect treatment effectiveness.

Results: In this study, we investigated the intracellular metabolism of gefitinib in a panel of EGFR wild-type gefitinib-sensitive and -resistant NSCLC cell lines, assessing the role of cytochrome P450 1A1 (CYP1A1) inhibition on gefitinib efficacy. Our results indicate that there is a significant difference in drug metabolism between gefitinib-sensitive and -resistant cell lines. Unexpectedly, only sensitive cells metabolized gefitinib, producing metabolites which were detected both inside and outside the cells. As a consequence of gefitinib metabolism, the intracellular level of gefitinib was markedly reduced after 12-24 h of treatment. Consistent with this observation, RT-PCR analysis and EROD assay showed that mRNA and activity of CYP1A1 were present at significant levels and were induced by gefitinib only in sensitive cells. Gefitinib metabolism was elevated in crowded cells, stimulated by exposure to cigarette smoke extract and prevented by hypoxic condition. It is worth noting that the metabolism of gefitinib in the sensitive cells is a consequence and not the cause of drug responsiveness, indeed treatment with a CYP1A1 inhibitor increased the efficacy of the drug because it prevented the fall in intracellular gefitinib level and significantly enhanced the inhibition of EGFR autophosphorylation, MAPK and PI3K/AKT/mTOR signalling pathways and cell proliferation.

Conclusion: Our findings suggest that gefitinib metabolism in lung cancer cells, elicited by CYP1A1 activity, might represent an early assessment of gefitinib responsiveness in NSCLC cells lacking activating mutations. On the other hand, in metabolizing cells, the inhibition of CYP1A1 might lead to increased local exposure to the active drug and thus increase gefitinib potency.

BACKGROUND

Gefitinib is an orally active, selective EGFR TKI used in the treatment of patients with advanced-NSCLC carrying activating EGFR mutations [1]. In fact, it is well established that gefitinib is more active in some patient subgroups, such as Asians, females, never smokers and adenocarcinoma histotypes which have a higher probability of harbouring activating mutations in the tyrosine kinase domain, the most frequent being L858R in exon 21 and Del (746-750) in exon 19 [1]. As a consequence most of the NSCLCs containing wild-type EGFR receptor are excluded and hence the role of gefitinib for the treatment of NSCLC is limited. However, some studies have shown that patients without mutations responded to gefitinib with response rates reaching 6.6% [2,3]. In addition to cancer cell genomic determinants of sensitivity, some pharmacokinetic parameters may also play a role in the variable response to gefitinib and other TKIs [4].

When administered at 250 mg/day, gefitinib is 60% orally absorbed and 90% plasma protein-bound [5,6]. The very high distribution volume of gefitinib (1400 litres) clearly indicates that the drug is extensively distributed in tissues such as liver, kidney, gastrointestinal tract, lung and in tumors [7]. A tendency to accumulate in the lung was observed with concentrations 10 times higher than in plasma [8]. We have recently demonstrated in NSCLC cell lines that the uptake of gefitinib is an essentially active process leading to intracellular gefitinib concentrations more than two hundred times higher than outside the cells [9].

There are few data on gefitinib intracellular metabolism in tumors, the majority of the available data concerns liver metabolism. In vitro and in vivo studies indicate that in the liver gefitinib is mainly metabolized by cytochrome P450-dependent (CYP) activities, including CYP3A4, CYP3A5 and CYP2D6 [10-12]. The main metabolic pathway characterized by using human liver microsomes include morpholine ring opening, O-demethylation of the methoxy-substituent on the quinazoline ring structure and oxidative defluorination of the halogenated phenyl group [13,14].

A study investigating the contribution of individual CYPs to gefitinib metabolism demonstrated that gefitinib disappeared with similar clearance when incubated with CYP3A4 or CYP2D6 enzymes, less efficiently with CYP3A5 or CYP1A1, whereas CYP1A2 and CYP1B1 were not involved in the metabolism of the drug [12]. Incubation with CYP3A4 and to a lesser extent CYP3A5, produced a similar range of metabolites as that produced by liver microsomes [11], but the main plasma metabolite, the O-desmethyl derivative present at plasma concentrations similar to gefitinib [10], was formed predominantly through the CYP2D6 enzyme.

CYP1A1 is one of the three members of the CYP1 family mainly expressed in extra-hepatic tissue, involved in the metabolism of a large number of xenobiotics as well as a small number of endogenous substrates [15]. Being expressed at a significant level in human lung [16], it might play a role in the metabolism of gefitinib by lung tumor cells and its activity might be involved in the variability of the drug response.

In experiments using lung microsomes, CYP1A1 was shown to produce significant amounts of the parahydroxyaniline metabolite derived from oxidative defluorination of gefitinib. Hydroxyaniline metabolites produced by CYP1A1 can be oxidized to reactive quinoneimine derivatives that form adducts with nucleophilic groups of macromolecules or GSH and may be related to clinically relevant hepatotoxicity or interstitial lung disease [8].

Both mRNA and protein CYP1A1 levels in human lung are greatly induced by tobacco smoke [17] and it has been reported that lung microsomes from smokers may generate 12 times more gefitinib-derived reactive metabolites as compared to non-smokers [8].

The present study was designed to investigate gefitinib metabolism in a panel of EGFR wild-type NSCLC cell lines either sensitive or resistant to gefitinib. Our objective was to define a possible potential role of gefitinib metabolism in early evaluation of tumor response to gefitinib, to analyze conditions or factors that can alter tumor gefitinib metabolism and to test the effect of CYP1A1 inhibition on gefitinib efficacy.

MATERIALS AND METHODS

Cell culture

The human NSCLC cell lines H322, Calu-3, H292, H460, H1299, A549, Calu-1 and SKLU-1 were cultured as recommended. Cell lines obtained from American Type Culture Collection (Manassas, VA, USA) were immediately expanded and frozen. Every four months all the cell lines were restarted from a frozen vial of the same batch of cells and no additional authentication was done in our laboratory. All cells were maintained under standard cell culture conditions at 37°C in a water-saturated atmosphere of 5% CO_2 in air. As previously reported [18], cells showing in proliferation assays IC_{50} for gefitinib < 1 μM were considered sensitive (H322, H292, Calu-3) and cell lines with IC_{50} > 8 μM (H460, H1299, A549, Calu-1 and SKLU-1) were considered resistant.

Hypoxia

Hypoxic conditions (0.5% O_2) were established by placing the cells in a tissue culture incubator (Binder GmbH, Tuttlingen, Germany) with controlled O2 levels.

Preparation of cigarette smoke extract (CSE)

CSE preparation was made according to Carp and Janoff [19], with slight modifications. Briefly, one cigarette without filter was combusted using a modified syringe-driven apparatus and the smoke was bubbled through 50 ml of serum-free cell culture medium. This solution, considered to be 100% CSE, was filtered diluted with medium and applied to cell cultures within 30 min of preparation.

CYP1A1 genotyping

Genomic DNA was isolated using a PureGene DNA purification system (GENTRA SYSTEMS, Minneapolis, MN) and both the rs 4646903 (3798 T > C, variant allele CYP1A1*2A) and the rs 1048943 (2454 A > G, variant allele CYP1A1*2C) polymorphisms of the CYP1A1 gene that were characterized according to previously published methods, with minimal changes [20,21]. All the tested cell lines carried a wild type homozygous genotype for both the polymorphisms.

Drug treatment

Gefitinib (ZD1839/Iressa) and metabolites [morpholine ring-opening (M537194, M1), oxidative defluorinated (M387783, M2) and O-desmethyl (M523595, M3) derivatives] were kindly provided by AstraZeneca. a-naphthoflavone (a-NAP) was from Sigma Aldrich (St. Louis, MO, USA).

Cetuximab, erlotinib and lapatinib were from inpatient pharmacy. RAD001 and NVP-BEZ235 were provided by Novartis Institutes for BioMedical Research (Basel, Switzerland). Wortmannin, PD98059 and U0126 were from Sigma-Aldrich (St. Louis, MO).

Uptake measurements

[3H]gefitinib uptake by cells was determined as described recently [9].

Liquid chromatography tandem mass spectrometry (LCMS/MS)

For LC-MS/MS analysis, the medium samples were treated with ethyl acetate, dried under nitrogen and refilled with methanol and aqueous formic acid (0.1 M), while the ethanolic extracts were diluted with aqueous formic acid (0.1 M).

LC analyses were carried out with an Agilent HP 1100 pump coupled with a API4000 triple-quadrupole mass spectrometer (Sciex, Concord, Canada) equipped with a TurboIonSprayTM interface and configured in Selected Reaction Monitoring (SRM) mode. Chromatography was performed on a Synergi Hydro-RP column (5 × 2.0 mm i. d., 2 µm; Phenomenex) using variable proportions of 10 mM aqueous formic acid and methanol/acetonitrile (95/5, v/v) mixture as the mobile phase.

The analytes were ionized in positive ion mode and the following SRM transitions were monitored: m/z 447 ($[M+H]^+$) → 128 for Gefitinib; m/z 421 ($[M+H]^+$) → 320 for Metabolite 1; m/z 445 ($[M+H]^+$) → 128 for Metabolite 2; m/z 433 ($[M+H]^+$) → 128 for Metabolite 3 and m/z 394 ($[M+H]^+$) → 336 for Internal Standard. Erlotinib was used as Internal Standard.

Determination of cell growth

Cell number and viability were evaluated by cell counting, crystal violet staining and MTT colorimetric assay as previously described [18].

Western blot analysis

Procedures for protein extraction, solubilization, and protein analysis by 1-D PAGE are described elsewhere [22]. Anti-EGFR, anti-phospho-EGFR (Tyr1068), antiphospho-p44/42 MAPK, anti-p44/42 MAPK, anti-phospho-AKT (Ser473), anti-AKT and anti-actin were from Cell Signaling Technology (Beverly, MA, USA).

Real-Time RT-PCR

Total RNA was isolated by the TRIzol® reagent (Invitrogen, Carlsbad, CA, USA) and reverse-transcribed as previously described [23]. The transcript levels of CYP1A1, CYP1A2, CYP2D6, CYP3A4 and CYP3A5 genes were assessed by Real-Time qRT-PCR on an iCycler iQ Multicolor RealTime PCR Detection System (Bio-Rad, Hercules, CA, USA). Primers and probes included: CYP1A1-F (5'-TCCAAGAGTCCACCCTTCC-3'), CYP1A1-R (5'-AAGCATGATCAGTGTAGGGATCT-3'), CYP1A1-probe (5'-FAM CAGCCACC 3'DQ); CYP1A2-F (5'-GGCTTCTACATCCCCAAGAA-3'), CYP1A2-R (5'-CAGCTCTGGGTCATGGTTG-3'), CYP1A2-probe (5'-FAM CAGTGGCA3'DQ); CYP2D6-F (5'-CTTCCAAAAGGCTTTCCTGA-3'), CYP2D6-R (5'-CAGGTCATCCTGTGCTCAGTT-3'), CYP2D6-probe (5'-FAM GCTGGATG 3'DQ); CYP3A4-F (5'-

GATGGCTCTCATCCCAGACTT-3'), CYP3A4-R (5'AGTCCATGTGAATGGGTTCC-3'), CYP3A4-probe (5'-FAM TCCTCCTG 3'DQ); CYP3A5-F (5'-TGCCCAGTATGGAGATGTATTG-3'), CYP3A5-R (5'-GCTGTAGG CCCCAAAGATG-3'), CYP3A5-probe (5'-FAM GGAAGCAG3'DQ); PGK1-F (5'-GGAGAACCTCCGCTTTCAT-3'), PGK1-R (5'-CTGGCTCGGCTTTAACCTT-3'), PGK1-probe (5'-FAM GGAGGAAG 3'DQ); RPL13-F (5'-ACAGCTGCTCAGCTTCACCT-3'), RPL13-R (5'-TGGCAGCATGCCATAAATAG-3'), RPL13-probe (5'-FAMCAGTGGCA3'DQ); HPRT-F (5'-TGACCTTGATTTATTTTGCATACC-3'), HPRT-R (5'CGAGCAAGACGTTCAGTCCT-3'), HPRT-probe (5'-FAM GCTGAGGA3'DQ).

The amplification protocol consisted of 15 min at 95°C followed by 40 cycles at 94°C for 20 s and at 60°C for 1 min. The relative transcript quantification was calculated using the geNorm algorithm for Microsoft Excel™ after normalization by expression of the control genes [phosphoglycerate kinase1 (PGK1), ribosomal protein L13 (RPL13) and hypoxanthine-guanine-phosphoribosyltransferase (HPRT)] and expressed in arbitrary units (a.u.).

EROD assay

The CYP1A1 ethoxyresorufin-O-deethylase activity (EROD) was determined in intact cells as described by Kennedy and Jones [24] with 5 µM ethoxyresorufin in growth medium as substrate in the presence of 1.5 mM salicylamide, to inhibit conjugating enzymes. The assay was performed at 37°C. The fluorescence of resorufin generated by the conversion of ethoxyresorufin by CYP1A1 was measured first, immediately after addition of reagents and then every 10 min for 60 min at 37°C in a Tecan infinite 200 fluorescence plate reader with excitation of 530 nm and emission at 595 nm. A standard curve was constructed using resorufin.

RNA interference assay

Cells were transfected with Invitrogen Stealth™ siRNA against CYP1A1 (1:1:1 mixture of #102535, #102537 and #175787) or scramble negative control (1:1:1 mixture of #12935-200, #12935-300 and #12935-400) with a final concentration of 30 nM. The transfection was carried out according to the Invitrogen forward transfection protocol for Lipofectamine™ RNAiMAX transfection reagent. After 48 h of transfection, the transfection medium was aspirated and replaced with exposure medium.

Statistical analysis

The statistical analyses were carried out using GraphPad Prism version 5.00 software (GraphPad Software Inc., San Diego, CA). Results are expressed as mean values ± standard deviations (SD) for the indicated number of independent measurements. Differences between the mean values recorded for different experimental conditions were evaluated by Student's t-test, and P values are indicated where appropriate in the figures and in their legends. A P value < 0.05 was considered as significant.

RESULTS

Intracellular and extracellular levels of gefitinib in sensitive and resistant NSCLC cell lines

In the first part of the study we evaluated the accumulation kinetics of 0.1 µM radiolabeled gefitinib in H322-sensitive and H1299-resistant cell lines during 24 h of treatment. Figure 1A shows a progressive

decrease of the level of intracellular radiolabeled gefitinib only in the sensitive cell line. The decrease was detectable starting from 6 h of treatment, reaching a minimum level after 16 h. Similar results were obtained with a higher (1 μM) gefitinib concentration (not shown).

We then analyzed the effect of the intracellular gefitinib level on EGFR autophosphorylation in H322 cells. As reported in Figure 1B after 0.5 h, gefitinib inhibited EGFR autophosphorylation by around 50% and 80% at doses of 0.1 μM and 1 μM respectively; after 24 h these inhibitions were significantly reduced indicating a correlation between the intracellular gefitinib level and the inhibition of EGFR phosphorylation, confirming our previous results [9].

In an attempt to investigate whether the fall in intracellular gefitinib could be related to a lower influx, an enhanced efflux or metabolism of the drug, we firstly measured 5 min of [3H]gefitinib uptake in H322 cells treated with gefitinib for 0.5 h and 24 h (Figure 1C) and the level of intracellular gefitinib in the presence of inhibitors of specific efflux transporters (Figure 1D). As shown in Figure 1C, the initial rate of [3H]gefitinib uptake at 0.5 h and at 24 h was similar, suggesting that in the presence of an extracellular fixed concentration of drug, its influx is constant over time. Since it has been reported that gefitinib interacts with ABCG2 and to a lesser extent with ABCB1 [25], the intracellular levels of the radiolabeled drug were determined after dosing cells with the respective inhibitors Fumitremorgin C (Sigma Aldrich) and PSC833 (kindly provided by Novartis). We demonstrated only a slight increase in gefitinib content at 24 h in the presence of Fumitremorgin C (inhibition of ABCG2), whereas the inhibition of ABCB1 pump was ineffective (Figure 1D).

We then analyzed the distribution of radioactivity among intracellular, extracellular and macromoleculelinked compartments in another sensitive, EGFR wild-type cell line (Calu-3) and in resistant H1299 after 0.5 h and 24 h of treatment with radiolabeled gefitinib. As shown in Figure 2A, Calu-3 showed a significant drop in intracellular radioactivity, with a parallel increase in extracellular radioactivity after 24 h of incubation; by contrast, the radioactivity distribution was unchanged between 0.5 h and 24 h in H1299 cells. The amount of radioactivity in the NaOH fraction (macromoleculelinked) was less than 10% in both cell lines.

Since the measured radioactivity may be associated, at least in part, with gefitinib metabolites, the actual amount of gefitinib was monitored intracellularly and in the medium by LC-MS/MS after 0.5 h and 24 h of treatment in a panel of NSCLC cell lines showing either sensitivity (H322, H292, Calu-3) or resistance (H460, H1299, A549, Calu-1, SKLU-1) to the drug. As shown in Figure 2B, the intracellular level of gefitinib was markedly reduced at 24 h (more than 80%) in all the sensitive cell lines, whereas the resistant ones showed a slight reduction (lower than 20%). Figure 2C shows that in sensitive cell lines, the extracellular level of gefitinib after 24 h of treatment was markedly reduced indicating that the increased radioactivity in the medium at 24 h (Figure 2A) was not due to gefitinib itself but to radiolabeled molecules probably derived from intracellular metabolism of gefitinib and then extruded into the extracellular compartment.Taken together these results clearly demonstrate that the observed decrease in gefitinib content, evident only in sensitive cells, was due to a high rate of gefitinib metabolism.

Employing the standards kindly provided by AstraZeneca, we analyzed the appearance of the three main gefitinib metabolites (M1; M2; M3) inside and outside the cells after 0.5, 6 and 24 h of treatment with 0.1 μM gefitinib. LC-MS/MS analysis (Figure 3A) showed that the M1 metabolite was present at a very low level in the intracellular compartment, mainly in sensitive cell lines, whereas M2 and M3 were undetectable.

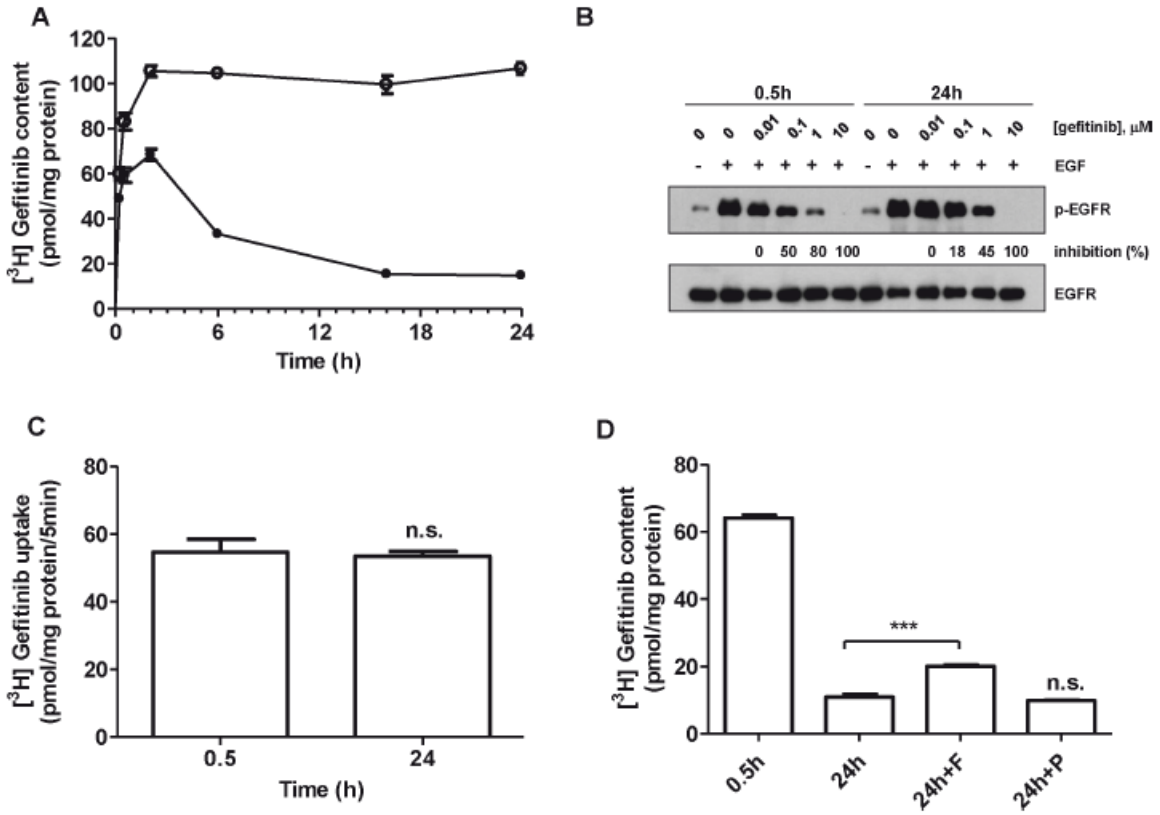

Figure 1. Intracellular content of gefitinib in NSCLC cell lines and its effect on EGFR autophosphorylation. (A) Time course of 0.1 µM [3H]gefitinib accumulation in H322 (●) and H1299 (○) cell lines. Each point represents the mean ± SD of four independent determinations. **(B)** H322 cells were incubated for 0.5 h and 24 h with the indicated extracellular concentrations of gefitinib before stimulation with 0.1 µg/ml EGF for 5 min. Western blot analysis was performed by using monoclonal antibodies directed to p-EGFR(p-Tyr1068) and to EGFR. The immunoreactive spots were quantified by densitometric analysis, ratios of phosphotyrosine/total EGFR were calculated and values are expressed as percentage of inhibition versus control. The experiment, repeated three times, yielded similar results. **(C)** H322 cells were incubated with 0.1 µM gefitinib for 0.5 h or 24 h and then the initial rate (5 min) of 0.1 µM [3H]gefitinib uptake was measured. Each bar represents the mean ± SD of four independent determinations. **(D)** H322 cells were exposed to 0.1 µM [3H]gefitinib for 0.5 h and 24 h, in the absence or in the presence of 10 µM Fumetrimorgin C (F) or PSC833 (P) and then intracellular gefitinib content was determined. Values given are the means (± SD) of three independent determinations (***P < 0.001).

Production of gefitinib metabolites by NSCLC cell lines and their effect on cell growth and EGFR autophosphorylation

The M1 metabolite was also present in the extracellular compartment (Figure 3B) at concentrations between 0.01 and 0.05 µM only in sensitive cell lines. We then tested on sensitive and resistant cell lines whether metabolites M1, M2 and M3, when present in the growth medium at concentrations equivalent to gefitinib, were able to exert similar biological effects than gefitinib. As shown in Figure 3C, gefitinib and its metabolites inhibited, in a dose-dependent manner, cell proliferation in sensitive H322 cells with IC_{50} values of 0.13, 0.7, 0.5 and 1.4 µM for gefitinib, M1, M2 and M3 respectively. Figure 3D shows that gefitinib and metabolites inhibited with the same potency EGFR autophosphorylation. These results were further confirmed in both Calu-3 and H292 cell lines.

It should be noted that metabolites were only effective in all the resistant cells at very high concentrations (IC_{50} > 20 µM) (see Figure 3E for H1299) indicating that the metabolites themselves did not have an additive toxic effect (IC_{50} for gefitinib 9 µM).

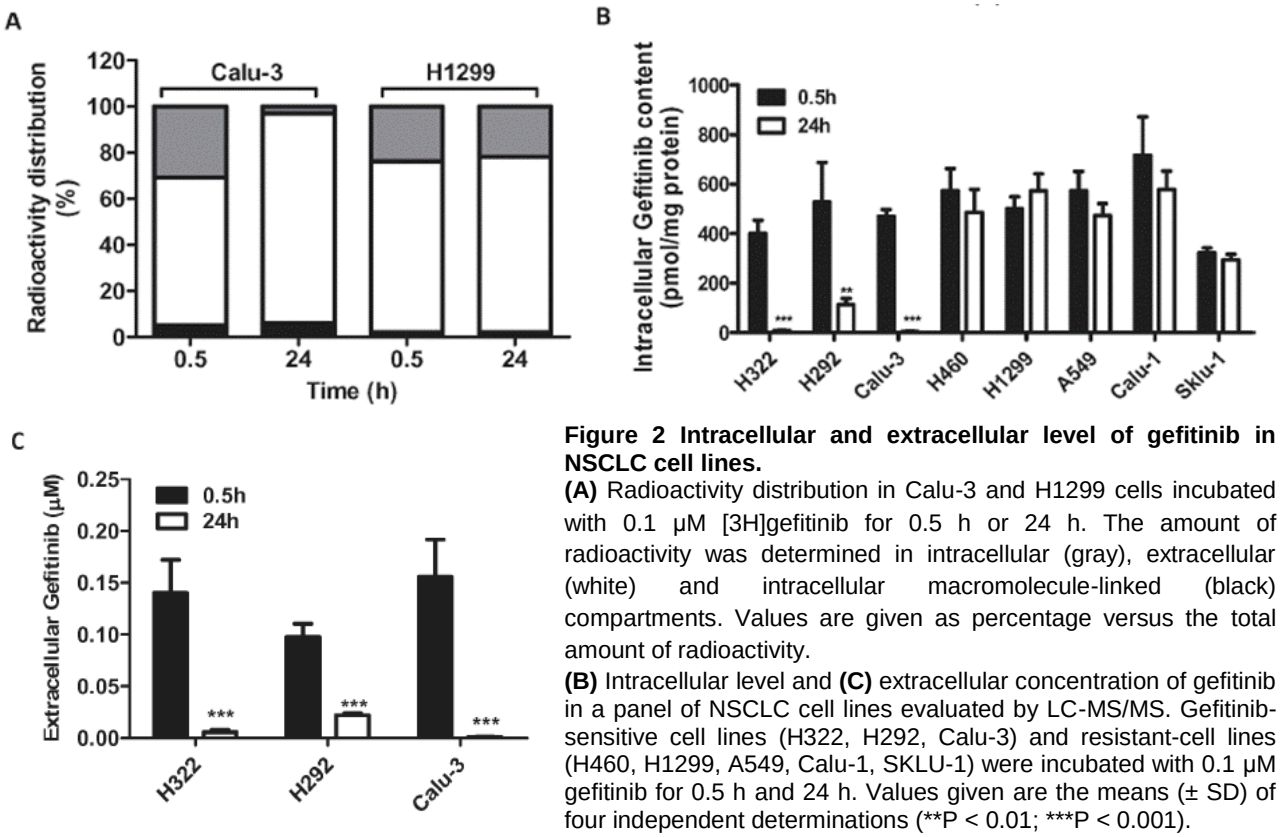

Figure 2 Intracellular and extracellular level of gefitinib in NSCLC cell lines.
(A) Radioactivity distribution in Calu-3 and H1299 cells incubated with 0.1 µM [3H]gefitinib for 0.5 h or 24 h. The amount of radioactivity was determined in intracellular (gray), extracellular (white) and intracellular macromolecule-linked (black) compartments. Values are given as percentage versus the total amount of radioactivity.
(B) Intracellular level and **(C)** extracellular concentration of gefitinib in a panel of NSCLC cell lines evaluated by LC-MS/MS. Gefitinib-sensitive cell lines (H322, H292, Calu-3) and resistant-cell lines (H460, H1299, A549, Calu-1, SKLU-1) were incubated with 0.1 µM gefitinib for 0.5 h and 24 h. Values given are the means (± SD) of four independent determinations (**P < 0.01; ***P < 0.001).

Effect of gefitinib on CYP mRNAs expression and EROD activity in NSCLC cell lines

The baseline transcript levels of CYP1A1, CYP1A2, CYP2D6, CYP3A4 and CYP3A5 were determined in both sensitive and resistant cell lines by RT-PCR and data are summarized in Figure 4A. CYP1A1 and CYP1A2 were expressed at significant levels only in H322, H292 and Calu-3 cells; CYP2D6 was detected in all cell lines; whereas CYP3A4 was undetected. CYP3A5 was present at high level only in A549 cells.

The inducibility of individual CYP genes by gefitinib was then investigated and the levels of CYP1A1, CYP1A2, CYP2D6 and CYP3A5 mRNAs were assessed after treating cells with the drug. After 6 h, significantly higher gene expression levels of CYP1A1 and CYP1A2 were observed in all sensitive cell lines. By contrast no significant modulation of gene expression was observed in resistant cell lines (Figure 4B).

In order to evaluate whether modulation of the CYP1A1 transcript levels was associated with changes in the respective enzyme activity levels, we measured the activity of 7-ethoxyresorufin-O-deethylase (EROD), a commonly-used indicator of CYP1A activity [26], both basally and after exposure of cells to gefitinib. In untreated cells, EROD activity was detectable only in sensitive cells, and gefitinib caused a significant increase in this activity (3-6 fold induction) with a maximum at 16-24 h (Figure 5A). Although both CYP1A1 and CYP1A2 carry out EROD activity, the 1A1 form has a much higher specific EROD activity than 1A2 [27]. A further demonstration of CYP1A1 involvement came from the use of 10 µM a-NAP, a CYP1A1 inhibitor [28,29] or from CYP1A1 silencing using siRNAs that significantly inhibited both baseline and gefitinib-induced EROD activity (Figure 5B).

We then tested the effect of other EGFR inhibitors (erlotinib, cetuximab, lapatinib) and of inhibitors of MAPK and PI3K/AKT/mTOR signalling transduction pathways on EROD activity in H322 cell line. As shown in Figure 5C erlotinib, cetuximab and lapatinib induced a significant increase in EROD activity comparable to

that induced by gefitinib. Both MEK inhibitors (PD98059 and U0126) strongly activated CYP1A1. In contrast, no increase in the activity was detectable after incubation with the inhibitors of PI3K/AKT/mTOR pathway tested (wortmannin, PI3K inhibitor; RAD001 mTOR inhibitor; NVP-BEZ235 PI3K and mTOR inhibitor).

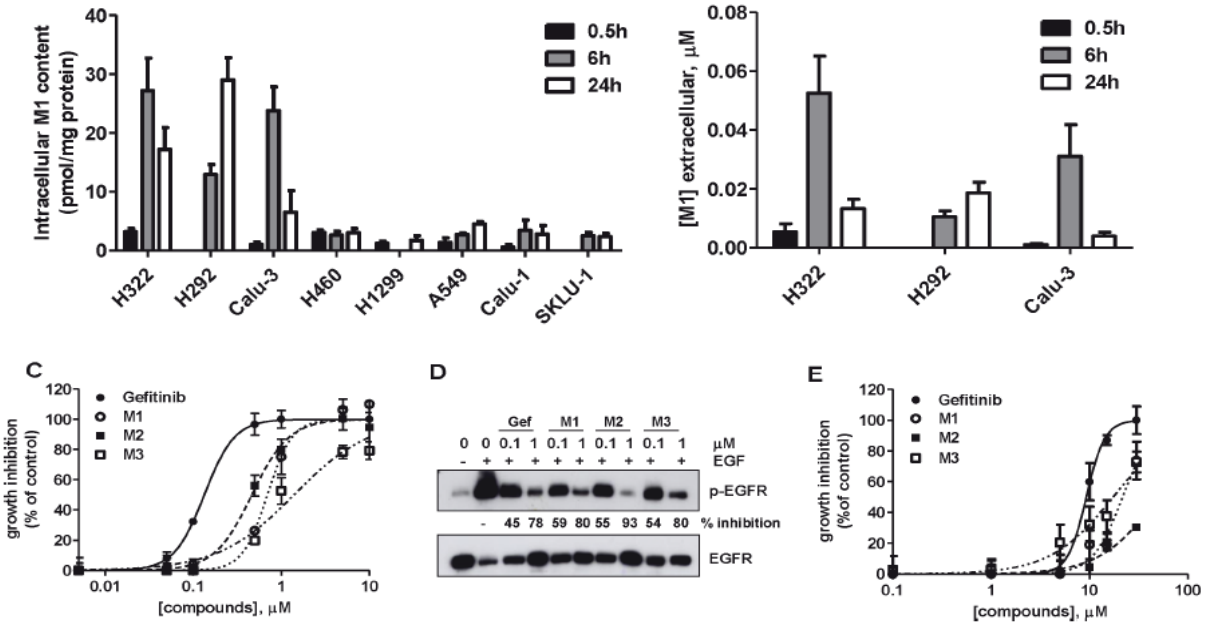

Figure 3. Production and biological activity of gefitinib metabolites. Cells were incubated with 0.1 µM gefitinib for 0.5, 6 or 24 h and then the M1 content was determined both in the intracellular **(A)** and extracellular **(B)** compartment, through LC-MS/MS analysis. M1 levels calculated for each cell line were expressed as pmol/mg of protein (intracellular) or µM (extracellular). Values given are the means (± SD) of three independent determinations **(C)** H322 cells were exposed for 72 h to different concentrations of gefitinib or its metabolites (ranging from 0.05 to 10 µM) and then cell growth was assessed using crystal violet staining. Data are expressed as percent inhibition of cell proliferation versus control cells. The mean values of three independent measurements (± SD) are shown. **(D)** H322 cells were incubated for 0.5 h with the indicated concentrations of gefitinib and metabolites, before stimulation with 0.1 µg/ml EGF for 5 min. Western blot analysis was performed by using monoclonal antibodies directed to p-EGFR (p-Tyr1068) and to EGFR. The immunoreactive spots at each point were quantified by densitometric analysis, ratios of phosphotyrosine/total EGFR were calculated and values expressed as percentage of inhibition versus control. The experiment, repeated three times, yielded similar results. **(E)** H1299 cells were exposed for 72 h to different concentrations of gefitinib or its metabolites (ranging from 1 to 30 µM) and then cell growth was assessed using crystal violet staining. Data are expressed as percent inhibition of cell proliferation versus control cells. The mean values of three independent measurements (± SD) are shown.

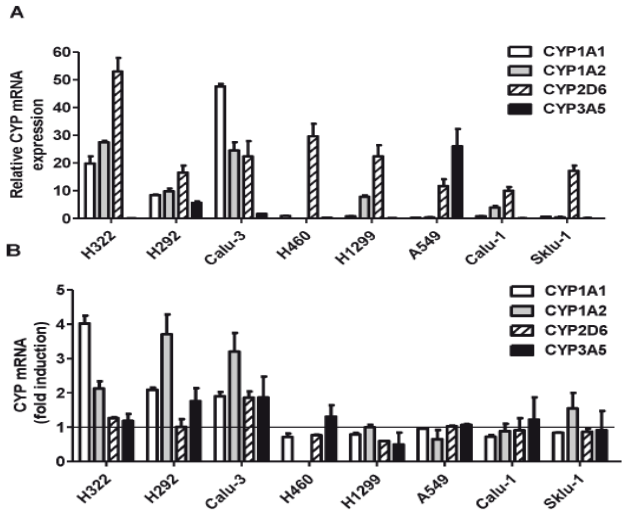

Figure 4. Effect of gefitinib on CYP mRNAs expression. **(A)** Basal expression of CYP1A1, 1A2, 2D6 and 3A5 mRNAs in NSCLC cell lines was detected by RT-PCR. The mean values of three independent measurements (± SD) are shown. It is to note that CYP3A4 was undetected. **(B)** The cells were exposed to 0.1 µM gefitinib for 6 h and then gefitinib induction of CYP1A1, 1A2, 2D6 and 3A5 mRNAs was evaluated by RT-PCR and expressed as fold induction relative to basal expression. The mean values of three independent measurements (± SD) are shown.

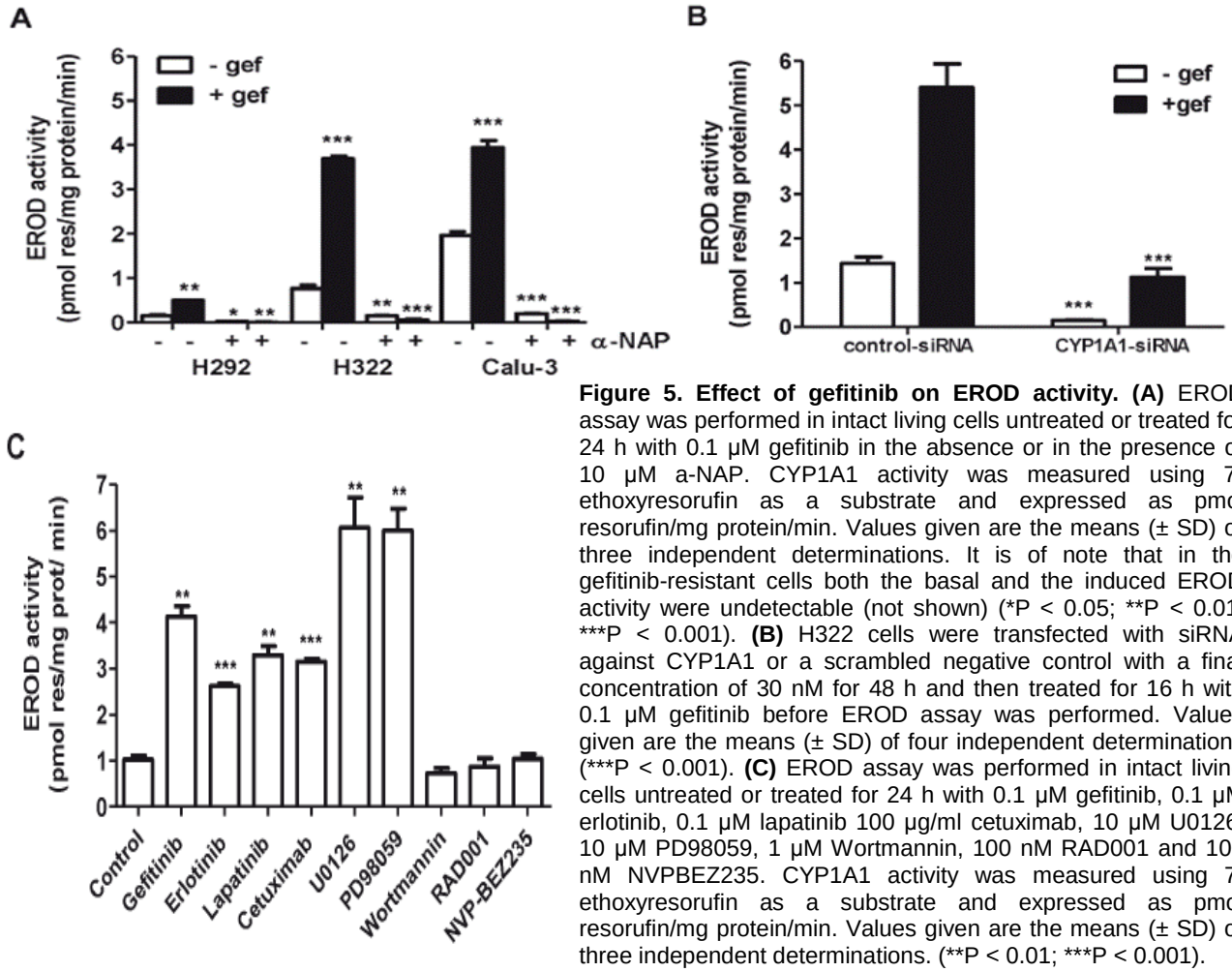

Figure 5. Effect of gefitinib on EROD activity. (A) EROD assay was performed in intact living cells untreated or treated for 24 h with 0.1 μM gefitinib in the absence or in the presence of 10 μM a-NAP. CYP1A1 activity was measured using 7-ethoxyresorufin as a substrate and expressed as pmol resorufin/mg protein/min. Values given are the means (± SD) of three independent determinations. It is of note that in the gefitinib-resistant cells both the basal and the induced EROD activity were undetectable (not shown) (*P < 0.05; **P < 0.01; ***P < 0.001). **(B)** H322 cells were transfected with siRNA against CYP1A1 or a scrambled negative control with a final concentration of 30 nM for 48 h and then treated for 16 h with 0.1 μM gefitinib before EROD assay was performed. Values given are the means (± SD) of four independent determinations (***P < 0.001). **(C)** EROD assay was performed in intact living cells untreated or treated for 24 h with 0.1 μM gefitinib, 0.1 μM erlotinib, 0.1 μM lapatinib 100 μg/ml cetuximab, 10 μM U0126, 10 μM PD98059, 1 μM Wortmannin, 100 nM RAD001 and 100 nM NVPBEZ235. CYP1A1 activity was measured using 7-ethoxyresorufin as a substrate and expressed as pmol resorufin/mg protein/min. Values given are the means (± SD) of three independent determinations. (**P < 0.01; ***P < 0.001).

Effect of hypoxia, cigarette smoke extract and cell density on gefitinib metabolism

Since it is known that hypoxia downregulates the expression and activity of many CYPs including CYP1A1 [30], we evaluated whether hypoxia could prevent gefitinib metabolism and its intracellular loss. The simultaneous exposure of H322 cells to gefitinib and hypoxia (Figure 6A) almost completely prevented gefitinib catabolism inside the cells. Differently, CYP1A1 activity was strongly induced in Calu-3 cells exposed to 2.5% cigarette smoke extract (CSE) for 24 h (see inset Figure 6B) and consequently gefitinib consumption (Figure 6B) was significantly expedited. Moreover, as expected, cell density strongly affected the reduction in the intracellular level of gefitinib at 24 h in the Calu-3 line (Figure 6C) and consequently cells seeded at high and low density but with a similar growth-rate quotient, exhibited a significant difference in the sensitivity to gefitinib. Indeed, as shown in Figure 6D, cells at low density showed a 15-fold higher sensitivity to gefitinib (IC_{50} 0.4 μM) as compared to cells at high density (IC_{50} 6 μM).

Effects of CYP1A1 inhibition on the intracellular level of gefitinib, EGFR autophosphorylation and inhibition of cell growth

In an attempt to better characterize the role of CYP1A1 in sensitive cells, we measured the intracellular content of radiolabeled gefitinib in Calu-3 cells in the presence of 10 μM a-NAP. This inhibitor almost completely abolished the fall in intracellular gefitinib levels after 24 h of treatment (Figure 7A) and the

intracellular appearance of the M1 metabolite (not shown).

To further demonstrate that a-NAP was able to maintain a high level of effective drug, Calu-3 cells were treated for 24 h with gefitinib in the presence or absence of a-NAP and then the medium was collected (conditioned media) and extracts from H322 cells exposed to conditioned media for 2 h were prepared to examine the inhibition of EGFR autophosphorylation by Western blot analysis. As shown in Figure 7B in H322 cells EGFR autophosphorylation was unaffected when cells were treated with gefitinib-conditioned medium collected from Calu-3 in the absence of a-NAP, in contrast when the inhibitor was present in the gefitinib-conditioned medium, EGFR autophosphorylation was completely inhibited. These results strongly suggest that in sensitive cells the metabolites released into the medium (low amount of M1 and other undetermined compounds) were ineffective in EGFR inhibition. The high and constant drug level inside the cells obtained in the presence of a-NAP maintained a significant inhibition of EGFR p44/42 MAPK and AKT phosphorylation even after a prolonged period (48 h) of treatment (Figure 7C) when compared with cells incubated with gefitinib alone.

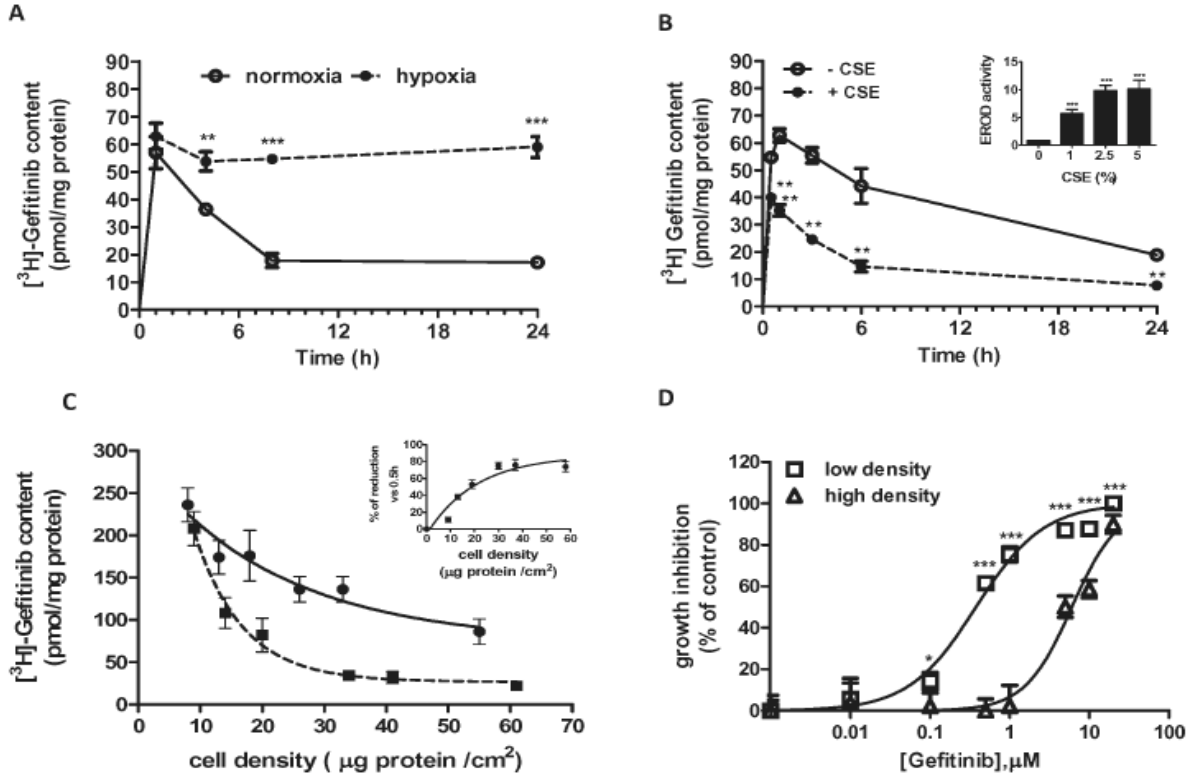

Figure 6. Conditions affecting gefitinib metabolism: hypoxia, cigarette smoke extract and cell density. (A) H322 cells were incubated with 0.1 µM [3H]gefitinib under normoxia or hypoxia for the indicated times. Values given of gefitinib content, expressed as pmol/mg of protein, are the means (± SD) of four independent determinations (**P < 0.01; ***P < 0.001). **(B)** Calu-3 cells were treated for 24 h with 2.5% of CSE and then exposed to 0.1 µM [3H]gefitinib for the indicated times. Values given are the means (± SD) of three independent determinations (**P < 0.01; ***P < 0.001). Inset: EROD assay performed in cells untreated or treated for 24 h with 1, 2.5 or 5% CSE expressed as pmol Res/mg protein/min. **(C)** Calu-3 cells were seeded at different cell density (from 7000 to 70000 cells/cm2) and after 24 h incubated for 0.5 h (●) or 24 h (■) with 0.1 µM [3H]gefitinib. Then, the intracellular [3H]gefitinib content was determined and plotted versus final cell density expressed as µg protein/cm2. Inset: values are expressed as % of reduction versus 0.5 h value. **(D)** Calu-3 seeded at low and high density (7000 and 70000 cells/cm2 respectively)were exposed for 72 h to different concentrations of gefitinib. Cell growth was assessed using crystal violet staining. Data are expressed as percent inhibition of cell proliferation versus control cells. The mean values of three independent measurements (± SD) are shown (*P < 0.05; ***P < 0.001).

Sensitive cell lines were then treated with gefitinib in the presence of 10 μM a-NAP for 72 h in order to evaluate the effects of CYP1A1 inhibition on efficacy of gefitinib in inhibiting cell proliferation. In the presence of the inhibitor the IC_{50} for gefitinib, evaluated by crystal violet staining (Figure 7D-F) and confirmed by cell counting and MTT assay (not shown), was reduced 15, 3 and 6 times in Calu-3, H322 and H292 cells respectively.

Overall, these results show that inhibition of CYP1A1 is associated with reduced gefitinib metabolism, increased intracellular gefitinib content and increased drug efficacy in cultured NSCLC cells.

DISCUSSION

The cytochrome P450 system consists of a large number of enzyme subfamilies involved in the oxidative metabolism of xenobiotics including drugs. They are expressed mainly in the liver, but extra-hepatic expression of a number of these enzymes does occur [31]. Although the primary site of gefitinib metabolism is the liver, tumor cell metabolism can significantly affect treatment effectiveness. However, to our knowledge, no studies have been performed addressing gefitinib metabolism in lung tumor cells.

The present study shows that the drop in gefitinib content observed in EGFR wild-type gefitinib-sensitive cell lines after 24 h of treatment was mainly due to gefitinib metabolism by CYP1A1 activity and not related to a time-dependent modification of influx or efflux processes. Our results indicate that there is a significant difference between gefitinib-sensitive and -resistant cell lines with regard to drug metabolism. Surprisingly, only sensitive cells were able to metabolize gefitinib and as a consequence, after 24 h of treatment, gefitinib disappeared both inside and outside the cells. The majority of radiolabeled gefitinib metabolites were present in the extracellular compartment as not well defined metabolites since we could barely detect the M1 metabolite and M2 or M3 were undetectable. In any case the metabolites present in the medium were not effective in inhibiting EGFR autophosphorylation as demonstrated by the conditioned medium experiment.

It has been reported that both gefitinib and its desmethyl metabolite (M3) formed through CYP2D6, inhibited with a similar potency and selectivity subcellular EGFR tyrosine kinase activity [32]. However, M3 was 15 times less active in a cell-based assay and consequently it was assumed that this metabolite was unlikely to contribute to the activity of gefitinib in vivo due to poor cell penetration.

On the contrary, when metabolites M1, M2 and M3 were tested in our responsive cell models at concentrations equivalent to that of gefitinib, they exhibited a significant inhibition of EGFR autophosphorylation and proliferation in intact cells, indicating their ability to enter cells and to interact with the catalytic domain of EGFR. Finally, in gefitinib resistant cell lines M1, M2 and M3 metabolites were poorly effective (IC_{50} > 20 μM in proliferation assay) indicating that at least these metabolites did not produce additive toxic effects in NSCLC cell lines.

In contrast to its abundant hepatic expression, CYP3A4 seems to play a minor role in lung metabolism, being expressed in only about 20% of cases [33]. Realtime PCR analysis confirmed the lack of expression of this isoform in our NSCLC cell models, as reported for A549 cells [34]. CYP2D6 was detected in all cell lines, whereas both CYP1A1 and CYP1A2 were expressed at significant levels in sensitive cells. Inducibility of CYP1A1 and CYP1A2 transcripts by gefitinib was clearly demonstrated in sensitive cell lines, while induction of CYP1A1 mRNA was not detected in resistant cell lines. EROD activity demonstrated a 3-6 fold induction of CYP1A1 elicited by gefitinib in sensitive cells. To the best of our knowledge, this is the first time that the

induction by gefitinib of relevant metabolic enzyme(s) has been demonstrated.

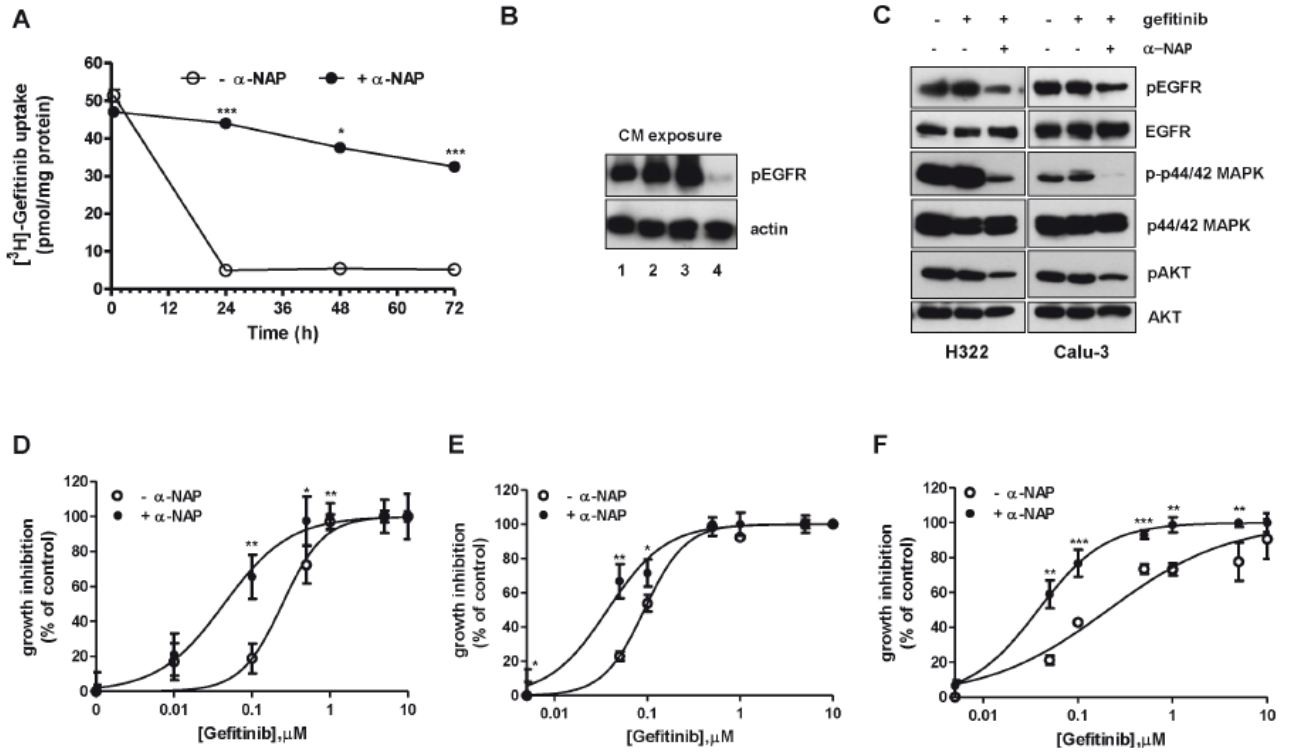

Figure 7. Effects of CYP1A1 inhibition on intracellular level of gefitinib, EGFR autophosphorylation and inhibition of cell growth. (A) Calu-3 cells were incubated with 0.1 μM [3H]gefitinib for 0.5, 24, 48 or 72 h in the absence or in the presence of 10 μM a-NAP. Values given of gefitinib content, expressed as pmol/mg of protein, are the means (± SD) of four independent determinations. a-NAP was renewed after 36 h of gefitinib treatment. (***P < 0.001). **(B)** Calu-3 cells were treated with 0.1 μM gefitinib for 24 h in the absence or in the presence of 10 μM a-NAP, then the conditioned media (CM) were collected and extracts were prepared from H322 cells exposed for 2 h to CM. The effect of CM on EGF (0.1 μg/ml for 5 min)-induced EGFR autophosphorylation was examined by Western blotting using monoclonal antibodies directed against pEGFR(Tyr1068) and actin. The experiment, repeated twice, yielded similar results. Line 1: CM from control cells; line 2: CM from gefitinib treated cells; line 3: CM from a-NAP treated cells; line 4: CM from a-NAP and gefitinib treated cells. **(C)** H322 and Calu-3 cells were incubated for 48 h with 0.1 μM gefitinib in the absence or in the presence of 10 μM a-NAP. Before protein extraction cells were stimulated with 0.1 μg/ml EGF for 5 min. Western blot analysis was performed by using monoclonal antibodies directed against pEGFR(Tyr1068), EGFR, p-p44/42 MAPK, p44/42 MAPK, pAKT (Ser473), AKT. The experiment, repeated three times, yielded similar results. a-NAP was renewed after 24 h of gefitinib treatment. **(D)** Calu-3, **(E)** H322, **(F)** H292 were exposed for 72 h to different concentrations of gefitinib in the absence or in the presence of 10 μM a-NAP. Cell growth was assessed using crystal violet staining as described in Materials and Methods. Data are expressed as percent inhibition of cell proliferation versus control cells. The mean values of three independent measurements (± SD) are shown. a-NAP was renewed after 36 h of gefitinib treatment (*P < 0.05; **P < 0.01; ***P < 0.001).

The reason why gefitinib induces CYP expression and activity only in sensitive cells could be ascribed to the ability of gefitinib to inhibit EGFR downstream signal transduction pathway. It has been recently demonstrated that EGF represses the dioxin-mediated induction of CYP1A1 in normal human keratinocytes preventing recruitment of the p300 coactivator [35]. Therefore, EGFR signalling is a repressor of the aryl hydrocarbon receptor and regulates the transcription of numerous genes including CYP1A1. In this context, EGFR inhibitors such as gefitinib, erlotinib, lapatinib or cetuximab might affect the induction of CYP1A1 in those cell types in which the drug effectively inhibits signalling controlled by EGFR. The inhibition of MAPK pathway might represent a link between EGFR inhibition and CYP1A1 induction since PD98059 and U0126, well known MEK1/2 inhibitors, induced CYP1A1 activity as did gefitinib in H322 cells, while none of

PI3K/AKT/mTOR inhibitors tested was effective. It is noteworthy that constitutive activation of signaling pathways downstream of EGFR is a recognized mechanism or resistance against reversible EGFR tyrosine kinase inhibitors [5].

We surmise that gefitinib metabolism is a consequence and not the cause of drug responsiveness and might be useful for early evaluation of response to gefitinib in tumor lacking activating mutations.

Since CYP1A1 inducibility strongly correlates with CYP1A1 gene polymorphism [36] we also tested the genotypic asset of our cell lines regarding the two main polymorphic forms of CYP1A1 (CYP1A1*2A and CYP1A1*2C). All the tested cell lines carried a wild type homozygous genotype for both the polymorphisms and so we can exclude that different genotypes are involved in the different capability of metabolizing gefitinib.

The role of CYP1A1 polymorphism as a predictor of clinical outcome to EGFR-TKIs in patients with advanced lung cancer has very recently been reported [37]. The authors note that CYP1A1*2A polymorphism correlates with the response to EGFR-TKIs of NSCLC, wild type T/T patients having an improved response of inhibitors versus T/C and C/C alleles.

Studies have shown that the hepatic metabolism of gefitinib is primarily catalyzed via CYP3A4, consequently the effects of known inducers (phenytoin, carbamezepine, rifampicin) and inhibitors (ketoconazole, itraconazole, erythromycin and claritromycin) of CYP3A4 activity have been investigated [6].

Our results indicate that, in NSCLC cells metabolizing gefitinib, CYP1A1 inhibition could lead to increased local exposure to the active drug. In fact, inhibition by a-naphthoflavone was associated with lower gefitinib metabolism and consequently with a prolonged exposure to locally active drug. This leads to enhanced inhibition of EGFR, MAPK and AKT phosphorylation and cell proliferation, with the result of reduced IC_{50} for gefitinib in proliferation assays of EGFR wild-type NSCLC cell lines.

From a medicinal chemistry perspective, these results stress the importance of considering drug pharmacokinetics at the intratumoral cellular level, focusing on the roles of transport and metabolism in the target cells. While the structure of gefitinib makes it a substrate of transporters [9], thus enhancing its activity toward intracellular targets, it also harbors metabolic liabilities in tumor cells. From this point of view, its interaction with CYP3A4 seems mainly related to total-body exposure gefitinib, while CYP1A1 is mainly responsible of its metabolism in tumor cells. A program of structural optimization should thus consider the effects of structure modulation on all these processes in combination.

In addition, a strategy of increasing gefitinib activity by using specific CYP inhibitors, could be pursued in the context of optimizing the use of gefitinib for the treatment of EGFR wild-type gefitinib-sensitive tumors.

Interstitial lung disease (ILD) has been reported as a serious adverse effect of gefitinib treatment [38]. The incidence of acute ILD during gefitinib treatment varies between different ethnic groups occurring more frequently in Japanese patients (4%-6%) than in Caucasian (0.2-0.3%) [39]. Although the precise mechanism of ILD induced by gefitinib remains unknown, it has been proposed that bioactivation of gefitinib by CYP1A1 in the lung may be related to the risk of developing ILD mainly in smokers [8]. In this context the optimisation of CYP1A1 inhibition may not only improve gefitinib efficacy but even reduce the incidence of ILD.

ACKNOWLEDGEMENTS

This work was supported by: Associazione Italiana per la Ricerca sul Cancro (AIRC), Milan grant IG 8856; AstraZeneca SpA Basiglio (MI); Associazione Augusto per la vita (Novellara, RE); Associazione Davide Rodella, Montichiari, BS; Ministero della Salute (Programma straordinario di ricerca oncologica 2006) Regione Emilia Romagna; Associazione Marta Nurizzo, Brugherio MI; Associazione Chiara Tassoni, Parma; A.VO.PRO.RI.T., Parma.

REFERENCES

1. Cataldo VD, Gibbons DL, Perez-Soler R, Quintas-Cardama A: Treatment of non-small-cell lung cancer with erlotinib or gefitinib. N Engl J Med 2011, 364:947-955.
2. Douillard JY, Shepherd FA, Hirsh V, Mok T, Socinski MA, Gervais R, Liao ML, Bischoff H, Reck M, Sellers MV, et al: Molecular predictors of outcome with gefitinib and docetaxel in previously treated non-small-cell lung cancer: data from the randomized phase III INTEREST trial. J Clin Oncol 2010, 28:744-752.
3. Hirsch FR, Varella-Garcia M, Bunn PA Jr, Franklin WA, Dziadziuszko R, Thatcher N, Chang A, Parikh P, Pereira JR, Ciuleanu T, et al: Molecular predictors of outcome with gefitinib in a phase III placebo-controlled study in advanced non-small-cell lung cancer. J Clin Oncol 2006, 24:5034-5042.
4. Janne PA, Gray N, Settleman J: Factors underlying sensitivity of cancers to small-molecule kinase inhibitors. Nat Rev Drug Discov 2009, 8:709-723.
5. Engelman JA, Janne PA: Mechanisms of acquired resistance to epidermal growth factor receptor tyrosine kinase inhibitors in non-small cell lung cancer. Clin Cancer Res 2008, 14:2895-2899.
6. van Erp NP, Gelderblom H, Guchelaar HJ: Clinical pharmacokinetics of tyrosine kinase inhibitors. Cancer Treat Rev 2009, 35:692-706.
7. Huang Y, Sadee W: Membrane transporters and channels in chemoresistance and -sensitivity of tumor cells. Cancer Lett 2006, 239:168-182.
8. Li X, Kamenecka TM, Cameron MD: Bioactivation of the epidermal growth factor receptor inhibitor gefitinib: implications for pulmonary and hepatic toxicities. Chem Res Toxicol 2009, 22:1736-1742.
9. Galetti M, Alfieri RR, Cavazzoni A, La Monica S, Bonelli M, Fumarola C, Mozzoni P, De Palma G, Andreoli R, Mutti A, et al: Functional characterization of gefitinib uptake in non-small cell lung cancer cell lines. Biochem Pharmacol 2010, 80:179-187.
10. Swaisland HC, Cantarini MV, Fuhr R, Holt A: Exploring the relationship between expression of cytochrome P450 enzymes and gefitinib pharmacokinetics. Clin Pharmacokinet 2006, 45:633-644.
11. McKillop D, McCormick AD, Millar A, Miles GS, Phillips PJ, Hutchison M: Cytochrome P450-dependent metabolism of gefitinib. Xenobiotica 2005, 35:39-50.
12. Li J, Zhao M, He P, Hidalgo M, Baker SD: Differential metabolism of gefitinib and erlotinib by human cytochrome P450 enzymes. Clin Cancer Res 2007, 13:3731-3737.
13. McKillop D, Hutchison M, Partridge EA, Bushby N, Cooper CM, Clarkson-Jones JA, Herron W, Swaisland HC: Metabolic disposition of gefitinib, an epidermal growth factor receptor tyrosine kinase inhibitor, in rat, dog and man. Xenobiotica 2004, 34:917-934.
14. McKillop D, McCormick AD, Miles GS, Phillips PJ, Pickup KJ, Bushby N, Hutchison M: In vitro metabolism of gefitinib in human liver microsomes. Xenobiotica 2004, 34:983-1000.
15. Androutsopoulos VP, Tsatsakis AM, Spandidos DA: Cytochrome P450 CYP1A1: wider roles in cancer progression and prevention. BMC Cancer 2009, 9:187.
16. Bieche I, Narjoz C, Asselah T, Vacher S, Marcellin P, Lidereau R, Beaune P, de Waziers I: Reverse transcriptase-PCR quantification of mRNA levels from cytochrome (CYP)1, CYP2 and CYP3 families in 22 different human tissues. Pharmacogenet Genomics 2007, 17:731-742.
17. Thum T, Erpenbeck VJ, Moeller J, Hohlfeld JM, Krug N, Borlak J: Expression of xenobiotic metabolizing enzymes in different lung compartments of smokers and nonsmokers. Environ Health Perspect 2006, 114:1655-1661.
18. La Monica S, Galetti M, Alfieri RR, Cavazzoni A, Ardizzoni A, Tiseo M, Capelletti M, Goldoni M, Tagliaferri S, Mutti A, et al: Everolimus restores gefitinib sensitivity in resistant non-small cell lung cancer cell lines. Biochem Pharmacol 2009, 78:460-468.
19. Carp H, Janoff A: Possible mechanisms of emphysema in smokers. In vitro suppression of serum elastase-inhibitory capacity by fresh cigarette smoke and its prevention by antioxidants. Am Rev Respir Dis 1978, 118:617-621.
20. Drakoulis N, Cascorbi I, Brockmoller J, Gross CR, Roots I: Polymorphisms in the human CYP1A1 gene as susceptibility factors for lung cancer: exon-7 mutation (4889 A to G), and a T to C mutation in the 3'-flanking region. Clin Investig 1994, 72:240-248.
21. Hayashi SI, Watanabe J, Nakachi K, Kawajiri K: PCR detection of an A/G polymorphism within exon 7 of the CYP1A1 gene. Nucleic Acids Res 1991, 19:4797.
22. Cavazzoni A, Alfieri RR, Carmi C, Zuliani V, Galetti M, Fumarola C, Frazzi R, Bonelli M, Bordi F, Lodola A, et al: Dual mechanisms of action of the 5-benzylidene-hydantoin UPR1024 on lung cancer cell lines. Mol Cancer Ther 2008, 7:361-370.
23. Alfieri RR, Bonelli MA, Cavazzoni A, Brigotti M, Fumarola C, Sestili P, Mozzoni P, De Palma G, Mutti A, Carnicelli D, et al: Creatine as a compatible osmolyte in muscle cells exposed to hypertonic stress. J Physiol 2006, 576:391-401.
24. Kennedy SW, Jones SP: Simultaneous measurement of cytochrome P4501A catalytic activity and total protein concentration with a fluorescence plate reader. Anal Biochem 1994, 222:217-223.
25. Ozvegy-Laczka C, Hegedus T, Varady G, Ujhelly O, Schuetz JD, Varadi A, Keri G, Orfi L, Nemet K, Sarkadi B: High-affinity interaction of tyrosine kinase inhibitors with the ABCG2 multidrug transporter. Mol Pharmacol 2004, 65:1485-1495.
26. Shimada T, Gillam EM, Sutter TR, Strickland PT, Guengerich FP, Yamazaki H: Oxidation of xenobiotics by recombinant human cytochrome P450 1B1. Drug Metab Dispos 1997, 25:617-622.
27. Doostdar H, Burke MD, Mayer RT: Bioflavonoids: selective substrates and inhibitors for cytochrome P450 CYP1A and CYP1B1.

Toxicology 2000, 144:31-38.

28. Shimada T, Yamazaki H, Foroozesh M, Hopkins NE, Alworth WL, Guengerich FP: Selectivity of polycyclic inhibitors for human cytochrome P450s 1A1, 1A2, and 1B1. Chem Res Toxicol 1998, 11:1048-1056.
29. Dubey RK, Gillespie DG, Zacharia LC, Barchiesi F, Imthurn B, Jackson EK: CYP450- and COMT-derived estradiol metabolites inhibit activity of human coronary artery SMCs. Hypertension 2003, 41:807-813.
30. Fradette C, Du Souich P: Effect of hypoxia on cytochrome P450 activity and expression. Curr Drug Metab 2004, 5:257-271.
31. van Schaik RH: CYP450 pharmacogenetics for personalizing cancer therapy. Drug Resist Updat 2008, 11:77-98.
32. McKillop D, Guy SP, Spence MP, Kendrew J, Kemp JV, Bushby N, Wood PG, Barnett S, Hutchison M: Minimal contribution of desmethyl-gefitinib, the major human plasma metabolite of gefitinib, to epidermal growth factor receptor (EGFR)-mediated tumour growth inhibition. Xenobiotica 2006, 36:29-39.
33. Anttila S, Hukkanen J, Hakkola J, Stjernvall T, Beaune P, Edwards RJ, Boobis AR, Pelkonen O, Raunio H: Expression and localization of CYP3A4 and CYP3A5 in human lung. Am J Respir Cell Mol Biol 1997, 16:242-249.
34. Hukkanen J, Lassila A, Paivarinta K, Valanne S, Sarpo S, Hakkola J, Pelkonen O, Raunio H: Induction and regulation of xenobioticmetabolizing cytochrome P450s in the human A549 lung adenocarcinoma cell line. Am J Respir Cell Mol Biol 2000, 22:360-366.
35. Sutter CH, Yin H, Li Y, Mammen JS, Bodreddigari S, Stevens G, Cole JA, Sutter TR: EGF receptor signaling blocks aryl hydrocarbon receptormediated transcription and cell differentiation in human epidermal keratinocytes. Proc Natl Acad Sci USA 2009, 106:4266-4271.
36. Zhou SF, Liu JP, Chowbay B: Polymorphism of human cytochrome P450 enzymes and its clinical impact. Drug Metab Rev 2009, 41:89-295.
37. Nie Q, Yang XN, An SJ, Zhang XC, Yang JJ, Zhong WZ, Liao RQ, Chen ZH, Su J, Xie Z, Wu YL: CYP1A1*2A polymorphism as a predictor of clinical outcome in advanced lung cancer patients treated with EGFR-TKI and its combined effects with EGFR intron 1 (CA)n polymorphism. Eur J Cancer 2011, 47:1962-1970.
38. Inoue A, Saijo Y, Maemondo M, Gomi K, Tokue Y, Kimura Y, Ebina M, Kikuchi T, Moriya T, Nukiwa T: Severe acute interstitial pneumonia and gefitinib. Lancet 2003, 361:137-139.
39. Kudoh S, Kato H, Nishiwaki Y, Fukuoka M, Nakata K, Ichinose Y, Tsuboi M, Yokota S, Nakagawa K, Suga M, et al: Interstitial lung disease in Japanese patients with lung cancer: a cohort and nested case-control study. Am J Respir Crit Care Med 2008, 177:1348-1357.

Chapter 10

Combined use of anti-ErbB mAbs and erlotinib enhances antibody-dependent cellular cytotoxicity of wild-type EGFR erlotinib-sensitive NSCLC cell lines

Cavazzoni A, Alfieri RR, Cretella D, Saccani F, Ampollini L, Galetti M, Quaini F, Graiani G, Madeddu D, Mozzoni P, Galvani E, La Monica S, Bonelli M, Fumarola C, Mutti A, Carbognani P, Tiseo M, Barocelli E, Petronini PG & Ardizzoni A

MOLECULAR CANCER 2012

11(1):91.

ABSTRACT

Background: The epidermal growth factor receptor (EGFR) is an established target for anti-cancer treatment in different tumour types. Two different strategies have been explored to inhibit this pivotal molecule in epithelial cancer development: small molecules TKIs and monoclonal antibodies. ErbB/HER-targeting by monoclonal antibodies such as cetuximab and trastuzumab or tyrosine-kinase inhibitors as gefitinib or erlotinib has been proven effective in the treatment of advanced NSCLC

Results: In this study we explored the potential of combining either erlotinib with cetuximab or trastuzumab to improve the efficacy of EGFR targeted therapy in EGFR wild-type NSCLC cell lines. Erlotinib treatment was observed to increase EGFR and/or HER2 expression at the plasma membrane level only in NSCLC cell lines sensitive to the drug inducing protein stabilization. The combined treatment had marginal effect on cell proliferation but markedly increased antibody-dependent, NK mediated, cytotoxicity in vitro. Moreover, in the Calu-3 xenograft model, the combination significantly inhibited tumour growth when compared with erlotinib and cetuximab alone.

Conclusion: Our results indicate that erlotinib increases surface expression of EGFR and/or HER2 only in EGFR-TKI sensitive NSCLC cell lines and, in turns, leads to increased susceptibility to ADCC both in vitro and in a xenograft models. The combination of erlotinib with monoclonal antibodies represents a potential strategy to improve the treatment of wild-type EGFR NSCLC patients sensitive to erlotinib.

INTRODUCTION

The epidermal growth factor receptor (EGFR, ErbB1, HER1) is the prototypic member of the ErbB family of receptor tyrosine kinases (TKs), which further consists of ErbB2-4 (HER2-4). The ErbB receptors share a similar protein structure, consisting of an extracellular ligand binding domain, a single transmembrane domain and an intracellular C-terminal domain with tyrosine kinase activity [1]. Upon specific binding of EGF-like ligands to the extracellular domain, ErbB receptors dimerize, either as homo- or heterodimers, and undergo autophosphorylation at specific tyrosine residues within the intracellular domain. The phosphorylated tyrosines serve as docking sites for adapter molecules, such as Grb2 and the p85 subunit of PI3K, which activate a complex downstream network. The activated signaling pathways, including the Ras/MAPK, Akt/mTOR kinase and STAT cascades, in turn regulate transcription factors and other proteins involved in cell proliferation, survival, motility and differentiation [2]. Two main strategies targeting ErbB receptors have been developed: small-molecule inhibitors of the tyrosine kinase domain (EGFR tyrosine kinase inhibitors [TKIs], such as erlotinib and gefitinib), and monoclonal antibodies (such as cetuximab, anti-EGFR and trastuzumab, anti-HER2), directed against the extracellular domain, which inhibit phosphorylation/activation and promote internalization. EGFR and HER2 are overexpressed in 40-80% and 25-30%, respectively, of non-small cell lung cancer (NSCLC) patients and their overexpression has been frequently correlated with a poor prognosis [3,4].

Erlotinib is an effective treatment for NSCLC patients and has been registered as a second and third-line treatment of NSCLC regardless of EGFR mutation status [5].

Gefitinib has been registered for the therapy of advanced NSCLC harbouring activating EGFR mutations in the tyrosine kinase domain, the most frequent being L858R in exon 21 and Del (746-750) in exon 19 [6]. Although mutations in EGFR are useful predictors for the activity of EGFR-TKI, they cannot be used as the only criterion to determine who should receive anti-EGFR therapy and it is becoming increasingly clear that even patients with EGFR wild-type can benefit from EGFR-TKI [5,7,8].

Cetuximab is a chimeric IgG1 monoclonal antibody (mAb) that blocks ligand binding to EGFR, leading to a decrease in receptor dimerization, autophosphorylation, and activation of signaling pathways [9]. In addition the binding of cetuximab initiates EGFR internalization and degradation which leads to signal termination. Moreover, unlike EGFR-TKIs, cetuximab can induce antibody dependent cellular cytotoxicity (ADCC) activity, an important immunologic antitumour effect. Cetuximab in combination with chemotherapy has been approved by the FDA for the treatment of metastatic colorectal cancer and of locally advanced head and neck cancer.

Two randomized phase III trials in NSCLC patients, evaluating cetuximab in addition to first-line chemotherapy, showed a small benefit in overall survival for the experimental treatment, which was considered insufficient by the EMA for marketing approval [10,11]. However, a subgroup analysis of the FLEX phase III trial recently demonstrated a larger survival benefit from the experimental treatment in patients with high immunohistochemical EGFR expression [12].

Trastuzumab, registered for the treatment of HER2 positive breast cancer, has also been tested in phase II trials as a single agent and in combination with cytotoxic chemotherapy for patients with NSCLC. These trials have not yet produced any convincing evidence of an improved antitumour activity by adding

trastuzumab to standard chemotherapy in NSCLC [13,14].

Several preclinical studies on cell lines from different tumour types indicated that the association between EGFR/HER2 mAbs with TKIs displays an increased efficacy [15].

In this study we explored the potential of combining erlotinib with either cetuximab or trastuzumab in order to improve the efficacy of EGFR targeted therapy in EGFR wild-type sensitive NSCLC cell lines. Our results indicate that EGFR-TKI increases surface expression of EGFR and/or HER2 only in erlotinib sensitive NSCLC cell lines and, in turns, leads to increased susceptibility to ADCC both in vitro and in xenograft models.

MATERIALS AND METHODS

Cell Culture

The human NSCLC cell lines H322, H292, Calu-3, H1299, A549, H1703 and Calu-1 were obtained from American Type Culture Collection (Manassas, VA, USA) and were cultured as recommended. The PC9, HCC827 and HCC827GR5 cell lines were kindly provided by Dr P. Jänne (Dana-Farber Cancer Institute, Boston MA). All cells were maintained under standard cell culture conditions at 37°C in a water-saturated atmosphere of 5% CO_2 in air. As previously reported [31] cells showing by proliferation assays IC_{50} for erlotinib<1μM were considered sensitive (H322, H292, Calu-3, PC9, HCC827) while cell lines with IC_{50}>5 μM (H1299, A549, H1703, Calu-1, HCC827GR5) were considered resistant.

Drug treatment

Erlotinib, gefitinib, cetuximab, trastuzumab and rituximab were from inpatient pharmacy. RAD001, NVP-BKM-120 and NVP-BYL-719 were from Novartis. Stock solutions of 20 mM drugs were prepared in dimethylsulfoxide (DMSO) (with the exception of mAbs), stored at -20°C and diluted in fresh medium for use. The final concentration of DMSO never exceeded 0.1% v/v.

Western blot analysis

Procedures for protein extraction, solubilization, and protein analysis by 1-D PAGE are described elsewhere [32,33]. Fifty μg of proteins from lysates were resolved by 7.5% SDS-PAGE and transferred to nitrocellulose membranes. Membranes were incubated with: 1:1000 rabbit polyclonal anti-EGFR; 1:1000 rabbit mAb anti-HER2/ErbB2; 1:1000 rabbit mAb anti-Phospho-p70S6K (Thr421/Ser424); 1:1000 mouse mAb anti-Phospho-p44/42 MAPK (ERK1/2); 1:1000 rabbit mAb anti-p44/42 MAPK (ERK1/2) (Cell Signaling Technology, Beverly, MA, USA); 1:1000 mouse mAb anti- Transferrin Receptor (Invitrogen Corporation, Camarillo, CA, USA); 1:3000 mouse mAb anti-Actin (Sigma–Aldrich, St Louis, MO, USA). Blots were then washed and incubated with HRP-anti-mouse or HRP-anti-rabbit antibodies at 1:20000 dilution (Pierce, Rockford, IL, USA). Immunoreactive bands were visualized using an enhanced chemiluminescence system (ImmobilionTM Western Cemiluminescent HRP Substrate, Millipore USA).

Cell surface protein isolation

Calu-3 cells were grown in T75 flasks and treated with 0.5 μM erlotinib for 24 h. Cells were incubated with EZ-LINK Sulfo-Biotin (Pierce) for 2 h at 4 °C with gentle rotation. The reaction was stopped by washing

twice with 25 mM Tris-HCl (pH 7.5) in PBS (phosphate-buffered saline) and cells were scraped into ice-cold lysis buffer (50 mmol/l HEPES, pH 7.0, 10% glycerol, 1% TritonX-100, 5 mmol/l EDTA (ethylenediaminetetraacetic acid), 1 mmol/l $MgCl_2$, 25 mmol/l NaF, 50 µg/ml leupeptin, 50 µg/ml aprotinin, 0.5 mmol/l orthovanadate, and 1 mmol/l phenylmethylsulfonyl fluoride). Lysates were centrifuged at 15000 g for 20 min at 4 °C, and supernatants were removed and assayed for protein concentration using the Dc Protein assay (Bio-Rad, CA, USA). A volume of 500 µl of lysis buffer containing equal amount of proteins was incubated with UltraLink Immobilized NeutrAvidin protein (Pierce) for 2 h at 4 °C with gentle rotation, washed three times with lysis buffer before suspension in SDS (sodium dodecyl sulfate)-loading buffer and then resolved by SDS-PAGE.

Flow Cytometry

For the determination of EGFR and HER2 protein membrane levels, NSCLC cell lines H322, Calu-3 and H292 were treated with 1 µM erlotinib for 24h. One million cells per condition were then incubated with Isotype control Monoclonal Mouse IgG1/R-PE (Ancell IRP, Bayport, MN, USA), PE mouse anti-Human EGFR (Calu-3 and H322 cells) (BD Biosciences, San Josè, CA, USA) or PE mouse anti-Human HER2 (H322 and H292) (BD Biosciences). After the incubation the analysis was performed with an EPICS-XL flow cytometer.

For the relative quantization of EGFR or HER2 binding sites, NSCLC cell lines H322, Calu-3, H292 were treated with 1 µM erlotinib for 24h. One million cells were then dispensed for each condition and treated with either 20 µg/ml rituximab (Isotype control), cetuximab (Calu-3 and H322) or trastuzumab (H292) for 1h. After the incubation with PE-anti-human-IgG (BD Biosciences), the analysis was performed with an EPICS-XL flow cytometer.

The values of mean fluorescence intensity (MFI) were converted in units of equivalent fluorochrome (MEF) using the FluoroSpheres 6-Peak Kit (Dako, CA, USA).

Quantitative Real-Time PCR

Total RNA was isolated by the TRIzol® reagent (Invitrogen, Carlsbad, CA, USA) and reverse transcribed as previously described [33]. The transcript levels of EGFR gene were assessed by Real-Time qRT-PCR on an iCycler iQ Multicolor RealTime PCR Detection System (Bio-Rad, Hercules, CA, USA).

Primers and probes included: EGFR-F (5'-GCCTTGACTGAGGACAGCA-3'), EGFR-R (5-TTTGGGAACGGACTGGTTTA-3), EGFR-probe (5'-FAM CTTCCTCC3'DQ); PGK1-F (5'-GGAGAACCTCCGCTTTCAT-3'), PGK1-R (5'-CTGGCTCGGCTTTAACCTT-3'), PGK1-probe (5'-FAM GGAGGAAG 3'DQ); RPL13-F (5'-ACAGCTGCTCAGCTTCACCT-3'), RPL13-R (5'-TGGCAGCATGCCATAAATAG-3'), RPL13-probe (5'-FAMCAGTGGCA3'DQ); HPRT-F (5'-TGACCTTGATTTATTTTGCATACC-3'), HPRT-R (5'CGAGCAAGACGTTCAGTCCT-3'), HPRT-probe (5'-FAM GCTGAGGA 3'DQ).

The amplification protocol consisted of 15 min at 95°C followed by 40 cycles at 94°C for 20s and at 60°C for 1 min. The relative transcript quantification was calculated using the geNorm algorithm for Microsoft ExcelTM after normalization by expression of the control genes [phosphoglycerate kinase1 (PGK1), ribosomal protein L13 (RPL13) and hypoxanthine-guanine-phosphoribosyltransferase (HPRT)] and

expressed in arbitrary units (a.u.).

MTT Assay

The cells were seeded into 96-well plate in quadruplicate and were exposed to various treatments. After 72 h, 100 µl of 3-(4,5-dimethylthiazol-2-yl)-2,5 diphenyltetrazolium bromide (MTT) solution (1 mg/ml, Sigma-Aldrich) was added to each well and incubated. After 4 h, crystalline formation was dissolved with DMSO and the absorbance at 570 nm was measured using the microplate-reader 550 (BioRad).

Isolation and culture of NK cells

Human PBMC were isolated from buffy coat of healthy donors by using a Lympholyte-H density gradient centrifugation (Cederlane Burlington, Ontario, Canada). Highly purified CD56+ natural killer (NK) cells were obtained by magnetic separation using the NK Cell Isolation Kit and the autoMACS Separator (Miltenyi Biotec, Cologne, Germany) according to the user manual.

Purified NK cells were resuspended in culture medium (RPMI 1640 without phenol red and supplemented with heat inactivated 10% FCS, 50 U/ml penicillin, 50 U/ml streptomycin, 2 mmol/l glutamine) plated and preincubated at 37 °C for up to18 h in the presence of human Interleukin-2 (IL-2, 100 U/ml, Miltenyi Biotec).

ADCC assay

Antibody-dependent cell-mediated cytotoxicity (ADCC) was measured with the CytoTox 96 non-radioactive cytotoxicity assay (Promega, Madison, WI, USA) according to manufacturer's instructions. $2x10^3$ Calu-3, H322, H292 or H1299 cells were treated for 24 h with 1 µM erlotinib, and then seeded with purified NK cells (ratio of 1:25 and 1:50) in a 96-well plate and incubated with 10 µg/ml cetuximab or trastuzumab. After 4 hours the lactate dehydrogenase (LDH) release was determined and the percentage of cytotoxicity was calculated after correcting for background absorbance values according to the following formula:

$$\% \text{ Cytotoxicity} = \frac{\text{Experimental - Effector spontaneous - Target spontaneous}}{\text{Target maximum - Target spontaneous}} \times 100$$

Tumour xenografts

All experiments involving animals were performed in accordance with Guiding Principles in the Care and Use of Animals (DL117/92). Twenty-four Balb/c-Nude female mice (Charles River Laboratories, Calco, Italy) were housed in a protected unit for immunodeficient animals with 12-hour light/dark cycles and provided with sterilized food and water ad libitum. At the time of xenograft establishment, mice were 8 weeks old and weighted ~20g. 200 µl of matrigel (BD Biosciences) and sterile PBS (1:1) containing $1x10^7$ Calu3 cells, were subcutaneously injected on the right flank of each mouse (using a 1ml syringe, needle G25). When tumour volume reached an average size of 300 mm^3, 14 days after injection, animals were randomized into four groups and the treatment started. After 4 weeks, mice were euthanized by cervical dislocation and tumours collected for immunohistochemistry and histological analysis.

Erlotinib (25mg/Kg) was administered orally in 1% methylcellulose, 0.2% Tween 80 in sterilized water 5 days/week. Cetuximab (2mg/Kg) was intraperitoneally injected in sterile saline solution 2 days/week. Control group received both oral gavage of 1% methylcellulose, 0.2% Tween 80 in sterilized water 5 days/week and i.p. injection of sterile saline solution (0.9%) 2 days/week.

Dosages of drugs were chosen halving the one used in a previous study in NSCLC-xenograft models, in order to avoid the complete inhibition of tumour growth by the single agent treatment and to better highlight the effect of erlotinib-cetuximab combination [19,34].

Tumour xenografts were measured twice a week, tumour volume was determined using the formula: (length x width^2)/2. Final data are expressed as percent of volume increase: (tumour volume/pre-treatment tumour volume) x 100.

Morphometric and Immunohistochemical Analysis of Tumour Xenografts

Formalin fixed samples were embedded in paraffin. From each tumour serial sections of 5 µm thickness were obtained and stained with Haematoxylin and Eosin (H&E), Masson's Trichrome and for immunohistochemistry. Morphometric analysis was performed in order to evaluate: (a) the numerical density of neoplastic cells, (b) the volume fraction of interstitial inflammatory cells, (c) the volume fraction of fibrosis and (d) the fraction of proliferating and apoptotic cells.

In particular, for each section stained with H&E, a quantitative evaluation of tissue composition was performed. To better define the fraction occupied by neoplastic and non-neoplastic cells, sections were stained with pancytokeratin antibodies (monoclonal mouse, 1:500, o.n. 4°C, Dako) revealed through biotin-streptavidin-DAB system, as repeatedly described. The numerical density (n/mm^2) of pancytokeratin positive neoplastic cells was computed.

In addition, cell proliferation and apoptotic death were investigated by fluorescence microscopy. Thus, Ki67 labeling (rabbit polyclonal antibody, Vector) and the Terminal deoxynucleotidyltransferase (TdT)–mediated dUTP nick end labeling (TUNEL) assay (Roche Diagnostics, Italy) on cytokeratinpos neoplastic cells were revealed by specific fuorescent probes.

The area occupied by interstitial cells was expressed as percentage of the total area explored. By the same approach, the volume fraction of fibrosis was calculated on Masson's Trichrome stained sections. To define the volume fractions, the number of points overlying each tissue components was counted and expressed as percentage of the total number of points explored.

All these morphometric measurements were obtained with the aid of a grid defining a tissue area of 0.23 mm^2 and containing 42 sampling points each covering an area of 0.0052 mm^2.

All these evaluations were performed on the entire section of each tumour sample of each experimental group of animals using an optical microscope (250X final magnification).

Statistical analysis

Statistical analyses were carried out using GraphPad Prism version 5.00 software (GraphPad Software Inc., San Diego, CA). Results are expressed as mean values ± standard deviations (SD) for the indicated number of independent measurements. Differences between the mean values recorded for different

experimental conditions were evaluated by Student's t-test, and P values are indicated where appropriate in the figures and in their legends. A P value <0.05 was considered as significant.

For *in vivo* studies comparison among groups was made using analysis of variance (two-way ANOVA repeated measures) followed by Bonferroni's post-test. Analysis was performed using Prism 5.0 (GraphPad Software) and differences were considered significant when P value was below 0.05. The nature of the interaction between erlotinib and cetuximab was calculated using the Bliss interaction model [35].

RESULTS

Differential effects of Erlotinib on EGFR and HER2 expression in sensitive and resistant NSCLC cell lines.

Firstly, we evaluated the effect of erlotinib on total EGFR and HER2 protein levels in sensitive NSCLC cell lines (Calu-3, H322 and H292 cell lines carrying wild-type EGFR; PC9 and HCC827 carrying EGFR E746-A750del mutation) and in resistant cell lines (A549, H1299, H1703 and Calu-1 intrinsically resistant carrying wild-type EGFR; HCC827GR5 with MET amplification as mechanism of acquired resistance to TKI) [16]. As shown in Figure 1A, erlotinib induced accumulation of EGFR protein in Calu-3 and H322 cells while HER2 accumulated in H322, H292, PC9 and HCC827 cells in a dose-dependent manner. The EGFR/Actin and HER2/Actin ratios obtained after treatment at 1 μM or 10 nM erlotinib were calculated and values expressed as fold differences versus control (Figure 1B). In contrast, EGFR and HER2 protein accumulation was not observed in any cancer cell line with intrinsic resistance to EGFR inhibitors until the concentration of 10 μM. Indeed the ratios EGFR/Actin or HER2/Actin were similar or even lower than those calculated in untreated cells (Figure 1C) and similar results were obtained with gefitinib (not shown). A representative Western blotting of resistant H1299 cell line is reported in Figure 1D.

The different effect of TKIs on HER2 expression between sensitive and resistant NSCLC cell lines was confirmed in the HCC827 parental and in the HCC827GR5 resistant clone treated for 48 h with gefitinib (Figure 1E).

Erlotinib increases the cell surface expression of EGFR and HER2 in erlotinib sensitive NSCLC cell lines

EGFR and HER2 expression on the plasma membrane was quantified by flow cytometry in sensitive EGFR wild-type NSCLC cell lines Calu-3, H322 and H292 after exposure to 1 μM erlotinib for 24 h. The drug enhanced surface expression calculated as molecules of equivalent soluble fluorophore of EGFR in Calu-3 (Figure 2A), H322 (Figure 2C, 2D), and of HER2 in H292 (Figure 2B) and H322 (Figure 2C, 2D) cell lines. In H322 cell line, the increase in EGFR and HER2 surface expression was dose and time dependent (Figure 2C, 2D). Western blot analysis of isolated cell surface membrane proteins (inset Figure 2A) confirmed the increase of EGFR in erlotinib treated Calu-3 cells.

Exploiting the ability of cetuximab and trastuzumab to bind EGFR and HER2, we used these mAbs as primary antibodies for flow cytometry analysis. By this approach, as shown in Figure 3, we confirmed that the surface density of cetuximab and trastuzumab-binding sites, respectively, on Calu-3 (Figure 3A), H322 (3B) and H292 (3C) cells were increased after 1 μM erlotinib treatment. These results suggest that erlotinib enhanced cell surface expression of EGFR or HER2 on sensitive NSCLC cells, leading to an increase of

mAbs binding to cancer cell surface.

A

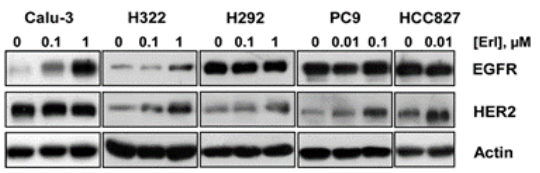

B

Sensitive NSCLC cell lines	EGFR	RAS	EGFR/Actin	HER2/Actin
CALU-3	WT	WT	5.8	1
H322	WT	WT	2.4	2.5
H292	WT	WT	1	1.6
PC9	Mut (E746A750del)	WT	1	2.1
HCC827	Mut (E746A750del)	WT	1	1.5

C

Resistant NSCLC cell lines	EGFR	RAS	EGFR/Actin	HER2/Actin
HCC827 GR5	Mut (E746A750del)	WT	1	1.1
A549	WT	G12S	1.2	1
H1299	WT	Q61K	1	1
H1703	WT	WT	0.9	0.9
Calu-1	WT	G12S	0.6	0.7

D

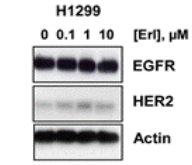

E

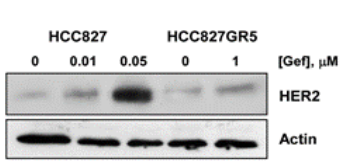

Figure 1. Erlotinib induces EGFR and HER2 protein accumulation only in sensitive NSCLC cell lines. (A) Calu-3, H322, H292, PC9 and HCC827 cell lines were treated with the indicated concentrations of erlotinib for 48 h. At the end of the drug treatment cell lysates were immunoblotted to detect the indicated proteins. The immunoreactive spots were quantified by densitometric analysis, ratios of EGFR/Actin and HER2/Actin were calculated at 1µM erlotinib for Calu-3 H322 and H292 or 10 nM for PC9 and HCC827 and values are expressed as fold increase versus control **(B)**. **(C)** HCC827GR5, A549, H1299, H1703, Calu-1 cell lines were treated with 1 µM erlotinib for 48 h and at the end of treatment cell lysates were immunoblotted to detect the indicated proteins. The immunoreactive spots were quantified by densitometric analysis, ratios of EGFR/Actin and HER2/Actin were calculated and values are expressed as fold increase versus control. **(D)** Representative Western blotting of resistant H1299 cell line exposed to increased concentration of erlotinib. **(E)** HCC827 parental cell line and HCC827GR5 resistant clone were treated with the indicated doses of gefitinib and processed as above. The results are from representative experiments. Each experiment, repeated three times, yielded similar results.

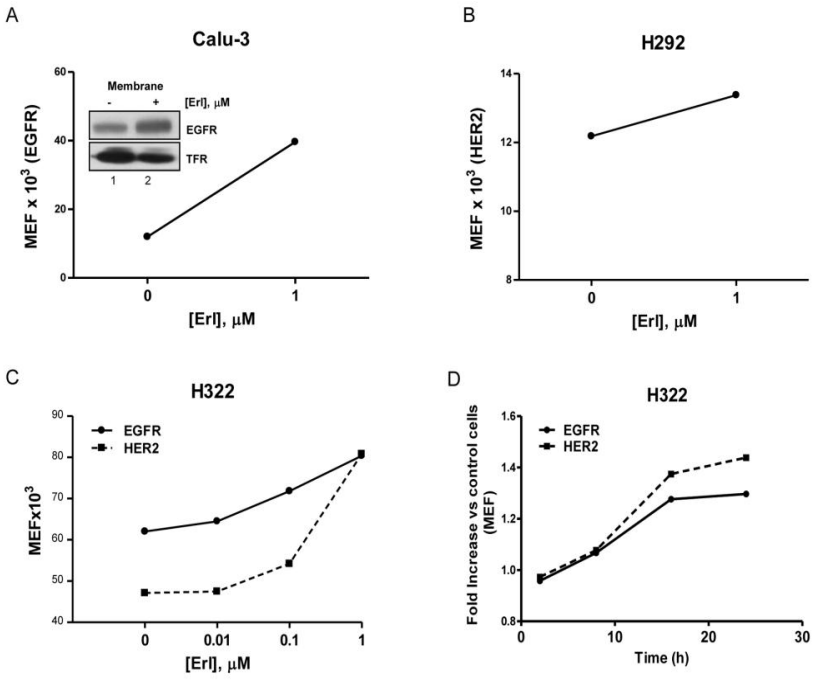

Figure 2. **EGFR and HER2 increase at the plasma-membrane level.** Calu-3 **(A)** and H292 **(B)** cell lines were treated with 1 µM erlotinib for 24 h, H322 cell line was treated with increasing concentration of erlotinib **(C)** or with 1 µM erlotinib for the indicated period of time **(D)**. At the end of the treatment, cell surface expression of EGFR and/or HER2 were evaluated by flow cytometry and the quantification is reported as Molecules of Equivalent Fluorophore [MEF] or as fold increase versus untreated control cells **(D)**. Inset Fig 2A: Western blot analysis of EGFR protein membrane level in Calu-3 after treatment with 1 µM erlotinib for 24h. Whole cells were labeled with biotin and membrane bound proteins were pulled down with neutrAvidin beads. The results are from representative experiments. Each experiment, repeated three times, yielded similar results.

Erlotinib induces EGFR protein stabilization

The possibility that the higher EGFR level observed in Calu-3 cells exposed to erlotinib was due to protein stabilization or increased synthesis was then explored. As shown in Figure 4A, EGFR level increased after 2 h of erlotinib treatment and reached a plateau after 24 h. Furthermore, the maximum level was maintained during time in the presence of the drug. However, after 48 h of erlotinib removal, EGFR expression was reduced to level comparable to untreated cells (Figure 4B). Calu-3 cells were also treated with erlotinib in the presence of specific inhibitors of mRNA (Actynomicin D) and protein (Cycloheximide) synthesis. As shown in Figure 4C, the erlotinib- induced EGFR protein increase was neither influenced by Actynomicin D nor Cycloheximide treatment indicating that the higher level of EGFR after erlotinib treatment could be ascribed to post-transcriptional mechanisms such as protein stabilization. Moreover, we analyzed EGFR transcript level by real time PCR after erlotinib treatment (Figure 4D). Erlotinib did not affect EGFR mRNA level when compared to untreated cells.

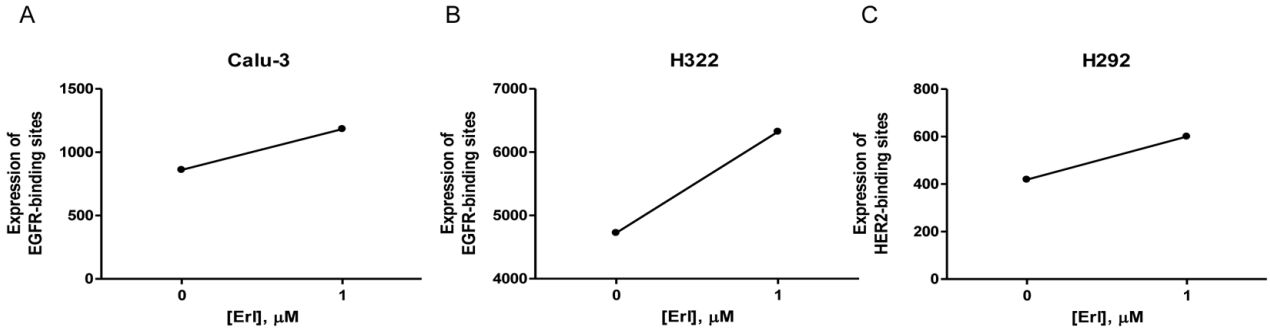

Figure 3. Erlotinib induces the increase of cetuximab and trastuzumab binding sites. Calu-3 **(A)**, H322 **(B)** and H292 **(C)** cell lines were treated with erlotinib for 24h. Binding sites were assessed by flow cytometry using cetuximab (Calu-3, H322) and trastuzumab (H292) as primary antibodies followed by PE-anti-human IgG exposure. Binding sites quantification is reported as Molecules of Equivalent Fluorophore [MEF]. The results in A, B, C are from representative experiments. Each experiment, repeated three times, yielded similar results.

With the aim to clarify why the increased level of EGFR was induced only in sensitive cells, we then tested the effect of EGFR inhibitors (gefitinib, erlotinib, cetuximab, lapatinib) and of inhibitors of MAPK and PI3K/AKT/mTOR signaling transduction pathways on EGFR accumulation in Calu-3 cell line. Gefitinib, erlotinib, lapatinib significantly inhibited the phosphorylation of p70S6K and p44/42 and induced a significant increase in EGFR protein level (Figure 4E). The MEK inhibitor U0126 strongly enhanced EGFR expression, in contrast no increase in the EGFR level was observed after incubation with the inhibitors of PI3K/AKT/mTOR pathway tested (NVP-BKM-120 and NVP-BYL-719 PI3K inhibitors and RAD001 mTOR inhibitor).

Effects of erlotinib and cetuximab combined treatment on NSCLC cell growth and antibody-dependent cell-mediated cytotoxicity

We then investigated the effect of targeting EGFR by both the TKI erlotinib and the mAb cetuximab in a cell viability assay (Figure 5). We treated Calu-3, H322 and H1299 cells with erlotinib, cetuximab (doses ranged from 1 to 50 μg/ml) or the combination based on the schedule erlotinib 24 h followed by the combination of erlotinib with cetuximab for 72 h. As expected Calu-3 (Figure 5A) and H322 (Figure 5B) cells

were responsive to erlotinib and cetuximab treatment, whereas H1299 (Figure 5C) cells were resistant to both the single regimens. Comparing the experimental combination points with that expected by the Bliss criterion, an additive effect was observed only in the Calu-3 cells. In fact, in the H322 cells we failed to observe any improvement treating cells with the combined treatment and H1299 remained resistant.

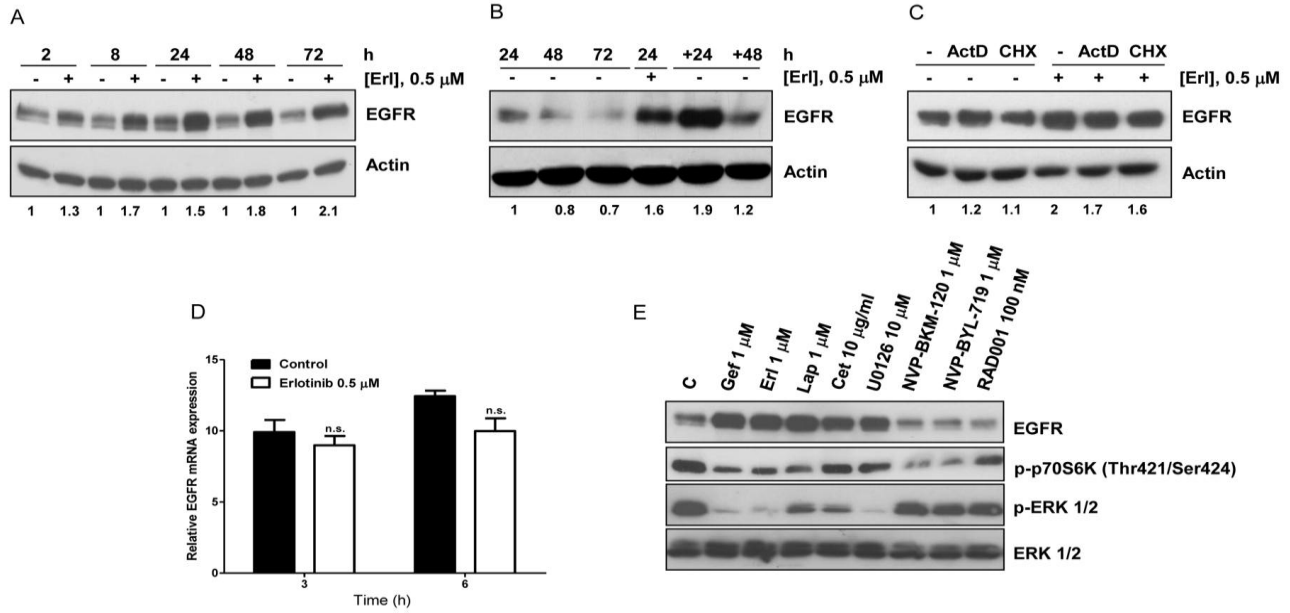

Figure 4. Erlotinib induces EGFR protein accumulation through protein stabilization. (A) Calu-3 cells were treated for the indicated period of time with 0.5 μM erlotinib. At the end of drug treatments cell lysates were immunoblotted to detect EGFR protein. **(B)** Calu-3 cells were treated with 0.5 μM erlotinib for 24h then the drug was removed and drug-free medium was added for further 24 and 48 h. Then, cell lysates were immunoblotted to detect the EGFR protein levels. **(C)** Calu-3 cells were treated for 24h with erlotinib 0.5 μM, in the absence/presence of 0.1 μg/ml actynomicin D and 2 μg/ml cyclohexymide. At the end of the experiment, cell lysates were immunoblotted to detect the indicated proteins. The immunoreactive spots were quantified by densitometric analysis, ratios of EGFR/Actin were calculated and values are expressed as fold increase versus control. **(D)** Calu-3 cells were exposed to 0.5 μM erlotinib for the indicate period of time and the EGFR mRNA was detected by RT-PCR. The mean values of two independent measurements (± SD) are shown. (E) EGFR, p-P70S6K, p-P44/42 and P44/42 were detected by Western blotting in Calu-3 cells untreated or treated for 24 h with 1 μM gefitinib, erlotinib and lapatinib, 10 μg/ml cetuximab, 10 μM U0126, 1 μM NVP-BKM-120 and NVP-BYL-719 and 100 nM RAD001. The results are from representative experiments. Each experiment, repeated three times, yielded similar results.

Moreover, cell death, evaluated by morphological analysis, caspase-3 activation and cleavage, was negligible under any of the tested treatments at all the time points analyzed (not shown) suggesting that the combined erlotinib-cetuximab treatment exerted a cytostatic and not a cytotoxic effect.

Since the engagement of immune component system is one of the main mechanisms of the activity of specific mAbs directed to ErbB family members in vivo, we examined whether erlotinib could enhance cetuximab- or trastuzumab-mediated ADCC by NK cells. As shown respectively in Figure 6 A-B cetuximab-dependent cytotoxicity in the presence of IL-2 activated NK cells was higher in Calu-3 and H322 cells previously treated with erlotinib compared with cells treated with cetuximab alone. Similarly, trastuzumab-dependent cytotoxicity was higher in H322 and H292 cells (Figure 6 C-D) previously treated with erlotinib compared with cells treated with trastuzumab alone. On the contrary, the combination of erlotinib with cetuximab did not significantly modify the mAb dependent cytotoxicity in H1299 resistant cancer cells.

Effect of erlotinib and cetuximab on Calu-3 xenografts

To extend our results in vivo, we tested the combination of erlotinib with cetuximab in a Calu-3 xenograft model (Figure 7). When tumours were well established (14 days post-injection, average volume of 300 mm3) mice were randomized into four treatment groups receiving erlotinib alone, cetuximab alone, the combination, or vehicles as described in the Methods section. Drug treatments were well tolerated, and no signs of toxicity were detected during the study.

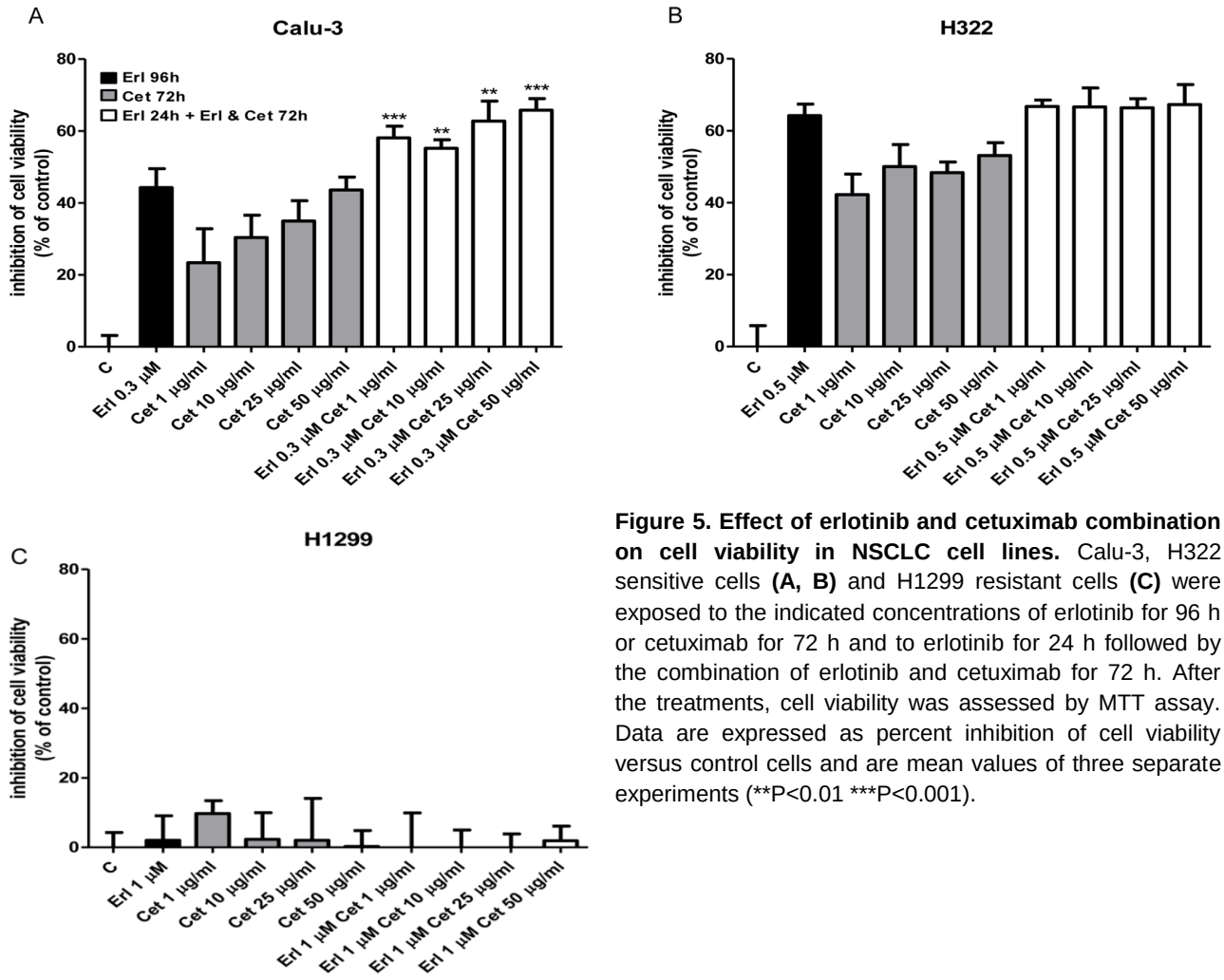

Figure 5. Effect of erlotinib and cetuximab combination on cell viability in NSCLC cell lines. Calu-3, H322 sensitive cells **(A, B)** and H1299 resistant cells **(C)** were exposed to the indicated concentrations of erlotinib for 96 h or cetuximab for 72 h and to erlotinib for 24 h followed by the combination of erlotinib and cetuximab for 72 h. After the treatments, cell viability was assessed by MTT assay. Data are expressed as percent inhibition of cell viability versus control cells and are mean values of three separate experiments (**P<0.01 ***P<0.001).

The treatment with either erlotinib or cetuximab as single agent delayed tumour growth. However, the significance of the treatment versus the control was observed only with cetuximab as single agent or in combination. Interestingly, the treatment with the combination of erlotinib plus cetuximab significantly inhibited tumour growth when compared to both the single agent treatments. The histologic analysis of tumour samples showed that the subcutaneous injection of Calu-3 strikingly reproduced within four weeks the morphological features of human adenocarcinoma (Figures 8A, 8B1-4, 8C-1). Neoplastic epithelial cells clearly expressed cytokeratin (Figure 8C-2) and were organized in secretory glands surrounded by cellularized collagen as evidenced by Masson's trichrome staining (Figure 8C-4). Regressive phenomena and changes in size of neoplastic glands together with intense stromal reaction were observed in histologic samples of tumours from treated mice. Interestingly, cetuximab clearly resulted in dense inflammatory

periglandular infiltrates mostly composed of lymphocytes (Figure 8C-3). Thus, the real impact of treatment on tumour mass within the nodules was assessed by the morphometric analysis of tissue composition. By this quantitative approach, in agreement with gross anatomic measurements, we documented that the combination of erlotinib with cetuximab was the most effective treatment on tumour growth inhibition (Figure 8D).

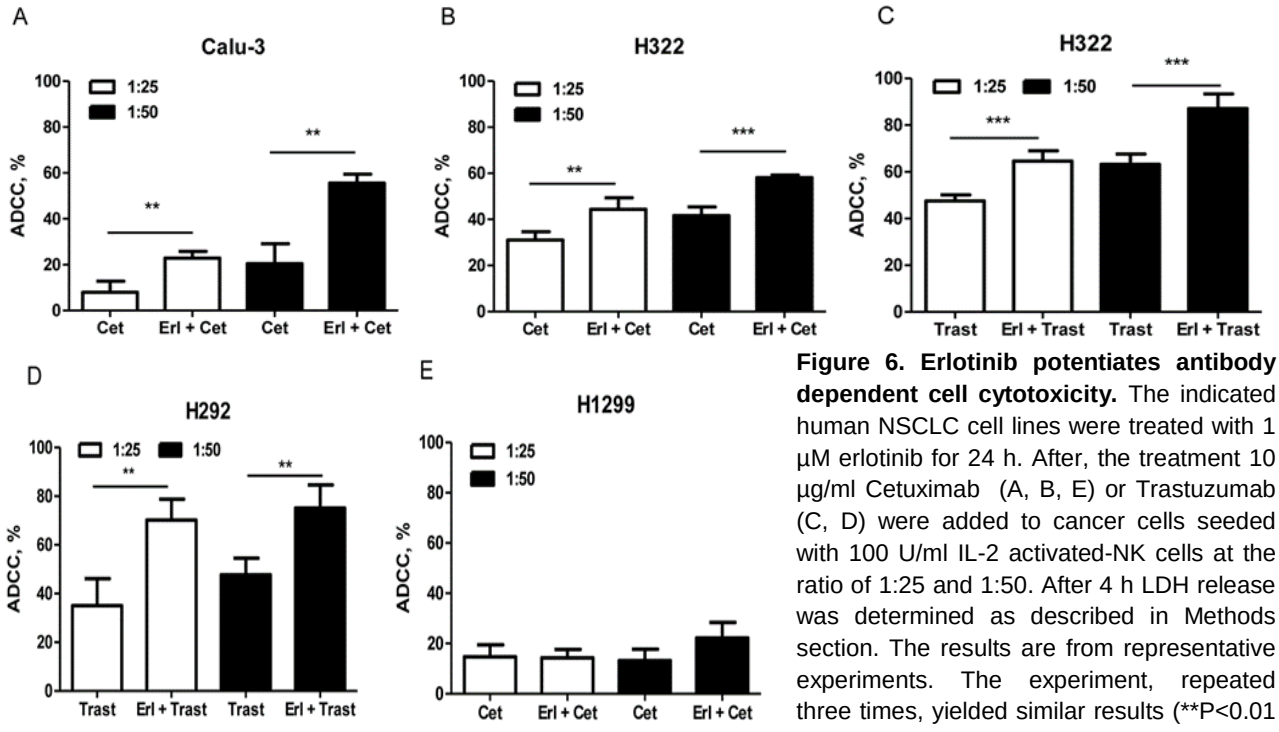

Figure 6. Erlotinib potentiates antibody dependent cell cytotoxicity. The indicated human NSCLC cell lines were treated with 1 µM erlotinib for 24 h. After, the treatment 10 µg/ml Cetuximab (A, B, E) or Trastuzumab (C, D) were added to cancer cells seeded with 100 U/ml IL-2 activated-NK cells at the ratio of 1:25 and 1:50. After 4 h LDH release was determined as described in Methods section. The results are from representative experiments. The experiment, repeated three times, yielded similar results (**P<0.01 ***P<0.001).

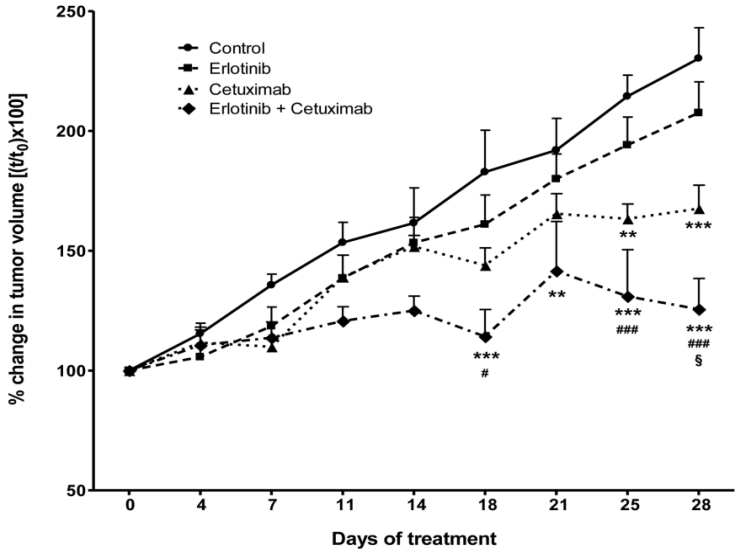

Figure 7. Antitumour activity of erlotinib and cetuximab on Calu-3 xenografts. Calu-3 cells were suspended in matrigel and sterile PBS (1:1) and implanted s.c. (right flank) on female BALB/c-Nude mice. Tumours were allowed to establish growth after implantation for 14 days, and the treatments started when tumours reached an average volume of 300 mm3. Vehicle, erlotinib (25 mg/Kg, orally 5 days/week), cetuximab (2 mg/Kg i.p. twice weekly), or erlotinib plus cetuximab were administered for the duration of the study. Data are expressed as percent change in tumour volume ± SEM of 6 mice per group. (**p<0.01, ***p<0.001 vs control; #p<0.05, ###p<0.001 vs erlotinib; §p<0.05 vs cetuximab; two-way ANOVA followed by Bonferroni post-test).

This contention was further supported by the immunofluorescence analysis of Ki67 labelling on tumour tissues at the end of the experimental protocol (Figure 9). Erlotinib was able to reduce proliferation of neoplastic cytokeratinpos cells only in association with cetuximab whereas cetuximab had a negative impact

on cycling cells also as individual agent. The TUNEL assay indicated that, according with in vitro data, apoptosis was not a significant ongoing cellular event implicated in the effect of different treatments.

We have calculated that 0.026+/-0.016% neoplastic cells were undergoing apoptosis in untreated tumours. Similar low numbers were obtained after Erlotinib or Cetuximab single treatment whereas Erl+Cet increased the amount of TUNEL positive neoplastic cells although reaching a rate of 0.12+/-0.03%. However, we cannot exclude that apoptotic cell death may have contributed to the positive effect of tumor shrinkage at earlier times after drug administration. Thus, these experimental observations suggest that targeting EGFR by the combination of small molecules and antibodies increases the in vitro and in vivo anti-proliferative activity of both individual agents and seems to be a potent therapeutic strategy against NSLC.

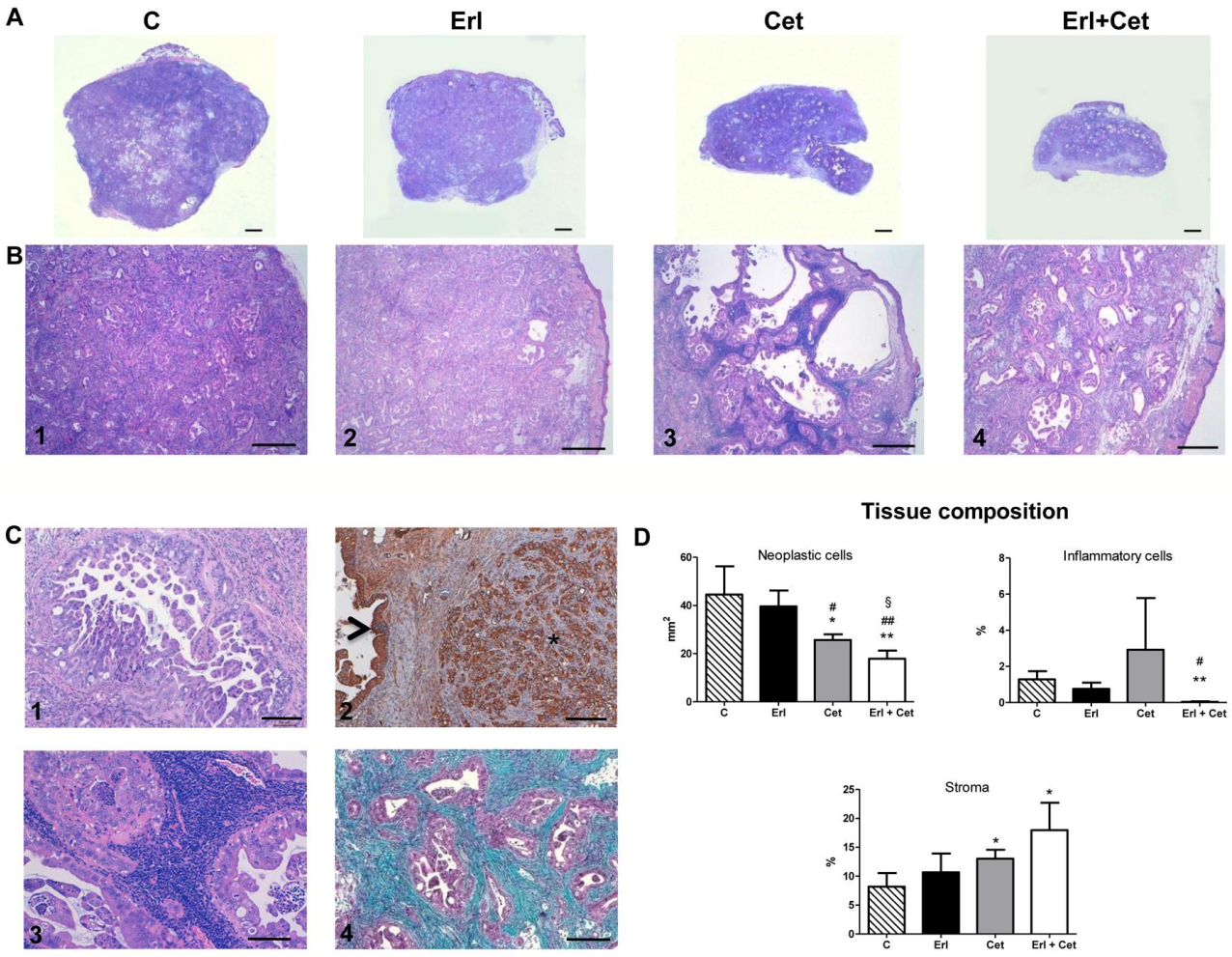

Figure 8 Hystological analysis of tumours. (A) Selected examples of H&E stained sections of the entire subcutaneous xenografted tumour induced by Calu-3 injection in untreated (C) and erlotinib (Erl), cetuximab (Cet) or erlotinib+cetuximab (Erl + Cet) treated BALB/c nude mice (scale bars: 1 mm). The same samples are shown with higher magnification in corresponding panels **(B)** (scale bars: 500 μm). **(C)** Representative morphological details of the control neoplastic epithelium (1, H&E) expressing cytokeratin (2,***** brown-immunoperoxidase) that also depicts the epidermis (arrowhead). The presence of inflammatory interstitial cells in a cetuximab treated tumour (3, H&E) and the intense collagen deposition (bluish) surrounding neoplastic glands (purple) in a Erl + Cet treated tumour (4, Masson's trichrome) are shown (scale bars: 100 μm). **(D)** Bar-graphs illustrating the quantitative measurements of neoplastic, inflammatory cells and stromal compartments composing the tumours. (*p<0.05, **p<0.01, vs control; $^{\#}$p<0.05, $^{\#\#}$p<0.01 vs erlotinib; §p<0.05 vs cetuximab).

DISCUSSION

The potential for dual-agent molecular targeting of the ErbB family has been clearly demonstrated in pre-clinical models and confirmed on the clinical setting for HER2-targeting agents in breast cancer. However, little is known about this therapeutic strategy for different targets in other tumour types.

In our current study we demonstrated that the combination of erlotinib with cetuximab or trastuzumab may enhance the antitumour activity of EGFR-TKI in NSCLC cell lines harbouring wild-type EGFR and in xenograft models.

The efficacy of the association between an EGFR/HER2 mAbs with TKIs has been documented in preclinical studies in several cell lines originating from different tumour types [15]. In EGFR wild-type H292 and A549 NSCLC cell lines, the combination of either gefitinib or erlotinib with cetuximab was reported to enhance growth inhibition in comparison to single treatment, particularly in the H292 gefitinib sensitive cell line [17]. In the A549 cell line, expressing both EGFR and HER2, the combination of gefitinib with trastuzumab significantly inhibited cell growth and proliferation [18]. In Calu-3 xenograft models, the combined treatment of erlotinib and pertuzumab showed an enhanced antitumour activity [19].

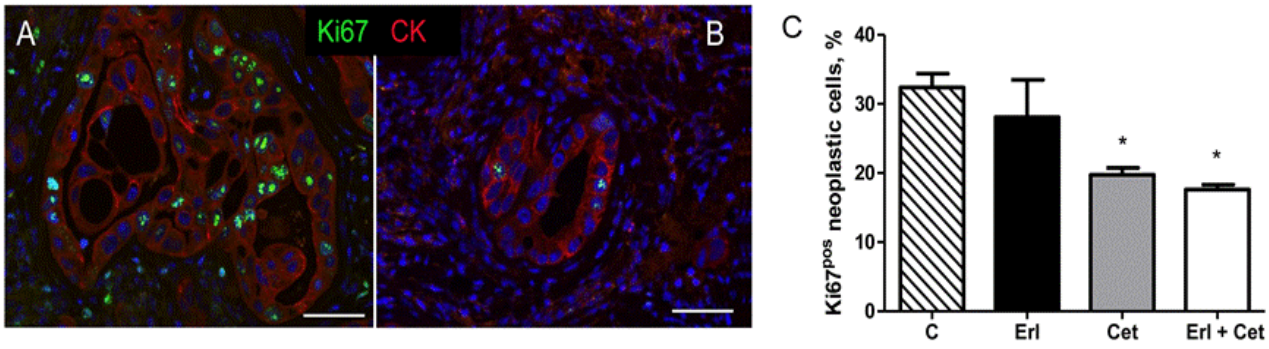

Figure 9. Immunohistochemical analysis of cellular proliferation. Immunofluorescence images of Ki67 (green) nuclear labelling of cytokeratin (CK, red) positive neoplastic cells in sections of xenograft tumours from an untreated **(A)** and Erl + Cet treated **(B)** BALB/c nude mouse. **(C)** Bar-graph illustrating the effect of the different treatments on the percentage of cycling (Ki67pos) neoplastic cells within the tumour. CTRL, untreated; ERL, erlotinib; CET, cetuximab; COMB, combination with erlotinib and cetuximab. * $p<0.01$ vs CTRL.

A correlation between cetuximab efficacy and EGFR expression has been reported in preclinical studies [20] and recently confirmed in clinical trials. Thus, the phase III FLEX study involving patients with advanced NSCLC showed a strong correlation between high tumour EGFR overexpression and the efficacy of adding cetuximab to platinum based first-line chemotherapy [12].

The combination of a TKI and a mAb was explored as a potential strategy to overcome acquired resistance to first-generation EGFR-TKIs. Kim and colleagues demonstrated that the combination of lapatinib with cetuximab overcame gefitinib resistance due to the secondary T790M mutation in NSCLC by inducing enhanced cytotoxicity both in vitro and in vivo [21]. Furthermore, the association of cetuximab with afatinib has been shown to be effective to overcome T790M-mediated drug resistance [22].

However, the combination of erlotinib with cetuximab did not lead to a significant radiological response in NSCLC patients with clinically defined acquired resistance to erlotinib indicating that this strategy is not sufficient to overcome acquired resistance to erlotinib [23].

The mechanisms leading to an enhanced activity of combining a TKI with a monoclonal antibody have

been ascribed, in other cancer cell models, either to a more efficient inhibition of TK receptors [17] or to an increased targeted receptors on plasma membrane induced by TKIs [24, 25]. Scaltriti and colleagues showed that lapatinib enhanced the effects of trastuzumab by inducing HER-2 stabilization and accumulation at the cell surface of breast cancer cell lines [24], and Mimura et al. reported that lapatinib induced accumulation of HER-2 and EGFR on esophageal cancer cell lines evoking trastuzumab- and cetuximab-mediated ADCC [25].

ADCC, one of the killing mechanisms of the immune system mediated by Natural Killer cells, plays a pivotal role in the anti-cancer effects exerted by mAbs. Therefore, increasing the ADCC activity is an important objective in the development of novel therapeutic approaches.

It has been recently demonstrated that the EGFR inhibitors gefitinib and erlotinib enhance the susceptibility to NK cell mediated lysis of A549, NCI-H23 and SW-900 lung cancer cell lines [26] by the induction of ULBP1 (a ligand of the NK cell activation receptor NKG2D). These data indicate that EGFR blockade could not be the only mechanism of action of EGFR inhibitors in vivo. The efficacy of these inhibitors in lung cancer may be at least in part mediated by increased susceptibility to NK activity. Moreover, cetuximab serves as a potent stimulus for NK functions including INF-gamma production [27] and is also associated with a complement-mediated immune response [28].

We here demonstrated that erlotinib induces an accumulation of EGFR and/or HER2 protein at the plasma membrane level only in TKI sensitive NSCLC cell lines whereas, in resistant cells (both, intrinsic or MET amplification-mediated acquired resistance), this enhancement was not observed. The anti-tumour effect of drug combination was more evident in ADCC experiments compared with cell viability experiments. In the Calu-3 xenograft model, the combined treatment resulted in a lower rate of tumour growth, suggesting the involvement of NK activity as a determinant factor to improve the efficacy of the combined treatment. Moreover, regressive phenomena and changes in size of neoplastic glands together with intense stromal reaction were observed in histologic samples of tumours from mice treated with cetuximab alone or the combination.

The reason why EGFR inhibitors such as gefitinib, erlotinib or lapatinib induce EGFR accumulation only in sensitive cells could be ascribed to their ability to inhibit signal transduction pathways downstream EGFR. The constitutive activation of signaling pathways downstream of EGFR (i.e. presence of RAS mutations) is indeed a recognized mechanism of resistance against reversible EGFR-TKIs [29]. The inhibition of the MAPK pathway might represent a link between EGFR inhibition and EGFR accumulation since U0126, a well-known MEK1/2 inhibitor, induced EGFR accumulation in Calu-3 cells, while none of PI3K/AKT/mTOR inhibitors tested was effective. A correlation between MAPK pathway and protein degradation by the ubiquitin system was described for the pro-apoptotic BH3-only protein BIM, indeed in the absence of MAPK activation, BIM protein accumulated in the cell promoting activation of apoptotic cell death [30].

Considering that EGFR TKIs, in particular erlotinib, demonstrated to be effective only in a small percentage of NSCLC patients not harboring EGFR mutations, our preclinical results could support clinical trials on the combinations of erlotinib and cetuximab or trastuzumab aiming to improve treatment efficacy. Although the addition of cetuximab to erlotinib is insufficient to overcome erlotinib resistance in EGFR-driven lung adenocarcinoma [23], the clinical potential of dual-agent molecular targeting of the EGFR in patients with EGFR wild-type tumours remains to be elucidated and may represents an interesting research area to

be pursued.

CONCLUSIONS

In this study we explored the potential of combining erlotinib with cetuximab or trastuzumab in improving the efficacy of EGFR targeted therapy in EGFR wild-type erlotinib-sensitive NSCLC cell lines. Our results indicate that erlotinib, through ERK inhibition, increases surface expression of EGFR and/or HER2 only in erlotinib sensitive NSCLC cell lines and in turn leads to increased susceptibility to ADCC both in vitro and in xenografts models.

These data prompt future adequate clinical trials that will give the ultimate proof of the utility of this combined treatment for the care of NSCLC patients carrying wild-type EGFR that are sensitive to TKIs.

ACKNOWLEDGEMENTS

This work was supported by: Associazione Italiana per la Ricerca sul Cancro (AIRC), Milan grant IG 8856; Associazione Augusto per la Vita (Novellara, RE); Associazione Davide Rodella, Montichiari, BS; Associazione Chiara Tassoni, Parma; A.VO.PRO.RI.T., Parma.

REFERENCES

1. Schlessinger J: Ligand-induced, receptor-mediated dimerization and activation of EGF receptor. Cell 2002, 110:669-672.
2. Normanno N, De Luca A, Bianco C, et al. Epidermal growth factor receptor (EGFR) signaling in cancer. Gene 2006, 366:2-16.
3. Hirsch FR, Varella-Garcia M, Bunn PA, et al. Epidermal growth factor receptor in non-small-cell lung carcinomas: correlation between gene copy number and protein expression and impact on prognosis. J Clin Oncol 2003, 21:3798-3807.
4. Liu L, Shao X, Gao W, et al. The role of human epidermal growth factor receptor 2 as a prognostic factor in lung cancer: a meta-analysis of published data. J Thorac Oncol 2010, 5:1922-1932.
5. Shepherd FA, Rodrigues Pereira J, Ciuleanu T, et al. Erlotinib in previously treated non-small-cell lung cancer. N Engl J Med 2005, 353:123-132.
6. Cataldo VD, Gibbons DL, Perez-Soler R, et al. Treatment of non-small-cell lung cancer with erlotinib or gefitinib. N Engl J Med 2011, 364:947-955.
7. Douillard JY, Shepherd FA, Hirsh V, et al. Molecular predictors of outcome with gefitinib and docetaxel in previously treated non-small-cell lung cancer: data from the randomized phase III INTEREST trial. J Clin Oncol 2010, 28:744-752.
8. Cappuzzo F, Ciuleanu T, Stelmakh L, et al. Erlotinib as maintenance treatment in advanced non-small-cell lung cancer: a multicentre, randomised, placebo-controlled phase 3 study. Lancet Oncol 2010, 11:521-529.
9. Mendelsohn J, Baselga J: Status of epidermal growth factor receptor antagonists in the biology and treatment of cancer. J Clin Oncol 2003, 21:2787-2799.
10. Pirker R, Pereira JR, Szczesna A, et al. Cetuximab plus chemotherapy in patients with advanced non-small-cell lung cancer (FLEX): an open-label randomised phase III trial. Lancet 2009, 373:1525-1531.
11. Lynch TJ, Patel T, Dreisbach L, et al. Cetuximab and first-line taxane/carboplatin chemotherapy in advanced non-small-cell lung cancer: results of the randomized multicenter phase III trial BMS099. J Clin Oncol 2010, 28:911-917.
12. Pirker R, Pereira JR, von Pawel J, et al. EGFR expression as a predictor of survival for first-line chemotherapy plus cetuximab in patients with advanced non-small-cell lung cancer: analysis of data from the phase 3 FLEX study. Lancet Oncol 2012, 13:33-42.
13. Langer CJ, Stephenson P, Thor A, et al. Trastuzumab in the treatment of advanced non-small-cell lung cancer: is there a role? Focus on Eastern Cooperative Oncology Group study 2598. J Clin Oncol 2004, 22:1180-1187.
14. Gatzemeier U, Groth G, Butts C, et al. Randomized phase II trial of gemcitabine-cisplatin with or without trastuzumab in HER2-positive non-small-cell lung cancer. Ann Oncol 2004, 15:19-27.
15. Matar P, Rojo F, Cassia R, et al. Combined epidermal growth factor receptor targeting with the tyrosine kinase inhibitor gefitinib (ZD1839) and the monoclonal antibody cetuximab (IMC-C225): superiority over single-agent receptor targeting. Clin Cancer Res 2004, 10:6487-6501.
16. Engelman JA, Zejnullahu K, Mitsudomi T, et al. MET amplification leads to gefitinib resistance in lung cancer by activating ERBB3 signaling. Science 2007, 316:1039-1043.
17. Huang S, Armstrong EA, Benavente S, et al. Dual-agent molecular targeting of the epidermal growth factor receptor (EGFR): combining anti-EGFR antibody with tyrosine kinase inhibitor. Cancer Res 2004, 64:5355-5362.
18. Nakamura H, Takamori S, Fujii T, et al. Cooperative cell-growth inhibition by combination treatment with ZD1839 (Iressa) and trastuzumab (Herceptin) in non-small-cell lung cancer. Cancer Lett 2005, 230:33-46.
19. Friess T, Scheuer W, Hasmann M. Combination treatment with erlotinib and pertuzumab against human tumor xenografts is superior to monotherapy. Clin Cancer Res 2005, 11:5300-5309.
20. Kimura H, Sakai K, Arao T, et al. Antibody-dependent cellular cytotoxicity of cetuximab against tumor cells with wild-type or mutant epidermal growth factor receptor. Cancer Sci 2007, 98:1275-1280.
21. Kim HP, Han SW, Kim SH, et al. Combined lapatinib and cetuximab enhance cytotoxicity against gefitinib-resistant lung cancer cells. Mol Cancer Ther 2008, 7:607-615.
22. Regales L, Gong Y, Shen R, et al. Dual targeting of EGFR can overcome a major drug resistance mutation in mouse models of EGFR mutant lung cancer. J Clin Invest 2009, 119:3000-3010.
23. Janjigian YY, Azzoli CG, Krug LM, et al. Phase I/II trial of cetuximab and erlotinib in patients with lung adenocarcinoma and acquired resistance to erlotinib. Clin Cancer Res 2011, 17:2521-2527.
24. Scaltriti M, Verma C, Guzman M, et al. Lapatinib, a HER2 tyrosine kinase inhibitor, induces stabilization and accumulation of HER2 and potentiates trastuzumab-dependent cell cytotoxicity. Oncogene 2009, 28:803-814.
25. Mimura K, Kono K, Maruyama T, et al. Lapatinib inhibits receptor phosphorylation and cell growth and enhances antibody-dependent cellular cytotoxicity of EGFR- and HER2-overexpressing esophageal cancer cell lines. Int J Cancer 2011, 129:2408-2416.
26. Kim H, Kim SH, Kim MJ, et al. EGFR inhibitors enhanced the susceptibility to NK cell-mediated lysis of lung cancer cells. J Immunother 2011, 34:372-381.
27. Roda JM, Joshi T, Butchar JP, et al. The activation of natural killer cell effector functions by cetuximab-coated, epidermal growth factor receptor positive tumor cells is enhanced by cytokines. Clin Cancer Res 2007, 13:6419-6428.
28. Hsu YF, Ajona D, Corrales L, et al. Complement activation mediates cetuximab inhibition of non-small cell lung cancer tumor growth in vivo. Mol Cancer 2010, 9:139.
29. Engelman JA, Janne PA: Mechanisms of acquired resistance to epidermal growth factor receptor tyrosine kinase inhibitors in non-small cell lung cancer. Clin Cancer Res 2008, 14:2895-2899.
30. Ley R, Balmanno K, Hadfield K, et al. Activation of the ERK1/2 signaling pathway promotes phosphorylation and proteasome-dependent degradation of the BH3-only protein, Bim. J Biol Chem 2003, 278:18811-18816.
31. La Monica S, Galetti M, Alfieri RR, et al. Everolimus restores gefitinib sensitivity in resistant non-small cell lung cancer cell

lines. Biochem Pharmacol 2009, 78:460-468.
32. Cavazzoni A, Alfieri RR, Carmi C, et al. Dual mechanisms of action of the 5-benzylidene-hydantoin UPR1024 on lung cancer cell lines. Mol Cancer Ther 2008, 7:361-370.
33. Alfieri RR, Galetti M, Tramonti S, et al. Metabolism of the EGFR tyrosin kinase inhibitor gefitinib by cytochrome P450 1A1 enzyme in EGFR-wild type non small cell lung cancer cell lines. Mol Cancer 2011, 10:143.
34. Steiner P, Joynes C, Bassi R, et al. Tumor growth inhibition with cetuximab and chemotherapy in non-small cell lung cancer xenografts expressing wild-type and mutated epidermal growth factor receptor. Clin Cancer Res 2007, 13:1540-1551.
35. Bonelli MA, Fumarola C, Alfieri RR, et al. Synergistic activity of letrozole and sorafenib on breast cancer cells. Breast Cancer Res Treat 2010, 124:79-88.

Chapter 11

Summarizing discussion

SUMMARIZING DISCUSSION

The majority of patients with lung tumors present cancers histologically classified as non-small cell lung cancer (NSCLC) in advanced stage disease. Until recently, platinum-based doublet chemotherapy regimens were the standard treatment for patients with a good performance status. In CHAPTER 2, tymidylate synthase (TS) is reviewed as a well-established target for the treatment of several tumor types, including NSCLC, given its pivotal role in DNA replication/repair and cancer cell proliferation. Furthermore, its role as a transforming factor and a potential oncogene has been recognized [1,2]. The inhibition of TS represents an anti-metabolite approach to control tumor cell growth, and TS inhibitors could be considered one of the first 'targeted' drugs having been designed to interfere with a specific molecular target. In particular, the TS inhibitor pemetrexed emerged for its approval and widespread use for first-/second-line and maintenance therapy in NSCLC. Although TS overexpression represents the most studied cause of resistance to the treatment with the drug, other mechanisms of resistance to antifolate treatment have been described which can also affect pemetrexed activity [3]. However, despite multiple studies evaluating different schedules, doses and combinations, the results obtained from the treatment with chemotherapy remain disappointing with only about 30% of responding patients, the median survivals ranging from 8 to 12 months and 1-year survival rates varying from 33 to 46% [4-8]. A therapeutic plateau has been reached with cytotoxic chemotherapy alone in the treatment of advanced NSCLC and new treatment options are needed.

New insights into the molecular biology of cancer and mechanisms of tumorigenesis have identified key biological processes and several potential molecular targets for anti-cancer treatment [9]. Mutations, chromosomal rearrangements, DNA copy number abnormalities or epigenetic changes such as methylation or microRNAs regulation have been highlighted among the genetic alterations involved in cancer development and progression and new targeted therapies have been developed. A number of these novel agents have proven clinical efficacy or are lately yielding promising results, with the epidermal growth factor receptor (EGFR) tyrosine kinase inhibitors (TKIs) gefitinib and erlotinib, the anti-EGFR monoclonal antibody (mAb) cetuximab, the angiogenesis inhibitor bevacizumab and the ALK/c-MET inhibitor crizotinib having already been granted regulatory approval for the treatment of advanced NSCLC.

Along with its ligands (e.g. EGF, TGF-α, and amphiregulin) EGFR is frequently overexpressed and negatively correlated with prognosis in many types of human malignancies, including NSCLC [10-12]. In particular, overexpression of EGFR has been found in 40-80% of NSCLC cases and EGFR mutations were also described and correlated with malignancy "oncogene-addiction" [13]. Besides, overexpression of the ligand for ErbB3 and ErbB4, neuregulin-1, has also been reported in NSCLC [14]. Taken together, these findings make EGFR an attractive target for cancer therapy [15]. CHAPTER 3, reviews the various anti-EGFR agents that have been approved or are currently undergoing clinical investigation in NSCLC. To date, two classes of EGFR inhibitors are available for clinical use in many countries, including either, small-molecule TKIs that compete with ATP for the interaction with the intracellular domain, and mAbs which contend with ligands at the extracellular domain [16]. Both classes exert antitumor activity with various potential implications for clinical efficacy correlated to the different administration way and mechanism of action. An association with therapeutic response to EGFR-TKIs has been observed with the discovery of somatic EGFR mutations in NSCLC, and in particular the exon 21 missense point mutation L858R and the

in-frame deletions in exon 19 [17-20]. These mutations, also known as activating mutations, confer tumor cell dependency on EGFR signaling and are the most commonly studied predictive biomarkers of response to gefitinib and erlotinib [21-23] being observed in 15 to 40% of cases [10,24-27]. Although the introduction of these new agents has improved NSCLC treatment, oncologists are still facing relevant inter-individual variability in drug reactivity, toxicity and cancer outcomes, which might not only be caused by clinical and cancer molecular characteristics [23]. To date, it is not completely clear which patient characteristics are risk factors for EGFR-TKI-induced toxicity, and the large interindividual variability in toxic effects prompts the identification of novel pharmacogenetic markers. Thus, inherited genetic determinants, which can be assessed in blood tissue, may complement common clinical factors for the prediction of clinical outcome and toxicity. CHAPTER 4 describes the main results achieved in the evaluation of the genetic polymorphisms or pharmacogenetics of EGFR targeted therapy. Several germline polymorphisms of EGFR and genes involved in anti-EGF agent activity, metabolism and transport have been studied as predictors of outcome and toxicity. Multiple studies reported the correlation between short EGFR intron 1 CA repeats and clinical response to EGFR-TKI treatment in patients affected by NSCLC [28-33]. This variant was also associated with grade 2/3 skin rash, but controversial results were reported by other studies in which the role of polymorphisms in ABCG2 was suggested to predict gastrointestinal toxicity [34]. These controversial data might be clarified within future studies, which should evaluate the feasibility of sampling more accessible tissue (i.e., blood) compared to cancer specimens, showing whether germline and somatic genotypes of drug transporters, drug metabolism enzymes and drug targets are correlated with the gene expression or functional activity in the tumors. Moreover, most clinical observations need to be confirmed in larger populations, and there needs to be clinical validation of a more robust approach to genotyping of patients as the multiple-gene approach may overcome the limitations of the single-gene approach.

However, the clinical success of the new targeted agents has also been limited by the emergence of acquired resistance, which leads to tumor relapse after initial response to therapy [35]. Resistance to these drugs can be caused by several mechanisms, which are partially overlapping with the main factors involved in resistance towards conventional chemotherapy, such as increased drug elimination, decreased drug uptake, drug inactivation and alterations of drug targets [36]. Genetic changes, such as the occurrence of the secondary EGFR-T790M mutation or the amplification of c-Met, -account for about 70% of the resistant cases to gefitinib and erlotinib [37]. Recent data overviewed in CHAPTER 5 showed that drug resistance mechanisms can also be regulated by epigenetic modifications, including alterations in microRNAs which act as key post-transcriptional regulators of gene expression [38]. In particular, up-regulation of miR-214 has been correlated with gefitinib resistance in NSCLC cells and its expression was inversely correlated with the expression of the oncosuppressor PTEN [39]. Furthermore, the stable expression, after gefitinib treatment, of several miRNAs (miR-30b, miR-30c, miR-221 and miR-222) which limit apoptosis induction, is also associated with gefitinib resistance [40]. Moreover, ontological annotation of the 13-gene miRNA signature (miR-140-3p, miR-628-5p, miR-518f, miR-636, miR-301a, miR-34c, miR-224, miR-197, miR-205, miR135b, miR-200b, miR-200c, and miR-141) and its potential targets revealed enrichment in the components of epithelial-to-mesenchymal transition (EMT), including Wnt pathway, which can be used to predict erlotinib sensitivity [41]. Multiple studies reported also that the deregulation of several miRNAs, such as miR155,

let7a-2, miR-21 and miR-146, correlated with outcome in NSCLC patients [42-45]. However, only few data are available on the correlation of miRNAs expression with NSCLC patients' outcome after treatment with EGFR inhibitors.

Various types of EGFR mutations have been identified to date, which are differentially related to response to EGFR-TKIs treatment [17]. In particular, deletions in the exon 19 have been shown to be related with better response to TKIs than the L858R substitution [46]. Moreover, the T790M mutation is associated with acquired resistance to EGFR-TKIs [47,48]. Covalent alkylation of a cysteine residue (Cys797), positioned at the entrance of the ATP binding site, was the additional mechanism of second-generation irreversible EGFR-TKIs, which had been shown to overcome resistance to gefitinib [49-53]. In CHAPTER 3 several inhibitors of this class which have progressed to clinical investigation in patients that initially responded to gefitinib and subsequently relapsed are presented [54]. EGFR irreversible covalent inhibitors are characterized by a heterocyclic core structure (driving portion) carrying an electrophilic functionality (warhead) that covalently interacts with the specific cysteine residue in the target protein [55-59]. The intrinsic reactivity of the warhead known in literature is associated with both advantages, and augmented metabolic degradation and toxicity, due to reactions with non-target proteins [60,61]. In CHAPTER 6 we described the systematic analysis of functional groups that are able to covalently interact with cysteine residues of EGFR, focusing on a new chemical entity containing a 3-aminopropanamide moiety [62-64]. These compounds possess a particular profile of reactivity, being non-reactive directly, but able to covalently modify their biological target after bioconversion via β-elimination to the corresponding α,β-unsaturated carbonyl compound. Notably, the newly synthesized 3-aminopropanamides suppressed proliferation of gefitinib-resistant NSCLC cells at significantly lower concentration than gefitinib and blocked mutated T790M EGFR activity with a long-lasting effect on the enzyme autophosphorylation in the resistant cellular model. Finally, these drugs acted as prodrugs, releasing the active derivative in the intracellular environment, although were stable in other conditions. In CHAPTER 7 we demonstrated the activity of the novel 3-aminopropanamide inhibitors in in vitro and in vivo models of NSCLC cells harbouring EGFR-T790M. Several molecular mechanisms are affected by these compounds which are involved in complex processes as cellular migration and ability to growth as three-dimensional spheroidal systems. Furthermore, accumulating evidence suggests that specific sub-populations of cancer cells within the bulk of tumors undergo different degree of EMT, and this process has been related with the acquisition of stem cell-like characteristics. Both EMT and stemness are implicated in the pathogenesis and chemoresistance of heterogeneous malignant tumors [65,66]. Our compounds demonstrated to be very promising anticancer agents by attacking different key mechanisms involved in the resistance of NSCLC cells to the first-generation EGFR-TKIs gefitinib and erlotinib, including the EMT process. Moreover, the 3-aminopropanamide derivatives also retained their activity in vivo leading to tumor shrinkage. These data should prompt future trials that will give the ultimate proof of the utility of these novel anticancer agents for the treatment of lung cancer.

Angiogenesis is the multi-step process whereby new blood vessels are formed from the existing vasculature. The key player in tumor angiogenesis is the vascular endothelial growth factor (VEGF) pathway [68]. Two main strategies are currently available to inhibit the VEGF pathway: i) direct VEGF inhibition by

mAbs like bevacizumab, or ii) VEGFR inhibition by TKIs such as sorafenib, sunitinib, montasenib and cediranib. Currently bevacizumab, in combination with platinum-based chemotherapy, is the only angiogenesis inhibitor that has been approved for the treatment of advanced non-squamous NSCLC [69,70]. Trials evaluating other angiogenesis inhibitors have shown modest results and further research is needed. By targeting the EGFR- and RAF-dependent cancer cell proliferation and the VEGFR-2-dependent tumor angiogenesis pathways, the combination of erlotinib with sorafenib offers the potential advantage of blocking key pathways in different cell types, namely cell proliferation in the tumor and angiogenesis in endothelial cells. Several studies demonstrated that NSCLC is characterized by dysregulation of molecular mechanisms involved in cell proliferation and angiogenesis [71]. In CHAPTER 8, we demonstrated the highly synergistic interaction between erlotinib and sorafenib in NSCLC cells. Several molecular mechanisms and determinants involved in the synergistic interaction of erlotinib and sorafenib against NSCLC cells have been characterized, focusing on cells harbouring K-Ras and EGFR-T790M mutations. In these cells, sorafenib reduced ERK and Akt phosphorylation, which was additionally reduced by drug combination, and favoured apoptosis induction. The combination with erlotinib and sorafenib also significantly reduced E2F-1 expression, while increased Raf-kinase-inhibitor protein (RKIP) expression was observed with both erlotinib and the combination, favouring sorafenib activity. The modulation of all these determinants influences the cytotoxicity of this combination and, although the extrapolation of in vitro data to the clinical setting should be considered with caution, these results may have implications for the rational development of chemotherapeutic regimes including erlotinib and sorafenib or other emerging multikinase inhibitor of angiogenic, stromal and oncogenic kinases, such as regorafenib [72].

However, not all the patients with activating mutations of EGFR respond to EGFR-TKIs treatment, and conversely, some EGFR mutation negative patients do respond. Other biomarkers for predicting treatment efficacy need to be identified. In CHAPTER 9 we described the results of an investigation on the role of cytochrome P450 1A1 (CYP1A1) inhibition on intracellular metabolism of gefitinib in both sensitive and resistant EGFR wild-type NSCLC cell lines. Differences in drug metabolism between gefitinib-sensitive and -resistant cells were observed. Unexpectedly, gefitinib was metabolized only by sensitive cells in which mRNA and activity of CYP1A1 were induced by the drug. Furthermore, the treatment with a CYP1A1 inhibitor increased the efficacy of gefitinib preventing the reduction of its intracellular level and enhancing the inhibition of EGFR and cell proliferation. Our results suggest that gefitinib metabolism in lung cancer cells might represent an early assessment of response to gefitinib treatment in NSCLC cells lacking activating mutations. On the other hand targeting CYP1A1 might lead to increased local exposure to the active drug increasing its potency.

The approach of combining TKIs and mAbs directed against different regions of the same target may result in improved inhibition of the molecule. Recently published preclinical and clinical studies evaluating the combination of erlotinib with the anti-EGFR mAb cetuximab, reported the synergism of this combination in colon cancer cell lines and in chemotherapy-refractory colorectal cancer patients [67]. In CHAPTER 10 we explored the potential of combining erlotinib with either cetuximab or trastuzumab in wild-type EGFR NSCLC cells. Increased EGFR and/or HER2 expression due to protein stabilization was observed in sensitive NSCLC cell lines after erlotinib treatment. The combination with TKI and mAb slightly affected cell

proliferation while markedly increased antibody-dependent, NK mediated, cytotoxicity in vitro. Moreover, the combination showed higher activity than single agent treatments by reducing tumour growth in xenografts. Our results indicate that by stabilizing surface expression of EGFR and/or HER2, erlotinib leads to increased susceptibility to ADCC both in vitro and in vivo. The combination with erlotinib and mAbs might represent a potential strategy to improve the efficacy of anti-EGFR treatment in mutation negative NSCLC patients sensitive to the TKI.

To conclude, the introduction of targeted therapies has clearly led to some progress in the treatment of advanced NSCLC. Combining bevacizumab with chemotherapy as first-line treatment demonstrated a survival prolongation beyond the historical bench mark of 12 months. EGFR-TKIs have proven superior efficacy when compared to standard chemotherapy in patients with activating EGFR mutations, and these are now the recommended first-line treatment for such patients. Cetuximab in combination with platinum-based chemotherapy has been approved for the first-line treatment of EGFR-protein expressing NSCLC patients with good performance status and the extraordinary response seen in ALK-positive NSCLC patients accelerated the FDA approval of the potent ALK/c-MET inhibitor crizotinib. However, despite the progress made, several important issues in the clinical development of these targeted agents remained unresolved. There is a need to identify when and how these agents should be safely and effectively integrated with conventional therapies so as to maximize clinical benefit and minimize toxicity. Moreover, despite these new therapies, a large proportion of patients do not benefit from the currently available molecular targeted agents. Further elucidation of other driver mutations that lead to oncogene addiction will identify new potentially “drugable” targets and is thus essential in the pursuit to improve the treatment and prognosis of these patients. Finally, with the increasing knowledge on tumorigenesis, resistance mechanisms, development of novel treatment strategies and emerging imaging and biochemical techniques we are moving towards personalized treatment approach for advanced NSCLC.

REFERENCES

1. Rahman L, Voeller D, Rahman M, et al. Thymidylate synthase as an oncogene: a novel role for an essential DNA synthesis enzyme. Cancer Cell 2004;5:341-51
2. Chen M, Rahman L, Voeller D, et al. Transgenic expression of human thymidylate synthase accelerates the development of hyperplasia and tumors in the endocrine pancreas. Oncogene 2007;26:4817-24
3. Assaraf YG. Molecular basis of antifolate resistance. Cancer Metastasis Rev 2007;26:153-81
4. Fossella F, Pereira JR, von Pawel J, et al. Randomized, multinational, phase III study of docetaxel plus platinum combinations versus vinorelbine plus cisplatin for advanced non-small-cell lung cancer: the TAX 326 study group. J Clin Oncol. 2003 Aug 15;21(16):3016-24.
5. Kelly K, Crowley J, Bunn PA Jr, et al. Randomized phase III trial of paclitaxel plus carboplatin versus vinorelbine plus cisplatin in the treatment of patients with advanced non--small-cell lung cancer: a Southwest Oncology Group trial. J Clin Oncol. 2001 Jul 1;19(13):3210-8
6. Le Chevalier T, Scagliotti G, Natale R, et al. Efficacy of gemcitabine plus platinum chemotherapy compared with other platinum containing regimens in advanced non-small-cell lung cancer: a meta-analysis of survival outcomes. Lung Cancer. 2005 Jan;47(1):69-80.
7. Scagliotti GV, De Marinis F, Rinaldi M, et al. Phase III randomized trial comparing three platinum-based doublets in advanced non-small-cell lung cancer. J Clin Oncol. 2002 Nov 1;20(21):4285-91.
8. Schiller JH, Harrington D, Belani CP, et al. Comparison of four chemotherapy regimens for advanced non-small-cell lung cancer. N Engl J Med. 2002 Jan 10;346(2):92-8.
9. Hanahan D, Weinberg RA. The hallmarks of cancer. Cell. 2000 Jan 7;100(1):57-70.
10. Hirsch FR, Varella-Garcia M, Bunn PA, et al. Epidermal growth factor receptor in non small-cell lung carcinomas: correlation between gene copy number and protein expression and impact on prognosis. J Clin Oncol 2003; 21(20):3798–807.
11. Suzuki S, Dobashi Y, Sakurai H, et al. Protein overexpression and gene amplification of epidermal growth factor receptor in nonsmall cell lung carcinomas. An immunohistochemical and fluorescence in situ hybridization study. Cancer 2005; 103(6):1265–73.
12. Sato M, Shames DS, Gazdar AF, Minna JD. A translational view of the molecular pathogenesis of lung cancer. J Thorach Oncol 2007; 2(4):327–43.
13. Shigematsu H, Lin L, Takahashi T, et al. Clinical and biological features associated with epidermal growth factor receptor gene mutations in lung cancers. J Natl Cancer I 2005; 97(5):339–46.
14. Sharma SV, Settleman J. ErbBs in lung cancer. Exp Cell Res 2009; 315(4):557–71.
15. Weinstein IB, Joe A. Oncogene addiction. Cancer Res 2008; 68(9):3077–80; discussion 3080.
16. Cappuzzo F, Ligorio C, Jänne PA, et al. Prospective study of gefitinib in epidermal growth factor receptor fluorescence in situ hybridization-positive/phospho-Akt-positive or never smoker patients with advanced non-small-cell lung cancer: the ONCOBELL trial. J Clin Oncol 2007; 25(16):2248–55.
17. Wellcome trust sanger institute: Catalogue of somatic mutations in cancer. Available on: http://www.sanger.ac.uk/perl/genetics/CGP/cosmic?action=gene&ln=EGFR
18. De Pas T, Toffalorio F, Manzotti M, et al. Activity of epidermal growth factor receptor-tyrosine kinase inhibitors in patients with non-small cell lung cancer harboring rare epidermal growth factor receptor mutations. J Thorach Oncol 2011; 6(11):1895–901.
19. Pao W, Miller V, Zakowski M, et al. EGF receptor gene mutations are common in lung cancers from “never smokers” and are associated with sensitivity of tumors to gefitinib and erlotinib. P Natl Acad Sci USA 2004; 101(36):13306–11.
20. Mok TS, Wu Y-L, Thongprasert S, et al. Gefitinib or carboplatin-paclitaxel in pulmonary adenocarcinoma. N Engl J Med 2009; 361(10):947–57.
21. Lynch TJ, Bell DW, Sordella R, et al. Activating mutations in the epidermal growth factor receptor underlying responsiveness of non-small-cell lung cancer to gefitinib. N Engl J Med 2004; 350(21):2129–39.
22. Paez JG, Jänne PA, Lee JC, et al. EGFR mutations in lung cancer: correlation with clinical response to gefitinib therapy. Science 2004; 304(5676):1497–500.
23. Sharma SV, Bell DW, Settleman J, Haber DA. Epidermal growth factor receptor mutations in lung cancer. Nat Rev Cancer 2007; 7(3):169–81.
24. Eberhard DA, Johnson BE, Amler LC, et al. Mutations in the epidermal growth factor receptor and in KRAS are predictive and prognostic indicators in patients with non-small-cell lung cancer treated with chemotherapy alone and in combination with erlotinib. J Clin Oncol 2005; 23(25):5900–9.
25. Kim YT, Kim T-Y, Lee DS, et al. Molecular changes of epidermal growth factor receptor (EGFR) and KRAS and their impact on the clinical outcomes in surgically resected adenocarcinoma of the lung. Lung Cancer 2008; 59(1):111–8.
26. Marks JL, Broderick S, Zhou Q, et al. Prognostic and therapeutic implications of EGFR and KRAS mutations in resected lung adenocarcinoma. J Thorach Oncol 2008; 3(2):111–6.
27. Tomizawa Y, Iijima H, Sunaga N, et al. Clinicopathologic significance of the mutations of the epidermal growth factor receptor gene in patients with non-small cell lung cancer. Clin Cancer Res 2005; 11(19 Pt 1):6816–22.
28. Liu G, Gurubhagavatula S, Zhou W et al. Epidermal growth factor receptor polymorphisms and clinical outcomes in non-small-cell

lung cancer patients treated with gefitinib. Pharmacogenomics J 2008; 8(2), 129–138.

29. Ichihara S, Toyooka S, Fujiwara Y et al. The impact of epidermal growth factor receptor gene status on gefitinib-treated Japanese patients with non-small-cell lung cancer. Int. J. Cancer 2007; 120(6), 1239–1247.
30. Gregorc V, Hidalgo M, Spreafico A et al. Germline polymorphisms in EGFR and survival in patients with lung cancer receiving gefitinib. Clin. Pharmacol. Ther. 2008; 83(3), 477–484.
31. Han SW, Jeon YK, Lee KH et al. Intron 1 CA dinucleotide repeat polymorphism and mutations of epidermal growth factor receptor and gefitinib responsiveness in non-small-cell lung cancer. Pharmacogenet. Genom. 2007; 17(5), 313–319.
32. Ma F, Sun T, Shi Y et al. Polymorphisms of EGFR predict clinical outcome in advanced non-small-cell lung cancer patients treated with gefitinib. Lung Cancer 2009; 66(1), 114–119.
33. Dubey S, Stephenson P, Levy DE et al. EGFR dinucleotide repeat polymorphism as a prognostic indicator in non-small cell lung cancer. J. Thorac. Oncol. 2006; 1(5), 406–412.
34. Lemos C, Giovannetti E, Zucali PA et al. Impact of ABCG2 polymorphisms on the clinical outcome and toxicity of gefitinib in non-small-cell lung cancer patients. Pharmacogenomics 2011; 12(2), 159–170.
35. Allen KE, Weiss GJ. Resistance may not be futile: microRNA biomarkers for chemoresistance and potential therapeutics. Mol Cancer Ther. 2010;9:3126-3136.
36. Broxterman HJ, Gotink KJ, Verheul HM. Understanding the causes of multidrug resistance in cancer: a comparison of doxorubicin and sunitinib. Drug Resist Updat. 2009;12:114–26.
37. Galvani E, Peters GJ, Giovannetti E. EGF receptor-targeted therapy in non-small-cell lung cancer: role of germline polymorphisms in outcome and toxicity. Future Oncol. 2012;8:1015-29.
38. Fojo T. Multiple paths to a drug resistance phenotype: mutations, translocations, deletions and amplification of coding genes or promoter promoter regions, epigenetic changes and microRNAs. Drug Resist Updat. 2007;10:59–67.
39. Wang YS, Wang YH, Xia HP, Zhou SW, Schmid-Bindert G, Zhou CC. MicroRNA-214 regulates the acquired resistance to gefitinib via the PTEN/AKT pathway in EGFR-mutant cell lines. Asian Pac J Cancer Prev. 2012;13:255-60.
40. Garofalo M, Romano G, Di Leva G, Nuovo G, Jeon YJ, Ngankeu A, et al. EGFR and MET receptor tyrosine kinase-altered microRNA expression induces tumorigenesis and gefitinib resistance in lung cancers. Nat Med. 2011;18:74-82.
41. Bryant JL, Britson J, Balko JM, Willian M, Timmons R, Frolov A, et al. A microRNA gene expression signature predicts response to erlotinib in epithelial cancer cell lines and targets EMT. Br J Cancer. 2012;106:148-56.
42. Markou A, Tsaroucha EG, Kaklamanis L, Fotinou M, Georgoulias V, Lianidou ES. Prognostic value of mature microRNA-21 and microRNA-205 overexpression in non-small cell lung cancer by quantitative real-time RT-PCR. Clin Chem. 2008;54:1696-704.
43. Raponi M, Dossey L, Jatkoe T, Wu X, Chen G, Fan H, et al. MicroRNA classifiers for predicting prognosis of squamous cell lung cancer. Cancer Res. 2009;69:5776-83.
44. Patnaik SK, Kannisto E, Knudsen S, Yendamuri S. Evaluation of microRNA expression profiles that may predict recurrence of localized stage I non-small cell lung cancer after surgical resection. Cancer Res. 2010;70:36-45.
45. Voortman J, Goto A, Mendiboure J, Sohn JJ, Schetter AJ, Saito M, et al. MicroRNA expression and clinical outcomes in patients treated with adjuvant chemotherapy after complete resection of non-small cell lung carcinoma. Cancer Res. 2010;70:8288-98.
46. Jiang J, Greulich H, Jänne PA et al. Epidermal growth factor-independent transformation of Ba/F3 cells with cancer-derived epidermal growth factor receptor mutants induces gefitinib-sensitive cell cycle progression. Cancer Res. 2005; 65(19):8968-74.
47. Kobayashi S, Ji H, Yuza Y, et al. An alternative inhibitor overcomes resistance caused by a mutation of the epidermal growth factor receptor. Cancer Res. 2005; 65(16):7096-101.
48. Pao W, Miller VA, Politi KA, et al. Acquired resistance of lung adenocarcinomas to gefitinib or erlotinib is associated with a second mutation in the EGFR kinase domain. PLoS Med. 2005; 2(3):e73.
49. Fry DW; Bridges AJ; Denny WA; et al. Specific, irreversible inactivation of the epidermal growth factor receptor and erbB2, by a new class of tyrosine kinase inhibitor. *Proc. Natl. Acad. Sci. U.S.A.* 1998, *95*, 12022–12027.
50. Blair JA; Rauh D; Kung C; et al. Structure-guided development of affinity probes for tyrosine kinases using chemical genetics. *Nature Chem. Biol.* 2007, *3*, 229–238.
51. Kwak EL; Sordella R; Bell DW; et al. Irreversible inhibitors of the EGF receptor may circumvent acquired resistance to gefitinib. *Proc. Natl. Acad. Sci. U.S.A.* 2005, *102*, 7665–7670.
52. Carter TA; Wodicka LM; Shah NP; et al. Inhibition of drug-resistant mutants of ABL, KIT, and EGF receptor kinases. *Proc. Natl. Acad. Sci. U.S.A.* 2005, *102*, 11011–11016.
53. Godin-Heymann N; Ulkus L; Brannigan BW; et al. The T790M “gatekeeper” mutation in EGFR mediates resistance to low concentration of an irreversible EGFR inhibitor. *Mol. Cancer Ther.* 2008, *7*, 874–879.
54. Singh J; Petter RC; Kluge AF. Targeted covalent drugs of the kinase family. *Curr. Opin. Chem. Biol.* 2010, *14*, 475–480.
55. sTsou HR; Mamuya N; Johnson BD; et al. 6-Substituted-4-(3-bromophenylamino)quinazolines as putative irreversible inhibitors of the epidermal growth factor receptor (EGFR) and human epidermal growth factor receptor (HER-2) tyrosine kinases with enhanced antitumor activity. *J. Med. Chem.* 2001, *44*, 2719–2734.
56. Smaill JB; Showalter HDH; Zhou H; et al. Tyrosine kinase inhibitors. 18. 6-Substituted 4-anilinoquinazolines and 4-anilinopyrido[3,4-d]pyrimidines as soluble, irreversible inhibitors of the Epidermal Growth Factor Receptor. *J. Med. Chem.* 2001, *44*, 429–440.
57. Mishani E; Abourbeh G; Jacobson O; et al. High-affinity Epidermal Growth Factor Receptor (EGFR) irreversible inhibitors with

diminished chemical reactivities as Positron Emission Tomography (PET)-imaging agent candidates of EGFR overexpressing tumors. *J. Med. Chem.* 2005, *48*, 5337–5348.

58. Carmi C; Lodola A; Rivara S; et al. Epidermal growth factor receptor irreversible inhibitors: Chemical exploration of the cysteine-trap portion. *Mini Rev. Med. Chem.* 2011, *11*, 1019–1030.
59. Zhou W; Ercan D; Chen L; et al. Novel mutant-selective EGFR kinase inhibitors against EGFR T790M. *Nature*, 2009, *462*, 1070–1074.
60. Jänne PA; von Pawel J; Cohen RB; Crino, et al. Multicenter, randomized, phase II trial of CI-1033, an irreversible pan-ERBB inhibitor, for previously treated advanced non small-cell lung cancer. *J. Clin. Oncol.* 2007, *25*, 3936–3944.
61. Besse B; Eaton KD; Soria JC; et al. Neratinib (HKI-272), an irreversible pan-ErbB receptor tyrosine kinase inhibitor: preliminary results of a phase 2 trial in patients with advanced non-small cell lung cancer. *Eur. J. Cancer* 2008, *Suppl. 6*, 64.
62. Carmi C; Cavazzoni A; Zuliani V; et al. 5-Benzylidene-hydantoins as new EGFR inhibitors with antiproliferative activity. *Bioorg. Med. Chem. Lett.* 2006, *16*, 4021–4025.
63. Zuliani V; Carmi C; Rivara M; et al. 5-Benzylidene-hydantoins: Synthesis and antiproliferative activity on A549 lung cancer cell line. *Eur. J. Med. Chem.* 2009, *44*, 3471–3479.
64. Cavazzoni A; Alfieri RR; Carmi C; et al. Dual mechanisms of action of the 5-benzylidene-hydantoin UPR1024 on lung cancer cell lines. *Mol. Cancer Ther.* 2008, *7*, 361–370.
65. Jung M-J, Rho J-K, Kim Y-M, *et al.*. Upregulation of CXCR4 is functionally crucial for maintenance of stemness in drug-resistant non-small cell lung cancer cells. Oncogene 2012; 1-13.
66. Thomson S, Buck E, Petti F, *et al.*. Epithelial to mesenchymal transition is a determinant of sensitivity of non-small-cell lung carcinoma cell lines and xenografts to epidermal growth factor receptor inhibition. Cancer Res 2005; 65(20):9455-62.
67. Weickhardt AJ, Price TJ, Chong G, et al. Dual Targeting of the Epidermal Growth Factor Receptor Using the Combination of Cetuximab and Erlotinib: Preclinical Evaluation and Results of the Phase II DUX Study in Chemotherapy-Refractory, Advanced Colorectal Cancer. J Clin Oncol 2012; 30(13):1505–12.
68. Ferrara N. Vascular endothelial growth factor: basic science and clinical progress. Endocr Rev. 2004; 25(4):581-611.
69. Sandler A, Gray R, Perry MC, et al. Paclitaxel-carboplatin alone or with bevacizumab for non-small-cell lung cancer. N Engl J Med. 2006 Dec 14;355(24):2542-50.
70. Reck M, von Pawel J, Zatloukal P, et al. Phase III trial of cisplatin plus gemcitabine with either placebo or bevacizumab as first-line therapy for nonsquamous non-small-cell lung cancer: AVAil. J Clin Oncol. 2009; 27(8):1227-34.
71. Giovannetti E, Honeywell R, Hanauske AR, et al. Pharmacological aspects of the enzastaurin-pemetrexed combination in non-small cell lung cancer (NSCLC). Curr Drug Targets. 2010;11:12-28.
72. Mross K, Frost A, Steinbild S, et al. A Phase I Dose-Escalation Study of Regorafenib (BAY 73-4506), an Inhibitor of Oncogenic, Angiogenic, and Stromal Kinases, in Patients with Advanced Solid Tumors. Clin Cancer Res. 2012;18:2658-67.

Appendix A

SUPPORTING INFORMATION

Chapter 6

Irreversible Inhibition of EGFR Activity by 3-Aminopropanamides

EXPERIMENTAL PROCEDURES

*Synthesis. Experimental procedures for the synthesis of compounds **25-27a**,**b** (Scheme 1 in the main text), **29-35** (Scheme 2 in the main text), and **41b**, **42b**, **43a**,**b** and **45** (Scheme 3 in the main text).*

Ethyl 4-(3-bromoanilino)quinazolin-6-ylcarbamate (**25**). Ethyl chloroformate (133 µL, 1.40 mmol) was added dropwise to a stirred solution of 6-amino-4-(3-bromoanilino)quinazoline 4 (400 mg, 1.27 mmol) in anhydrous pyridine (10 mL) at 0 °C. The mixture was warmed to room temperature and stirred for 5 h. Pyridine was removed under reduced pressure and the solid residue was washed with 10% acetic acid solution and water until neutrality. The crude product 25 was dried in vacuo and used in the next step without further purification: MS (APCI) m/z 387.1; 1H NMR (CD3OD, 300 MHz) δ 1.37 (t, J = 7.1 Hz, 3H), 4.30 (q, J = 7.2 Hz, 2H), 7.40 (t, J = 8.0 Hz, 1H), 7.49 (m, 1H), 7.75 (ddd, J = 7.9, 2.3, 1.2 Hz, 1H), 7.80 (d, J = 9.0 Hz, 1H), 7.95 (dd, J = 9.1, 2.3 Hz, 1H), 8.07 (t, J = 1.9 Hz, 1H), 8.63 (d, J = 2.1 Hz, 1H), 8.68 (s, 1H).

4-(3-Bromoanilino)-6-methylaminoquinazoline (**26**). Ethyl carbamate 25 was dissolved in anhydrous THF (30 mL) and cooled in an ice bath. Red-Al (1.17 mL, 5.08 mmol) was added by small portions and the resulting mixture was heated at reflux overnight. The reaction was then cooled to 0 °C and quenched with 30% KOH solution (1.2 mL). The crude product was purified by silica gel chromatography (AcOEt/n-hexane, 60:40 to 99:1) to give 26 as a yellow solid (60%): mp 145 °C; MS (APCI) m/z 329.1, 331.3; 1H NMR (CD3OD, 300 MHz) δ 2.89 (s, 3H), 7.09 (d, J = 2.4 Hz, 1H), 7.23 (m, 3H), 7.51 (d, J = 9.0 Hz, 1H), 7.70 (m, 1H), 8.04 (br s, 1H), 8.28 (s, 1H).

N-(4-(3-Bromoanilino)quinazolin-6-yl)-3-chloropropanamide (**27a**). A stirring suspension of amine 4 (300 mg, 0.95 mmol) and 3-chloropropionyl chloride (3 mL, 31.3 mmol) was heated to 50 °C and stirred for 5 h. Methanol (6 mL) was then added dropwise and the mixture was evaporated under reduced pressure. The solid residue was washed with Et2O and water, dried under reduced pressure and purified by silica gel chromatography (CH2Cl2/MeOH, 98:2 to 95:5) to afford 27a as a white solid (86%): MS (APCI) m/z 409.3, 407.4; 1H NMR (CDCl3, 300 MHz) δ 2.96 (t, J = 6.2 Hz, 2H), 3.95 (t, J = 6.2 Hz, 2H), 7.31-7.33 (m, 2H), 7.78 (m, 3H), 8.14 (s, 1H), 8.55 (s, 1H), 8.72 (s, 1H).

N-(4-(3-Bromoanilino)quinazolin-6-yl)-3-chloro-N-methylpropanamide (**27b**).
4-(3-Bromoanilino)-6-methylaminoquinazoline 26 was reacted with 3-chloropropionil chloride as described for compound 27a. The product 27b obtained as a pale yellow solid (75%) was used in the next step without further purification: mp 176-179 °C; MS (APCI): m/z 419.1, 420.3, 421.2, 422.2; 1H NMR (CD3OD, 300 MHz) δ 2.67 (br s, 2H), 3.42 (s, 3H), 3.78 (m, 2H), 7.33 (m, 2H), 7.78 (m, 1H), 7.83 (dd, J = 8.9, 2.2 Hz, 1H), 7.92 (d, J = 8.7 Hz, 1H), 8.17 (s, 1H), 8.42 (br s, 1H), 8.66 (s, 1H).

7-Chloroquinazolin-4(1*H*)-one (**29**). 2-Amino-4-chlorobenzoic acid 28 (5.0 g, 29.1 mmol) and formamidine acetate (6.1 g, 58.3 mmol) in methoxyethanol (35 mL) were stirred at reflux overnight. The clear reaction mixture was then cooled to rt, the solvent was removed under vacuum and the solid residue was

washed several times with aqueous NH3 (0.01M) to yield a light brown powder (94%): mp 254-255 °C; MS (APCI) m/z 181.3, 183.1; 1H NMR (DMSO-d6, 300 MHz) δ 7.54 (dd, J = 8.5, 1.9 Hz, 1H), 8.72 (d, J = 1.9 Hz, 1H), 8.11 (d, J = 8.5 Hz, 1H), 8.14 (s, 1H), 12.40 (br s, 1H).

7-Chloro-6-nitroquinazolin-4(1*H*)-one (**30**). A solution of 29 (1.18 g, 6.5 mmol) in conc. H2SO4 (3.5 mL, 65 mmol) and fuming HNO3 (3.5 mL) was heated at 100 °C for 1 h. After cooling to rt, the solution was poured onto ice-water and the precipitant was collected by filtration. The light yellow solid was crystallized twice from AcOH to give 30 as a bright yellow solid (70%): mp (AcOH) >230 °C; MS (APCI) m/z 224.1, 226.0; 1H NMR (DMSO-d6, 300 MHz) δ 8.05 (s, 1H), 8.32 (s, 1H), 8.69 (s, 1H), 12.79 (br s, 1H).

7-Ethoxy-6-nitroquinazolin-4(1*H*)-one (**31**). 7-Chloroquinazoline derivative 30 (700 mg, 3.10 mmol) was added to a solution of Na (422 mg, 18.6 mmol) in anhydrous EtOH (110 mL) and the mixture was stirred at reflux for 3 days. The dark solution was neutralized with AcOH, the solvent was removed under reduced pressure, and residue was extracted from AcOEt/H2O. The organic layer was evaporated to dryness and the crude product was purified by silica gel chromatography (CH2Cl2/MeOH/AcOH, 96:3:1) to afford 31 as a white solid (50%): mp (EtOH) >230 °C; MS (APCI) m/z 236.3; 1H NMR (DMSO-d6, 300 MHz)δ 1.43 (t, J = 7.0 Hz, 3H), 4.38 (q, J = 7.0 Hz, 2H), 8.26 (s, 1H), 8.44 (s, 1H), 8.55 (s, 1H), 12.54 (br s, 1H).

4-Chloro-7-ethoxy-6-nitroquinazoline (**32**). A suspension of 31 (314 mg, 1.34 mmol) in $POCl_3$ (15 mL) was heated to reflux for 30 min. The clear solution was then evaporated under reduced pressure and the residue was dissolved in CH2Cl2 and washed with aqueous NaHCO3. The organic layer was dried and the solvent removed to obtain 32 (99%) that was used the next step without further purification: 1H NMR (CDCl3, 300 MHz) δ 1.57 (t, J = 7.0 Hz, 3H), 4.37 (q, J = 7.0 Hz, 2H), 7.54 (s, 1H), 8.62 (s, 1H), 9.07 (s, 1H).

4-(3-Chloro-4-fluoroanilino)-7-ethoxy-6-nitroquinazoline (**33**).

4-Chloro-7-ethoxy-6-nitroquinazoline 32 (381 mg, 1.51 mmol) and 3-chloro-4-fluoroaniline (438 mg, 3.01 mmol) in i-PrOH (16 mL) were heated to reflux and conc HCl (3 drops) was added. The mixture was stirred and refluxed for 30 min and then basified by addition of Et3N. The solvent was removed under reduced pressure, the solid residue was dissolved in Et2O and filtered, then the solvent was removed under reduced pressure and the residue was further dissolved in AcOEt and washed with H2O. The organic layer was evaporated to dryness giving 33 (99%) that was used in the next step without further purifications: MS (APCI) m/z 363.2, 365.3; 1H NMR (DMSO-d6, 400 MHz) δ 1.43 (t, J = 7.0 Hz, 3H), 4.09 (q, J = 7.0 Hz, 2H), 7.51 (s, 1H), 7.53 (t, J = 9.1 Hz, 1H), 7.77 (ddd, J = 9.1, 4.0, 2.8 Hz, 1H), 8.11 (dd, J = 6.7, 2.4 Hz, 1H), 8.83 (s, 1H), 9.34 (s, 1H), 10.85 (br s, 1H).

6-Amino-4-(3-chloro-4-fluoroanilino)-7-ethoxyquinazoline (**34**). Iron powder (225 mg, 4.04 mmol) and AcOH (0.33 mL, 5.77 mmol) were added to a solution of 6-nitroquinazoline 33 (488 mg, 1.35 mmol) in EtOH/H2O 7:3 (60 mL) and the mixture was heated to reflux for 2 h. 30% NH3 solution was added to basify the solution, then the solvent was removed under reduced pressure. The residue was dissolved in AcOEt and washed with H2O. The organic layer was evaporated to give the reduced product 34 (89%): mp 206-

208 °C; MS (APCI) m/z 333.4, 335.3; 1H NMR (MeOD, 400 MHz) δ 1.57 (t, J = 6.9 Hz, 3H), 4.34 (q, J = 6.9 Hz, 2H), 7.11 (s, 1H), 7.33 (t, J = 8.9 Hz, 1H), 7.48 (s, 1H), 7.64 (ddd, J = 8.8, 4.1, 2.7 Hz, 1H), 7.93 (dd, J = 6.6, 2.5 Hz, 1H), 8.56 (s, 1H).

3-Chloro-N-(4-(3-Chloro-4-fluoroanilino)-7-ethoxyquinazolin-6-yl)propanamide (**35**).

6-aminoquinazoline 34 was reacted with 3-chloropropionil chloride as described for compound 27a. The resulting solid residue (99%) was used in the next step without no further purification: MS (APCI) m/z 425.3, 427.4; 1H NMR (MeOD, 300 MHz) δ 1.59 (t, J = 7.0 Hz, 3H); 3.06 (t, J = 6.2 Hz, 2H), 3.93 (t, J = 6.2 Hz, 2H), 4.40 (q, J = 7.0 Hz, 2H), 7.28 (s, 1H), 7.35 (t, J = 8.9 Hz, 1H), 7.63 (ddd, J = 8.9, 4.1, 2.8 Hz, 1H), 7.91 (dd, J = 6.6, 2.6 Hz, 1H), 8.73 (s, 1H), 9.13 (s, 1H).

N-(4-(3-Chloro-4-(pyridin-2-ylmethoxy)anilino)-3-cyano-7-ethoxyquinolin-6-yl)acetamide (**41b**).

A mixture of N-(4-chloro-3-cyano-7-ethoxyquinolin-6-yl)acetamide 40 (400 mg, 1.39 mmol), 3-chloro-4-(pyridine-2-ylmethoxy)aniline 45 (295 mg, 1.25 mmol), and pyridine hydrochloride (145 mg, 1.25 mmol) in i-PrOH (3.5 mL) was refluxed overnight. The solid was filtered, washed with H2O and Et2O to afford the coupling product 41b (99%): 1H NMR (DMSO-d6, 300 MHz) δ 1.50 (t, J = 6.9 Hz, 3H), 2.19 (s, 3H), 4.33 (q, J = 6.9 Hz, 2H), 5.35 (s, 2H), 7.38 (m, 3H), 7.51 (s, 1H), 7.61 (m, 2H), 7.92 (td, J = 7.8, 1.9 Hz, 1H), 8.62 (d, J = 4.1 Hz, 1H), 8.93 (s, 1H), 9.03 (s, 1H), 9.60 (s, 1H), 10.91 (br s, 1H).

6-Amino-4-(3-chloro-4-(pyridin-2-ylmethoxy)anilino)-7-ethoxyquinoline-3-carbonitrile (**42b**).

Acetamide 41b was suspended in conc HCl (1.22 mL) and H2O (0.6 mL), and the mixture was stirred at reflux for 5 h. The solvent was then evaporated and the residue was treated with aqueous NaHCO3, filtered, washed with H2O and dried. Silica gel chromatography purification (CH2Cl2/MeOH, 96:4) afforded 42b (78%): MS (APCI) m/z 446.1; 1H NMR (DMSO-d6, 300MHz) δ 1.43 (t, J = 6.9 Hz, 3H), 4.21 (q, J = 6.9 Hz, 2H), 5.24 (s, 2H), 5.41 (s, 2H), 7.03 (d, J = 8.7 Hz, 1H), 7.21 (m, 4H), 7.36 (m, 1H), 7.57 (d, J = 7.7 Hz, 1H), 7.87 (td, J = 7.7, 1.5 Hz, 1H), 8.24 (s, 1H), 8.58 (d, J = 4.4 Hz, 1H), 9.13 (s, 1H).

3-Chloro-N-(4-(3-chloro-4-fluoroanilino)-3-cyano-7-ethoxyquinolin-6-yl)propanamide (**43a**).

6-Amino-4-(3-chloro-4-fluoroanilino)-7-ethoxyquinoline-3-carbonitrile 42a was reacted with 3-chloropropionil chloride as described for compound 27a. Silica gel chromatography purification (CH2Cl2/MeOH, 98:2 to 95:5) afford 43a as a pale yellow solid (99%): MS (APCI) m/z 536.3, 538.5; 1H NMR (DMSO-d6, 300 MHz) δ 1.47 (t, J = 7.1 Hz, 3H), 3.01 (t, J = 6.5 Hz, 2H), 3.90 (t, J = 6.3 Hz, 2H), 4.31 (q, J = 7.4 Hz, 2H), 5.29 (s, 2H), 7.19-7.27 (m, 2H), 7.36-7.39 (m, 3H), 7.59 (d, J = 7.8 Hz, 1H), 7.88 (t, J = 7.7 Hz, 1H), 8.48 (s, 1H), 8.73 (d, J = 4.0 Hz, 1H), 8.87 (s, 1H), 9.52 (s, 1H), 9.64 (s, 1H).

3-Chloro-N-(4-(3-chloro-4-(pyridin-2-ylmethoxy)anilino)-3-cyano-7-ethoxyquinolin-6-yl)propanamide (**43b**).

6-Amino-4-(3-chloro-4-(pyridine-2-ylmethoxy)anilino)-7-ethoxyquinoline-3-carbonitrile 42b was reacted with 3-chloropropionil chloride as described for compound 27a. Silica gel chromatography purification (CH2Cl2/MeOH, 98:2 to 95:5) gave 43b as a pale yellow solid (99%): MS (APCI) m/z 536.3, 538.5; 1H NMR (DMSO-d6, 300 MHz) δ 1.47 (t, J = 7.1 Hz, 3H), 3.01 (t, J = 6.5 Hz, 2H),

3.90 (t, J = 6.3 Hz, 2H), 4.31 (q, J = 7.4 Hz, 2H), 5.29 (s, 2H), 7.19-7.27 (m, 2H), 7.36-7.39 (m, 3H), 7.59 (d, J = 7.8 Hz, 1H), 7.88 (t, J = 7.7 Hz, 1H), 8.48 (s, 1H), 8.73 (d, J = 4.0 Hz, 1H), 8.87 (s, 1H), 9.52 (s, 1H), 9.64 (s, 1H).

3-Chloro-4-(pyridine-2-ylmethoxy)aniline (**45**). 4-Anilino-2-chlorophenol 44 (200 mg, 1.39 mmol) was dissolved in anhydrous DMF (1.6 mL), benzaldehyde (155 µL, 1.53 mmol) and the mixture was stirred at rt for 10 min. Potassium carbonate was then added (768 mg, 5.56 mmol) followed by picolyl chloride hydrochloride (273 mg, 1.67 mmol). The reaction was stirred at 50 °C for 24 h, then the solvent was removed under reduced pressure and the residue was carefully added of 2N HCl. Upon complete dissolution, the product was extracted with EtOAc and the aqueous layer was basified with 2N NaOH. The resulting precipitate was washed with water and dried to give 45 (95%) that was used in the next step without further purification: MS (APCI) m/z 235.3; 1H NMR (DMSO-d6, 300MHz) δ 4.94 (s, 2H), 5.07 (s, 2H), 6.45 (dd, J = 8.7, 2.7 Hz, 1H), 6.65 (d, J = 2.7 Hz, 1H), 6.91 (d, J = 8.7 Hz, 1H), 7.33 (m, 1H), 7.54 (d, J = 7.8 Hz, 1H), 7.84 (td, J = 7.7, 1.8 Hz, 1H), 8.55 (d, J = 4.2 Hz, 1H).

In vitro Stability assays.

Chemical stability was tested at fixed ionic strength (µ = 0.15 M), under physiological (0.01 M PBS, pH 7.4), and alkaline (0.01 M borate buffer, pH 9.0) pH conditions, at 37°C. Stock solutions of **3** and **5** were prepared in DMSO, and each sample was incubated at a final concentration of 1 µM in prewarmed buffered solutions (final concentration of DMSO: 1% v/v). At regular time points, aliquots were sampled and immediately injected into the HPLC system. For rat plasma stability assays, rat plasma was quickly thawed and diluted to 80% (v/v) with 0.1 M PBS, pH 7.4. Compound stock solution in DMSO was added (final compound concentration: 1 µM, DMSO concentration: 1% v/v) and maintained at 37 °C. Aliquots of solution were sampled, two volumes of acetonitrile were added and the mixture was centrifuged (4 °C, 8,000 g, 10 min) and analyzed by RP-HPLC.

Analytical Method.

HPLC column used was a RP-C18 Supelco Discovery (Supelco, Bellefonte, PA, USA), 5 µm, 150 x 4.6 mm i.d. Mobile phases consisted of water and methanol, both additioned with trifluoroacetic acid (TFA) at 0.05% v/v and at a flow rate of 1 mL min-1. Conditions chosen were the following: Eluent A: methanol + 0.05% TFA; Eluent B: water + 0.05% TFA. T(0 min): 40% A: 60% B; T(10 min) 90% A:10% B returning to initial conditions after 0.5 min, followed by 5 min re-equilibration time. Injection volume: 10 µL. Single ions at m/z [M+H]+ = 414.3 amu (5); 315.2 (4); 369.2 (3); 468.1 (45) were monitored. MS potentials were optimized by Flow Injection Analysis (FIA) of stock solutions of compounds in 1:1 water:methanol additioned with 0.05% trifluoroacetic acid. The following parameters were retained for optimal analyte detection: nebulizer gas: 13 psi; turbo ion spray gas: 13 psi; curtain gas: 10 psi; cone voltage: 45 V; skimmer voltage: 295 V; entrance potential: 4.6 V; ion source temperature: 450°C. The dwell time used for acquiring data for each SIM analysis was 1000 ms. For HR-MS analysis, HPLC column was a RP-C18 Supelco Discovery (Supelco, Bellefonte, PA, USA), 5 µm, 150 x 4.6 mm i.d. thermostated at 30°C. Mobile phases consisted of water and methanol, both additioned with formic acid (FA) at 0.1% v/v and at a flow rate of 1 mL min-1. Conditions

chosen were the following: Eluent A: methanol + 0.1% FA; Eluent B: water + 0.1% FA. T(0 min): 30% A: 70% B; T(2 min) 30% A:70% B; T(12 min) 95% A:5% B; T(14 min) 95% A:5% B returning to initial conditions after 0.5 min, followed by 5 min re-equilibration time. LTQ-Orbitrap mass analyzer operated in scan mode in the 200-600 uma range (scan mode). Detection was in positive polarity. Tuning parameters for ESI source were chosen as follows: Source Voltage (kV): 3; Sheath Gas Flow Rate: 25; Aux Gas Flow Rate: 10; Sweep Gas Flow Rate: 10; Capillary Voltage (V): 9; Capillary Temperature (°C): 275; Tube Lens Voltage (V): 105.

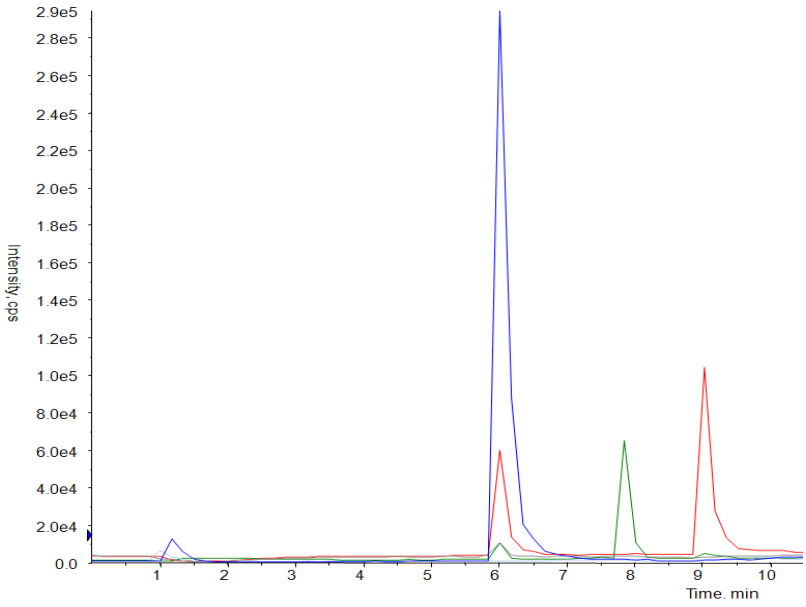

Figure S1. HPLC-MS chromatogram of compound 5 (UPR1157) after 24 h incubation under alkaline conditions (pH 9.0) at 37 °C. Mass balance studies revealed 77% of 5 (blue) recovered after 24 h, with acrylamide 3 (19%, in red) and amine 4 (4%, in green) as degradation products.

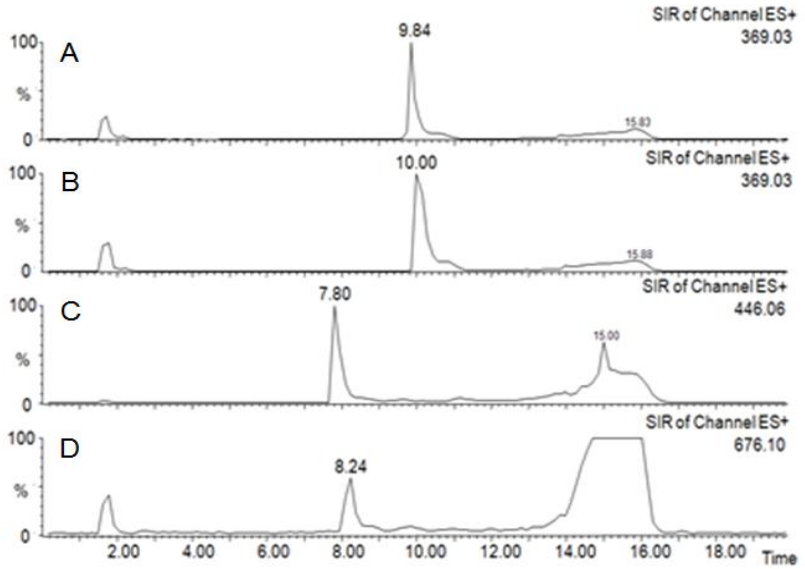

Figure S2. HPLC-MS chromatograms of compound 3 incubated in the presence of LMW thiols cysteamine and GSH. As a title of example, reported in Figure S2 are LC/MS traces corresponding to the formation of GSH- (*m*/*z* = 676.10) and cysteamine- (*m*/*z* = 446.06) conjugates by compound **3** (*m*/*z* = 369.03) after 1 h incubation at 37 °C. **(A)** Acrylamide **3** incubated in the presence of cysteamine (*t* = 0, *m*/*z* = 369.03); **(B)** Acrylamide **3** incubated in the presence of GSH (*t* = 0, *m*/*z* = 369.03); **(C)** Acrylamide **3** incubated in the presence of cysteamine (*t* = 1 h, *m*/*z* = 446.06); **(D)** Acrylamide **3** incubated in the presence of GSH (*t* = 1 h, *m*/*z* = 676.10).

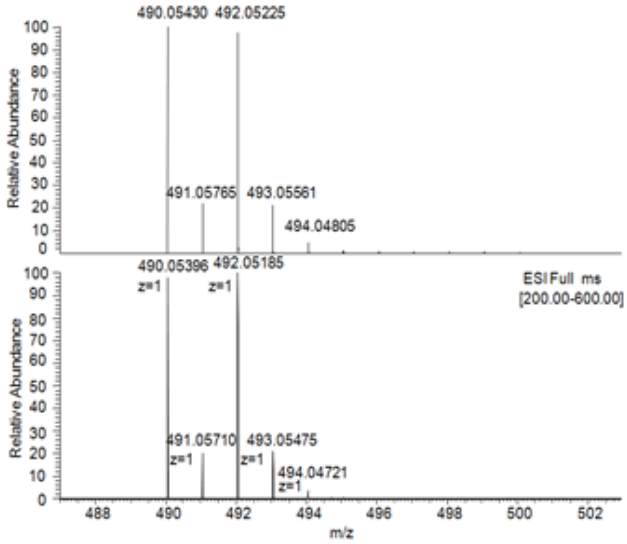

Figure S3. The unique identity of the conjugate formed by compounds **3** and **5** with cysteine in A549 cell lysate was confirmed by high resolution mass spectrometry employing a LTQ Orbitrap mass analyzer (Thermo). Below is the comparison between the calculated (first row) and experimental (second row) high resolution spectrum of the observed cysteine conjugate of compound **5** in cell lysates.

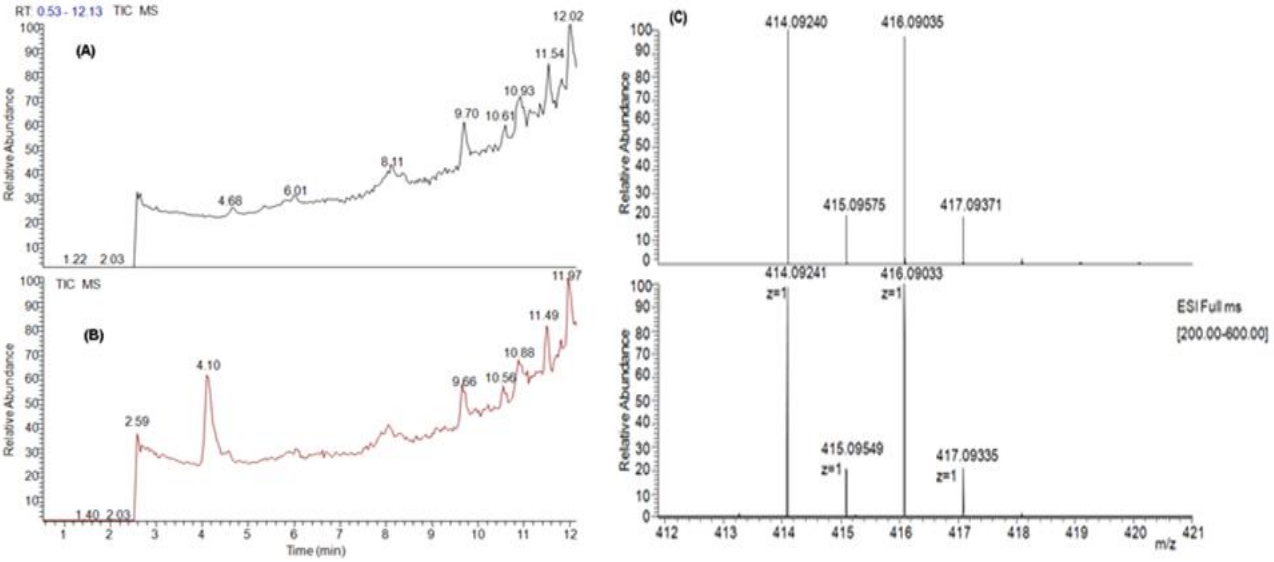

Figure S4. Total Ion Chromatogram (TIC) of A549 cell lysate control **(A)** compared to incubation in the presence of compound **5 (B)**. The peak at R_t = 4.10 min corresponds to **5** and has the HRMS spectrum reported below: the calculated **(C-first row)** and experimental **(C-second row)**.

Table S1. Quantification of intracellular concentration of compounds **3**, **4** and **5** in A549 cells.

Compound	nmol/mg prot[a] mean (± SEM)	
	1 h	8 h
3	< LOD[b]	< LOD[b]
4	0.050 ± 0.01	< LOD[b]
5	0.105 ± 0.01	< LOD[b]

[a] Intracellular nmol of compound per mg of protein detected 1 h or 8 h after 1 h incubation with the compound (1 µM); data were normalized for the protein content in each cellular sample; mean ± SEM, n = 3. [b] limit of detection (LOD) = 20 pmol/mL.

Table S2. ErbB2 tyrosine kinase inhibition.

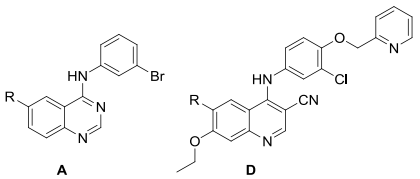

Compd	Series	R	ErbB2 kinase assay IC_{50} (μM)[a]
5	A	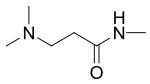	>10
20	D	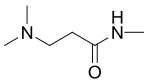	0.97 ± 0.05
21	D	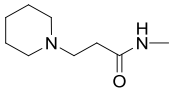	0.98 ± 0.01

[a] Concentration to inhibit by 50% ErbB2 tyrosine kinase activity. IC_{50} values were measured by the phosphorylation of a peptide substrate using homogeneous time resolved fluorescence (see Experimental Section in the main text). Mean values of three independent experiments ± SEM are reported.

Table S3. Elemental Analysis Data.

Compound	Formula	C Calcd % Found %	H Calcd % Found %	N Calcd % Found %
3	$C_{17}H_{13}BrN_4O$	55.30 54.96	3.55 3.83	15.17 14.98
4	$C_{14}H_{11}BrN_4 \cdot 3/2H_2O$	49.92 49.73	3.65 3.92	16.63 16.23
5	$C_{19}H_{20}BrN_5O$	55.08 54.69	4.87 4.89	16.90 16.53
6	$C_{22}H_{24}BrN_5O \cdot 3/4H_2O$	56.47 56.46	5.49 5.43	14.96 14.77
7	$C_{21}H_{22}BrN_5O_2 \cdot 1/3H_2O$	54.56 54.75	4.94 4.99	15.15 14.88
8	$C_{22}H_{25}BrN_6O \cdot 1/2H_2O$	55.23 55.22	5.48 5.54	17.57 17.28
9	$C_{20}H_{22}BrN_5O$	56.08 56.48	5.18 5.15	16.35 16.13
10	$C_{19}H_{16}ClFN_4O_2 \cdot 2/3CH_3CH_2OH$	58.49 58.31	4.83 4.75	13.42 13.09
11	$C_{21}H_{23}ClFN_5O_2 \cdot 2/3H_2O$	56.81 56.92	5.53 5.58	15.78 15.47
12	$C_{24}H_{27}ClFN_5O_2 \cdot 1H_2O$	58.83 59.20	5.97 5.97	14.29 14.08
13	$C_{23}H_{25}ClFN_5O_3 \cdot 2/3H_2O$	56.85 57.22	5.46 5.44	14.41 14.09
14	$C_{21}H_{16}ClFN_4O_2 \cdot 1/2H_2O$	60.07 60.09	4.08 3.95	13.35 13.15
15	$C_{23}H_{23}ClFN_5O_2 \cdot 1H_2O$	58.29 57.93	5.35 5.32	14.78 14.69
16	$C_{26}H_{27}ClFN_5O_2 \cdot 1/2CH_3CH_2OH$	62.48 62.15	5.83 5.58	13.50 13.82
17	$C_{25}H_{25}ClFN_5O_3 \cdot 1/2CH_3CH_2OH$	59.94 60.22	5.42 5.47	13.44 13.23
18	$C_{27}H_{22}ClFN_5O_3 \cdot 2/3CH_3OH$	63.74 64.04	4.99 4.76	13.42 13.04
19	$C_{29}H_{29}ClFN_6O_3 \cdot 1/2H_2O$	62.81 62.81	5.23 5.40	15.41 15.10
20	$C_{32}H_{33}ClFN_6O_3 \cdot 3/2H_2O$	62.79 63.08	5.93 6.12	13.73 13.35
21	$C_{31}H_{31}ClFN_6O_4$	63.42 63.08	5.32 6.48	14.32 13.92

Sommario

SOMMARIO

Nonostante la continua evoluzione in campo farmacologico per l'introduzione di nuovi e sempre piú efficaci chemioterapici e l'avanzamento nel settore diagnostico, la prognosi per i pazienti affetti da carcinoma polmonare non a piccole cellule (NSCLC) in stadio avanzato rimane negativa. La risposta al trattamento standard con chemioterapia é limitata dalla considerevole tossicitá associata a questo tipo di trattamento e allo sviluppo di meccanismi di resistenza.

La comprensione della biologia del tumore polmonare ha portato nell'ultimo decennio all'identificazione di bersagli molecolari utili per lo sviluppo di nuove terapie mirate con limitata tossicitá. Il recettore per il fattore di crescita dell'epidermide (EGFR) é uno dei bersagli molecolari più comunemente studiati per il quale iperespressione e deregolazione nei tumori polmonari sono state ampiamente documentate. Con la recente introduzione nella pratica clinica degli inibitori reversibili dell'attività tirosin chinasica (TKI) di EGFR, gefitinib ed erlotinib, é emersa la necessitá di identificare biomarcatori che permettano di prevedere e selezionare i pazienti che possano trarre il maggior beneficio da questo tipo di trattamento. La scoperta di mutazioni attivanti di EGFR nel 2004 ha portato successivamente all'approvazione di gefitinib per il trattamento in prima linea di pazienti con tali alterazioni del recettore. Sebbene la maggior parte dei pazienti trattati in prima linea con EGFR-TKI tragga inizialmente beneficio dalla terapia, dopo circa 10-12 mesi invariabilmente si osserva lo sviluppo di resistanza alla stessa con la conseguente progressione del tumore. I meccanismi di resistenza acquisita finora descritti includono la mutazione secondaria di EGFR T790M che occorre nel 50% dei casi, l'amplificazione di MET (5-15%), la mutazione di PI3KCA (5%) e la trasformazione in microcitoma (SCLC) (14%).

Nel caso di resistenza associata alla presenza della mutazione T790M, dati sperimentali hanno provato che la crescita tumorale conserva la propria dipendenza dall'attivitá del recettore. Per il trattamento di tali pazienti esiste pertanto l'esigenza di sviluppare nuove molecole che, avendo come bersaglio lo stesso EGFR, permettano di superare la resistenza acquisita agli inibitori tradizionali. Inibitori di EGFR di seconda generazione ad attività irreversibile, tra cui dacomitinib e afatinib, sono attualmente in studio in trials clinici. Questi composti sono in grado di interagire covalentemente con uno specifico e altamente conservato residuo di cisteina (Cys797) presente nel sito attivo dell'enzima che conferirebbe loro notevoli vantaggi rispetto ai convenzionali inibitori competitivi dell'ATP. Tenendo conto delle conoscenze acquisite nel campo degli inibitori di cistein-proteasi e degli inibitori di EGFR, nuovi inibitori irreversibili di EGFR/ErbB-2 in grado di superare la resistenza acquisita al trattamento con inibitori tradizionali sono stati sviluppati dal nostro gruppo e differenti aspetti dell'attività di tali composti sono stati studiati. Questi derivati 3-aminopropanamidici si sono dimostrati attivi su EGFR-T790M *in vitro* e *in vivo*, mostrando ridotta tossicitá rispetto ad altri inibitori di seconda generazione quale il canertinib. Inoltre, sono stati osservati effetti inibitori su altri importanti processi quali la migrazione cellulare e la trasformazione epitelio-mesenchimale. Questi risultati estendono potenzialmente l'uso di tali inibitori anche ai casi di NSCLC che abbiano sviluppato resistenza al trattamento con EGFR-TKIs anche diversi dalla mutazione secondaria del bersaglio.

Un'ulteriore strategia per il superamento della resistenza primaria o acquisita al trattamento con EGFR-TKI é l'identificazione di nuove combinazioni efficaci che associno farmaci diretti contro bersagli importanti per lo sviluppo e la crescita tumorale. Attraverso esperimenti preclinici abbiamo dimostrato il sinergismo

della combinazione erlotinib-sorafenib la quale, inibendo contemporaneamente le vie di segnalazione di EGFR e Raf aumenta la citotossicitá dei due farmaci.

Seppur in numero ridotto, alcuni pazienti negativi per le mutazioni attivanti di EGFR hanno ottenuto benefici dal trattamento con gefitinib o erlotinib durante gli studi clinici evidenziando come la sensibilitá al trattamento non sia imputabile al solo stato di EGFR. Per ottimizzare l'uso di questi farmaci si rende altresí necessaria l'identificazione di nuovi biomarcatori che possano prevedere la risposta al trattamento con EGFR-TKI. Il nostro gruppo ha dimostrato che l'induzione del citocromo P450-1A1, coinvolto nel metabolismo del gefitinib nel tessuto polmonare, a seguito di una prima esposizione al farmaco, potrebbe essere utilizzato come strategia per identificare precocemente i pazienti che possono trarre benefici dal trattamento stesso. Inoltre, l'inibizione dell'enzima puó potenziare l'effetto del farmaco in pazienti giá responsivi alla terapia. Un incremento nell'efficacia della terapia puó essere altresí ottenuto dalla combinazione di EGFR-TKI con l'anticorpo monoclonale anti-EGFR cetuximab. Dati da noi raccolti in studi preclinici hanno dimostrato che la stabilizzazione del bersaglio da parte di erlotinib ne causa l'accumulo a livello di membrana cellulare dove cetuximab compete con i ligandi per l'interazione con il recettore. Oltre ad impedire la normale attivazione di EGFR, il legame con il recettore attiva il processo di citotossicitá cellulo-mediata anticorpo-dipendente che riduce ulteriormente il numero delle cellule tumorali.

In conclusione, é necessario definire quando e come questi farmaci a bersaglio molecolare debbano essere impiegati, anche in combinazione con chemioterapici, per ottenere il massimo effetto con ridotta tossicitá. Inoltre, l'identificazione di nuove molecole coinvolte nella crescita tumorale potenzialmente utilizzabili come bersaglio per nuovi farmaci sono necessari per migliorare la prognosi di pazienti affetti da NSCLC ed evolvere nella direzione di una terapia sempre piú personalizzata.

Acknowledgements

Doing a PhD has been the most exciting and challenging experience of my life. During these years in which I learnt, worked, learnt how to work, faced with tricky situations and had fun I realized that looking carefully it's always possible to find people willing to help you out, to teach you, to encourage you, to listen to you and make your day with a smile.

I of course would like to thank my supervisors Prof. Roberta Alfieri and Prof. Pier Giorgio Petronini for the great opportunity to do this PhD. I am thankful for the time, help and suggestions you have dedicated to me throughout these years.

Maricla, Silvia, Claudia, Andrea and Mara, you were there when I started and became good colleagues and friends. It seems yesterday you were teaching me how to prepare nasty solutions (trypsin and lysis buffer) and perform protein measurements and Western blot, and I swear I learnt them. Francesca, I'm glad we have the chance to collaborate; I've a lot of things to learn from you.

Carla, Gabry and Marco, thanks for making my days with a smile and helping me out with the "unusual" requests I came out with. I wouldn't defend my thesis without the great work you've always done to help me.

I also would like to thank Prof. Frits Peters for the opportunity you gave me to work in your lab and the attention and time you dedicated to my research.

Elisa, I have never met anyone working as hard as you do with so much passion. You are a source of inspiration. I could never thank you enough for all that you taught me (and hopefully you will go on teaching me in the future) and for all the time and effort you dedicated to helping me.

Also a special thanks to the other researchers/students that helped out during their internships with their insights and hard working.